LANDSLIDING AND RHIZOBIOTA LINK THE SHORT- AND LONG-TERM CARBON CYCLE THROUGH SILICATE ROCK WEATHERING

by

YAKSHI NICOLE ORTIZ-MALDONADO

A thesis presented to the Department of Biology

FACULTY OF NATURAL SCIENCES

UNIVERSITY OF PUERTO RICO

RIO PIEDRAS CAMPUS

in partial fulfillment of the requirements for the degree of

MASTER OF SCIENCE IN BIOLOGY

May 2021

San Juan, Puerto Rico

This thesis has been accepted by the faculty of the:

DEPARTMENT OF BIOLOGY
FACULTY OF NATURAL SCIENCES
UNIVERSITY OF PUERTO RICO
RIO PIEDRAS CAMPUS

In partial fulfillment of the requirements for the degree of

MASTER OF SCIENCE IN BIOLOGY

Thesis Committee:

Carla Restrepo, Ph.D. (Advisor)

Filipa Godoy-Vitorino, Ph.D.

Zomary Flores, Ph.D.

Riccardo Papa, Ph.D.

Thesis Defense: May 14, 2021

TABLE OF CONTENTS

TABLES AND FIGURES LEGEND

TABLES

CHAPTER 2

CHAPTER 3

FIGURES

SUPPLEMENTAL MATERIAL

TABLES

CHAPTER 2

CHAPTER 3

FIGURES

CHAPTER 2

CHAPTER 3

ABBREVIATION LIST

APC – Absolute percent change

CIA – Chemical Index of Alteration

CIW – Chemical Index of Weathering

LD_i – Limit of Detection

LQ_i – Limit of Quantification

OMC – Optimizing Measuring Conditions

PIA – Plagioclase Index of Alteration

PWI – Product of Weathering Index

QIIME2 – Quantitative Insights Into Microbial Ecology 2

REM – Relative Element Mobility

RR – Ruxton Ratio

STI – Silica-Titania Index

UP – Utuado Pluton

V – Vogt Index

WIP – Weathering Index of Parker

ABSTRACT

The microbial community inhabiting the root-soil contact interface, rhizobiomes, represent a critical link between plant, ecosystems, and geomorphic processes. In landslides where fresh silicate rocks are exposed, rhizobiomes may set in motion several biogeochemical transformations with local to global impacts. Given the prevalence of landslides in humid mountains wordwide and the understudied role of rhizobiomes in these environments, I designed a field study to address two aims: 1) characterize the composition, and function of plant rhizobiomes established in “landslide-like” areas, and 2) evaluate the role of rhizobiomes in (Ca,Mg)-silicate rock weathering through an rock incubation experiement. I found two key results: 1) that the distinctive biotic and abiotic factors between landslides and forests habitats were important in structuring microbial community composition and functioning, and 2) that rock weathering occurrs faster in landslides compared to forest, and that the resulting nutrient mobilization drives microbial diversity and composition.

DEDICATION

A mi madre, Noemi, mi padre, Ernesto y a mis hermanos Tania, Giovanni, Edwin, Christian y Alex. Los amo de aquí al infinito y con la misma intensidad del calor del sol.

ACKNOWLEDGEMENTS

I am thankful to my advisor, Dr. Carla Restrepo, for her patience, compromise, and confidence in me and my committee members Dr. Filipa Godoy, Dr. Zomary Flores and Dr. Riccardo Papa, for their invaluable help.

I would like to acknowledge the contribution other people to this project. Dr. José García Arrarás and Griselle Valentin allowed me to work in their lab and made sure that I always had everything that I needed. Dr. Elvira Cuevas and Larry Diaz, and Dr. Ram Katiyar and William Perez allowed me to use their equipment for chemical analyses of soils and rocks. Dr. Eugenio Santiago and Dr. Stephen Hughes helped with the identification of plants and rocks, respectively. The University of Puerto Rico Sequencing and Genomic Facility of the and its staff, Silvia Planas, and Yadira Ortiz sequenced the biological samples and were willing to answer numerous questions. The Material Characterization Center, and its staff, Maria Cepeda and Christopher Boccheciamp helped with the processing of geological samples. Dr. Lee Taylor and his lab at the University of New Mexico provided primers for fungal analyses. Dr. Abdulmehdi S. Ali and the Earth and Planetary Sciences Department of the University of New Mexico provided training in WDXRF analyses. Dr. Erika Marin-Spiotta and her lab at the University of Wisconsin helped with soil analysis. The University of Puerto Rico's High-Performance Computing facility and its staff, Dr. Humberto Ortiz and Jose Bonilla, provided constant technical support. Dr. Michael McLaren helped understand and analyze data with sequencing batch effects. Last but not least my gratitude goes to Doris and Gladys and their families who allowed me to do field work in their private land, and for making me feel part of their families.

This pioneering work could not have been possible without the financial support received from a number of institutions. I would like to acknowledge the support of the Puerto Rico Louis Stokes – Alliance for Minority Participation (Bridge to Doctorate Program; Grant No. HDR1400870) and the NASA Puerto Rico Space Grant Consortium (Grant No. NNX15AI11H). Their help was pivotal for the advancement of my research. I would also like to thank the Dean of Graduate Students and Research (DEGI) and the Biology Graduate Program of the University of Puerto Rico for their support to share my research results in national and international forums. I am thankful to the American Association for

the Advancement of Science (AAAS)-Caribbean Division and the Puerto Rico Science, Technology and Research Trust for their Hurricane Relief Grants Program, which allowed me to continue my research in the aftermath Hurricane Maria. Finally, support for this project came from on Institutional Development Award (IdeA to CR and FG) from the National Institute of General Medical Sciences of the National Institutes of Health (Grant No. P20 GM103475-14) and the National Science Foundation (NSF-DEB 1556878 to CR). To all of them my deepest gratitude.

Finally, I would also like to thank many people, that served as mentors, mentees, and life companions throughout my graduate life: I am thankful to Diana Delgado and Zuania Colón for their affection, support, and guidance; to Nydia Santiago, Emily Díaz, Ariel Barbosa and Edwin Navarro for allowing me to mentor them and for helping with different aspects of the research; to Alexander Ortiz and Jessica Pita for helping with field work; to Peter Delgado and Michel Alejandro for their love, companionship, and more than anything for their support in day to day life affairs. To all of you, thanks for the good memories and for allowing me to grow as a professional and as a person.

CHAPTER 1: LANDSLIDES: MICROBIALLY-MEDIATED HOTSPOTS OF BIOGEOCHEMICAL ACTIVITY

The rhizobiomes – the microbial community inhabiting the root-soil contact interface – represent a critical link between plant, ecosystems, and geomorphic processes within the critical zone-CZ (Calvaruso et al. 2006, Amundson et al. 2007, Brantley et al. 2007, Calvaruso et al. 2007, Uroz et al. 2011, Gadd 2013, Visioli et al. 2015). Here, rhizobiomes contribute to the decomposition of organic matter and the cycling of nutrients (Ehrenfeld et al. 2005, Bever et al. 2010, Larsen et al. 2015, Jackson et al. 2019) as well as the weathering of soil and rock (Calvaruso et al. 2006, Calvaruso et al. 2007, Turpault et al. 2009), ultimately sustaining ecosystems and life on Earth. In montainous areas, particularly in the tropics with their high weathering rates, the aforementioned links may be particularly important, yet they remain little-studied. In these environments, landsliding exposes fresh rock where rhizobiomes may set in motion several biogeochemical transformations with local to global impacts. Among these, the *weathering* of calcium and magnesium-bearing silicate rocks stand out due to their role in the carbon cycle (Berner 1992, Drever 1994b, Hilley and Porder 2008, Schwartzman 2017, Emberson et al. 2018) (Figure 1). To date, however, a limited number of studies has explored the role of rhizobiomes in rock weathering in these environments.

In mountainous environments underlain by calcium and magnesium-bearing silicate rocks, rhizobiomes may couple *landsliding* and rock weathering and ultimately, the short- and long-term carbon cycles (Fig. 1.1). First, weathering of a number of Ca, Mg-bearing silicate rocks often originates coarse textured soils that increase slope instability (Durgin 1977, Monroe 1979, Larsen and Torres-Sánchez 1996), especially in humid tropical environments (Ruxton and Berry 1957, Matsukura et al. 2007). The work of Guida et al.

(2014) albeit in regions underlain by different rocks, shows that rock weathering is enhanced by soil microorganisms, ultimately influencing landslide probability. Second, landslides expose little weathered substrates where the establishment of plants and their rhizobiomes might help mobilize nutrients, including Ca^{2+} and Mg^{2+}, contributing to the short-term carbon cycle. Third, landslides themselves transport and increase leaching of Ca^{2+} and Mg^{2+}, among other nutrients through streams and rivers to the sea (Berner et al. 1983, Berner and Kothavala 2001, McAdams et al. 2015). In marine ecosystems, these cations participate in further reactions that ultimately translate into the net fixation of CO_2 (Berner et al. 1983, Drever 1994, Berner and Kothavala 2001). Thus, humid steep environments create a feedback loop between landslides and soil production that will promote the exposure and weathering of (Ca, Mg)-silicate rocks, influencing the worldwide carbon cycle.

Indirect evidence for the role of landsliding and rhizobiomes on the mobilization of element nutrients through rock weathering may come from three broad sets of studies. A first set focuses on soil production as a function of rock weathering (Dixon and Riebe 2014). A second set involves mineral weathering experiments to study the role of bacteria and fungi associated to rhizobiomes. The last set encompasses studies of primary succession particularly in humid environments. Ultimately, these studies suggest that landslides may represent hot spots biogeochemical activity mediated by rhizobiomes.

The general processes outlined above are likely to be influenced by anthropogenic activities in gross and subtle ways. At one extreme, road construction and mining can exacerbate the formation of landslides and/or create and maintain "landslide-like" conditions (Molinelli 1984, Larsen and Torres-Sánchez 1996, Wills et al. 2001, Rollerson

et al. 2004, VanBuskirk et al. 2005, Muenchow et al. 2012, Brenning et al. 2015). At the other, deforestation and land use changes, such as agriculture and urbanization, may also increase landsliding (Sajinkumar et al. 2011).

LANDSLIDING AND SOIL PRODUCTION FUNCTIONS

The build-up of soil represents the combined effect of soil production and soil erosion (Dixon and von Blanckenburg 2012). Two existing models describe a negative relationship between soil production or weathering rates with soil thickness (Figure 1.2) (Cox 1980, Heimsath et al. 1997, Dixon and von Blanckenburg 2012, Dixon and Riebe 2014). The exponential and the humped models show that soil production rates are highest at lower and intermediate soil depths, respectively (Figure 1.2).

The above models suggest that landslide activity through its effect on soil depth may strongly influence soil production or rock weathering rates. At the same time, plants colonizing landslides may reduce soil erosion through the stabilizing role of roots and their rhizobiomes (Cammeraat et al. 2005, Walker and Shiels 2008, Tang et al. 2011). Using soil data from a landslide chronosequence in New Zealand (Trustrum and De Rose 1988), I was able to show a humped relationship between soil depth and soil production rates (Fig. 1.3) that further suggests that increased soil production rates at intermediate soil depths may be due to a synergism between environmental effects attributable to shallow soil thickness and the rhizobiomes influence on rock weathering (Figure 1.2).

A few studies have investigated microbial activity associated with weathering of silicate rocks. One set of studies focuses on microbial rock weathering in natural settings, and microbially-mediated dissolution experiments under lab and field conditions (Vuorinen et al. 1981, Bennett et al. 2001, Roberts 2004, Rogers and Bennett 2004, Gleeson et al. 2006). A second set of studies focuses on the effect of microbial metabolism on silicate weathering, particularly the production of organic acids, ligands and biofilms (Welch and Ullman 1993, Rogers et al. 1998, Welch et al. 1999, Kalinowski et al. 2000, Maurice et al. 2001, Welch et al. 2002, Neaman et al. 2006, Uroz et al. 2009b). A last, and at the same time least developed, set of studies have examined microbial rock weathering on whole silicate rocks with its multi-mineral complexity (Song et al. 2007, Wu et al. 2008, Song et al. 2010).

Microbial mineral-weathering have been assessed through *ex-situ* and *in-situ* experiments. *The ex-situ* experiments are very diverse, but central to them is the use of different substrates that are inoculated with different microbes to assess the role of microorganisms on rock weathering. In the batch experiments, the substrate used for the weathering experiment fluctuates from a single granulated or pulverized mineral to a whole silicate rock. On the other hand, the substrate is inoculated with either soil from the study site, specific culturable bacterial species (e.g. *Arthrobacter* spp., *Bacillus* spp., *Burkholderia* spp., *Collimonas* spp., *Janthinobacterium* spp., *Leifsonia* spp., *Polaromonas* spp., *Pseudomonas* spp., and *Streptomyces* spp.), fungal species (*Mucor hiemalis*, *Umbelopsis 19eg19inate19* and *Mortierella alpine*) or microbial exudates (e.g. siderophores and low molecular weight organic acids). Albeit the large variability in

methodologies, the results have been consistent in that the added microorganisms or their exudates increased rock weathering rates from 1.5 to 20 times as shown by the mobilization of Al, Si, Fe, Na, Ca, Mg, K (Vuorinen et al. 1981, Vandevivere et al. 1994b, Barker et al. 1998, Kalinowski et al. 2000, Maurice et al. 2001, Frey et al. 2010, Brunner et al. 2011). Therefore, rhizobiomes could be major contributors of soil production and further weathering of silicate rocks in areas prone to landslides.

The *in-situ* weathering experiments are fewer in number, and have been mostly based on incubation of experiments of crushed rocks or pure minerals that include root exclusion treatments (Quirk et al. 2012, Koele et al. 2014, Kirtzel et al. 2020). These studies have shown that mycorrhizal fungi form tunnels as they contribute to weathering of minerals and rocks. Unfortunately, these studies did not I a budget analyses to estimate rock weathering rates. These studies open two major questions. The first pertains to microorganisms involved in the succession of surfaces where bare rock has been exposed, including their contribution to weathering under natural settings. The second question pertains to root microbes, which have been widely studied, but their role in silicate rock weathering have only began to gain attention (Taylor et al. 2009). There are a number of bare rock surfaces, and among these landslides are the least investigated.

LANDSLIDING AND MICROBIAL PRIMARY SUCCESSION

The contribution of microorganisms to the diversity and functioning of landslides comes from two broad sets of studies that indicate that these bare rock surfaces experience extreme environmental, as well as oligotrophic, conditions (Geertsema and Pojar 2007, Restrepo et al. 2009). The first set of studies focuses on "primary substrates" created from the retreat

of glaciers, the deposition of lava and ash by volcanic activity, sand dunes, and human-made structures such as road cuts, mines, and buildings. These bare surfaces experience extreme UV radiation, temperature and moisture conditions, and lack of readily available nutrients which most likely has determined unique microbial life history strategies (Uroz et al. 2009a, Gadd 2013). On the one hand, microorganisms establishing in these environments need protection against desiccation, temperature fluctuations, and UV radiation. On the other hand, these microorganisms can take advantage of the sunlight as their energy source and the high concentration of rock-derived nutrients "trapped" in these little-weathered substrates. This combination of stressful and disturbed conditions suggests a rich array microbial traits and life-history strategies (Krause et al. 2014).

Traits that may allow microorganisms to colonize open areas that combine high levels of UV radiation, temperature, and desiccation include the production of pigments such as melanin, carotenoids, mycosporines (Gorbushina et al. 2003, Volkmann et al. 2003, Gorbushina et al. 2008), formation of biofilms through the production of exopolymeric substances (Gadd 2007, 2017), and occupation of pores and fissures in rocks to avoid direct exposure (Hoppert et al. 2004, Walker and Pace 2007, Omelon 2008, Gorbushina and Broughton 2009, Gadd 2017). Species among the Actinobacteria, Acidobacteria, Firmicutes and Cyanobacteria phyla, and Betaproteobacteria class are expected to be primary colonizer of landslide-disturbed habitats because they produce biofilms and acidify rock surfaces (Omelon 2008, Olsson-Francis et al. 2012), as well as melanized fungi which can overcome UV radiation (Gorbushina et al. 2003, Gorbushina and Broughton 2009).

A second set of traits involve oligotrophic life-history strategies that improves energy acquisition in low nutrient environments. Microbes growing in primary substrates either obtain energy through the sun (autotrophs that may include photoautotrophs, chemoautotrophs, lithoautotrophs) or through chemical reactions as their energy source (e.g., chemoorganotrophs, chemolithotrophs). Microbes also release nutrients "trapped" in rocks by producing exudates including low molecular weight organic acids, siderophores, and oxidoreductases (Ullman et al. 1996, Warscheid and Braams 2000, Hoppert et al. 2004, Gorbushina 2007, Roeselers et al. 2007, Omelon 2008, Gorbushina and Broughton 2009, Uroz et al. 2009a, Gadd 2017). Species within Verrucomicrobia, Acidobacteria, Basidiomycota and Glomeromycota phyla are known to be associated to oligotrophic environments (Ho et al. 2017), where they thrive with lower concentrations of bioavailable nutrients (Eilers et al. 2010), including soil C (Fierer et al. 2007) and N (Chen et al. 2014, Chen et al. 2016), while degrading recalcitrant compounds (Baldrian 2006). Other species, including various members of the Proteobacteria phyla and zygomyceteous fungi releases a variety of organic acids, including oxalate, citrate and malate to release mineral nutrients (Uroz et al. 2009a, Brunner et al. 2011).

The second set of studies focus directly on landslides. Albeit the increased recognition of the role of microbes on rock weathering in landslides (Emberson et al. 2018), only few studies have characterized microbial communities (Singh et al. 2001, Sparling et al. 2003, Li et al. 2005). The first approach relies on measuring microbial biomass and mycorrhizal inoculum (Singh et al. 2001, Li et al. 2005). The second approach estimated microbial diversity through phospholipid fatty acids measurements (DeGrood et al. 2005). These works have documented reduced microbial inoculum/diversity in landslide or landslide-

like disturbances and that both recover as ecosystems matured. These approaches cannot elucidate the complexity of microbial groups, their contributions to rock weathering and implications on biogeochemical cycles.

Given the prevalence of landslides in humid mountains wordwide and the understudied role of rhizobiomes in these environments, in particular in silicate rock weathering, I designed a field study to address two aims. Chapter 2 focuses on Aim 1 of my thesis to characterize the composition, structure, and function of plant rhizobiomes established in "landslide-like" areas, namely road cuts within an area underlain by (Ca,Mg)-silicate rocks. This field study that to my knowledge, is the first to provide a taxonomic and functional characterization of plant rhizobiomes established in landslide-like areas based on next generation sequencing-NGS. Chapter 3 focuses on Aim 2 to evaluate the role of rhizobiomes in (Ca,Mg)-silicate rock weathering. This "*in situ*" experiment, is also the first to my knowledge that estimates whole-silicate rock weathering rates associated with plant rhizobiomes. Finally, I use Chapter 4 to wrap up my work with an overall conclusion. Studying the role of rhizobiomes in Ca-Mg silicate rock weathering in landslide areas is critical to understand the contribution of microbial communities to the sequestration of carbon at short and long-temporal scales. The composition of rhizobiomes coupled with functional analysis will help us to quantify and understand in more detail the essential processes that enable ecosystem functioning at varying scales, from local to global.

CITED LITERATURE

Amundson, R., D. D. Richter, G. S. Humphreys, E. G. Jobbágy, and J. Gaillardet. 2007. Coupling between biota and earth materials in the Critical Zone. Elements 3:327-332.

Barker, W. W., S. A. Welch, S. Chu, and J. F. Banfield. 1998. Experimental observations of the effects of bacteria on aluminosilicate weathering. American Mineralogist 83:1551-1563.

Bennett, P. C., J. R. Rogers, W. J. Choi, and F. K. Hiebert. 2001. Silicates, silicate weathering, and microbial ecology. Geomicrobiology Journal 18:3-19.

Berner, R. A. 1992. Weathering, plants, and the long-term carbon-cycle. Geochimica Et Cosmochimica Acta 56:3225-3231.

Berner, R. A., and Z. Kothavala. 2001. GEOCARB III: A Revised model of atmospheric CO2. American Journal of Science 301:182-204.

Berner, R. A., A. C. Lasaga, and R. M. Garrels. 1983. The carbonate-silicate geochemical cycle and its effect on atmospheric carbon dioxide over the past 100 million years. American Journal of Science 283:641-685.

Bever, J. D., I. A. Dickie, J. M. Facelli, J. Klironomos, M. Moora, M. C. Rilling, W. D. Stock, M. Tibbett, and M. Zobel. 2010. Rooting theories of plant community ecology in microbial interactions. Trends in Ecology & Evolution 25:468-478.

Brantley, S. L., M. B. Goldhaber, and K. Vala Ragnarsdottlr. 2007. Crossing disciplines and scales to understand the Critical Zone. Elements 3:307-314.

Brenning, A., M. Schwinn, A. P. Ruiz-Páez, and J. Muenchow. 2015. Landslide susceptibility near highways is increased by 1 order of magnitude in the Andes of southern Ecuador, Loja province. Nat. Hazards Earth Syst. Sci. 15:45-57.

Brunner, I., M. Plotze, S. Rieder, A. Zumsteg, G. Furrer, and B. Frey. 2011. Pioneering fungi I Damma glacier forefield in the Swiss Alps can promote granite weathering. Geobiology 9:266-279.

Calvaruso, C., M.-P. Turpault, E. Leclerc, and P. Frey-Klett. 2007. Impact of ectomycorrhizosphere on the functional diversity of soil bacterial and fungal communities from a forest stand in relation to nutrient mobilization processes. Pages 567-577. Microbial Ecology.

Calvaruso, C., M. P. Turpault, and P. Frey-Klett. 2006. Root-associated bacteria contribute to mineral weathering and to mineral nutrition in trees: A budgeting analysis. Applied and Environmental Microbiology 72:1258-1266.

Cammeraat, E., R. van Beek, and A. Kooijman. 2005. Vegetation succession and its consequences for slope stability in SE Spain. Plant and Soil 278:135-147.

Cox, N. J. 1980. On the relationship between bedrock lowering ans regolith thickness. Earth Surface Processes 5:271-274.

Dalling, J. W., and E. V. J. Tanner. 1995. An experimental study of regeneration on landslides in Montane Rain Forest in Jamaica. Journal of Ecology 83:55-64.

DeGrood, S. H., V. P. Claassen, and K. M. Scow. 2005. Microbial community composition on native and drastically disturbed serpentine soils. Soil Biology & Biochemistry 37:1427–1435.

Dixon, J. L., and C. S. Riebe. 2014. Tracing and pacing soil across slopes. Elements 10:363-368.

Dixon, J. L., and F. von Blanckenburg. 2012. Soils as pacemakers and limiters of global silicate weathering. Comptes Rendus Geoscience:597–609.

Drever, J. I. 1994. The effect of land plants on weathering rates of silicate minerals. Geochimica et Cosmochimica Acta 58:2325-2332.

Durgin, P. B. 1977. Landslides and the weathering of granitic rocks. Reviews in Engineering Geology 3:127-131.

Ehrenfeld, J. G., B. Ravit, and K. Elgersma. 2005. Feedback in the plant-soil system. Annu. Rev. Environ. Resour. 30:75-115.

Emberson, R., A. Galy, and N. Hovius. 2018. Weathering of reactive mineral phases in landslides acts as a source of carbon dioxide in mountain belts. JGR Earth Surface 123:2695-2713.

Frey, B., S. R. Rieder, I. Brunner, M. Plotze, S. Koetzsch, A. Lapanje, H. Brandl, and G. Furrer. 2010. Weathering-associated bacteria from the Damma Glacier forefield: Physiological capabilities and impact on granite dissolution. Applied and Environmental Microbiology 76:4788-4796.

Gadd, G. M. 2013. Microbial roles in mineral transformations and metal cycling in the Earth's Critical Zone. Pages 115–165 in J. Xu and D. L. Sparks, editors. Molecular Environmental Soil Science. Springer Netherlands.

Gadd, G. M. 2017. Geomicrobiology of the built environment. Nature Microbiology 2:1-9.

Geertsema, M., and J. J. Pojar. 2007. Influence of landslides on biophysical diversity — A perspective from British Columbia. Geomorphology 89:55-69.

Gleeson, D. B., N. M. Kennedy, N. Clipson, K. Melville, G. M. Gadd, and F. P. McDermott. 2006. Characterization of bacterial community structure on a weathered pegmatitic granite. Microbial Ecology 51:526-534.

Gorbushina, A. A. 2007. Life on the rocks. Environmental Microbiology 9:1613-1631.

Gorbushina, A. A., and W. J. Broughton. 2009. Microbiology of the atmosphere-rock interface: How biological interactions and physical stresses modulate a sophisticated microbial ecosystem.431-450.

Gorbushina, A. A., and G. M. Gadd. 2006. Fungal activities in subaerial rock-inhabiting microbial communities. Pages 267-288 Fungi in Biogeochemical Cycles.

Gorbushina, A. A., E. R. Kotlova, and O. A. Sherstneva. 2008. Cellular responses of microcolonial rock fungi to long-term desiccation and subsequent rehydration. Stud Mycol 61:91-97.

Gorbushina, A. A., K. Whitehead, T. Dornieden, A. Niesse, A. Schulte, and J. I. Hedges. 2003. Black fungal colonies as units of survival: hyphal mycosporines synthesized by rock-dwelling microcolonial fungi. Canadian Journal of Botany 81:131-138.

Heimsath, A. M., W. E. Dietrich, K. Nishiizumi, and R. C. Finkel. 1997. The soil production function and landscape equilibrium. Nature 388:358-361.

Hilley, G. E., and S. Porder. 2008. A framework for predicting global silicate weathering and CO2 drawdown rates over geologic time-scales. PNAS 105:16855-16859.

Hoppert, M., C. Flies, W. Pohl, B. Gunzl, and J. Schneider. 2004. Colonization strategies of lithobiontic microorganisms on carbonate rocks. Environmental Geology 46:421-428.

Jackson, O., R. S. Quilliam, A. Stott, H. Grant, and S. J. A. 2019. Rhizosphere carbon supply accelerates soil organic matter decomposition in the presence of fresh organic substrates. Plant and Soil 440:473-490.

Kalinowski, B. E., L. J. Liermann, S. Givens, and S. L. Brantley. 2000. Rates of bacteria-promoted solubilization of Fe from minerals: a review of problems and approaches Chemical Geology 169:357-370.

Koele, N., I. A. Dickie, J. D. Blum, J. D. Gleason, and L. de Graaf. 2014. Ecological significance of mineral weathering in ectomycorrhizal and arbuscular mycorrhizal ecosystems from a field-based comparison. Soil Biology & Biochemistry 69:63-70.

Larsen, J., P. Jaramillo-López, M. Nájera-Rincón, and C. E. Gonzaléz-Esquivel. 2015. Biotic interactions in the rhizosphere in relation to plant and soil nutrient dynamics. Journal of Soil Science and Plant Nutrition 15:449-463.

Larsen, M. C., and A. J. Torres-Sánchez. 1996. Geographic relations of landslide Distribution and assessment of landslide hazards in the Blanco, Cibuco, and Coamo basins, Puerto Rico. U.S. Geological Survey, San Juan, Puerto Rico.

Li, Y., H. Ruan, X. Zou, and R. W. Myster. 2005. Response of major soil decomposers to landslide disturbance in a Puerto Rican rainforest. Soil Science 170:202-211.

Matsukura, Y., T. Hattanji, C. T. Oguchi, and T. Hirose. 2007. Ten year measurements of weathering rates of rock tablets on a forested hillslope in a humid temperate region, Japan. Z. Geomorph. N. F. 51:27-40.

Maurice, P. A., M. A. Vierkorn, L. E. Hersman, and J. E. Fulghum. 2001. Dissolution of well and poorly ordered kaolinites by an aerobic bacterium. Chemical Geology 180:81-97.

McAdams, B. C., A. M. Trierweiler, S. A. Welch, C. Restrepo, and A. E. Carey. 2015. Two sides to every range: Orographic influences on CO2 consumption by silicate weathering. Applied Geochemistry 63:472-483.

McNamara, C. J., T. D. t. Perry, K. A. Bearce, G. Hernandez-Duque, and R. Mitchell. 2006. Epilithic and endolithic bacterial communities in limestone from a Maya archaeological site. Microbial Ecology 51:51-64.

Molinelli, J. A. 1984. Geomorphic processes along the Autopista Las Americas in north central Puerto Rico Implications for highway construction, design, and maintenance. Clark University, Ann Monroe, Michigan.

Monroe, W. H. 1979. Map showing landslides and areas of susceptibility to landsliding in Puerto Rico. Department of the Interior, U.S. Geological Survey:Map I-1148.

Muenchow, J., A. Brenning, and M. Richter. 2012. Geomorphic process rates of landslides along a humidity gradient in the tropical Andes. Geomorphology 139 – 140:271-284.

Neaman, A., J. Chorover, and S. L. Brantley. 2006. Effects of organic ligands on granite dissolution in batch experiments at pH 6. American Journal of Science 306:451-473.

Olsson-Francis, K., A. E. Simpson, D. Wolff-Boenisch, and C. S. Cockell. 2012. The effect of rock composition on cyanobacterial weathering of crystalline basalt and rhyolite. Geobiology 10:434-444.

Omelon, C. R. 2008. Endolithic microbial communities in Polar Desert habitats. Geomicrobiology Journal 25:404-414.

Quirk, J., D. J. Beerling, S. A. Banwart, G. Kakonyi, M. E. Romero-Gonzalez, and J. R. Leake. 2012. Evolution of trees and mycorrhizal fungi intensifies silicate mineral weathering. Biology Letters 8:1006-1011.

Restrepo, C., L. R. Walker, A. B. Shiels, R. Bussmann, L. Claessens, S. Fisch, P. Lozano, G. Negi, L. Paolini, G. Poveda, C. Ramos-Scharrón, M. Richter, and E. Velázquez. 2009. Landsliding and its multiscale influence on mountainscapes. BioScience 59:685-698.

Roberts, J. A. 2004. Inhibition and enhancement of microbial surface colonization: the role of silicate composition. Chemical Geology 212:313-327.

Roeselers, G., M. C. van Loosdrecht, and G. Muyzer. 2007. Heterotrophic pioneers facilitate phototrophic biofilm development. Microbial Ecology 54:578-585.

Rogers, J. R., and P. C. Bennett. 2004. Mineral stimulation of subsurface microorganisms: release of limiting nutrients from silicates. Chemical Geology 203:91-108.

Rogers, J. R., P. C. Bennett, and W. J. Choi. 1998. Feldspars as source of nutrients for microorganisms. American Mineralogist 83:1532-1540.

Rollerson, T., D. Maynard, S. Higman, and E. Ortmayr. 2004. Klanawa landslide hazard mapping pilot project. Pages 1-24 oint Conference of IUFRO 3.06 Forest Operations under Mountainous Conditions and the 12th International Mountain Logging Conference, Vancouver B.C.

Ruxton, B. P., and L. Berry. 1957. The weathering of granite and associated erosional features in Hong Kong. Bulletin of the Geological Society of America 68:1263-1292.

Sajinkumar, K. S., S. Anbazhagan, A. P. Pradeepkumar, and V. R. Rani. 2011. Weathering and landslide occurrences in parts of Western Ghats, Kerala. Geological Society of India 78:249-257.

Schwartzman, D. W. 2017. Life's critical role in the long-term carbon cycle: the biotic enhancement of weathering. AIMS Geosciences 3:216-238.

Singh, K. P., T. N. Mandal, and S. K. Tripathi. 2001. Patterns of restoration of soil physicochemical properties and microbial biomass in different landslide sites in the sal forest ecosystem of Nepal Himalaya. Ecological Engineering 17:385-401.

Song, W., N. Ogawa, C. T. Oguchi, T. Hatta, and Y. Matsukura. 2007. Effect of Bacillus subtilis on granite weathering: A laboratory experiment. Catena 70:275-281.

Song, W., N. Ogawa, C. Takashima-Oguchi, T. Hatta, and Y. Matsukura. 2010. Laboratory experiments on bacterial weathering of granite and its constituent minerals. Géomorphologie: relief, processus, environnement 16:327-336.

Sparling, G., G. Ross, N. Trustrum, G. Arnold, A. West, T. Speir, and L. Schipper. 2003. Recovery of topsoil characteristics after landslip erosion in dry hill country of New Zealand, and a test of the space-for-time hypothesis. Soil Biology and Biochemistry 35:1575-1586.

Tang, J., Y. Mo, J. Zhang, and R. Zhang. 2011. Influence of biological aggregating agents associated with microbial population on soil aggregate stability. Applied Soil Ecology 47:153-159.

Taylor, L. L., J. R. Leake, J. Quirk, K. Hardy, S. A. Banwart, and D. J. Beerling. 2009. Biological weathering and the long-term carbon cycle: integrating mycorrhizal evolution and function into the current paradigm. Geobiology 7:171-191.

Trustrum, N. A., and R. C. De Rose. 1988. Soil depth-age relationship of landslides on deforested hillslopes, Taranaki, New Zealand. Geomorphology 1:143-160.

Turpault, M. P., C. Nys, and C. Calvaruso. 2009. Rhizosphere impact on the dissolution of test minerals in a forest ecosystem. Geoderma 153:147-154.

Ullman, W. J., D. L. Kirchman, S. A. Welch, and P. Vandevivere. 1996. Laboratory evidence for microbially mediated silicate mineral dissolution in nature. Chemical Geology 132:11-17.

Uroz, S., C. Calvaruso, M.-P. Turpault, and P. Frey-Klett. 2009a. Mineral weathering by bacteria: ecology, actors and mechanisms. Trends in Microbiology 17:378-387.

Uroz, S., C. Calvaruso, M. P. Turpault, A. Sarniguet, W. de Boer, J. H. J. Leveau, and P. Frey-Klett. 2009b. Efficient mineral weathering is a distinctive functional trait of the bacterial genus Collimonas. Soil Biology and Biochemistry 41:2178-2186.

Uroz, S., P. Oger, C. Lepleux, C. Collignon, P. Frey-Klett, and M.-P. Turpault. 2011. Bacterial weathering and its contribution to nutrient cycling in temperate forest ecosystems. Research in Microbiology 162:820-831.

VanBuskirk, C. D., R. J. Neden, J. W. Schwab, and F. R. Fsmith. 2005. Road and terrain attributes of road fill landslides in the Kalum Forest District. B.C. Ministry of Forests and Range, Province of British Columbia.

Vandevivere, P., S. A. Welch, W. J. Ullman, and D. L. Kirchman. 1994. Enhanced dissolution of silicate minerals by bacteria at near-neutral pH. Microb Ecol 27:241-251.

Visioli, G., S. D'Egidio, and A. M. Sanangelantoni. 2015. The bacterial rhizobiome of hyperaccumulators: future perspectives based on omics analysis and advanced microscopy. Frontiers in Plant Science 5:1-12.

Vuorinen, A., S. Mantere-Alhonen, R. Uusinoka, and P. Alhonen. 1981. Bacterial weathering of rapakivi granite. Geomicrobiology Journal 2:317-325.

Walker, J. J., and N. R. Pace. 2007. Endolithic microbial ecosystems. Annu Rev Microbiol 61:331-347.

Walker, L. R., and A. B. Shiels. 2008. Post-disturbance erosion impacts carbon fluxes and plant succession on recent tropical landslides Plant Soil 313:205-216.

Warscheid, T., and J. Braams. 2000. Biodeterioration of stone: a review. International Biodeterioration & Biodegradation 46:343-368.

Welch, S. A., W. W. Barker, and J. F. Banfield. 1999. Microbial extracellular polysaccharides and plagioclase dissolution. Geochimica Et Cosmochimica Acta 63:1405-1419.

Welch, S. A., A. E. Taunton, and J. F. Banfield. 2002. Effect of microorganisms and microbial metabolites on apatite dissolution. Geomicrobiology Journal 19:343-367.

Welch, S. A., and W. J. Ullman. 1993. The effect of organic acids on plagioclase dissolution rates and stoichiometry. Geochimica Et Cosmochimica Acta 57:2725-2736.

Wills, C. J., M. W. Manson, K. D. Brown, C. W. Davenport, and C. J. Domrose. 2001. Landslides in the Highway 1 corridor: Geology and slope stability along the Big Sur coast between Point Lobos and San Carpoforo Creek, Monterey and San Luis Obispo counties, California. California Department of Transportation.

Wu, L., A. D. Jacobson, and M. Hausner. 2008. Characterization of elemental release during microbe–granite interactions at T=28°C. Geochimica Et Cosmochimica Acta 72:1076-1095.

Zumsteg, A., J. Luster, H. Göransson, R. H. Smittenberg, I. Brunner, S. M. Bernasconi, J. Zeyer, and B. Frey. 2012. Bacterial, archaeal and fungal succession in the forefield of a receding glacier. Microbial Ecology 63:552-564.

FIGURES

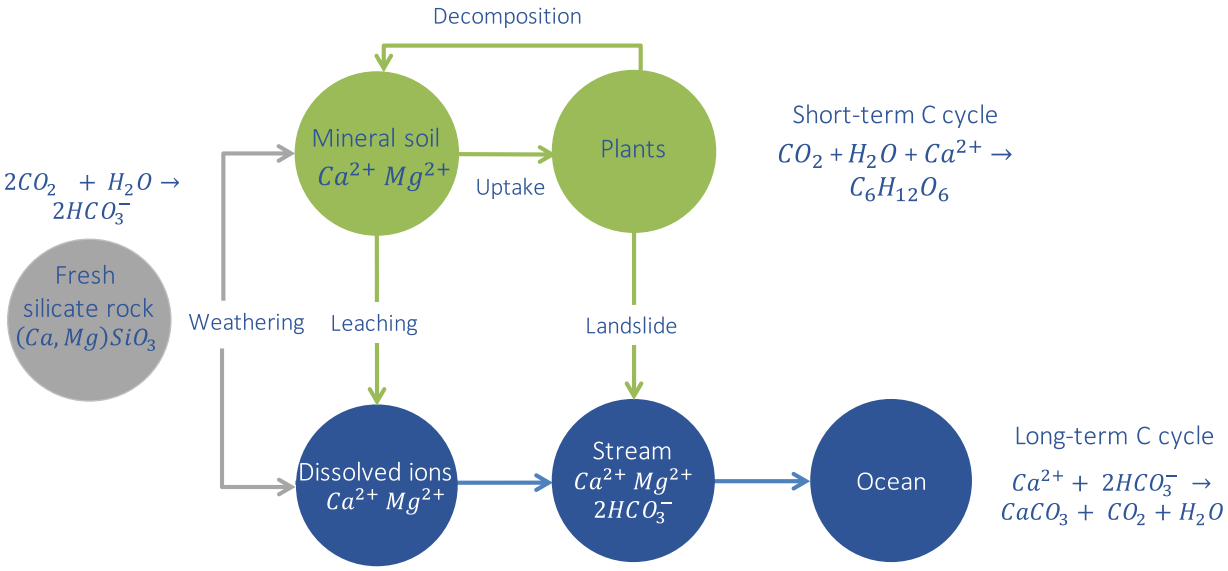

Figure 1.1. Conceptual model linking the weathering of silicate rocks (gray) to the short- (green) and long-term (blue) carbon cycles. Rhizobiomes may contribute to the weathering of silicate rocks. Weathering of Ca and Mg-silicate rocks contribute to the release of Ca^{2+} and Mg^{2+} cations. These cations can either be used by plants, contributing to the short-term carbon cycle, or subsequently leached and transported through streams and rivers to the sea (Berner et al. 1983, Berner and Kothavala 2001). In marine ecosystems, these cations participate in further reactions that ultimately translate into the net fixation of CO_2 (Berner et al. 1983, Drever 1994a, Berner and Kothavala 2001). Microbial contribution to the long-term carbon cycle may represent the missing CO_2 sink (Gorbushina and Krumbein 2005).

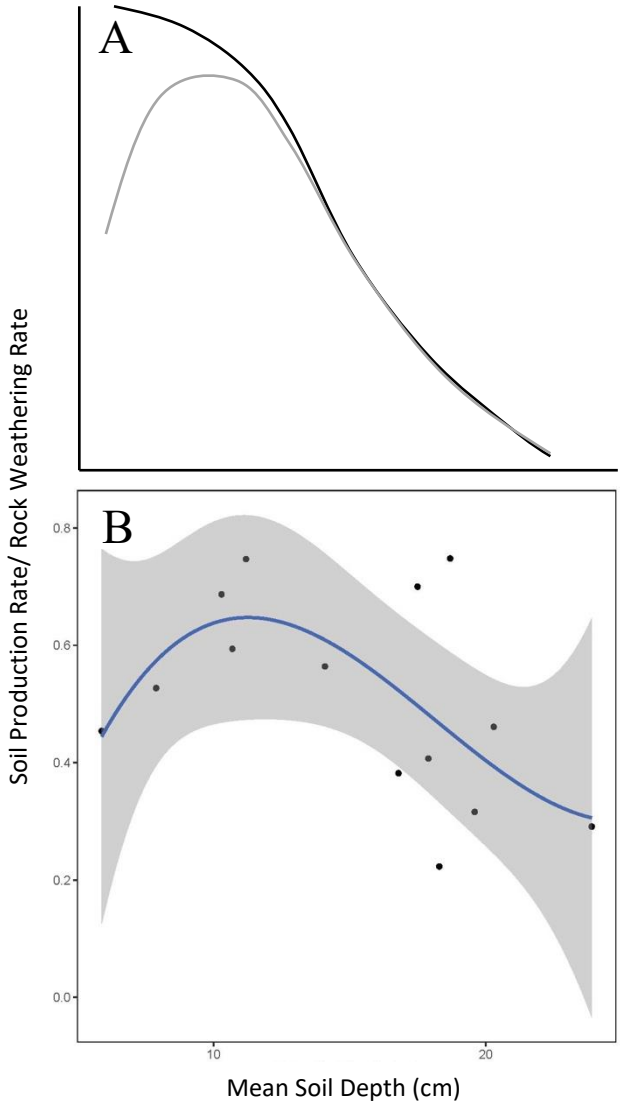

Figure 1.2. Soil production models as a function of soil depth. **A)** Two hypothetical soil production models, a function of the soil-saprolite interface depth, the exponential (black line) and the humped (grey line). **B)** Data from a landslide chronosequence in New Zealand (Trustrum and De Rose 1988) was plotted and fitted through a polynimial function. The resulting model resembled the humped soil production model.

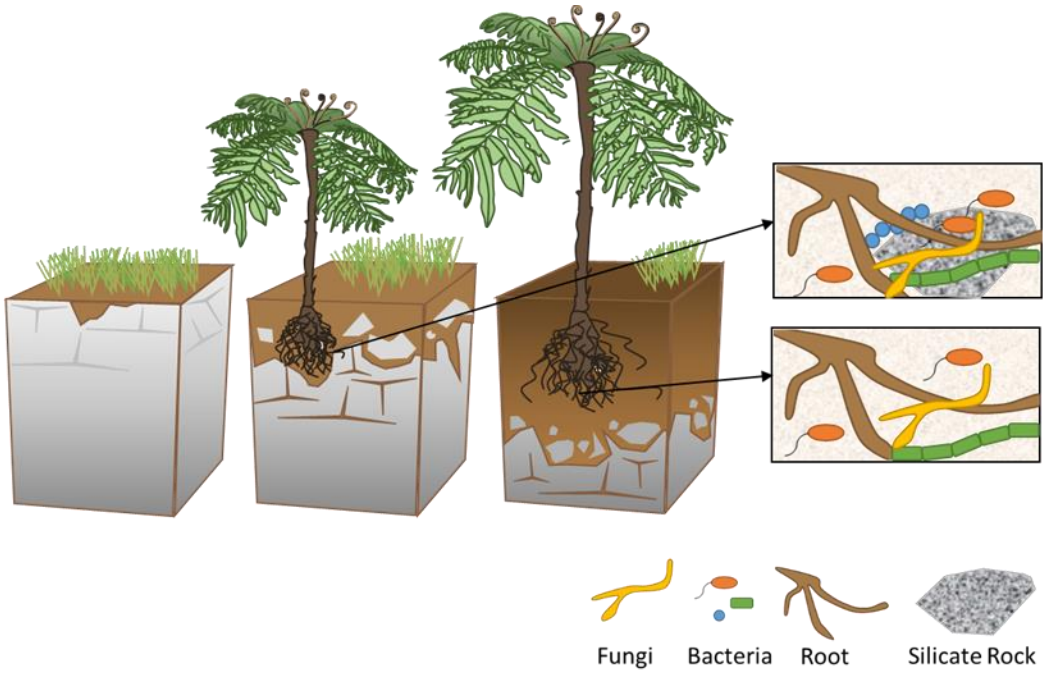

Figure 1.3. The rhizobiome-rock interface. Rhizobiomes of plants growing in landslides areas are in close contact with little weathered silicate rock. Under this case scenario, rhizobiomes might accelerate silicates rock weathering through the production of exudates. After the rhizobiome is no longer in contact with the silicate rock, the rock weathering rates might halt as shown in the Humped soil production model.

CHAPTER II: LANDSLIDING AND SILICATE ROCK WEATHERING INFLUENCE THE TAXONOMIC AND FUNCTIONAL COMPOSITION OF SOIL MICROBIOMES

INTRODUCTION

In areas where *primary* substrates have been exposed, complex interactions between the substrate, plants, and associated microorganisms are likely to yield hotspots of biogeochemical activity. Plant roots were originally postulated as the main contributors to this activity in areas underlain by silicate rocks (Berner 1992, Beerling and Berner 2005). Today, however, it is known that plant roots host diverse microbial communities – the rhizobiome – and that both bacteria (Leyval and Berthelin 1991, Calvaruso et al. 2006, Balogh-Brunstad et al. 2008, Uroz et al. 2009a, Quirk et al. 2012) and mycorrhizal fungi (Leake et al. 2008a, Koele et al. 2009, Taylor et al. 2009, Bonneville et al. 2011, Smits et al. 2012, Koele et al. 2014) play a critical role in soil formation, rock weathering and nutrient mobilization. One environment in which rhizobiomes may set in motion important biogeochemical transformations includes humid mountains, particularly those underlain by (Ca,Mg)-silicate rocks. In these environments, landslides expose slightly weathered substrates that are subjected to rhizobiome activity (Chapter 1). To date, however, little is known about the structure, composition, and functioning of rhizobiomes in landslides, including their role in rock weathering.

In areas undergoing primary or quasi-primary succession, abiotic and biotic factors influence soil microbial composition and their ecological function over time. In areas affected by landslides these abiotic factors include soil nutritional status and water retention, as well UV radiation and extreme temperatures fluctuations. Altogether, these abiotic factors affect microbial communities by selecting for microbes with oligotrophic life history strategies that allow them to thrive in ruderal and stressful conditions (Fierer et al. 2007, Krause et al. 2014). Among the traits needed to thrive in primary succession

habitats are the production of organic acids, siderophores and other exudates that weather rock and release nutrients (Kalinowski et al. 2000, Frey et al. 2010, Štyriaková et al. 2012, Schulz et al. 2013). Landsliding is known to affect microbial diversity and biomass, both of which have been found to increase as soil matures (Singh et al. 2001, DeGrood et al. 2005).

Biotic factors also influence microbial communities in areas undergoing primary succession. The presence of potential plant hosts with their root systems can affect microbial community composition. Yet, plant phylogeny and lifeform can further influence microbial communities in ways that suggest reciprocal feedbacks (Knelman et al. 2012, Yeoh et al. 2017). On the one hand, plant host phylogeny has been found to significantly alter rhizosphere microbial community composition (Edwards et al. 2015, Peiffer et al. 2015, Emmett et al. 2017, Yeoh et al. 2017), although this is not always true (Wagner et al. 2016). On the other hand, plant host lifeform can exert a distinct physico-chemical root conditions that alter soil nutrient mobility and rhizobiomes composition (Fu et al. 2020). Thus, as rock-derived nutrients are exchanged for carbon-rich root exudates with the plant (Grayston et al. 1996, Banfield et al. 1999, van Scholl et al. 2008, Lambers et al. 2009, Taylor et al. 2009, Uroz et al. 2011), rhizobiomes diverge from bulk soil microbial communities (Mendes et al. 2014). Plant roots creates metabolic hotspots that enable microbial growth and shape the microbial composition of the rhizobiome (Augusto et al. 2000, Turpault et al. 2009, Uroz et al. 2009a).

Here I focus on "landslide-like" areas underlain by Ca,Mg-silicate rocks to characterize the taxonomic and functional diversity of microbiomes using a metagenomics approach. Focusing on landslide-like and forest habitats, I 1) describe nutrient and weathering status

of soils, 2) characterize taxonomic microbial composition of rhizobiomes and bulk soil as a function of plant host, and 3) characterize microbial functional traits. I hypothesize that (1) species richness and composition will vary with habitat, microhabitats and plant host, and that (2) rhizobiomes of landslide-like habitat will have indicator species that enhances rock weathering. To our knowledge, this is the first research that characterizes the rhizobiomes of landslides or landslide-like habitats.

METHODS

STUDY AREA

This study took place in the vicinity of Cerro Punta, in the Central Mountain Range of Puerto Rico (centroid of sampling locations: 18° 9′ 55.44″ N, 66° 36′ 10.08″ W; mean elevation: 1060 m a.s.l.; Figure 2.1), a region classified as lower montane subtropical wet forest (Ewel and Whitmore 1973). The dominant land cover in the immediate surroundings of the study sites includes old growth forest interspersed with secondary forests of various ages, small shaded coffee plantations, and pastures. A primary road (PR-143) traverses the region in an E-W direction, and numerous secondary and tertiary roads run perpendicular from it. Most of these high elevation sites are within or adjacent to the Toro Negro State Forest.

This region is underlain by the Utuado pluton-UP (76 to 69 Mya,) the second largest reservoir of intrusive igneous rocks in Puerto Rico (Chen 1967). The UP is composed mainly of granodiorite (65%) and diorite (~32%). The UP granodiorite has high concentrations of plagioclase minerals, including Ca and Mg (Table S2.1) (Chen 1967, Smith et al. 1998). A combination of elevated mean annual precipitation (2560 mm) and

mean annual temperature (20.7 °C) (Weaver 1979, Birdsey and Jiménez 1985), creates ideal conditions for high chemical (Durgin 1977, Monroe 1979) and physical (Halsey et al. 1998) weathering activity, that together with historical forest clearing, hurricanes and earthquakes have a high potential for landsliding (Hughes and Schulz 2020, Lopez et al. 2020), that ultimately can contribute sediments to the stream network.

SAMPLING DESIGN

My sampling design included four main factors that can potentially influence microbial communities in areas subjected to landsliding: habitat ("landslide-like" and forest), microhabitat (rhizosphere and bulk soil), host plant life form (herbaceous ferns, tree ferns, and shrubs), host plant species (Table 2.1). In January of 2016, I identified two areas centered around Km 14.5 (Site 1 or "casa Doris") and Km 13 (Site 2 or "casa Gladys") of PR-143. In each site I identified a "landslide-like" habitat that was paired with a nearby "old-growth" forest habitat [Site 1: Landslide-like (18° 9′ 55.85″ N, 66° 36′ 19.14″ W) and forest (18° 10′ 4.69″ N, 66° 36′ 17.68″ W); Site 2: Landslide-like (18° 9′ 50.30″ N, 66° 36′ 1.93″ W) and forest (18° 9′ 51.93″ N, 66° 36′ 2.51″ W)] for a total of four areas (Figure 2.1). The "landslide-like" habitats represented road cuts created during the construction of PR-143 roughly 45 years ago. A combination of factors, including road maintenance and landslides, has kept the vegetation at these sites in early stages of succession, i.e. dominated by herbaceous plants, shrubs, and tree ferns (Birdsey and Jimenez 1985). Many of these species are known to colonize landslides in the Caribbean, and more broadly speaking the Neotropics (Ewel and Whitmore 1973, Sugden et al. 1985, Guariguata 1990, Walker 1994, Li et al. 2005, Keddy 2007, Judd and Ionta 2013).

At each site per habitat, I focused on three life forms and four plant morpho-species (one herbaceous fern, one tree fern, and two shrubs; Table 2.1) trying when possible to match species between habitats. Subsequent identification of the plants revealed that some morpho-species included >1 species. Nevertheless, in all but one case (shrub 2 for forest), I was unable to match species that were phylogenetically close (Table 2.1). For example, herbaceous ferns in the landslide-like habitats were represented by two species of Gleicheniaceae [*Gleichenia bifida* (Site 1) and *Dicranopteris pectinata* (Site 2)]. Similarly, the tree ferns were represented by two species of *Cyathea* [*Cyathea arborea* in landslide-like and *Cyathea pungens* in forest habitats]. The only case in which species were not phylogenetically close between sites corresponded to Shrub 2 of forests habitats due to the misidentification of plants in the field.

For each morpho-species at any given site I identified two individuals (each individual represents a sampling unit) and for each I collected 1) one sample of bulk soil to characterize soil properties and 2) three samples of roots and paired bulk soils ("biological replicates") to characterize microbial communities. The first set of soil samples were collected one meter away from the base of each plant: after removing the litter I used a 1.9 cm diameter soil corer to collect soil down to 10 cm. The second set of soil samples (paired bulk soils) were collected one meter away from the base of each plant following the procedure described above. In addition, I used a shovel to expose and collect root segments with attached soil. These soil samples for the microbial studies were immediately stored in 25 mL Eppendorf tubes filled with 25 mL of phosphate buffered saline (PBS) solution with 10% glycerol and placed in dry ice for a period < 36 hours. Once in the laboratory I stored the samples at -80 ºC until further processing.

SOIL ANALYTICAL METHODS

The bulk soil samples for chemical characterization were air-dried, and the soil aggregates were pulverized using a mortar and pestle. Afterwards the soils were sieved through a 10- (2 mm) and 100- (150 µm) mesh to remove rocks and roots and homogenize the soils. A first subsample of soil was used for C and N concentrations, and $\delta^{13}C$, $\delta^{15}N$ isotope analyses. The C and N analyses were performed at Erika Marin-Spiotta's Lab at the University of Wisconsin-Madison whereas the C and N isotope analyses at the UC-Davis Stable Isotope Facility. A second subsample of soils were processed further to estimate their elemental composition via Wavelength Dispersive X-Ray Fluorescence (WDXRF) spectrometer at the University of Puerto Rico-Rio Piedras (Ram Katiyar's Lab). First the soil samples were air dried and weighted. Then, these soil samples were sieved through a 230-mesh (63 µm), oven-dried (110 °C) for 12 hrs (Mori et al. 1999, Burke et al. 2009), and pulverized using a stainless-steel Retsch® ball mill at 17 rpm and sieved using a 270-mesh to obtain a 53 µm powdered soil (Markowicz et al. 1997).

The pulverized soil samples were turned into pressed pellets. I weighed 0.9 (± 0.0001) g of powdered soil to which I added 0.1 (± 0.0001) g of SpectroBlend wax binder from Chemplex® (Markowicz et al. 1997, Mori et al. 1999). This mixture was placed in a stainless-steel sample holder (without the stainless-steel balls) in a Retsch® ball mill for 6 min at 17 rpm (Demir et al. 2006). Subsequently I transferred the soil-binder mixture to a 13 mm tungsten carbide pellet die set and applied 3.5 tons of hydraulic pressure for 3 min in a Carver® Bench Top Standard press. The pressed pellets had 0.7534 g/cm^2 of weight thickness. All samples were stored in a desiccator prior to their analysis.

I ran quantitative analyses on the press pellets using a RIGAKU ZSX Primus II WDXRF spectrometer coupled to the ZSX software (Version 7.07). I used 13 rock and two soil reference materials and the ZSX software to generate calibration curves for each element with > 3 reference materials with certified values (Table S2.2). I used the empirical method (EMP) for matrix correction of all analyzed elements (Matsunami et al. 2010). In the Optimizing Measuring Conditions phase (OMC), I analyzed each element on each reference materials and manually selected the location of the highest intensity peak (I_P degree) for each element, provided background signal boundaries (I_{BG} degree), adjusted measuring time (s) and PHA range (Table S2.3). All samples, including the reference materials were analyzed under the conditions listed in Table S2.3. Every 6 measurements of samples with unknown concentration were followed by two analyses of SDC-1 reference material.

To assess the quality of the WDXRF analytical measurements, as well as the precision and accuracy and drifting detection, I estimated three quality indicators for each analyte. The first indicator is the Instrument Limit of Detection (ILD_i), that uses information from the calibration curve (Rousseau 2001):

$$ILD_i = (4.65\ x\ C_i/I_P - I_{BG})\ x\ \sqrt{I_{BG}/T_{BG}}\ \ [eq\ 1]$$

where C_i is the analyte concentration, I_P is the analyte peak intensity, I_{BG} is the background intensity, and T_{BG} is the background counting time or half of the total measuring time for the analyte. The ILD_i is a *theoretical* estimation of smallest concentration of the analyte that can be detected from the background signal (Rousseau 2001). The other two quality indicators are the Relative Standard Deviation (RSD) and the Relative Bias (Qi), which are related to measurements precision and accuracy, respectively (Marguí 2013).

$$RSD(\%) = SD/\overline{C_i}\ x\ 100 \quad [eq\ 2]$$

$$Q_i(\%) = |C_i - C_{cert}|/\ C_i\ x\ 100 \quad [eq\ 3]$$

where, *SD* is the analyte standard deviation, $\overline{C_i}$ is the analyte mean concentration and C_{cert} is the certified value of the analyte in the reference material SDC-1. The analyte values for Eq 2 and 3 are from the repeated analysis of SDC-1 reference material. All the quality indicator results are in Table S2.4.

DNA EXTRACTION, PCR AMPLIFICATION, SEQUENCING, AND BIOINFORMATICS

The bulk soil and root samples were allowed to slightly thaw within a week of soil sampling and to each 25 mL Eppendorf tube I added 12.5 μL of detergent polysorbate 20 (Tween 20) and subsequently placed them in a shaker (240 rpm) for 20 min (Ortiz et al. 2020). I removed the roots from the 25 mL tubes, and both the root-free rhizosphere and bulk soil samples were centrifuged at 4 ºC for 40 min at 4000 rpm. I discarded the supernatant of all samples and stored the soil at -80 ºC until further processing. To extract genomic DNA from each sample I used the PowerSoil™ DNA Isolation Kit (MO BIO Laboratories, Carlsbad, CA, United States) and followed their instructions.

I amplified and sequenced the *16SrRNA* V3-V4 region (*16S*) and *Internal Transcribed Spacer-2* (*ITS-2*) region following Illumina's 16S Metagenomic Sequencing Library Preparation protocol with some modifications. Prior to amplification of each sample, I measured gDNA concentrations using QuantiFluor (dsDNA system) kit with the Promega platform. I used the 16S-515F and 16S-805R and 5.8-Fun and ITS4-Fun primers with Illumina adapters to amplify the *16S* (Caporaso et al. 2011) and *ITS2* (Taylor et al. 2016) regions, respectively. I used slightly different parameters to amplify the *16S* and *ITS2*

regions. For the 16S, I ran the PCRs for each rhizosphere and bulk soil replicates using 12.5 ng of genomic DNA, 0.5 μL of each primer (10 μM), 12.5 μL of 2x KAPA HiFi HotStart ReadyMix and subsequently filled with PCR water until reaching a 25 μL reaction mixture. The thermocycling conditions were: initial denaturing at 95 °C for 3 min, followed by 25 cycles of denaturation at 95 °C for 30 s, 55 °C for 30 s, 72 °C for 30 s, and a final extension at 72 °C for 5 min (Eppendorf Mastercycler Nexus). To verify the amplicon size, I ran 1 μL of the PCR product on an Agilent 2100 Bioanalyzer (Bioanalyzer DNA 1000 chip).

For the *ITS*, I ran the PCRs for each rhizosphere and bulk soil replicate using 10 ng of genomic DNA, 0.25 μL of each primer (25 μM), 0.25 μL of Phusion® High-Fidelity DNA Polymerase, 5 μL of Phusion HF Buffer (5X), 0.5 μL of dNTPs (10 mM), 0.75 μL of DMSO, and subsequently filled with PCR water until reaching a 21 μL reaction mixture. The thermocycling conditions used for the *ITS2* samples were: initial denaturing at 96°C for 2 min, followed by 27 cycles of denaturation at 94 °C for 30 s, 58 °C for 30 s, 72 °C for 2 min, and a final extension at 72 °C for 10 min. In contrast to the *16S*-PCR's, I merged the *ITS*-amplicons of the three replicates of rhizosphere or bulk soil per plant. I purified the merged-*ITS* amplicons using PureLink PCR Purification kit from Invitrogen®, and resuspended the samples in 40 μL. Finally, I measured the purified-amplicon DNA concentration using Invitrogen® Qubit 4 fluorometer and then normalized the DNA concentration to up to 5 ng/μL. I did not make any further modifications to Illumina's 16S Metagenomic Sequencing Library Preparation protocol for any of the remaining steps.

Preparation of the *16S* and *ITS* Illumina libraries and sequencing were done at the UPR's Sequencing and Genomics Facility (SGF). A total of 318 samples were sequenced

using three Illumina MiSeq runs of 96 samples each. Thirteen *16S* samples were removed due to low sequence count and contamination.

The demultiplexed forward (fastq formatted) sequences from each MiSeq run were downloaded from Illumina's BaseSpace® and imported into Quantitative Insights Into Microbial Ecology 2 (QIIME2, v.2019.1) using the *demux emp-single* plugin (Boylen et al. 2018) and processed in three steps. First, I removed the primers using *Cutadapt* (Martin 2011), filtered (using a max-ee of 1), denoised, and dereplicated the sequences, and removed chimeras using DADA2 *denoise-single* plugin (Callahan et al. 2016). I truncated all the *16S* sequences to 230 bp due to a drop in the nucleotide's quality whereas the *ITS* was truncated in variable sizes based on quality of the nucleotides (< Q7). The *ITS2* amplicon size is variable (267-511 bp) (Taylor et al. 2016) thus truncating all sequences to the same length can create a bias towards taxa with short amplicons (Ihrmark et al. 2012). Second, following DADA2, I assigned taxonomy using Scikit-learn (Pedregosa et al. 2011) through the *classify-sklearn* plugin from QIIME 2. The classifier for *16S* was pre-trained using GreenGenes (99% similarity to 515F/806R-16S region) (Pruesse et al. 2007, Quast et al. 2013, Yilmaz et al. 2014, Glockner et al. 2017) whereas for *ITS* I used UNITE (dynamic similarity; version 8) (Nilsson et al. 2019) databases. I removed the sequences belonging to chloroplast, mitochondria (*16S*), and unidentified taxa (*16S* and *ITS*) and kept all ASV with > 10 reads in > 3 samples. The resulting ASVs were used to generate phylogenetic trees based on *de novo* construction (*16S* and *ITS*). To generate the phylogenetic trees, I aligned the representative sequences using Mafft (Katoh and Standley 2013), filtered the sequence gaps and highly un-conserved areas of the sequences using

Mask (Lane 1991), and subsequently built the phylogenetic trees with FastTree (Price et al. 2010) that I rooted with *phylogeny midpoint-root* plugin.

Because the *16S* and *ITS* samples were sequenced at different levels (i.e. replicates per individual vs individual, respectively) and because soil characterization sampling was done individual level (i.e. without microhabitat differentiation), I grouped the samples in two ways: 1) merging the *16S* replicates per individual while differentiating between rhizosphere and bulk soil samples (G1), matching *ITS* sequencing level, and 2) merging the *16S* and *ITS* replicates per individual without differentiating between rhizosphere and bulk soil samples (G2), matching soil sampling for elemental analyses. Subsequently the *16S* and *ITS* samples from both groups were respectively rarefied to even depth (Table S2.5).

Finally, I used Phylogenetic Investigation of Communities by Reconstruction of Unobserved States (PICRUSt2, v.2.3.0-b) to infer microbial gene content (Kegg Orthologs-KOs) from bacterial and archaeal taxa abundance (Douglas et al. 2020). I also used Funguild (Nguyena et al. 2016) to infer taxonomy-based ecological and fungal guild annotations.

DATA ANALYSES

Soil properties– I used the elemental composition of soils in two complimentary sets of analyses. The first set was aimed at characterizing the nutrient status of soils based on Center Log Ratio (CLR) and Isometric Log Ratios (ILR) transformation of their concentrations (Parent et al. 2012), whereas the second aimed at characterizing the soil weathering status based on known weathering indexes.

In compositional datasets (where each sample has a closed sum, often 100%), existing interdependencies, i.e., the concentration of one nutrient affects the concentration of others, causes self-redundancy (Parent et al. 2012). Center Log Ratio and Orthonormal balances (ILR-coordinates) are two important numerical transformation that try to eliminate these numerical biases that are brought by the nature of the instrument measurements. The ILR transformation is preferred because it removes the redundancy without sacrificing any component or analyte (Egozcue et al. 2003, Parent et al. 2012, Parent et al. 2013). However, I used both transformations to analyze the soil nutrients. Using the ILR transformation, required the calculation of the "filling value" (Fv), to close the sum to 100 weight %; this value represents all nutrients that were unaccounted for. Then, I clustered the nutrients from all samples using a complete-agglomerative hierarchical clustering analysis based on Euclidean distances as a basis for data-driven orthonormal transformation (Liu et al. 2019). Using the nutrients clusters, I used the sequentially binary partition (SBP) method to generate the groups of compositional parts (ILR transformation). The calculated ILR-compositional balances (Parent et al. 2012, Liu et al. 2019) were plotted on a CoDa dendrogram (Figure S2.2B) using the *compositions* R package. This analysis yielded 12 new variables (V1-V12).

The second set of analyses relied on the calculation of a number of weathering indexes based on the element oxide composition of soils and rock (Table S2.6) using criteria outlined in Prince and Velbel (2003). These indexes examine the ratio of "mobile" (Ca, Mg, Na, Si) to "immobile" (Al, Ti) elements that are depleted during weathering and are commonly used to characterize soil and rock weathering profiles (Jayawardena and Izawa

1994a, Prince and Velbel 2003, Burke et al. 2009, Fiantis et al. 2010, Che et al. 2012, Wilford 2012).

To reduce the number of variables for further analyses, I used the Variance Inflation Factor with a VIF threshold of 5.0 (vifcor function; *usdm* R package, v.1.1-18) to test for collinearity across the C and N isotopes, CLR-transformed nutrients, Orthonormal Balances, and Weathering Indexes variables. The resulting 10 from 34 variables (Figure S2.2) were further used for further analysis, including ANOVAs to test for differences between habitats and plant lifeforms.

Microbial communities – I conducted three sets of analyses to examine the extent to which bacterial, archaeal, and fungal taxonomic and functional diversity varied with habitat, microhabitat, life form, and species. Each set of analyses was conducted independently for bacteria/archaea and fungi. In a first set of analyses, I examined variation in alpha-diversity estimating species richness (Chao1), rarefaction curves (Chao1), and species diversity (Shannon). I further used ANOVA to test for differences among variables. Data analyses were done on R (R Core Team 2013) and plotted using *ggplot2* in the tidyverse R package (Wickham 2016, Wickham et al. 2019). The rarefaction curves were generated with *ggrare* in the Ranacapa R package (Kandlikar et al. 2018).

The ASVs relative abundances were used in a second set of analyses to examine taxonomic differential abundances and to identify indicator species. First, I generated barplots in *Phyloseq* R package (McMurdie and Holmes 2013a, McMurdie and Holmes 2014) to visualize microbial community composition. To test for taxonomical differential abundances between habitats, I used *ALDEx2* (v.1.16.0) and the results were visualized using bar plots. Then, I identified indicator species (ASVs) between habitats and habitat-

microhabitat interactions (Dufrene and Legendre 1997) using *labdsv* (Roberts 2016) and *Indicspecies* (De Cáceres and Legendre 2009, De Cáceres et al. 2011) R packages.

In a third and last set of analyses, I used species relative abundances in Non-metric Multidimensional Scaling (NMS) and Principal Coordinate Analysis (PcoA) ordinations to examine variation in the composition of microbial communities (beta diversity). I ran the NMDS based on Bray distances with proportions transformation of the data, and the PCA ordinations using a compositional approach which was based on Aitchison distances with prior replacing of zeroes with a pseudo count and CLR transformation. To test for the effect of habitat, microhabitat, and plant lifeform on microbial community compositions, I used PERMANOVAs in vegan R package (Anderson 2001, Oksanen et al. 2018).

Microbiomes-soil relationships – I examined relationships between microbial diversity and soil variables using two approaches. First, I used Pearson correlations to examine the relationship between Shannon diversity index and soil variables. Second, I used a NMDS ordination coupled with *envfit* (vegan R package) to fit soil variables into the ordination. Both of these approaches used G2 subset (Table 2.3) which do not distinguish microhabitats.

Microbial functional characterization- I tested for genes (KOs) and fungal guilds differential abundances between habitats using *ALDEx2* and the results were visualized using bar plots. A preliminary analysis of 7,182 KO's based on differential abundance revealed that 295 were differentially expressed as a function of habitat. These KO were annotated following three complimentary approaches: 1) based on KEGG Orthology (https://www.genome.jp/48eg/kegg2.html; accessed from July 2020 – April 2021) using Brite Hierarchy levels, 2) based on Geochip 5.0 functional gene array system (Shi et al.

2019), and 3) and on Grime's competitor/stress-tolerator/ruderal (CSR) traits (Wood et al. 2018). For the Brite Hierarchy levels, I searched the differentially abundant KOs in KEGG Orthology database and manually annotated each KO. For the GeoChip 5.0 genes, I searched the 1346 genes from Shi et al. (2019) in the KEGG database: a total of 918 genes matched 1 to 6 KO, 69 genes were associated to fungi and 359 genes were unclear or did not yield results. For the CSR traits, used the Brite Hierarchy levels and matched them to the CSR annotation based on Wood et al. (2018).

RESULTS

SOIL PROPERTIES

Of the 10 variables without collinearity (VIF value < 5), 8 differed between habitats and one differed between plant lifeforms (Table 2.2, Figure 2.2). Three variables (δ^{15}N, K, Mn) were higher in forests than in landslides, whereas five soil variables (δ^{13}C, Fe, V8, V11, CIW) were higher in landslides than forests. CIW was the only variable that differed between plant lifeform and was higher in shrubs than in herbaceous and tree ferns. The first two axis of a PCA based on ILR transformation of soil nutrients explained 78% of the variation among the data. Of the 12 orthonormal balances, four (V8, V10, V11 and V12) had higher correlation with the first two axes (Figure S2.1B). Three of these balances V8 (Ca|Na), V11 (Fe, Ti, P, Si, Al, Mg, F_v, Al | C, N, K, Mn), and V12 (Fe, Ti, P, Si, Al, Mg, F_v, Al, C, N, K, Mn | Ca, Na) were larger in landslides than forests, whereas V10 (P, Si, Al. Mg, F_v | Ti, Fe) was larger in forests than landslides.

MICROBIOMES

Species richness and diversity- The analysis of 4,917,139 *16S* and 3,072,956 *ITS* reads yielded a total of 10,148 and 2,422 ASVs, respectively (Table S2.5). After the rarefaction of G1 samples, the average reads per sample (n = 64) was 29,151 and 13,012 reads for *16S* and *ITS*, yielding a total of 10,080 and 2,422 ASVs, respectively (Table S2.5). After the rarefaction of G2 samples, the average read per sample (n = 32) was 59,736 and 47,150 reads for *16S* and *ITS*, yielding a total of 9,672 and 2,422 ASVs, respectively.

The species richness (Chao1) rarefaction curves suggest that most of the bacterial and archaeal, and fungal species richness was captured in the sampling, and reached species saturation (Figure S2.3). The *16S* species richness and diversity, but not *ITS*, differed between habitats, it was greater in forests than in landslides, (Figure 2.3; Table 2.3). Species diversity also differed significantly among microhabitat, whereas species richness and diversity differed across plant lifeform for *16S* (Table 2.3). Overall, *16S* diversity was significantly higher in rhizosphere than in bulk soil, while their species richness and diversity were significantly higher in tree fern than in herbaceous ferns and shrubs (Figure 2.3).

Taxonomic structure of microbial communities – Most archaeal and bacterial ASV were assigned to a phylum (100% and 95.5%, respectively), whereas < 20% of the ASVs were identified to genus and < 10% to species (7.8% archaea and 1% bacteria). In contrast to archaea and bacteria, all the fungal ASV were identified to the phylum level, while 59% of the fungal ASV, were identified to genus, and near 52% to species level.

The *16S* microbial communities were represented by 18 bacterial and 2 archaeal phyla. Nine bacterial phyla had relative abundances > 3%: Proteobacteria (40.7%), Verrucomicrobia (15.9%), Acidobacteria (14.6%), Planctomycetes (8.4%), Bacteroidetes

(5.6%), Chloroflexi (4.0%), Actinobacteria (3.9%), and Nitrospirae (3.6%) (Figure 2.4). The remaining 12 phyla represented < 3.4% of the reads (Figure S2.4). Among the Proteobacteria, the most abundant classes were the Alphaproteobacteria (64.2%), followed by the Gammaproteobacteria (18.9%), Deltaproteobacteria (10.3%), and Betaproteobacteria (6.5%). The fungal communities were represented by 11 phyla. Three fungal phyla had a relative abundance > 3%: Ascomycota (58.0%), Basidiomycota (33.0%), and Mortierellomycota (8.0%) (Figure 2.4). The remaining 8 phyla represents 2.6% of the reads (Figure S2.4). Among the Ascomycota, the most abundant classes were Sordariomycetes (32.3%), Eurotiomycetes (25.6%), Leotiomycetes (21.9%), Archaeorhizomycetes (12.2%), and Dothideomycetes (5.0%).

Indicator species and differentially abundant taxa – The Indicator Species Analysis identified 378 indicator taxa in landslides: 349 bacterial and 29 fungal, and 549 in forests: 1 archaeal, 521 bacterial and 27 fungal (Figure 2.5). In landslide and forest habitats, 7 and 31 taxa were indicator in the bulk soil and 40 and 43 in the rhizosphere, respectively (individual dots in the bottom part of the Extended Venn diagram; Figure 2.5; Table S2.7). At landslides, indicator species at rhizosphere included *Reyranella massiliensi, Phenylobacterium* spp., *Nevskia* spp., and *Rhodoplanes* spp. (Proteobacteria), *Sediminibacterium* spp. (Bacteroidetes), *Fimbriimonas* spp. (Armatimonadetes), *Acidicapsa borealis, Candidatus Solibacter* spp. (Acidobacteria), and order Diversisporales (Glomeromycota), whereas at bulk soil included Gemmataceae and Isosphaeraceae (Planctomycetes) and *Calceomyces lacunosus, Aspicilia* spp. (Ascomycota). At forests, indicator species at rhizosphere included *Woodsholea maritima, Dongia mobilis, Pedomicrobium* spp., *Mesorhizobium* spp., *Labrys* spp., *Leptothrix* spp.,

and *Steroidobacter* spp. (Proteobacteria), and *DA101* spp. (Verrucomicrobia), whereas at bulk soil included SAGMA-X (Crenarchaeota), *Rhodomicrobium vannielii* (Proteobacteria), *JG37-AG-70* spp. and *Nitrospira* spp. (Nitrospirae).

The differential abundance analysis with *ALDEx2* showed that 86 bacterial and 7 fungal ASVs were differentially abundant in the two habitats. In landslides, 71 bacterial and 4 fungal ASVs were differentially abundant, whereas in forest, 15 bacterial and 3 fungal ASVs were differentially abundant in forests (Table S2.8). In landslides, differentially abundant ASVs included *Koribacter versatilis*, and *Solibacter* spp. *(*Acidobacteria), *Gemmata* spp. (Planctomyces), and *Neurospora terricola* and *Leohumicola* spp. (Ascomycota) (Figure 2.6). In forest, differentially abundant ASVs included Micromonosporaceae (Actinobacteria), *Pirellula* spp. (Planctomycetes), and *Chloridium* spp. (Ascomycota) (Figure 2.6). ASVs belonging to *Rhodoplanes* spp. were differentially abundant in both habitats.

Beta diversity of microbial communities – In general, microbial community composition differed across habitat, microhabitat, and plant lifeform (Table 2.4). The NMDS ordinations for *16S* and *ITS* showed habitats separation along the first axis, and microhabitats separation along the second axis (Figure 2.7). A compositional approach using Aitchison distances showed a very similar trend (Figure S2.5). Yet, there was one notable difference among the two methods that I used. The separation between the microhabitats was less evident for the fungal communities using the compositional approach.

MICROBIOME – SOIL RELATIONSHIPS

Different soil variables correlated with *16S* and *ITS* Shannon species diversity index (Figure 2.8; Table 2.5). Irrespective of habitat (i.e., *Both* category), bacterial and archaeal diversity was correlated with 7 soil variables: positively correlated with 3 (δ^{15}N, K, and Mn) and negatively correlated with 4 (δ^{13}C, Fe, V8 and CIW). No variable was significantly correlated with bacterial and archaeal species diversity in landslides, whereas only K and Mn were correlated with *16S* species diversity in forests. In contrast, fungal species diversity was correlated with 2 variables, irrespective of the habitat: it was positively correlated with Mn and negatively correlated with δ^{15}N. In landslides, fungal species diversity was positively correlated with K and negatively correlated with δ^{13}C, δ15N, and V2, whereas in forests, species diversity was positively correlated with Fe and Mn, and negatively correlated with V8.

The Non-metric Multidimensional Scaling (NMDS) ordinations with soil variables fitted into the ordination showed that δ^{13}C, Fe and CIW had high correlation with the species composition at landslides, whereas δ^{15}N, K and Mn had high correlation with species composition at forests (Figure 2.9).

MICROBIAL FUNCTIONAL CHARACTERIZATION

PICRUSt2 resulted in 7,182 KEGG functional Orthologs (KOs). A total of 295 KOs were differently abundant between habitats: 44 were differentially abundant in landslides and 251 in forests. I used three strategies to describe the function of these KOs: 1) KEGG Brite Hierarchy annotation, 2) GeoChip 5.0 functional array descriptions, and 3) Competitive-Stress-Ruderal strategies annotations.

Based on the Brite hierarchy, I found that most of the differentially abundant genes were related to genetic information processing and metabolism. At landslides, more than half of the differentially abundant genes were related to metabolism and more than a quarter of the genes were related to carbohydrate metabolism (Table 2.6). At forests, on the other hand, half of the differentially abundant genes were related to genetic information processing, from which *translation* and *replication and repair* related genes stand out (Table 2.6). Based on the Geochip 5.0 gene array, I found that landslides differentially abundant genes related to carbon cycling (carbon degradation), plant growth promotion (anti-plant pathogens), and virulence, whereas forests had genes related to carbon cycling (carbon fixation), metal transport (K and Hg), nitrogen cycling (nitrification) and stress (Table S2.9). Finally, based on the CSR classifications, differentially abundant genes at landslides were not related to a CSR strategy in particular, although a quarter of the genes were related to plant exudates metabolism (Table S2.10). In contrast, differentially abundant genes at forests were associated to a ruderal life-history strategy.

FUNguild analysis resulted in 216 highly probable, 635 probable, 420 possible and 1151 unassigned ASVs to fungal guilds. From the assigned guilds, 54 were pathotrophs, 459 were saprotrophs, 210 were symbiotrophs and 548 were assigned to multiple guilds. The fungal guilds with the most species were generalists (i.e., ASVs that matched with the three trophic modes: symbiotrophs, pathotrophs and saprotrophs), arbuscular mycorrhizal fungi, soil saprotrophs and fungal parasites. Fungal parasites and plant saprotrophs were more abundant on landslides, while ectomycorrhizal, ericoid mycorrhizal, generalist saprotrophs, plant pathogens and wood saprotrophs were more abundant in forests. Arbuscular mycorrhizal, soil saprotrophs and generalist fungi were equally abundant in

landslides and forests. Two guild categories were significantly more abundant in landslides than in forest: saprotrophs and pathotrophs (Figure 2.10). Two guild categories were also more abundant in forest than landslides: saprotrophs and ectomycorrhizal (Figure 2.10).

DISCUSSION

Primary substrates with their extreme conditions represent unique habitats for the development of microbial communities and creating hotspots of biogeochemical activity. Focusing on "landslide-like" areas underlain by Ca,Mg-silicate rocks in montane tropical forests, I characterized the taxonomic and functional diversity of bacterial/archaeal and fungal communities using a metagenomics approach. Sampling of forests and "landslide" habitats, I found 1) large differences in soil attributes, including weathering rates, 2) distinctive communities of bacteria/archaea and fungi that were further affected by microhabitat, and plant lifeform, 3) distinct correlations between soil attributes and species diversity and composition, and 4) distinct microbial functional strategies across habitats. Altogether, these results shed new light into the identity and role of rhizobiomes in the weathering of Ca,Mg-silicate rocks in tropical mountains.

Soils – C and N isotopes, Fe, K, V8 (Ca|Na) orthonormal balance, and CIW weathering index were some of the soil attributes that differed across habitats. The higher $\delta^{13}C$ isotope values in landslides reflect different plant growth strategy to cope with higher temperatures (Wang et al. 2013) caused by the forest clearing during disturbances. Iron concentration was higher at landslides, but although its behavior is unpredictable, there have been documented cases where silicate weathering resulted in Fe accumulation in soils (Anderson et al. 2002, Riebe et al. 2003). Finally, based on CIW weathering index, landslide soil were more weathered that forest soils (Harnois 1988, Imam et al. 2019).

Microbial communities – The sampling design of my work identified a number of variables known to influence microbial communities in ecosystems undergoing development after disturbances, namely, habitats, microhabitat, and plant lifeform. I specifically studied microbial communities in "landslide-like" habitats and forests. Habitats consistently explained differences in species richness and diversity in bacteria/archaea but not fungi, and species composition in both groups of microorganisms. The microbial diversity and species richness was lower at landslides than forest habitats, which is consistent with studies done at landslides-like habitats which have found that microbial diversity is greatly reduced after a disturbance and increases as the ecosystem matures (DeGrood et al. 2005). The loss of microbial biomass and inoculum that occurs during the disturbance (Singh et al. 2001, Li et al. 2005) are probably the cause of differences in microbial diversity and composition in landslides. Nonetheless, very similar trends occur during microbial succession in distinct disturbances across distinct habitats (Nemergut et al. 2007, Mapelli et al. 2018, Ortiz-Álvarez et al. 2018), where the increase in potential niches and resource availability increases species diversity (Jackson 2003).

Microhabitats helped explain differences in microbial species diversity and community composition. Rhizosphere were separated from the bulk soil samples across the second axis of all ordinations, although this separation was weaker on fungal communities. Other studies have also found distinct microbial community composition across microhabitats (Mendes et al. 2014, Ortiz et al. 2020). This suggests a strong rhizosphere effect over bacterial and archaeal, and to a lesser extend fungal communities. A possible explanation is that each host plant reacts to environmental conditions though the production of root exudates (Philippot et al. 2013), affecting the microbial community composition and

functional role. However, the same might not be true for fungal communities, where it appears that during ecosystem succession, they were not affected by plant host presence. This is not the first time we have seen that bacteria and fungi have contrasting trajectories during microbial succession (Brown and Jumpponen 2014).

Plant host affects microbial community composition in two-ways. On the one hand, the samples from each microhabitat that came from the same plant host species were clustered together, respectively, for all microbial communities. On the other hand, even though plant host species were different, yet phylogenetically close between habitats, samples were mainly clustered by habitat, suggesting plant host lifeform had a minor role in shaping microbial community composition. These findings are consistent with Yeoh et al. (2017)'s work, which found plant host lifeform had a smaller effect that soil attributes in shaping the rhizobiomes microbial community across a chronosequence.

Differentially abundant species and indicator species analysis showed abiotic conditions are important to understand the differences found across habitats. For example, landslides were enriched with UV resistant - *Nevskia* (Hirsch 1992), heat resistant – *Leohumicola* (Hambleton et al. 2005), and low nutrient adapted- *Koribacter versatilis* (Campbell 2014) species. Bacteria in landslides also have diverse mechanisms of energy production, such as chemoheterotrophs – *Gemmata* (Fuerst 2017) and phototrophs – *Rhodoplanes* (Hiraishi and Ueda 1994). These characteristics are related to stressful environments, such as landslides.

Microbial communities – soil relationships – Various soil attributes correlated with microbial alpha and beta diversity. At landslides, $\delta^{13}C$, Fe and CIW weathering index correlated with species diversity, whereas at forests, Mn concentration correlated with

microbial species diversity and composition. These results contribute evidence to a growing body of knowledge stating that soil attributes are the major contributors to the shift in microbial communities across habitats (Berg and Smalla 2009, Lladó et al. 2018). Still, I do not discard the effect of other abiotic factors that were different across habitats, including soil maximum temperature, UV radiation (forest canopy closure), and soil water retention which are known to microbial community composition (Fierer et al. 2007, Krause et al. 2014).

Microbial functional characterization - Microbial communities of landslide-like habitats produced genes that suggest a different life history strategy to those of forests. The percent of genes related to stress-tolerance traits were similar in both habitats. Surprisingly, landslides, which are considered ruderal habitats, had a higher percent of competitive traits and genes related to the metabolisms of plant exudates, while forests, considered competitive habitats, were dominated by ruderal traits and foraging related genes. This is the opposite to what I expected because landslides are considered highly disturbed habitats with low nutrient availability (Osksanen and Ranta 1992, Matthews 2014) while forests are considered low-disturbance and low-stress habitats.

These contrasting results might suggest that landsliding promotes strong competence, due to its low concentration of readily available nutrients albeit rich in "trapped" nutrients. Thus, microbiomes here might be competing for plant derived compounds as genes related to plant growth promotion and carbon degradation were differentially abundant, and there was high abundance of fungal ASVs capable of degrading plant compounds in this habitat. Forest microbiome, on the other hand, had differentially abundant genes related to carbon fixation, nitrogen cycling, metal transport, and osmotic and oxygen limitation stresses,

although fungi might be doing the nutrient scavenging part given the higher abundance of ASVs with ectomycorrhizal and ericoid mycorrhizal associations. The opposite-to-expected results might be a due to the Twin Filter Theory (Grime and Pierce 2012, Ho et al. 2017, Wood and Franks 2018), where the environment exerts a first selection filter and pressures at finer scales act as a secondary filter.

Landslide-like habitats such as road cuts represent the perfect opportunity to study the dynamics associated to the exposure of primary substrates, in specific how microbial communities affect and are affected by the biogeochemical cycles. I was able to characterize taxonomically and functionally the rhizobiomes of plants growing in landslide-like habitats by combining NGS technologies and soil nutrient measurements across habitats, which to my knowledge has never been done before. In this study, I found that rhizobiomes composition at landslide-like habitats are influenced by habitat, plant host presence and lastly by plant host identity, and that both the microbiomes growing in each habitat have distinct life history strategies. This research is a first step to reach an understanding of the biogeochemical processes at tropical mountains and serves to corroborate frameworks that track microbial community changes across ecosystem succession.

Amundson, R., D. D. Richter, G. S. Humphreys, E. G. Jobbágy, and J. Gaillardet. 2007. Coupling between biota and earth materials in the Critical Zone. Elements **3**:327-332.

Anderson, M. J. 2001. A new method for non-parametric multivariate analysis of variance. Austral Ecology **26**:32-46.

Anderson, S. P., W. E. Dietrich, and G. H. Brimhall. 2002. Weathering profiles, mass-balance analysis, and rates of solute loss: Linkages between weathering and erosion in a small, steep catchment. GSA Bulletin **114**:1143-1158.

Augusto, L., M. P. Turpault, and J. Ranger. 2000. Impact of forest tree species on feldspar weathering rates. Geoderma **96**:215-237.

Autoridad de Carreteras y Transportación, P. Plan de Manejo de la Ruta Panorámica. Departamento de Transportación y Obras Públicas de Puerto Rico.

Baldrian, P. 2006. Fungal laccases-occurrence and properties. FEMS Microbiol Rev **30**:215-242.

Balogh-Brunstad, Z., C. K. Keller, R. A. Gill, B. T. Bormann, and C. Y. Li. 2008. The effect of bacteria and fungi on chemical weathering and chemical denudation fluxes in pine growth experiments Biochemistry **88**:153-167.

Banfield, J. F., W. W. Barker, S. A. Welch, and A. Tauton. 1999. Biological impact on mineral dissolution: Application of the lichen model to understanding mineral weathering in the rhizosphere. Proc. Natl. Acad. Sci **96**:3404-3411.

Barker, W. W., S. A. Welch, S. Chu, and J. F. Banfield. 1998. Experimental observations of the effects of bacteria on aluminosilicate weathering. American Mineralogist **83**:1551-1563.

Beerling, D. J. 2012. Atmospheric carbon dioxide: a driver of photosynthetic eukaryote evolution for over a billion years? Phil. Trans. R. Soc. B:477-482.

Beerling, D. J., and R. A. Berner. 2005. Feedbacks and the coevolution of plants and atmospheric CO_2Feedbacks and the coevolution of plants and atmospheric CO2. Proc. Natl. Acad. Sci **102**:1302-1305.

Bennett, P. C., J. R. Rogers, W. J. Choi, and F. K. Hiebert. 2001. Silicates, silicate weathering, and microbial ecology. Geomicrobiology Journal **18**:3-19.

Berg, G., and K. Smalla. 2009. Plant species and soil type cooperatively shape the structure and function of microbial communities in the rhizosphere. Pages 1–13. FEMS Microbiol Ecol.

Bergmann, G. T., S. T. Bates, K. G. Eilers, C. Lauber, J. G. Caporaso, W. Walters, R. Knight, and N. Fierer. 2011. The under-recognized dominance of Verrucomicrobia in soil bacterial communities. Soil Biology & Biochemistry **43**:1450-1455.

Bernasconi, S. M., A. Bauder, B. Bourdon, I. Brunner, E. Bünemann, I. Christl, N. Derungs, P. Edwards, D. Farinotti, B. Frey, E. Frossard, G. Furrer, M. Gierga, H. Göransson, K. Gülland, F. Hagedorn, I. Hajdas, R. Hindshaw, S. Ivy-Ochs, J. Jansa, T. Jonas, M. Kiczka, R. Kretzschmar, E. Lemarchand, J. Luster, J. Magnusson, E. A. D. Mitchell, H. Olde-Venterink, M. Plötze, B. Reynolds, R. H. Smittenberg, M. Stähli, F. Tamburini, E. T. Tipper, L. Wacker, M. Welc, J. G. Wiederhold, J. Zeyer, S. Zimmermann, and A. Zumsteg. 2011. Chemical and Biological Gradients along the Damma Glacier Soil Chronosequence, Switzerland Vadose Zone Journal **10**:867 - 883.

Berner, C., T. Johansson, and H. Wallander. 2012. Long-term effect of apatite on ectomycorrhizal growth and community structure. Mycorrhiza **22**:615–621.

Berner, R. A. 1992. Weathering, plants, and the long-term carbon-cycle. Geochimica Et Cosmochimica Acta **56**:3225-3231.

Berner, R. A., and Z. Kothavala. 2001. GEOCARB III: A Revised model of atmospheric CO2. American Journal of Science **301**:182-204.

Berner, R. A., A. C. Lasaga, and R. M. Garrels. 1983. The carbonate-silicate geochemical cycle and its effect on atmospheric carbon dioxide over the past 100 million years. American Journal of Science **283**:641-685.

Bever, J. D., I. A. Dickie, J. M. Facelli, J. Klironomos, M. Moora, M. C. Rilling, W. D. Stock, M. Tibbett, and M. Zobel. 2010. Rooting theories of plant community ecology in microbial interactions. Trends in Ecology & Evolution **25**:468-478.

Birdsey, R. A., and D. Jimenez. 1985. The Forests of Toro Negro. Usda Forest Service Southern Forest Experiment Station Research Paper:1-&.

Birdsey, R. A., and D. Jiménez. 1985. The Forests of Toro Negro. Pages 1-29 *in* U. S. D. o. Agriculture, editor. Forest Service, New Orleans, Louisiana.

Bonfante, P., and A. Genre. 2010. Mechanisms underlying beneficial plant-fungus interactions in mycorrhizal symbiosis. Nature Communications **1**.

Bonneville, S., D. J. Morgana, A. Schmalenberger, A. Bray, A. Brown, S. A. Banwar, and L. G. Benning. 2011. Tree-mycorrhiza symbiosis accelerate mineral weathering: Evidences from nanometer-scale elemental fluxes at the hypha–mineral interface. Geochimica Et Cosmochimica Acta **75**:6988 – 7005.

Boylen, E., J. R. Rideout, M. Dillon, N. A. Bokulich, C. Abnet, G. A. Al-Ghalith, H. Alexander, E. J. Alm, M. Arumugam, F. Asnicar, Y. Bai, J. E. Bisanz, K.

Bittinger, A. Brejnrod, C. J. Brislawn, C. T. Brown, B. J. Callahan, A. M. Caraballo-Rodríguez, J. Chase, E. Cope, R. Da Silva, P. C. Dorrestein, G. M. Douglas, D. M. Durall, C. Duvallet, C. F. Edwardson, M. Ernst, M. Estaki, J. Fouquier, J. M. Gauglitz, D. L. Gibson, A. Gonzalez, K. Gorlick, J. Guo, B. Hillmann, S. Holmes, H. Holste, C. Huttenhower, G. Huttley, S. Janssen, A. K. Jarmusch, L. Jiang, B. Kaehler, K. B. Kang, C. R. Keefe, P. Keim, S. T. Kelley, D. Knights, I. Koester, T. Kosciolek, J. Kreps, M. G. Langille, J. Lee, R. Ley, Y. Liu, E. Loftfield, C. Lozupone, M. Maher, C. Marotz, B. D. Martin, D. McDonald, L. J. McIver, A. V. Melnik, J. L. Metcalf, S. C. Morgan, J. Morton, A. T. Naimey, J. A. Navas-Molina, L. F. Nothias, S. B. Orchanian, T. Pearson, S. L. Peoples, D. Petras, M. L. Preuss, Pruesse E, L. B. Rasmussen, A. Rivers, M. S. Robeson II, P. Rosenthal, N. Segata, M. Shaffer, A. Shiffer, R. Sinha, S. J. Song, J. R. Spear, A. D. Swafford, L. R. Thompson, P. J. Torres, P. Trinh, A. Tripathi, P. J. Turnbaugh, S. Ul-Hasan, J. J. van der Hooft, F. Vargas, Y. Vázquez-Baeza, E. Vogtmann, M. von Hippel, W. Walters, Y. Wan, M. Wang, J. Warren, K. C. Weber, C. H. Williamson, A. D. Willis, Z. Z. Xu, J. R. Zaneveld, Y. Zhang, Q. Zhu, R. Knight, and J. G. Caporaso. 2018. QIIME 2: Reproducible, interactive, scalable, and extensible microbiome data science. PeerJ Preprints **6**:e27295v27292.

Brantley, S. L., M. B. Goldhaber, and K. Vala Ragnarsdottlr. 2007. Crossing disciplines and scales to understand the Critical Zone. Elements **3**:307-314.

Bray, J. R., and J. T. Curtis. 1957. An Ordination of the upland forest community of southern Wisconsin. Ecological Monographs **27**:325 - 349.

Brenning, A., M. Schwinn, A. P. Ruiz-Páez, and J. Muenchow. 2015. Landslide susceptibility near highways is increased by 1 order of magnitude in the Andes of southern Ecuador, Loja province. Nat. Hazards Earth Syst. Sci. **15**:45-57.

Brown, S. P., and A. Jumpponen. 2014. Contrasting primary successional trajectories of fungi and bacteria in retreating glacier soils. Molecular Ecology **23**:481-497.

Brunner, I., M. Plotze, S. Rieder, A. Zumsteg, G. Furrer, and B. Frey. 2011. Pioneering fungi fromthe Damma glacier forefield in the Swiss Alps can promote granite weathering. Geobiology **9**:266-279.

Burke, B. C., A. M. Heimsath, J. L. Dixon, J. Chappell, and K. Yoo. 2009. Weathering the escarpment: chemical and physical rates and processes, south-eastern Australia. Earth Surface Processes and Landforms **34**:768-785.

Buss, H. L., M. J. Schultz, C. F. Mathur, and S. L. Brantley. 2005. The coupling of biological iron cycling and mineral weathering during saprolite formation, Luquillo Mountains, Puerto Rico. Geobiology **3**:247-260.

Callahan, B. J., P. J. McMurdie, M. J. Rosen, A. W. Han, A. J. A. Johnson, and S. P. Holmes. 2016. DADA2: High-resolution sample inference from Illumina amplicon data. Nature Methods **13**:581-+.

Calvaruso, C., M.-P. Turpault, E. Leclerc, and P. Frey-Klett. 2007. Impact of ectomycorrhizosphere on the functional diversity of soil bacterial and fungal communities from a forest stand in relation to nutrient mobilization processes. Pages 567-577. Microbial Ecology.

Calvaruso, C., M.-P. Turpault, E. Leclerc, J. Ranger, J. Garbaye, S. Uroz, and P. Frey-Klett. 2010. Influence of forest trees on the distribution of mineral weathering-associated bacterial communities of the Scleroderma citrinum mycorrhizosphere. Applied and Environmental Microbiology **76**:4780-4787.

Calvaruso, C., M. P. Turpault, and P. Frey-Klett. 2006. Root-associated bacteria contribute to mineral weathering and to mineral nutrition in trees: A budgeting analysis. Applied and Environmental Microbiology **72**:1258-1266.

Cammeraat, E., R. van Beek, and A. Kooijman. 2005. Vegetation succession and its consequences for slope stability in SE Spain. Plant and Soil **278**:135-147.

Campbell, B. 2014. The Family Acidobacteriaceae. Pages 405-415 *in* E. Rosenberg, editor. The Prokaryotes – Other Major Lineages of Bacteria and the Archaea. Springer-Verlag, Berlin.

Caporaso, J. G., C. Lauber, L. Walters, D. Berg-Lyons, C. Lozupone, P. J. Turnbaugh, N. Fierer, and R. Knight. 2011. Global patterns of 16S rRNA diversity at a depth of millions of sequences per sample. Proc Natl Acad Sci **108**:4416-4522.

Ceryan, S. 2008. New chemical weathering indices for estimating the mechanical properties of rocks: a case study from the Kürtün Granodiorite, NE Turkey. Turkish Journal of Earth Sciences **17**:187-207.

Che, V. B., K. Fontijn, G. G. J. Ernst, M. Kervyn, M. Elburg, E. Van Ranst, and C. E. Suh. 2012. Evaluating the degree of weathering in landslide-prone soils in the humid tropics: The case of Limbe, SW Cameroon. Geoderma **170**:378-389.

Chen, C., J. Zhang, M. Lu, C. Qin, Y. Chen, L. Yang, Q. Huang, J. Wang, Z. Shen, and Q. Shen. 2016. Microbial communities of an arable soil treated for 8 years with organic and inorganic fertilizers. Biology and Fertility of Soils **52**:455-467.

Chen, J. 1967. Petrological and chemical studies of Utuado Pluton, Puerto Rico. Rice University.

Chen, Y., X. Zhang, J. Ye, H. Han, and S. Wan. 2014. Six-year fertilization modifies the biodiversity of arbuscular mycorrhizal fungi in a temperate steppe in Inner Mongolia. Soil Biology & Biochemistry **69**.

Clarkson, D. T., and J. B. Hanson. 1980. The mineral nutrition of higher plants. Annual Review of Plant Physiology **31**:239-298.

Cox, N. J. 1980. On the relationship between bedrock lowering ans regolith thickness. Earth Surface Processes **5**:271-274.

De Cáceres, M., and P. Legendre. 2009. Associations between species and groups of sites: indices and statistical inference. Ecology **90**:3566-3574.

De Cáceres, M., D. Sol, O. Lapiedra, and P. Legendre. 2011. A framework for estimating niche metrics using the resemblance between qualitative resources. Synthesising Ecology **120**:1341-1350.

DeGrood, S. H., V. P. Claassen, and K. M. Scow. 2005. Microbial community composition on native and drastically disturbed serpentine soils. Soil Biology & Biochemistry **37**:1427–1435.

Demir, F., G. Budak, E. Bayas, and Y. Sahin. 2006. Standard deviations of the error effects in preparing pellet samples for WDXRF spectroscopy. Nuclear Instruments and Methods in Physics Research B **243**:423-428.

Di Lionardo, D. P., F. Pinzari, D. Lunghini, O. Maggi, V. M. Granito, and A. M. Persiani. 2013. Metabolic profiling reveals a functional succession of active fungi during the decay of Mediterranean plant litter. Soil Biology & Biochemistry **60**:210-219.

Dixon, J. L., and C. S. Riebe. 2014. Tracing and pacing soil across slopes. Elements **10**:363-368.

Dixon, J. L., and F. von Blanckenburg. 2012. Soils as pacemakers and limiters of global silicate weathering. Comptes Rendus Geoscience:597–609.

Douglas, G. M., V. J. Maffei, J. R. Zaneveld, S. N. Yurgel, B. J. R., C. M. Taylor, C. Huttenhower, and M. G. Langille. 2020. PICRUSt2 for prediction of metagenome functions. Nature Biotechnology **38**:685-688.

Drever, J. I. 1994a. The effect of land plants on weathering rates of silicate minerals. Geochimica Et Cosmochimica Acta **58**:2325-2332.

Drever, J. I. 1994b. The effect of land plants on weathering rates of silicate minerals. Geochimica et Cosmochimica Acta **58**:2325-2332.

Dufrene, M., and P. Legendre. 1997. Species assemblages and indicator species: the need for a flexible asymmetrical approach. Ecological Monographs **67**:345-366.

Durgin, P. B. 1977. Landslides and the weathering of granitic rocks. Reviews in Engineering Geology **3**:127-131.

Edwards, J., C. Johnson, C. Santos-Medellín, E. Lurie, N. Kumar Podishetty, S. Bhatnagar, J. A. Eisen, and V. Sundaresan. 2015. Structure, variation, and assembly of the root-associated microbiomes of rice. PNAS:E911-E920.

Egozcue, J. J., and V. Pawlowsky-Glahn. 2005. CoDa-Dendrogram: a new exploratory tool.*in* G. a. B.-V. In: Mateu-Figueras, C. (Eds.), editor. Proceedings of the 2nd International Workshop on Compositional Data Analysis. Universitat de Girona.

Egozcue, J. J., V. Pawlowsky-Glahn, G. Mateu-Figueras, and C. Barcelo-Vidal. 2003. Isometric logratio transformations for compositional data analysis. Mathematical Geology **35**:279-300.

Ehrenfeld, J. G., B. Ravit, and K. Elgersma. 2005. Feedback in the plant-soil system. Annu. Rev. Environ. Resour. **30**:75-115.

Eilers, K. G., C. L. Lauber, and N. Fierer. 2010. Shifts in bacterial community structure associated with inputs of low molecular weight carbon compounds to soil. Soil Biology & Biochemistry **42**:896-903.

Emberson, R., A. Galy, and N. Hovius. 2018. Weathering of reactive mineral phases in landslides acts as a source of carbon dioxide in mountain belts. JGR Earth Surface **123**:2695-2713.

Emmett, B. D., N. D. Youngblut, D. H. Buckley, and L. E. Drinkwater. 2017. Plant phylogeny and life history shape rhizosphere bacterial microbiome of summer annuals in an agricultural field. Frontiers in Microbiology **8**:1-16.

Ewel, J. J., and J. L. Whitmore. 1973. The ecological life zones of Puerto Rico and the U.S. Virgin Islands. Institute of Tropical Forestry, Rio Piedras, P.R.,.

Fedo, C. M., H. W. Nesbitt, and G. M. Young. 1995. Unraveling the effects of potassium metasomatism in sedimentary rocks and paleosols, with implications for paleoweathering conditions and provenance. Geology **23**:921-924.

Fernandes, A. D., J. M. Macklaim, T. G. Linn, G. Reid, and G. B. Gloor. 2013. ANOVA-Like Differential Expression (ALDEx) Analysis for Mixed Population RNA-Seq. Plos One **8**:e67019.

Fernandes, A. D., J. N. S. Reid, J. M. Macklaim, T. A. McMurrough, R. D. Edgell, and G. B. Gloor. 2014. Unifying the analysis of high-throughput sequencing datasets: characterizing RNA-seq, 16S rRNA gene sequencing and selective growth experiments by compositional data analysis. Microbiome **2**.

Fiantis, D., M. Nelson, J. Shamshuddin, T. B. Goh, and E. Van Ranst. 2010. Determination of the geochemical weathering indices and trace elements content of new volcanic ash deposits from Mt. Talang (West Sumatra) Indonesia. Eurasian Soil Science **43**:1477-1485.

Fierer, N., M. A. Bradford, and R. B. Jackson. 2007. Towards an ecological classification of soil bacteria. Ecology **88**:1354-1364.

Frey, B., S. R. Rieder, I. Brunner, M. Plotze, S. Koetzsch, A. Lapanje, H. Brandl, and G. Furrer. 2010. Weathering-associated bacteria from the Damma Glacier forefield: Physiological capabilities and impact on granite dissolution. Applied and Environmental Microbiology **76**:4788-4796.

Fu, D., X. Wu, C. Duan, L. Zhao, and B. Li. 2020. Different life-form plants exert different rhizosphere effects on phosphorus biogeochemistry in subtropical mountainous soils with low and high phosphorus content. Soil & Tillage Research **199**.

Fuerst, J. A. 2017. Planctomycetes—New models for microbial cells and activities. Pages 1-27 Microbial Resources: From Functional Existence in Nature to Applications. Academic Press.

Gadd, G. M. 2007. Geomycology: biogeochemical transformations of rocks, minerals, metals and radionuclides by fungi, bioweathering and bioremediation. Mycological Research **111**:3-49.

Gadd, G. M. 2013. Microbial roles in mineral transformations and metal cycling in the Earth's Critical Zone. Pages 115–165 *in* J. Xu and D. L. Sparks, editors. Molecular Environmental Soil Science. Springer Netherlands.

Gadd, G. M. 2017. Geomicrobiology of the built environment. Nature Microbiology **2**:1-9.

Geertsema, M., and J. J. Pojar. 2007. Influence of landslides on biophysical diversity — A perspective from British Columbia. Geomorphology **89**:55-69.

Gleeson, D., F. Mathes, M. Farrell, and M. Leopold. 2016. Environmental drivers of soil microbial community structure and function at the Avon River Critical Zone Observatory. Sci Total Environ **571**:1407-1418.

Gleeson, D. B., N. M. Kennedy, N. Clipson, K. Melville, G. M. Gadd, and F. P. McDermott. 2006. Characterization of bacterial community structure on a weathered pegmatitic granite. Microbial Ecology **51**:526-534.

Glockner, F. O., P. Yilmaz, C. Quast, J. Gerken, A. Beccati, A. Ciuprina, G. Bruns, P. Yarza, J. Peplies, R. Westram, and W. Ludwig. 2017. 25 years of serving the community with ribosomal RNA gene reference databases and tools. Journal of Biotechnology **261**:169-176.

Gloor, G. B., J. M. Macklaim, and A. D. Fernandes. 2015. Displaying Variation in Large Datasets: Plotting a Visual Summary of Effect Sizes. Journal of Computational and Graphical Statistics.

Gorbushina, A. A. 2007. Life on the rocks. Environmental Microbiology **9**:1613-1631.

Gorbushina, A. A., and W. J. Broughton. 2009. Microbiology of the atmosphere-rock interface: How biological interactions and physical stresses modulate a sophisticated microbial ecosystem.431-450.

Gorbushina, A. A., E. R. Kotlova, and O. A. Sherstneva. 2008. Cellular responses of microcolonial rock fungi to long-term desiccation and subsequent rehydration. Stud Mycol **61**:91-97.

Gorbushina, A. A., and W. E. Krumbein. 2005. Ch 3: Role of microorganisms in wear down of rocks and minerals. Pages 59-84 Soil Biology. Springer-Verlag Berlin Heidelberg.

Gorbushina, A. A., K. Whitehead, T. Dornieden, A. Niesse, A. Schulte, and J. I. Hedges. 2003. Black fungal colonies as units of survival: hyphal mycosporines synthesized by rock-dwelling microcolonial fungi. Canadian Journal of Botany **81**:131-138.

Grayston, S. J., D. Vaughan, and D. Jones. 1996. Rhizosphere carbon flow in trees, in comparison with annual plants: the importance of root exudation and its impact on microbial activity and nutrient availability. Applied Soil Ecology **5**:29-56.

Grime, J. P., and S. Pierce. 2012. The evolutionary strategies that shape ecosystems. John Wiley & Sons, Oxford.

Guariguata, M. R. 1990. Landslide disturbance and forest regeneration in the Upper Luquillo Mountains of Puerto Rico. Pages 814 - 832. Journal of Ecology.

Guida, M., P. Losanno Cannavacciuolo, M. Cesarano, M. Borra, E. Biffali, R. D'Alessandro, and B. De Felice. 2014. Microbial diversity of landslide soils assessed by RFLP and SSCP fingerprints. J Appl Genetics **55**:403–415.

Halsey, D. P., D. J. Mitchell, and S. J. Dews. 1998. Influence of climatically induced cycles in physical weathering. Quarterly Journal of Engineering Geology and Hydrogeology **31**:359-367.

Hambleton, S., N. L. Nickerson, and K. A. Seifert. 2005. Leohumicola, a new genus of heat-resistant hyphomycetes. Studies in Mycology **53**:29-52.

Harnois, L. 1988. The CIW Index: A new chemical index of weathering. Sedimentary Geology **55**:319-322.

Heimsath, A. M., W. E. Dietrich, K. Nishiizumi, and R. C. Finkel. 1997. The soil production function and landscape equilibrium. Nature **388**:358-361.

Hilley, G. E., and S. Porder. 2008. A framework for predicting global silicate weathering and CO2 drawdown rates over geologic time-scales. PNAS **105**:16855-16859.

Hiraishi, A., and Y. Ueda. 1994. Rhodoplanes gen. nov., a new genus of phototrophic bacteria including Rhodopseudomonas rosea as Rhodoplanes roseus comb. nov. and Rhodoplanes elegans sp. nov. International Journal of Systematic and Evolutionary Microbiology **44**:665-673.

Hirsch, P. 1992. The genus Nevskia. Pages 4089-4092 *in* B. e. al., editor. The Prokaryotes. Springer Science+Business Media, New York.

Ho, A., D. P. Di Lionardo, and P. L. E. Bodelier. 2017. Revisiting life strategy concepts in environmental microbial ecology. FEMS Microbiol Ecol **93**:1-14.

Hoppert, M., C. Flies, W. Pohl, B. Gunzl, and J. Schneider. 2004. Colonization strategies of lithobiontic microorganisms on carbonate rocks. Environmental Geology **46**:421-428.

Hughes, K. S., and W. H. Schulz. 2020. Map depicting susceptibility to landslides triggered by intense rainfall, Puerto Rico. U.S. Geological Survey.

Ihrmark, K., I. T. Bodeker, K. Cruz-Martinez, H. Friberg, A. Kubartova, J. Schenck, Y. Strid, J. Stenlid, M. Brandstrom-Durling, K. E. Clemmensen, and B. D. Lindahl. 2012. New primers to amplify the fungal ITS2 region--evaluation by 454-sequencing of artificial and natural communities. FEMS Microbiol Ecol **82**:666-677.

Imam, M. H., C. T. Ogushi, T. Wakatsuki, and M. Ueda. 2019. Assessment of climate-induced degree of chemical weathering in some granite and granodiorite slopes of Japan. Modeling Earth Systems and Environment **5**:1751–1767.

Irfan, T. Y. 1996. Mineralogy, fabric properties and classification of weathered granites in Hong Kong. Quarterly Journal of Engineering Geology **29**:5-35.

Jackson, C. R. 2003. Changes in community properties during microbial succession. Oikos **101**:444-448.

Jackson, O., R. S. Quilliam, A. Stott, H. Grant, and S. J. A. 2019. Rhizosphere carbon supply accelerates soil organic matter decomposition in the presence of fresh organic substrates. Plant and Soil **440**:473-490.

Jayawardena, U. S., and E. Izawa. 1994a. Application of present indices of chemical weathering for precambrian metamorphic rocks in Sri Lanka. Bulletin of the International Association of Engineering Geology **49**:55-61.

Jayawardena, U. S., and E. Izawa. 1994b. A new chemical index of weathering for metamorphic silicate rocks in tropical regions: A study from Sri Lanka. Engineering Geology **36**:303-310.

Jenny, H. 1941. Factors of Soil Formation: A System of Quantitative Pedology. McGraw-Hill, New York.

Josse, J., and F. Husson. 2016. missMDA: A Package for Handling Missing Values in Multivariate Data Analysis. Journal of Statistical Software **70**:1-31.

Judd, W. S., and G. M. Ionta. 2013. Taxonomic studies in the Miconieae (Melastomataceae). X. Revision of the species of the Miconia crotonifolia complex. Brittonia **65**:66-95.

Kalinowski, B. E., L. J. Liermann, S. Givens, and S. L. Brantley. 2000. Rates of bacteria-promoted solubilization of Fe from minerals: a review of problems and approaches Chemical Geology **169**:357-370.

Kandlikar, G. S., Z. J. Gold, M. C. Cowen, R. S. Meyer, A. C. Freise, N. J. B. Kraft, J. Moberg-Parker, J. Sprague, D. J. Kushner, and E. E. Curd. 2018. ranacapa: An R package and Shiny web app to explore environmental DNA data with exploratory statistics and interactive visualizations [version 1]. F1000Research **7**:1734-1751.

Katoh, K., and D. M. Standley. 2013. MAFFT multiple sequence alignment software version 7: Improvements in performance and usability. Molecular Biology and Evolution **30**:772-780.

Keddy, P. 2007. Plants and vegetation: Origins, processes, consequences. Cambridge University Press.

Kirtzel, J., N. Ueberschaar, T. Deckert-Gaudig, K. Krause, V. Deckert, G. M. Gadd, and E. Kothe. 2020. Organic acids, siderophores, enzymes and mechanical pressure for black slate bioweathering with the basidiomycete Schizophyllum commune. Environmental Microbiology **22**:1535-1546.

Knelman, J. E., T. M. Legg, S. P. O'neill, C. L. Washenberg, A. González, C. C. Cleveland, and D. R. Nemergut. 2012. Bacterial community structure and function change in association with colonizer plants during early primary succession in a glacier forefield. Soil Biology & Biochemistry **46**.

Koele, N., I. A. Dickie, J. D. Blum, J. D. Gleason, and L. de Graaf. 2014. Ecological significance of mineral weathering in ectomycorrhizal and arbuscular mycorrhizal ecosystems from a field-based comparison. Soil Biology & Biochemistry **69**:63-70.

Koele, N., M. P. Turpault, E. E. Hildebrand, S. Uroz, and P. Frey-Klett. 2009. Interactions between mycorrhizal fungi and mycorrhizosphere bacteria during mineral weathering: Budget analysis and bacterial quantification. Soil Biology & Biochemistry **41**:1935-1942.

Krause, S., X. Le Roux, P. A. Niklaus, P. M. Van Bodegom, J. T. Lennon, S. Bertilsson, H.-P. Grossart, L. Philippot, and P. L. E. Bodelier. 2014. Trait-based approaches for understanding microbial biodiversity and ecosystem functioning. Frontiers in Microbiology **5**:1-10.

Lambers, H., C. Mougel, B. Jaillard, and P. Hinsinger. 2009. Plant-microbe-soil interactions in the rhizosphere: an evolutionary perspective. Plant and Soil **321**:83-115.

Lane, D. J. 1991. 16s/23s rrna sequencing. John Wiley and Sons, New York.

Larsen, J., P. Jaramillo-López, M. Nájera-Rincón, and C. E. Gonzaléz-Esquivel. 2015. Biotic interactions in the rhizosphere in relation to plant and soil nutrient dynamics. Journal of Soil Science and Plant Nutrition **15**:449-463.

Larsen, M. C., and A. J. Torres-Sánchez. 1996. Geographic relations of landslide Distribution and assessment of landslide hazards in the Blanco, Cibuco, and Coamo basins, Puerto Rico. U.S. Geological Survey, San Juan, Puerto Rico.

Lê, S., J. Josse, and F. Husson. 2008. FactoMineR: A Package for Multivariate Analysis. Journal of Statistical Software **25**:1-18.

Leake, J. R., A. L. Duran, K. E. Hardy, I. Johnson, D. J. Beerling, S. A. Banwart, and M. M. Smits. 2008a. Biological weathering in soil: the role of symbiotic root-associated fungi biosensing minerals and directing photosynthate-energy into grain-scale mineral weathering. Mineralogical Magazine **72**:85-89.

Leake, J. R., A. L. Duran, K. E. Hardy, I. Johnson, D. J. Beerling, S. A. Banwart, and M. M. Smits. 2008b. Biological weathering in soil: the role of symbiotic root-associated fungi biosensing minerals and directing photosynthate-energy into grain-scale mineral weathering. Mineralogical Magazine **72**:85-89.

Leyval, C., and J. Berthelin. 1991. Weathering of a mica by roots and rhizospheric microorganisms of pine. Soil Sci. Soc. Am. J. **55**:1009-1016.

Li, Y., H. Ruan, X. Zou, and R. W. Myster. 2005. Response of major soil decomposers to landslide disturbance in a Puerto Rican rainforest. Soil Science **170**:202-211.

Liermann, L. J., I. Albert, H. L. Buss, M. Minyard, and S. L. Brantley. 2015. Relating microbial community structure and geochemistry in deep regolith developed on volcaniclastic rock in the Luquillo Mountains, Puerto Rico. Geomicrobiology Journal **32**:494-510.

Liu, Y., E. J. M. Carranza, K. Zhou, and Q. Xia. 2019. Compositional balance analysis: An elegant method of geochemical pattern recognition and anomaly mapping for mineral exploration Natural Resources Research **28**:1269-1283.

Lladó, S., R. López-Mondéjar, and P. Baldrian. 2018. Drivers of microbial community structure in forest soils. Appl Microbiol Biotechnol **102**:4331–4338.

Lopez, A. M., K. S. Hughes, and E. Vanacore. 2020. Puerto Rico's winter 2019–2020 seismic sequence leaves the island on edge: Temblor.

Lunghini, D., V. M. Granito, D. P. Di Lionardo, O. Maggi, and A. M. Persiani. 2013. Fungal diversity of saprotrophic litter fungi in a Mediterranean maquis environment. Mycologia **105**:1499-1515.

Mapelli, F., R. Marasco, M. Fusi, B. Scaglia, G. Tsiamis, E. Rolli, S. Fodelianakis, K. Bourtzis, S. Ventura, F. Tambone, F. Adani, S. Borin, and D. Daffonchio. 2018. The stage of soil development modulates rhizosphere effect along a High Arctic desert chronosequence. The ISME Journal **12**:1188-1198.

Marguí, E. V. G., R. 2013. Chapter 3: Qualitative and Quantitative X-Ray Fluorescence Analysis. Pages 33-59 *in* J. M. Chalmers, editor. X-Ray Fluorescence Spectrometry and Related Techniques: An Introduction. Momentum Press, New York.

Markowicz, A., M. Dargie, and R. L. Walsh. 1997. Analysis of geological materials. Pages 15-20 Sampling, storage and sample preparation procedures for X ray fluorescence analysis of environmental materials. International Atomic Energy Agency, Vienna, Austria.

Marschner, H. 1995. Mineral Nutrition of Higher Plants. Second Edition edition. Academic Press, ndon.

Martin, M. 2011. Cutadapt removes adapter sequences from high-throughput sequencing reads. EMBnet. journal **17**:10.

Matsukura, Y., T. Hattanji, C. T. Oguchi, and T. Hirose. 2007. Ten year measurements of weathering rates of rock tablets on a forested hillslope in a humid temperate region, Japan. Z. Geomorph. N. F. **51**:27-40.

Matsunami, H., K. Matsuda, S. Yamasaki, K. Kimura, Y. Ogawa, Y. Miura, I. Yamaji, and N. Tsuchiya. 2010. Rapid simultaneous multi-element determination of soils and environmental samples with polarizing energy dispersive X-ray fluorescence (EDXRF) spectrometry using pressed powder pellets. Soil Science & Plant Nutrition **56**:530-540.

Matthews, T. J. 2014. Integrating Geoconservation and Biodiversity Conservation: Theoretical Foundations and Conservation Recommendations in a European Union Context. Geoheritage **6**:57-70.

Maurice, P. A., M. A. Vierkorn, L. E. Hersman, and J. E. Fulghum. 2001. Dissolution of well and poorly ordered kaolinites by an aerobic bacterium. Chemical Geology **180**:81-97.

McAdams, B. C., A. M. Trierweiler, S. A. Welch, C. Restrepo, and A. E. Carey. 2015. Two sides to every range: Orographic influences on CO2 consumption by silicate weathering. Applied Geochemistry **63**:472-483.

McMurdie, and Holmes. 2013a. Phyloseq: An R Package for Reproducible Interactive Analysis and graphics of Microbiome Census Data. Plos One **8**:e61217.

McMurdie, P. J., and S. Holmes. 2013b. phyloseq: An R package for reproducible interactive analysis and graphics of microbiome census data. Plos One **8**.

McMurdie, P. J., and S. Holmes. 2014. Shiny-phyloseq: Web application for interactive microbiome analysis with provenance tracking. Bioinformatics **31**:282-283.

Mendes, L. W., E. E. Kuramae, A. A. Navarrete, J. A. van Veen, and S. M. Tsai. 2014. Taxonomical and functional microbial community selection in soybean rhizosphere. The ISME Journal **8**:1577-1587.

Middelburg, J. J., C. H. Van Der Weijden, and J. R. W. Woittiez. 1988. Chemical processes affecting the mobility of major, minor and trace elements during weathering of granitic rocks. Chemical Geology **68**:253-273.

Molinelli, J. A. 1984. Geomorphic processes along the Autopista Las Americas in north central Puerto Rico Implications for highway construction, design, and maintenance. Clark University, Ann Monroe, Michigan.

Monroe, W. H. 1979. Map showing landslides and areas of susceptibility to landsliding in Puerto Rico. Department of the Interior, U.S. Geological Survey:Map I-1148.

Mori, P. M., S. Reeves, C. Teixeira-Correia, and M. Haukka. 1999. Development of a fused glass disc XRF facility and comparison with the pressed powder pellet technique at Instituto de Geociencias, Sao Paulo University. Brazilian Journal of Geology **23**:441-446.

Muenchow, J., A. Brenning, and M. Richter. 2012. Geomorphic process rates of landslides along a humidity gradient in the tropical Andes. Geomorphology **139 - 140**:271-284.

Neaman, A., J. Chorover, and S. L. Brantley. 2006. Effects of organic ligands on granite dissolution in batch experiments at pH 6. American Journal of Science **306**:451-473.

Nemergut, D. R., S. P. Anderson, C. C. Cleveland, A. P. Martin, A. E. Miller, A. Seimon, and S. K. Schmidt. 2007. Microbial community succession in an unvegetated recently deglaciated soil. Microbial Ecology **53**:110-122.

Nesbitt, H. W., and G. M. Young. 1982. Early Proterozoic climates and plate motions inferred from major element chemistry or lutites. Nature **299**:715–717.

Nguyena, N. H., Z. Song, S. T. Bates, S. Branco, L. Tedersoo, J. Menk, J. S. Schilling, and P. G. Kennedy. 2016. FUNGuild: An open annotation tool for parsing fungal community datasets by ecological guild. Fungal Ecology **20**:241-248.

Nilsson, R. H., K. H. Larsson, A. F. S. Taylor, J. Bengtsson-Palme, T. S. Jeppesen, D. Schigel, P. Kennedy, K. Picard, F. O. Glockner, L. Tedersoo, I. Saar, U. Koljalg, and K. Abarenkov. 2019. The UNITE database for molecular identification of fungi: handling dark taxa and parallel taxonomic classifications. Nucleic Acids Research **47**:D259-D264.

Oksanen, J., F. G. Blanchet, M. Friendly, R. Kindt, P. Legendre, D. McGlinn, P. R. Minchin, R. B. O'Hara, G. L. Simpson, P. Solymos, M. H. H. Stevens, E. Szoecs, and H. Wagner. 2018. vegan: Community ecology package. R package version 2.5-3.

Olsson-Francis, K., A. E. Simpson, D. Wolff-Boenisch, and C. S. Cockell. 2012. The effect of rock composition on cyanobacterial weathering of crystalline basalt and rhyolite. Geobiology **10**:434-444.

Omelon, C. R. 2008. Endolithic microbial communities in Polar Desert habitats. Geomicrobiology Journal **25**:404-414.

Ortiz-Álvarez, R., N. Fierer, A. de los Ríos, E. O. Casamayor, and A. Barberán. 2018. Consistent changes in the taxonomic structure and functional attributes of bacterial communities during primary succession The ISME Journal **12**:1658-1667.

Ortiz, Y., C. Restrepo, B. Vilanova-Cuevas, E. Santiago-Valentin, S. G. Tringe, and F. Godoy-Vitorino. 2020. Geology and climate influence rhizobiome composition of the phenotypically diverse tropical tree Tabebuia heterophylla. Plos One **15**:e0231083.

Osksanen, L., and E. Ranta. 1992. Plant strategies along mountain vegetation gradients: a test of two theories. Journal of Vegetation Science **3**:175-186.

Palarea-Albaladejo, J., and J. A. Martín-Fernández. 2015. zCompositions — R package for multivariate imputation of left-censored data under a compositional approach. Chemometrics and Intelligent Laboratory Systems **143**:85-96.

Parent, S. E., L. E. Parent, J. J. Egozcue, D. E. Rozane, A. Hernandes, L. Lapointe, V. Hebert-Gentile, K. Naess, S. Marchand, J. Lafond, D. Mattos, Jr., P. Barlow, and W. Natale. 2013. The plant ionome revisited by the nutrient balance concept. Front Plant Sci **4**:39.

Parent, S. E., L. E. Parent, D. E. Rozanne, A. Hernandes, and W. Natale. 2012. Nutrient balance as paradigm of soil and plant chemometrics.*in* R. N. Issaka, editor. Soil Fertility. IntechOpen.

Parker, A. 1970. An index of weathering for silicate rocks. Geological Magazine **107**:501-504.

Pedregosa, F., G. Varoquaux, A. Gramfort, V. Michel, B. Thirion, O. Grisel, M. Blondel, P. Prettenhofer, R. Weiss, V. Dubourg, J. Vanderplas, A. Passos, D. Cournapeau, M. Brucher, M. Perrot, and E. Duchesnay. 2011. Scikit-learn: machine learning in Python. Journal of Machine Learning Research **12**:2825-2830.

Peiffer, J. A., A. Spor, O. Koren, Z. Jin, S. G. Tringe, J. L. Dangl, E. S. Buckler, and R. E. Ley. 2015. Diversity and heritability of the maize rhizosphere microbiome under field conditions. PNAS **110**:6548-6553.

Philippot, L., J. M. Raaijmakers, P. Lemanceau, and W. H. van der Putten. 2013. Going back to the roots: the microbial ecology of the rhizosphere Pages 789–799. Nature reviews Microbiology.

Price, M. N., P. S. Dehal, and A. P. Arkin. 2010. FastTree 2-approximately maximum-likelihood trees for large alignments. Plos One **5**.

Prince, J. R., and M. A. Velbel. 2003. Chemical weathering indices applied to weathering profiles developed on heterogeneous felsic metamorphic parent rocks. Chemical Geology **202**:397-416.

Pruesse, E., C. Quast, K. Knittel, B. M. Fuchs, W. G. Ludwig, J. Peplies, and F. O. Glockner. 2007. SILVA: a comprehensive online resource for quality checked and aligned ribosomal RNA sequence data compatible with ARB. Nucleic Acids Research **35**:7188-7196.

Quast, C., E. Pruesse, P. Yilmaz, J. Gerken, T. Schweer, P. Yarza, J. Peplies, and F. O. Glockner. 2013. The SILVA ribosomal RNA gene database project: improved data processing and web-based tools. Nucleic Acids Research **41**:D590-D596.

Quirk, J., D. J. Beerling, S. A. Banwart, G. Kakonyi, M. E. Romero-Gonzalez, and J. R. Leake. 2012. Evolution of trees and mycorrhizal fungi intensifies silicate mineral weathering. Biology Letters **8**:1006-1011.

R Core Team. 2013. R: A language and environment for statistical computing. R Foundation for Statistical Computing, Vienna, Austria.

Reiche, P. 1950. A survey of weathering processes and products. University of New Mexico Press, Albuquerque.

Restrepo, C., L. R. Walker, A. B. Shiels, R. Bussmann, L. Claessens, S. Fisch, P. Lozano, G. Negi, L. Paolini, G. Poveda, C. Ramos-Scharrón, M. Richter, and E. Velázquez. 2009. Landsliding and Its Multiscale Influence on Mountainscapes. BioScience **59**:685-698.

Riebe, C. S., J. W. Kirchner, and R. C. Finkel. 2003. Long-term rates of chemical weathering and physical erosion from cosmogenic nuclides and geochemical mass balance. Geochimica Et Cosmochimica Acta **67**:4411-4427.

Roberts, D. W. 2016. Labdsv: ordination and multivariate analysis for ecology.

Roberts, J. A. 2004. Inhibition and enhancement of microbial surface colonization: the role of silicate composition. Chemical Geology **212**:313-327.

Rocha Filho, P., F. S. Antuenes, and M. F. G. Falcao. 1985. Quantitative influence of the weathering upon the mechanical properties of a young gneiss residual soil. First Int. Conf. Geomech. Trop. Lateric Sprolitic Soils Brasilia **1**:281-294.

Roeselers, G., M. C. van Loosdrecht, and G. Muyzer. 2007. Heterotrophic pioneers facilitate phototrophic biofilm development. Microbial Ecology **54**:578-585.

Rogers, J. R., and P. C. Bennett. 2004. Mineral stimulation of subsurface microorganisms: release of limiting nutrients from silicates. Chemical Geology **203**:91-108.

Rogers, J. R., P. C. Bennett, and W. J. Choi. 1998. Feldspars as source of nutrients for microorganisms. American Mineralogist **83**:1532-1540.

Rollerson, T., D. Maynard, S. Higman, and E. Ortmayr. 2004. Klanawa landslide hazard mapping pilot project. Pages 1-24 oint Conference of IUFRO 3.06 Forest Operations under Mountainous Conditions and the 12th International Mountain Logging Conference, Vancouver B.C.

Rousseau, R. M. 2001. Detection limit and estimate of uncertainty of analytical XRF results. The Rigaku Journal **18**:33-47.

Ruxton, B. P. 1968. Measures of the degree of chemical weathering of rocks. Journal of Geology **76**:518-527.

Ruxton, B. P., and L. Berry. 1957. The weathering of granite and associated erosional features in Hong Kong. Bulletin of the Geological Society of America **68**:1263-1292.

Sajinkumar, K. S., S. Anbazhagan, A. P. Pradeepkumar, and V. R. Rani. 2011. Weathering and landslide occurrences in parts of Western Ghats, Kerala. geological Society of India **78**:249-257.

Schulz, S., R. Brankatschk, A. Dumig, I. Kogel-Knabner, M. Schloter, and J. Zeyer. 2013. The role of microorganisms at different stages of ecosystem development for soil formation. Biogeosciences **10**:3983-3996.

Schwartzman, D. W. 2017. Life's critical role in the long-term carbon cycle: the biotic enhancement of weathering. AIMS Geosciences **3**:216-238.

Shi, Z., H. Yin, J. D. Van Nostrand, J. W. Voordeckers, Q. Tu, Y. Deng, M. Yuan, A. Zhou, P. Zhang, N. Xiao, D. Ning, Z. He, L. Wu, and J. Zhou. 2019. Functional

gene array-based ultrasensitive and quantitative detection of microbial populations in complex communities. Msystems **4**.

Singh, K. P., T. N. Mandal, and S. K. Tripathi. 2001. Patterns of restoration of soil physicochemical properties and microbial biomass in different landslide sites in the sal forest ecosystem of Nepal Himalaya. Ecological Engineering **17**:385-401.

Smith, A. L., J. H. Schellekens, and A. L. Muriel-Diaz. 1998. Batholiths as markers of tectonic change in the northeastern Caribbean. GSA Special Paper **322**:99-122.

Smits, M. M., S. Bonneville, L. G. Benning, S. A. Banwart, and J. R. Leake. 2012. Plant-driven weathering of apatite – the role of an ectomycorrhizal fungus Geobiology **10**:445–456.

Song, W., N. Ogawa, C. Takashima-Oguchi, T. Hatta, and Y. Matsukura. 2007. Effect of Bacillus subtilis on granite weathering: A laboratory experiment. Catena **70**:275-281.

Song, W., N. Ogawa, C. Takashima-Oguchi, T. Hatta, and Y. Matsukura. 2010. Laboratory experiments on bacterial weathering of granite and its constituent minerals. Géomorphologie: relief, processus, environnement **16**:327-336.

Sparling, G., G. Ross, N. Trustrum, G. Arnold, A. West, T. Speir, and L. Schipper. 2003. Recovery of topsoil characteristics after landslip erosion in dry hill country of New Zealand, and a test of the space-for-time hypothesis. Soil Biology and Biochemistry **35**:1575-1586.

Štyriaková, I., I. Štyriak, and H. Oberhänsli. 2012. Rock weathering by indigenous heterotrophic bacteria of Bacillus spp. at different temperature: a laboratory experiment. Mineral Petrology **105**:135-144.

Sugden, A. M., E. V. J. Tanner, and V. Kapos. 1985. Regeneration following clearing in a Jamaican montane forest: Results of a ten-year study. Journal of Tropical Ecology **1**:329-351.

Tang, J., Y. Mo, J. Zhang, and R. Zhang. 2011. Influence of biological aggregating agents associated with microbial population on soil aggregate stability. Applied Soil Ecology **47**:153-159.

Taylor, D. L., W. A. Walters, N. J. Lennon, J. Bochicchio, A. Krohn, J. G. Caporaso, and T. Pennanen. 2016. Accurate estimation of fungal diversity and abundance through improved lineage-specific primers optimized for Illumina amplicon sequencing. Applied and Environmental Microbiology **82**:7217-7226.

Taylor, L. L., J. R. Leake, J. Quirk, K. Hardy, S. A. Banwart, and D. J. Beerling. 2009. Biological weathering and the long-term carbon cycle: integrating mycorrhizal evolution and function into the current paradigm. Geobiology **7**:171-191.

Thorn, C. E., R. G. Darmody, J. C. Dixon, and P. Schlyter. 2002. Weathering rates of buried machine-polished rock disks, Karkevagge, Swedish Lapland. Earth Surf. Process. Landforms **27**:831-845.

Trustrum, N. A., and R. C. De Rose. 1988. Soil depth-age relationship of landslides on deforested hillslopes, Taranaki, New Zealand. Geomorphology **1**:143-160.

Turpault, M. P., C. Nys, and C. Calvaruso. 2009. Rhizosphere impact on the dissolution of test minerals in a forest ecosystem. Geoderma **153**:147-154.

Uhlig, D., J. A. Schuessler, J. Bouchez, J. L. Dixon, and F. Von Blanckenburg. 2017. Quantifying nutrient uptake as driver of rock weathering in forest ecosystems by magnesium stable isotopes. Biogeosciences **14**:3111-3128.

Ullman, W. J., D. L. Kirchman, S. A. Welch, and P. Vandevivere. 1996. Laboratory evidence for microbially mediated silicate mineral dissolution in nature. Chemical Geology **132**:11-17.

Uroz, S., C. Calvaruso, M.-P. Turpault, and P. Frey-Klett. 2009a. Mineral weathering by bacteria: ecology, actors and mechanisms. Trends in Microbiology **17**:378-387.

Uroz, S., C. Calvaruso, M. P. Turpault, J. C. Pierrat, C. Mustin, and P. Frey-Klett. 2007. Effect of the mycorrhizosphere on the genotypic and metabolic diversity of the bacterial communities involved in mineral weathering in a forest soil. Applied and Environmental Microbiology **73**:3019-3027.

Uroz, S., C. Calvaruso, M. P. Turpault, A. Sarniguet, W. de Boer, J. H. J. Leveau, and P. Frey-Klett. 2009b. Efficient mineral weathering is a distinctive functional trait of the bacterial genus Collimonas. Soil Biology and Biochemistry **41**:2178-2186.

Uroz, S., P. Oger, C. Lepleux, C. Collignon, P. Frey-Klett, and M.-P. Turpault. 2011. Bacterial weathering and its contribution to nutrient cycling in temperate forest ecosystems. Research in Microbiology **162**:820-831.

van den Boogaart, K. G. 2008. Using the R package "compositions".

van Scholl, L., T. W. Kuyper, M. M. Smits, R. Landeweert, E. Hoffland, and N. van Breemen. 2008. Rock-eating mycorrhizas: their role in plant nutrition and biogeochemical cycles. Plant and Soil **303**:35-47.

VanBuskirk, C. D., R. J. Neden, J. W. Schwab, and F. R. FSmith. 2005. Road and terrain attributes of road fill landslides in the Kalum Forest District. B.C. Ministry of Forests and Range, Province of British Columbia.

Vandevivere, P., S. A. Welch, W. J. Ullman, and D. L. Kirchman. 1994a. Enhanced dissolution of silicate minerals by bacteria at near-neutral pH. Microb Ecol **27**:241-251.

Vandevivere, P., S. A. Welch, W. J. Ullman, and D. L. Kirchman. 1994b. Enhanced dissolution of silicate minerals by bacteria at near-neutral pH. Microb Ecol **27**:241-251.

Visioli, G., S. D'Egidio, and A. M. Sanangelantoni. 2015. The bacterial rhizobiome of hyperaccumulators: future perspectives based on omics analysis and advanced microscopy. Frontiers in Plant Science **5**:1-12.

Vogt, T. 1927. Sulitjelmafeltets geologi og petrografi. Norges Geologiske Undersokelse **121**:1-560.

Volkmann, M., K. Whitehead, H. Rutters, J. Rullkotter, and A. A. Gorbushina. 2003. Mycosporine-glutamicol-glucoside: a natural UV-absorbing secondary metabolite of rock-inhabiting microcolonial fungi. Rapid Commun. Mass Spectrom. **17**:897-902.

Vuorinen, A., S. Mantere-Alhonen, R. Uusinoka, and P. Alhonen. 1981. Bacterial weathering of rapakivi granite. Geomicrobiology Journal **2**:317-325.

Wagner, M. R., D. S. Lundberg, T. G. del Rio, S. G. Tringe, J. L. Dangl, and T. Mitchell-Olds. 2016. Host genotype and age shape the leaf and root microbiomes of a wild perennial plant. Nature Communications **7**:1-15.

Walker, J. J., and N. R. Pace. 2007. Endolithic microbial ecosystems. Annu Rev Microbiol **61**:331-347.

Walker, L. R. 1994. Effects of fern thickets on woodland development on landslides in Puerto-Rico. Journal of Vegetation Science **5**:525-532.

Walker, L. R., and A. B. Shiels. 2008. Post-disturbance erosion impacts carbon fluxes and plant succession on recent tropical landslides Plant Soil **313**:205-216.

Wallander, H., L. O. Nilsson, D. Hagerberg, and E. Bååth. 2001. Estimation of the biomass and seasonal growth of external mycelium of ectomycorrhizal fungi in the field. New Phytol **151**:753–760.

Wang, G., J. Li, X. Liu, and L. X. 2013. Variations in carbon isotope ratios of plants across a temperature gradient along the 400 mm isoline of mean annual precipitation in north China and their relevance to paleovegetation reconstruction. Quaternary Science Reviews **63**:83-90.

Warscheid, T., and J. Braams. 2000. Biodeterioration of stone: a review. International Biodeterioration & Biodegradation **46**:343-368.

Weaver, P. L. 1979. Tree growth in several tropical forests of Puerto Rico. U.S. Dept. of Agriculture, Forest Service, Southern Forest Experiment Station, New Orleans, La.

Welch, S. A., W. W. Barker, and J. F. Banfield. 1999. Microbial extracellular polysaccharides and plagioclase dissolution. Geochimica Et Cosmochimica Acta **63**:1405-1419.

Welch, S. A., A. E. Taunton, and J. F. Banfield. 2002. Effect of microorganisms and microbial metabolites on apatite dissolution. Geomicrobiology Journal **19**:343-367.

Welch, S. A., and W. J. Ullman. 1993. The effect of organic acids on plagioclase dissolution rates and stoichiometry. Geochimica Et Cosmochimica Acta **57**:2725-2736.

Wickham, H. 2016. ggplot2: Elegant Graphics for Data Analysis. Springer-Verlag, New York.

Wickham, H., M. Averick, J. Bryan, W. Chang, L. D. McGowan, R. François, G. Grolemund, A. Hayes, L. Henry, J. Hester, M. Kuhn, T. L. Pedersen, E. Miller, S. M. Bache, K. Müller, J. Ooms, D. Robinson, D. P. Seidel, V. Spinu, K. Takahashi, D. Vaughan, C. Wilke, K. Woo, and H. Yutani. 2019. Welcome to the tidyverse. Journal of Open Source Software **4**:1686.

Wilford, J. 2012. A weathering intensity index for the Australian continent using airborne gamma-ray spectrometry and digital terrain analysis. Geoderma **183-184**:124-142.

Wills, C. J., M. W. Manson, K. D. Brown, C. W. Davenport, and C. J. Domrose. 2001. Landslides in the Highway 1 corridor: Geology and slope stability along the Big Sur coast between Point Lobos and San Carpoforo Creek, Monterey and San Luis Obispo counties, California. California Department of Transportation.

Wojcik, R., J. Donhauser, B. Frey, and L. G. Benning. 2020. Time since deglaciation and geomorphological disturbances determine the patterns of geochemical, mineralogical and microbial successions in an Icelandic foreland. Geoderma **379**:1-14.

Wood, J. L., and A. E. Franks. 2018. Understanding microbiomes through trait-based ecology. Microbiology Australia **39**:53-55.

Wood, J. L., C. Tang, and A. E. Franks. 2018. Competitive traits are more important than stress-tolerance traits in a cadmium-contaminated rhizosphere: a role for trait theory in microbial ecology. Frontiers in Microbiology **9**:1-12.

Wu, L., A. D. Jacobson, and M. Hausner. 2008. Characterization of elemental release during microbe–granite interactions at T=28°C. Geochimica Et Cosmochimica Acta **72**:1076-1095.

Yeoh, Y. K., P. G. Dennis, C. Paungfoo-Lonhienne, L. Weber, R. Brackin, M. A. Ragan, S. Schmidt, and P. Hugenholtz. 2017. Evolutionary conservation of a core root

microbiome across plant phyla along a tropical soil chronosequence. Nature Communications **8**:1-9.

Yilmaz, P., L. W. Parfrey, P. Yarza, J. Gerken, E. Pruesse, C. Quast, T. Schweer, J. Peplies, W. Ludwig, and F. O. Glockner. 2014. The SILVA and "All-species Living Tree Project (LTP)" taxonomic frameworks. Nucleic Acids Research **42**:D643-D648.

Zhalnina, K., K. B. Louie, Z. Hao, N. Mansoori, U. Nunes da Rocha, S. Shi, H. Cho, U. Karaoz, D. Loqué, B. P. Bowen, M. K. Firestone, T. R. Northen, and E. L. Brodie. 2018. Dynamic root exudate chemistry and microbial substrate preferences drive patterns in rhizosphere microbial community assembly. Nature Microbiology **3**:470 - 480.

Zumsteg, A., J. Luster, H. Göransson, R. H. Smittenberg, I. Brunner, S. M. Bernasconi, J. Zeyer, and B. Frey. 2012. Bacterial, archaeal and fungal succession in the forefield of a receding glacier. Microbial Ecology **63**:552-564.

TABLES

Table 2.1. Plant species sampled in forest and landslide-like habitats. The numbers represent the number of individuals sampled for each species. Three root and three soil samples were taken for individual.

			Landslide		Forest	
Lifeform	**Family**	**Species**	**Site 1**	**Site 2**	**Site 1**	**Site 2**
Herbaceous fern	Gleicheniaceae	*Gleichenia bifida*	2	-	-	-
Herbaceous fern	Gleicheniaceae	*Dicranopteris pectinata*	-	2	-	-
Herbaceous fern	Dennstaedtiaceae	*Dennstaedtia dissecta*	-	-	2	2
Tree fern	Cyatheaceae	*Cyathea arborea*	2	2	-	-
Tree fern	Cyatheaceae	*Cyathea pungens*	-	-	2	2
Shrub 1	Melastomataceae	*Tetrazygia crotonifolia*	2	2	-	-
Shrub 1	Melastomataceae	*Ossea krugiana*	-	-	2	-
Shrub 1	Melastomataceae	*Miconia affinis*	-	-	-	2
Shrub 2	Primulaceae	*Myrsine coriacea*	2	2	-	-
Shrub 2	Thymelaeaceae	*Daphnopsis philippiana*	-	-	2	1
Shrub 2	Myrtaceae	*Eugenia stahli*	-	-	-	1

Table 2.2. Results of two-way ANOVAs for soil attributes across habitats and plant host lifeform.

	Habitat (H)		**Plant lifeform (Lf)**		**H x Lf**	
Df	**1**		**2**		**2**	
	SS	**F**	**SS**	**F**	**SS**	**F**
Isotopes						
$\delta^{13}C$	113.33	66.31***	5.57	1.63	2.48	0.72
$\delta^{15}N$	8.33	9.81**	2.02	1.19	1.42	0.84
CLR - Nutrients						
Fe	0.20	69.51***	0.01	1.71	0.00	0.03
K	0.27	32.49***	0.01	0.79	0.00	0.09
Mn	0.22	5.27*	0.05	0.66	0.02	0.28
Orthonormal Balances						
V1	0.00	0.09	0.09	2.23	0.08	2.01
V2	0.00	0.49	0.01	1.33	0.00	0.19
V8	0.20	2.98 .	0.14	1.05	0.07	0.52
V11	3.57	10.34**	0.05	0.07	1.00	1.45
Weathering Index						
CIW	154.48	21.13***	48.53	3.32 .	25.69	1.76

*** $P \leq 0.001$; ** $P \leq 0.01$; * $P \leq 0.05$; . $P \leq 0.10$

Table 2.3. Results of a three-way ANOVAs for 16S and ITS diversity metrics across habitats, microhabitats and lifeform. Values are F values.

		16S		*ITS*	
	Df	**Richness**	**Diversity**	**Richness**	**Diversity**
Habitat (H)	1	15.69***	46.51***	0.67	0.07
Microhabitat (Mh)	1	1.85	10.75**	0.48	0.03
Lifeform (Lf)	2	7.32***	3.59*	1.36	0.48
H x Mh	1	0.83	0.57	0.13	1.26
H x Mh x Lf	4	0.53	0.34	1.32	0.84

*** $p < 0.001$; ** $p < 0.01$; * $p < 0.05$; . $p < 0.10$

Table 2.4. Results of a PERMANOVA testing the effect of habitat, microhabitat, and plant lifeform on microbial community composition.

		16S				***ITS***			
		Bray		**Aitchison**		**Bray**		**Aitchison**	
	Df	$\mathbf{R^2}$	***F***	$\mathbf{R^2}$	***F***	$\mathbf{R^2}$	***F***	$\mathbf{R^2}$	***F***
Habitat (H)	1	0.23	21.54^{***}	0.18	15.36^{***}	0.14	10.56^{***}	0.13	9.30^{***}
Microhabitat (Mh)	1	0.07	6.51^{***}	0.05	4.04^{***}	0.04	2.72^{***}	0.03	1.87^{**}
Plant Lifeform (Lf)	2	0.05	2.16^{**}	0.05	2.28^{**}	0.04	1.35^{*}	0.04	1.29^{*}
H x Mh	7	0.02	1.85^{*}	0.02	1.46 .	0.02	1.73^{*}	0.02	1.25 .
H x Mh x Lf	1	0.06	0.97	0.07	1.03	0.08	0.97	0.08	0.94

*** $p < 0.001$; ** $p < 0.01$; * $p < 0.05$; **.** $p < 0.10$

Table 2.5. Pearson correlation coefficients between Shannon diversity index with soil variables.

	16S			***ITS***		
	Both	**Landslide**	**Forest**	**Both**	**Landslide**	**Forest**
Isotopes						
$\delta^{13}C$	-0.64***	-0.30	0.22	-0.08	-0.30 .	-0.03
$\delta^{15}N$	0.38*	0.03	0.08	-0.23 .	-0.43*	-0.01
CLR-Nutrients						
Fe	-0.67***	-0.15	-0.25	0.08	-0.05	0.32 .
K	0.67***	0.10	0.65**	0.11	0.36*	0.00
Mn	0.55**	0.25	0.47 .	0.25*	0.11	0.38*
Orthonormal balances						
V1	-0.07	0.02	-0.21	-0.05	-0.02	-0.07
V2	-0.14	-0.07	-0.06	-0.06	-0.38*	0.20
V8	-0.33 .	-0.18	-0.18	-0.10	0.28	-0.45**
V11	-0.24	0.09	0.31	-0.07	-0.02	-0.18
Weathering Index						
CIW	-0.56**	-0.29	-0.24	-0.09	0.03	-0.19

*** $p < 0.001$; ** $p < 0.01$; * $p < 0.05$; . $p < 0.10$

Table 2.6. Brite hierarchy classification of differentially abundant KOs. Bold and plain text belong to the first and second level of the Brite classification, respectively.

	Forest		Landslide	
	Count	**%**	**Count**	**%**
Cellular Processes	**0**	**0.00**	**1**	**0.02**
Cellular community	0	0.00	1	0.02
Environmental Information Processing	6	0.02	1	0.02
Membrane transport	3	0.01	1	0.02
Signal transduction	3	0.01	0	0.00
Genetic Information Processing	**133**	**0.53**	**4**	**0.09**
Folding, sorting and degradation	11	0.04	0	0.00
Replication and repair	23	0.09	0	0.00
Transcription	18	0.07	3	0.07
Translation	73	0.29	1	0.02
Others	8	0.03	0	0.00
Metabolism	**72**	**0.29**	**24**	**0.55**
Amino acid metabolism	4	0.02	1	0.02
Biosynthesis of other secondary metabolites	1	0.00	0	0.00
Carbohydrate metabolism	10	0.04	12	0.27
Energy metabolism	17	0.07	0	0.00
Glycan biosynthesis and metabolism	4	0.02	0	0.00
Lipid metabolism	4	0.02	0	0.00
Metabolism of cofactors and vitamins	14	0.06	0	0.00
Metabolism of other amino acids	2	0.01	1	0.02
Metabolism of terpenoids and polyketids		0.00	3	0.07
Nucleotide metabolism	1	0.00	0	0.00
Xenobiotics biodegradation and metabolism	1	0.00	1	0.02
Others	14	0.06	6	0.14
Organismal systems	**1**	**0.00**	**0**	**0.00**
Others	1	0.00	0	0.00
Signaling and Cellular Processes	**15**	**0.06**	**12**	**0.27**
Others	15	0.06	12	0.27
Uncharacterized protein	**24**	**0.10**	**2**	**0.05**
Total	*251*		*44*	

Figure 2.1. Map of study area. Site 1 (circles) and Site 2 (triangles). Forests (black filled symbol) and landslide-like areas (open symbol). Green line limits of the Toro Negro State Forest protected area. Granodiorite shown in light green. Road PR-143 cuts through the area.

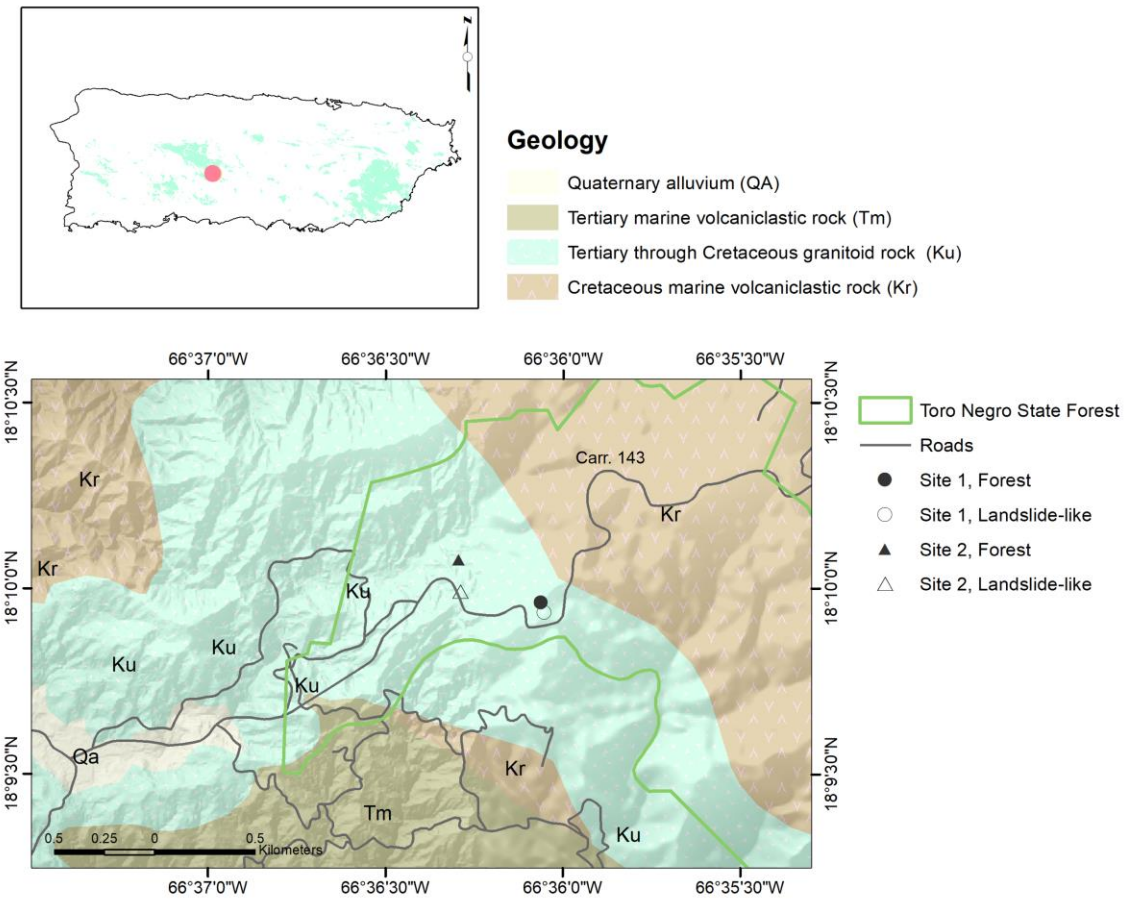

Figure 2.2. Mean soil attributes across habitat and plant lifeform.

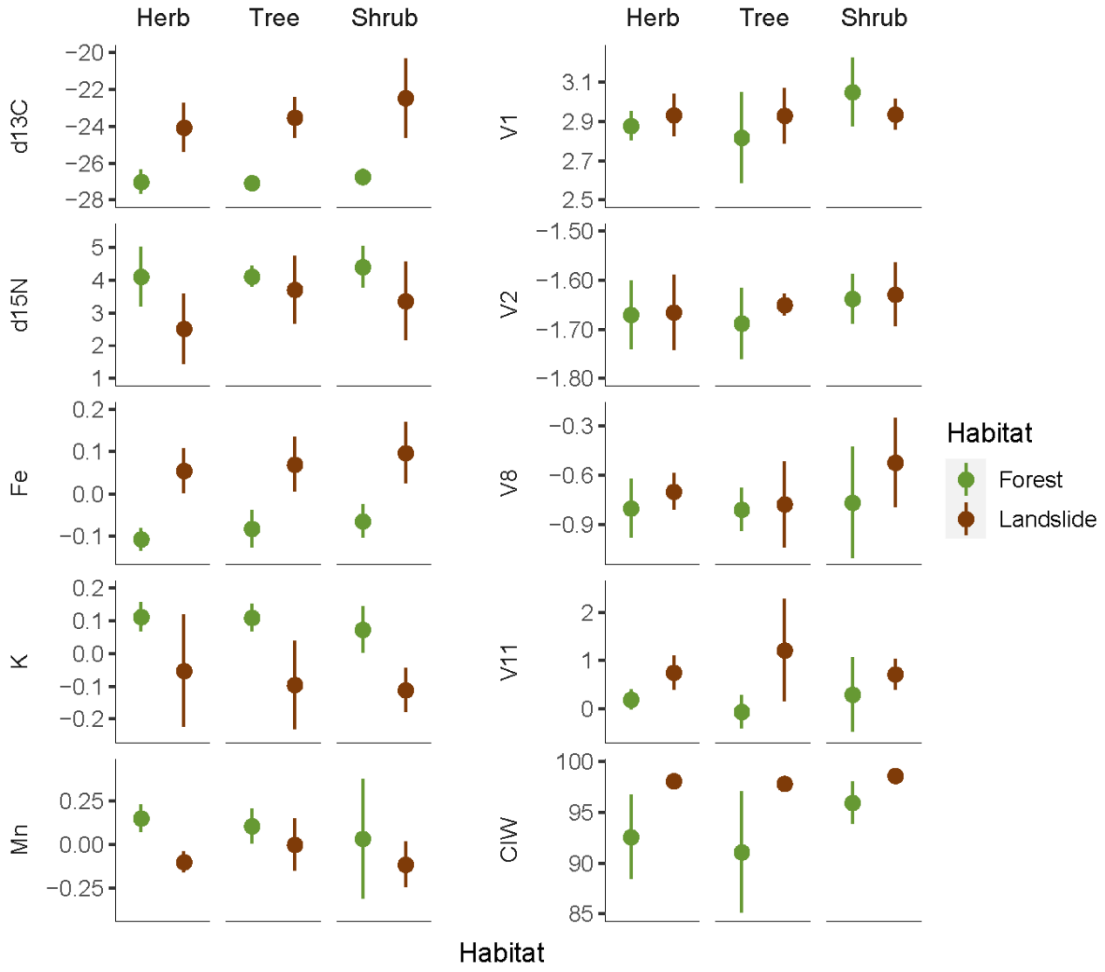

Figure 2.3. Mean species richness and species diversity for *16S* and *ITS* ASVs in forest and landslides across plant lifeform and microhabitats.

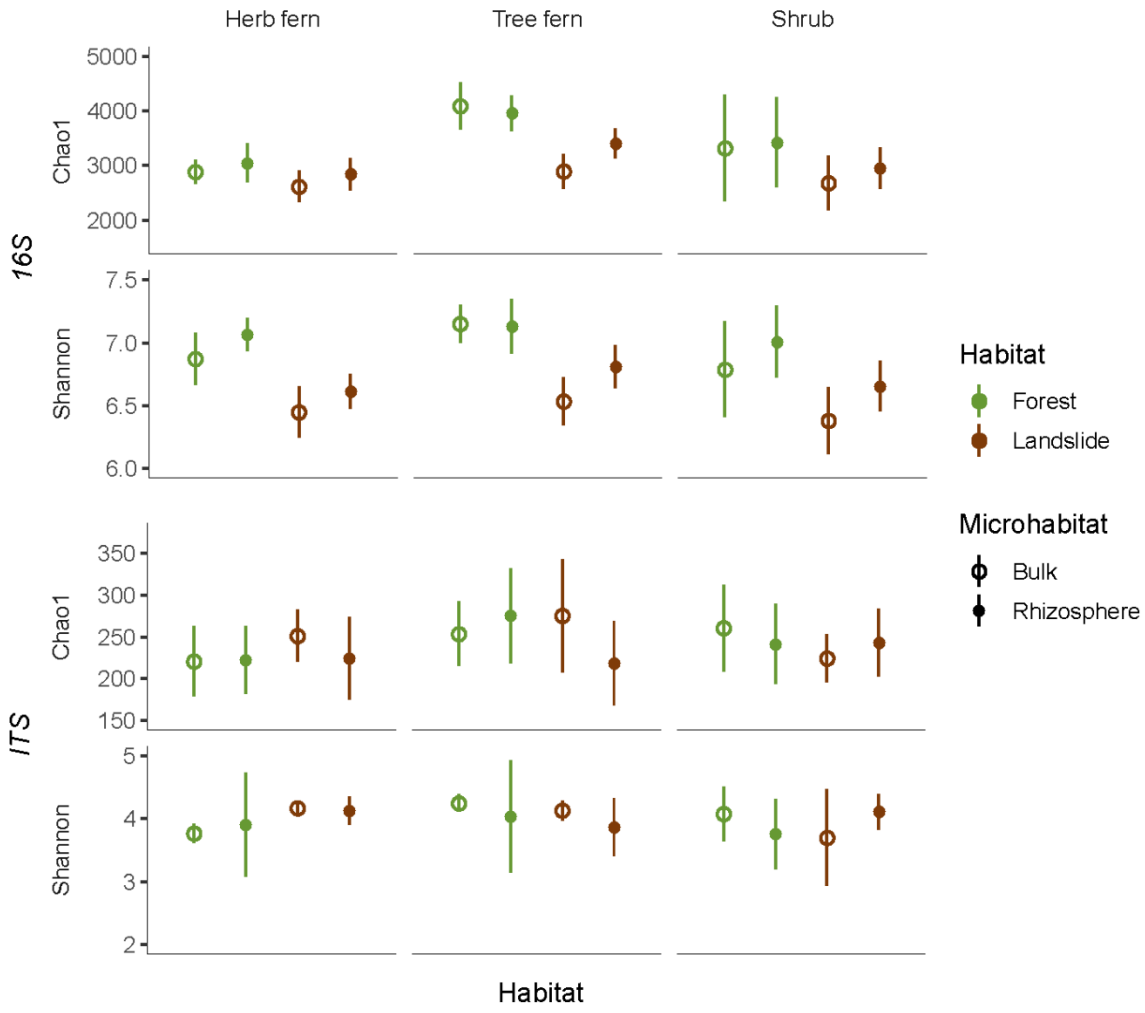

Figure 2.4. Taxonomic composition at phylum-level bacteria, archaea and fungi across habitats, microhabitats, and plant species. Phyla with < 1% relative abundance were excluded.

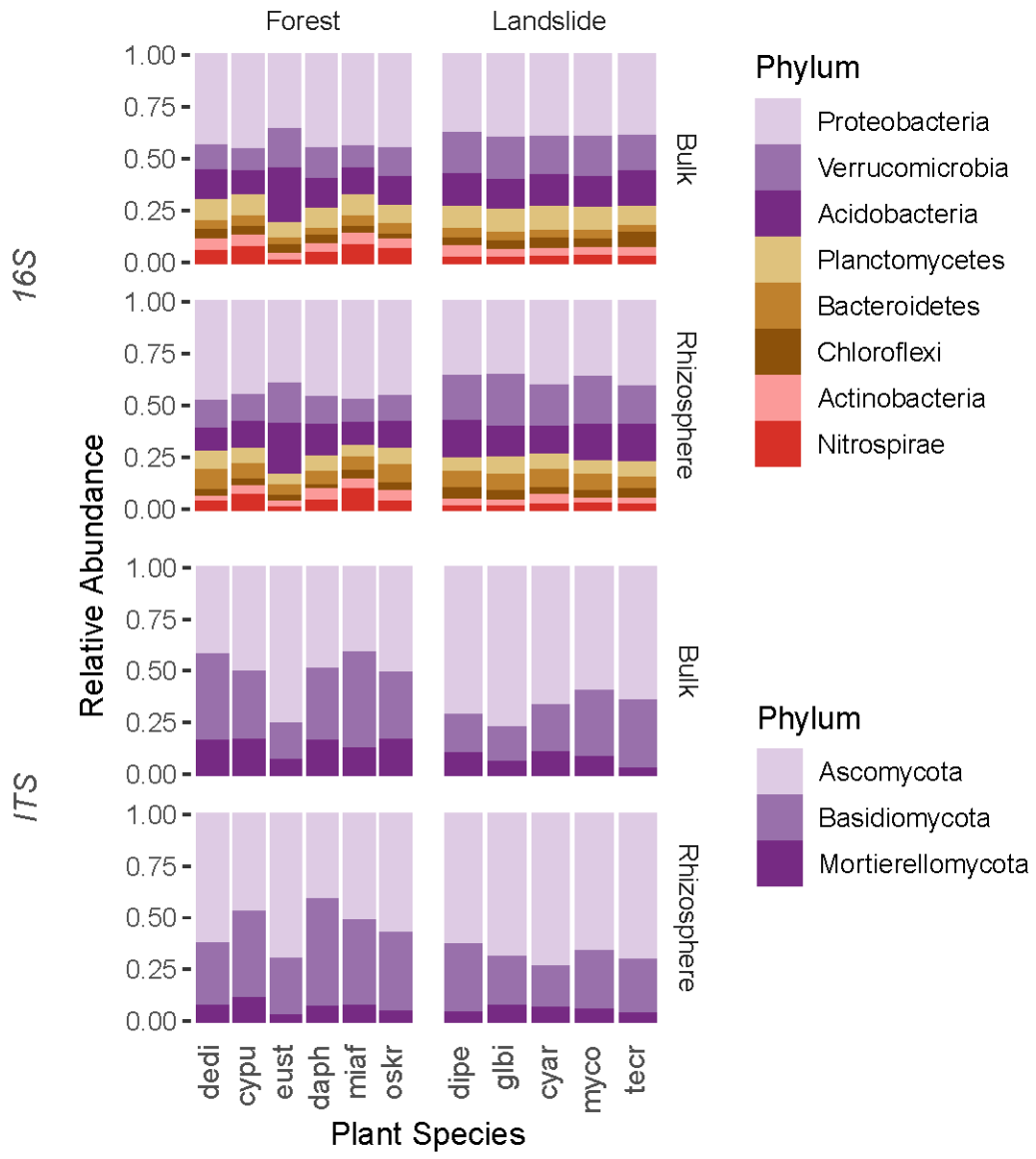

Figure 2.5. Extended Venn Diagram of indicator species.

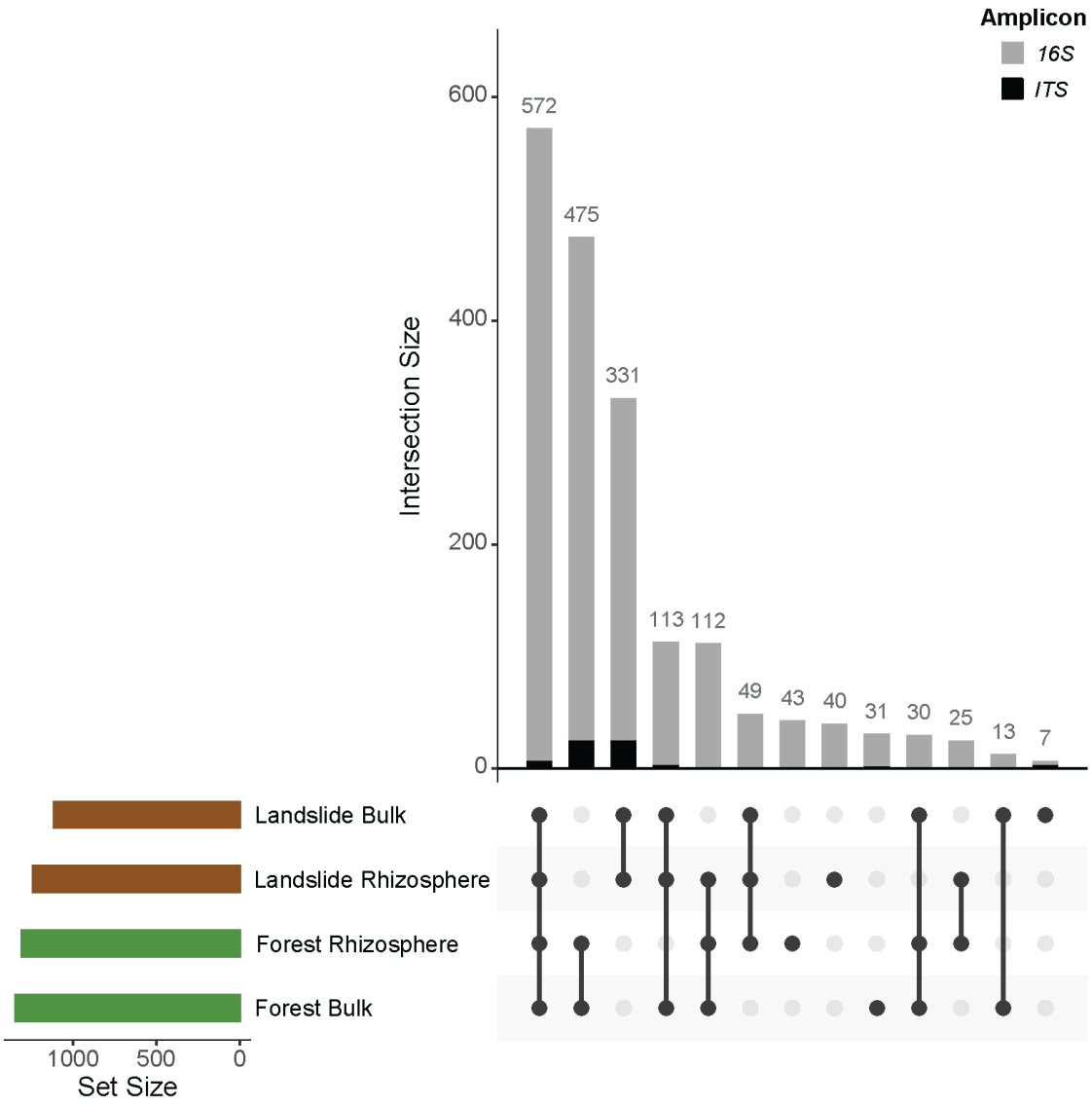

Figure 2.6. Mean CLR-transformed abundances of most differentially abundant taxa between habitats. Differentially abundant ASVs are identified by the phylum and the lowest taxonomical classification available.

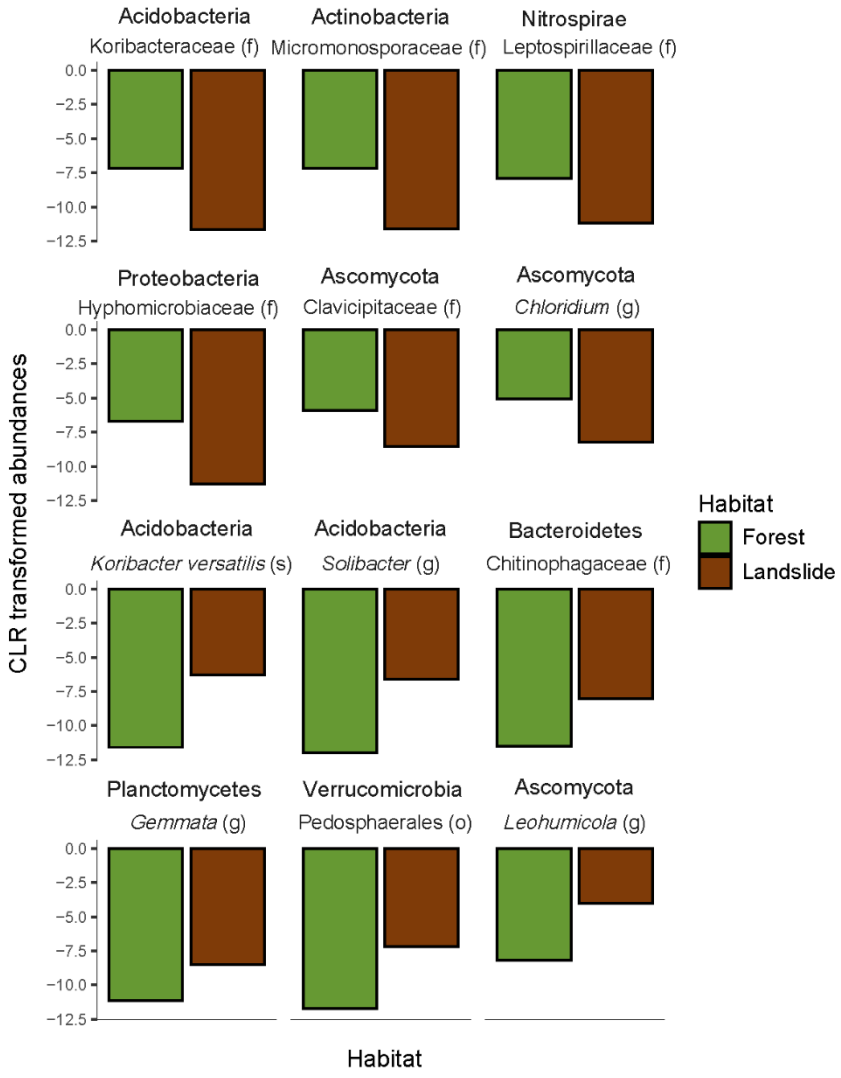

Figure 2.7. NMDS ordination based on the Bray-Curtis distances for *16S* and *ITS*.

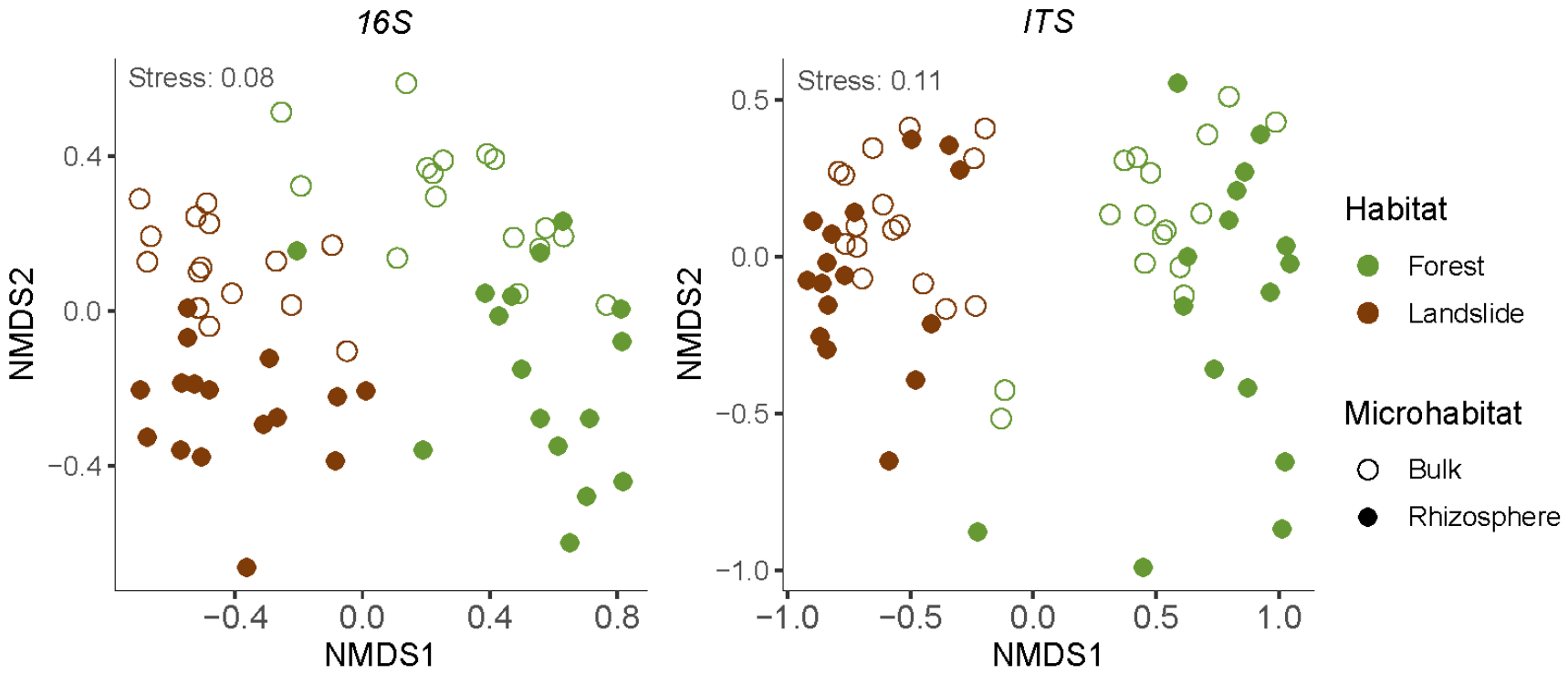

Figure 2.8. Pearson correlation coefficients between Shannon diversity index and soil attributes per habitat.

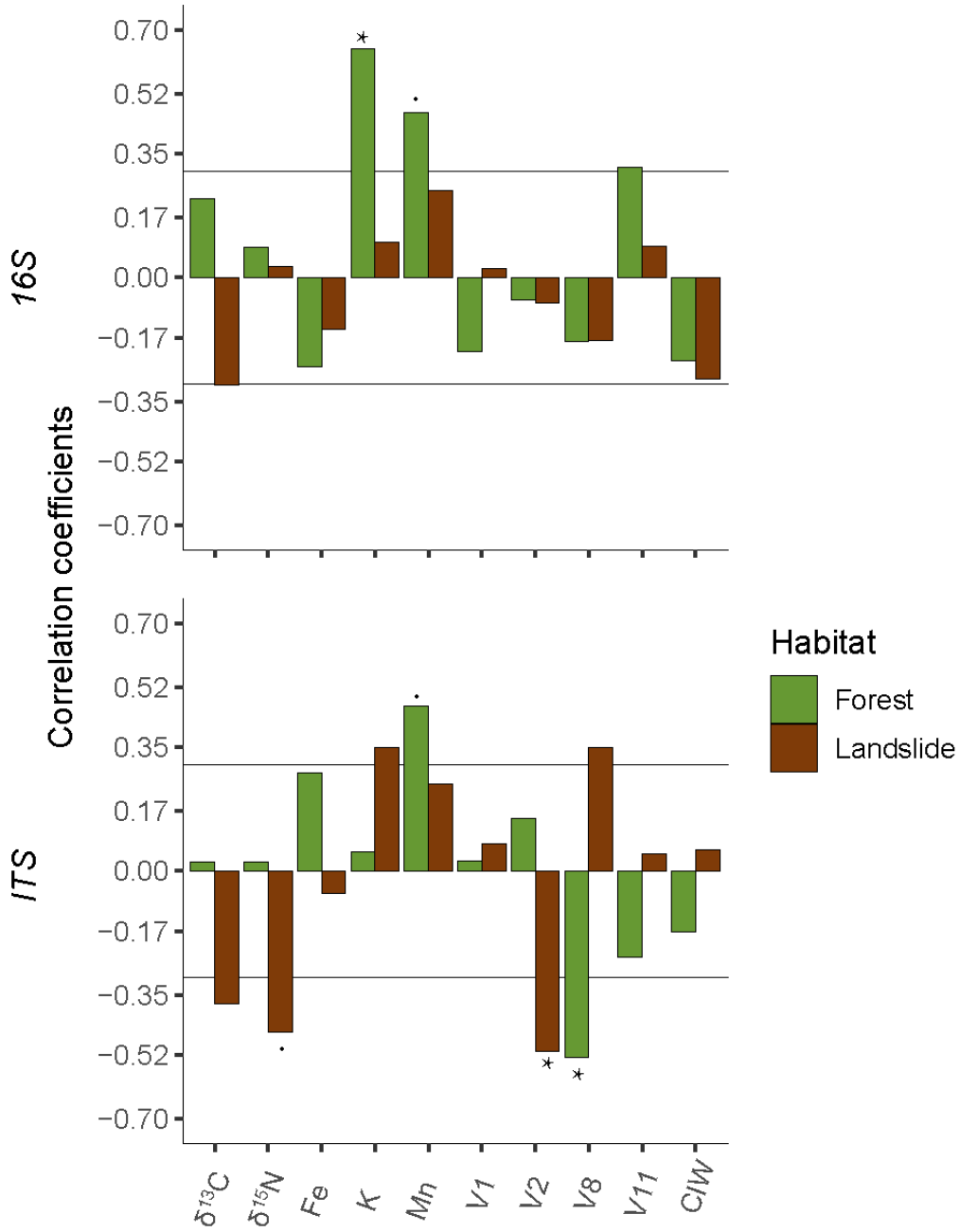

Figure 2.9. NMDS ordination based on the Bray-Curtis distance *16S* and *ITS* without distinguishing between microhabitats. Variables in bold were significative ($p < 0.05$) on the *envfit* test (Vegan R package) and the length of the arrow represents the r^2 value.

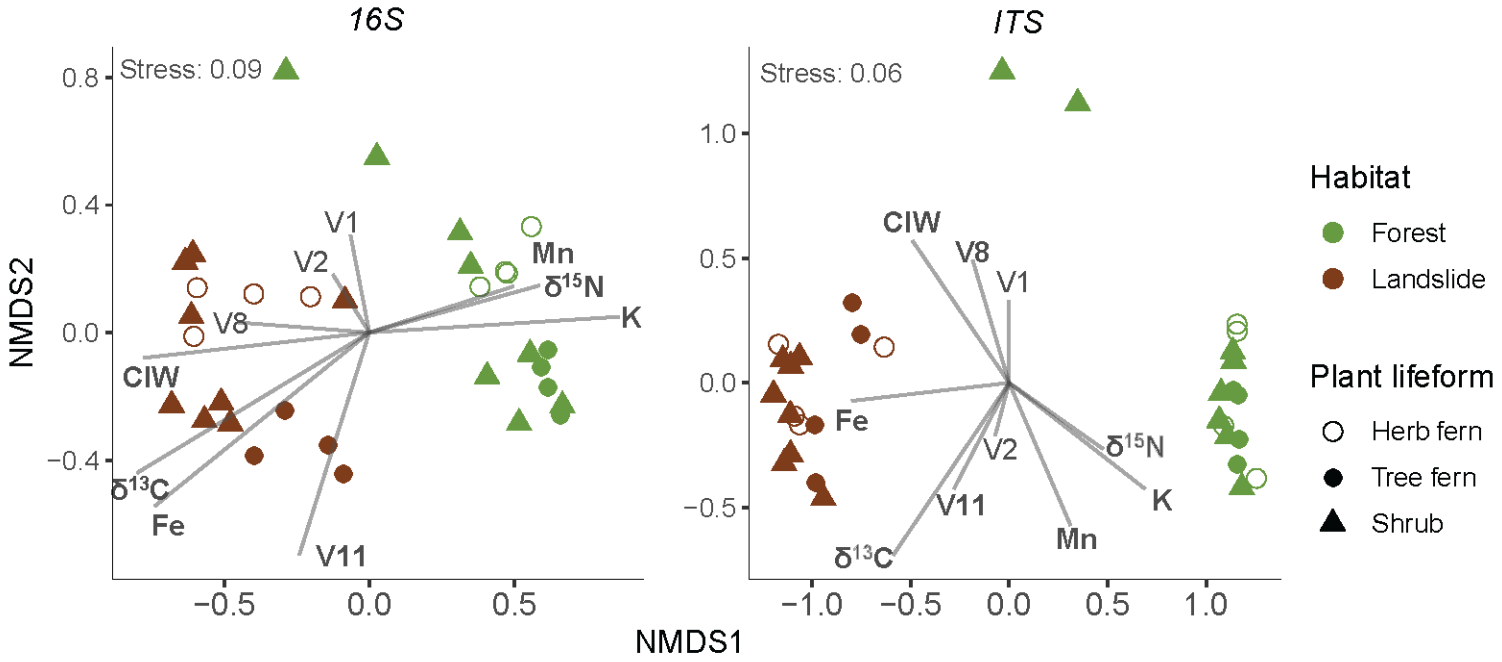

Figure 2.10. Mean CLR-transformed abundances of differentially abundant fungal guilds across habitats.

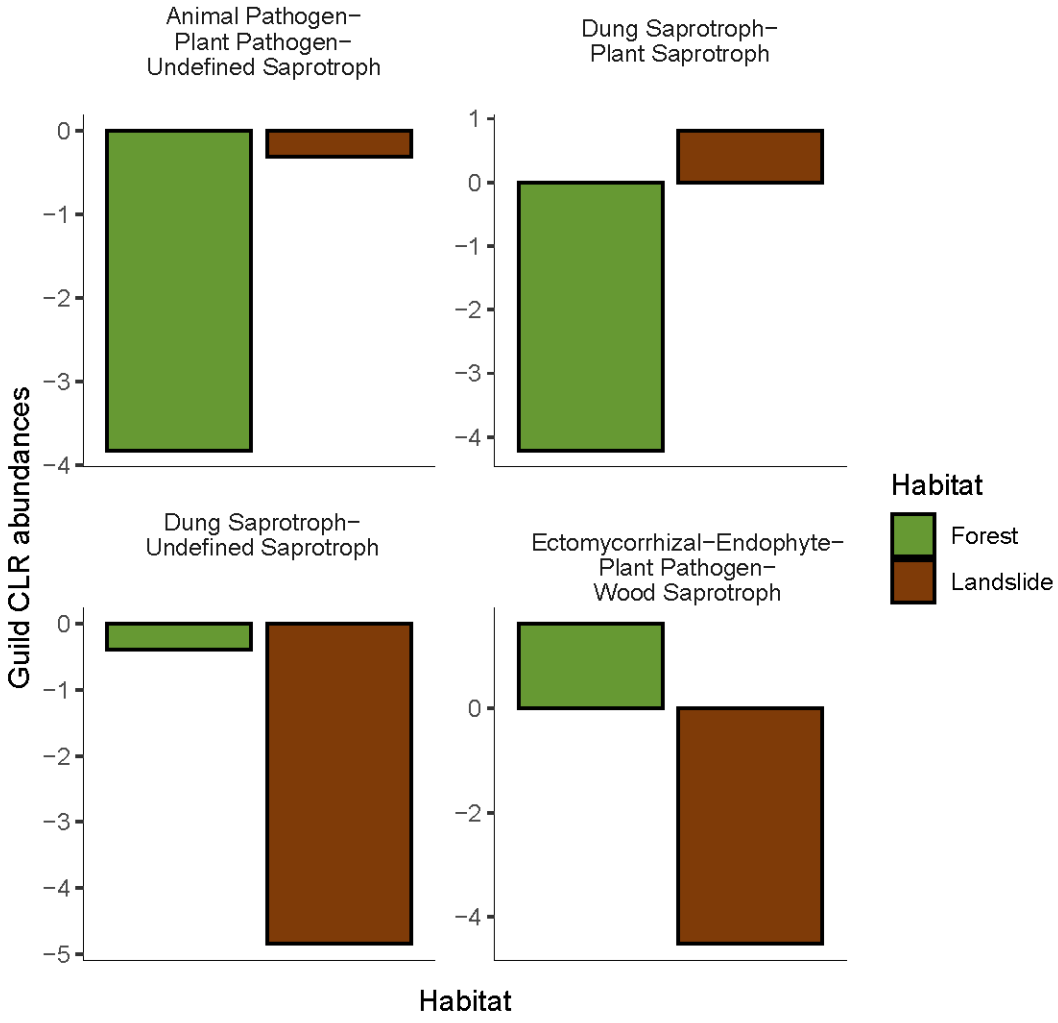

SUPPLEMENTARY TABLES AND FIGURES

Table S2.1. Average concentration of elements in granitic rocks of the Utuado pluton. Major and minor elements are given in weight %, while trace elements (Fe^{3+} – Cd) are given in ppm (Adapted from Chen 1967).

	Granodiaorite		Diorite	
Element	Mean	Sd	Mean	Sd
Al	8.10	0.49	9.50	0.87
Ca	3.05	0.52	5.76	1.11
Fe_T	3.70	0.77	5.55	0.62
K	2.40	0.51	0.70	0.35
Mg	1.44	0.37	2.22	0.33
Na	2.57	0.22	2.09	0.45
Si	29.45	4.26	24.75	1.72
Ti	0.38	0.23	0.37	0.08
Mn	0.08	0.02	1.47	0.04
Fe^{3+}	3.70	0.77	5.55	0.61
Sr	172.27	27.71	181.75	11.39
Ni	53.33	12.61	51.57	5.26
Rb	87.89	29.88	22.00	4.00
Co	12.66	2.37	13.80	1.93
Li	5.40	2.66	7.53	1.73
Cd	0.23	0.04	0.29	0.03

Table S2.2. Soil and rock standards used to calibrate a quantitative application using WDXRF spectroscopy. Soil/rock type and sampling location are included.

Standard	Name	Location
GSP-2	Granodiorite	Colorado, USA
BHVO-2	Basalt	Hawaii, USA
BCR-2	Basalt	Oregon, USA
RGM-2	Rhyolite	California, USA
AGV-2	Andesite	Oregon, USA
DTS-2b	Dunite	Washington, USA
NOD-A-1	Manganese Module	Atlantic Ocean
SDC-1	Mica Schist	Washington DC, USA
SBC-1	Shale	Pennsylvania, USA
STM-2	Syenite	Oregon, USA
SRM2709a	San Joaquin Soil	California, USA
SRM2711	Montana Soil	Montana, USA
JG-2	Japan Granite	Japan
JP-1	Peridotite	Japan
VS2124-81	Lujavrite	Russia

Table S2.3. Selected parameters for quantitative elemental composition measurements per element using WDXRF spectroscopy.

Analyte	Unit	Element line	Target method	Kv-ma	Filter	Slit	Crystal	Detector	Peak (deg)	Time (sec)	Bg1 (deg)	Bg2 (deg)	Pha1	Pha2
Al_2O_3	Mass%	Ka	Rh	30-120	Out	S4	PET	PC	144.770	40	139.000	148.000	120	280
CaO	Mass%	Ka	Rh	40-90	Out	S4	LIF(200)	PC	113.124	40	110.000	116.000	120	280
Fe_2O_3	Mass%	Ka	Rh	60-60	Out	S2	LIF(200)	SC	57.476	20	55.500	59.000	100	330
K_2O	Mass%	Ka	Rh	40-90	Out	S4	LIF(200)	PC	136.674	40	134.000	140.000	130	270
MgO	Mass%	Ka	Rh	30-120	Out	S4	RX25	PC	38.450	40	-	41.000	100	300
Na_2O	Mass%	Ka	Rh	30-120	Out	S4	RX35	PC	25.554	40	-	28.000	120	300
P_2O_5	Mass%	Ka	Rh	30-120	Out	S4	GE	PC	141.060	40	138.000	144.000	100	300
SiO_2	Mass%	Ka	Rh	30-120	Out	S4	PET	PC	109.030	40	106.000	112.000	100	300
TiO_2	Mass%	Ka	Rh	60-60	Out	S2	LIF(200)	SC	86.110	20	84.000	88.000	100	330
MnO	Mass%	Ka	Rh	60-60	Out	S2	LIF(200)	SC	62.950	20	60.000	65.000	80	320

Table S2.4. Quality indicators of instrument stability, precision, and accuracy in major oxides measurement.

Analyte	**C_{cert} (Wt %)**	**$\overline{C_i}$ (Wt %)**	**SD**	**ILD (Wt%)**	**RSD (%)**	**Q_i (%)**
Al_2O_3	15.80	15.59	0.05	0.22	0.33	0.01
CaO	1.40	1.49	0.01	0.09	0.38	0.07
Fe_2O_3	6.32	6.30	0.10	0.06	1.61	0.01
K_2O	3.28	3.25	0.01	0.07	0.37	0.01
MgO	1.69	1.64	0.03	0.51	1.93	0.03
Na_2O	2.05	2.29	0.01	0.31	0.46	0.12
P_2O_5	0.16	0.19	0.00	0.10	2.22	0.17
SiO_2	65.80	65.32	0.41	0.40	0.63	0.01
TiO_2	1.01	1.02	0.04	0.14	3.90	0.03
MnO	0.11	0.11	0.00	0.07	2.90	0.04

C_{cert} is the certified value of the SDC-1 reference material; $\overline{C_i}$ is the analyte mean concentration measured in 21 repetition; ILD is the Instrument Limit of Detection of each analyte; RSD is the Relative Standard Deviation of each analyte; Q is the Relative Bias of each analyte.

Table S2.5. Number of bacterial, archaeal, and fungal sequences and ASVs before and after rarefying to even depth for each grouping. G1 – replicates were grouped by individual while maintaining the microhabitats separately; G2 – replicates were grouped by individual without differentiating between microhabitats.

	Processing step	**Group**	**B Bacteria**	**A Archaea**	***16S* B+A**	***ITS* Fungi**
Sequences	Raw		7,944,350	31,855	8,015,551	3,544,081
	FS 1		5,097,156	21,900	5,119,056	3,440,387
	FS 2	G1	4,897,650	19,489	4,917,139	2,924,200
	Rarefied	G1	1,857,818	7,846	1,865,664	777,280
	FS 2	G2	4,869,493	19,315	4,888,808	2,774,392
	Rarefied	G2	1,903,977	7,575	1,911,552	1,261,120
Seqs per sample	Raw		44,135	177	44,530	53,698
	FS 1		28,317	122	28,439	53,756
	FS 2	G1	76,525	304	76,830	45,690
	Rarefied	G1	29,028	122	29,151	12,145
	FS 2	G2	152,171	603	152,775	86,699
	Rarefied	G2	59,499	237	59,736	39,410
ASVs	Raw		114,827	638	129,795	7,866
	FS 1		41,672	357	42,029	7,836
	FS2	G1	10,082	66	10,148	1,714
	Rarefied	G1	10,081	66	10,147	1,714
	FS 2	G2	9,608	64	9,672	1,491
	Rarefied	G2	9,608	64	9,672	1,491
Phyla	Raw		52	3	55	15
	FS 1		27	3	29	15
	FS 2	G1	18	2	20	11
	Rarefied	G1	18	2	20	11
	FS 2	G2	18	2	20	15
	Rarefied	G2	18	2	20	10

Filtering step (FS 1) 1 consisted of removing unidentified, chloroplast and mitochondria associated sequences for *16S* and removing contaminant sequences for *ITS*. Filtering step 2 (FS 2) consisted of filtering ASVs by abundance (minimum read 11) and occurrence (minimum samples 4).

Table S2.6. Weathering indexes used in this study. Adapted from (Prince and Velbel 2003). OFV is the Optimal Fresh Value; OWV is the Optimal Weathered Value

Index	Formula	OFV	OWV	Reference
Chemical Index of Alteration (CIA)	$100\ x\ \left(\frac{Al_2O_3}{Al_2O_3 + CaO +\ Na_2O + K_2O}\right)$	<50	100	(Nesbitt and Young 1982)
Chemical Index of Weathering (CIW)	$100\ x\ \left(\frac{Al_2O_3}{Al_2O_3 + CaO + Na_2O}\right)$	<50	100	(Harnois 1988)
Plagioclase Index of Alteration (PIA)	$100\ x\ \left(\frac{Al_2O_3 -\ K_2O}{Al_2O_3 + CaO + Na_2O -\ K_2O}\right)$	<50	100	(Fedo et al. 1995)
Vogt (V)	$\frac{Al_2O_3 + K_2O}{MgO + CaO + Na_2O}$	<1	∞	(Vogt 1927)
Product of Weathering Index (PWI)	$100\ x\ \left(\frac{SiO_2}{TiO_2 +\ Fe_2O_3 +\ SiO_2 +\ Al_2O_3}\right)$	>50	0	(Reiche 1950)
Ruxton Ratio (RR)	$RR = \frac{SiO_2}{Al_2O_3}$	>10	0	(Ruxton 1968)
Silica-Titania Index (STI)	$100\ x\ \left(\frac{\left({}^{SiO_2}/_{TiO_2}\right)}{\left({}^{SiO_2}/_{TiO_2}\right) + \left({}^{SiO_2}/_{Al_2O_3}\right) + \left({}^{Al_2O_3}/_{TiO_2}\right)}\right)$	>90	0	(Jayawardena and Izawa 1994b)
Si/SiAlFe (S.SAF)	$100\ x\ \left(\frac{2Na_2O}{0.35} + \frac{MgO}{0.90} + \frac{2K_2O}{0.25} + \frac{CaO}{0.70}\right)$	>100	0	(Parker 1970)

CIA – chemical index of alteration; CIW – chemical index of weathering; V – vogt; PWI – product of weathering index; RR – ruxton ratio; STI – silica-titania index; WIP – weathering index of parker

Table S2.7. Selected Indicator Species and their respective abundances per habitat and microhabitat. *Ab* is the taxon abundance, *R* and *B* refers to the number of ASVs associated to rhizosphere and bulk soil samples from each habitat. Selected indicator species had an indicator value higher than 0.8 and a p value <0.05. Indicator species in this table represent the individual dots at the bottom of the Extended Venn Diagram in Figure 2.5.

						Landslide			***Forest***		
Kingdom	**Phylum**	**Class**	**Order**	**Family**	**Genus/Species**	**Ab**	**R**	**B**	**Ab**	**R**	**B**
Archaea						*7*	*0*	*0*	*73*	*0*	*1*
	Crenarchaeota	Thaumarchaeota	Cenarchaeales	SAGMA-X		7	0	0	73	0	1
Bacteria						*5730*	*39*	*4*	*11742*	*43*	*28*
	Acidobacteria	Acidobacteria-6	iii1-15	RB40		99	1	0	353	2	0
		Acidobacteriia	Acidobacteriales	Acidobacteriaceae		284	2	0	9	0	0
					Acidicapsa borealis	65	1	0	4	0	0
				Koribacteraceae		32	0	0	1095	0	3
		Solibacteres	Solibacterales	Solibacteraceae		264	1	0	1	0	0
					Candidatus Solibacter	186	1	0	3	0	0
	Actinobacteria	Actinobacteria	Actinomycetales	Micromonosporaceae	*Actinoplanes globisporus*	121	1	0	17	0	0
		Thermoleophilia	Gaiellales	Gaiellaceae		3	0	0	347	1	2
	Armatimonadetes	[Fimbriimonadia]	[Fimbriimonadales]	[Fimbriimonadaceae]	*Fimbriimonas*	43	1	0	90	1	0
		Armatimonadia	Armatimonadales	Armatimonadaceae		52	1	0	1	0	0
		Chthono-monadetes	Chthonomonadales	Chthonomonadaceae		528	6	0	46	0	0
	Bacteroidetes	[Saprospirae]	[Saprospirales]	Chitinophagaceae		994	6	0	670	5	0
					Sediminibacterium	125	1	0	36	0	0
		Cytophagia	Cytophagales	Cytophagaceae		9	0	0	272	3	0
		Sphingobacteriia	Sphingobacteriales	Sphingobacteriaceae		193	2	0	19	0	0
	Chloroflexi	Ktedonobacteria	Thermo-gemmatisporales	Thermo-gemmatisporaceae		1	0	0	160	0	1

						Landslide			*Forest*		
Kingdom	**Phylum**	**Class**	**Order**	**Family**	**Genus/Species**	**Ab**	**R**	**B**	**Ab**	**R**	**B**
	Nitrospirae	Nitrospira	Nitrospirales	Nitrospiraceae	*JG37-AG-70*	1	0	0	358	0	2
					Nitrospira	0	0	0	365	0	1
	Planctomycetes	Planctomycetia	Gemmatales	Gemmataceae		390	0	2	264	0	2
					Gemmata	61	1	0	7	0	0
				Isosphaeraceae		187	0	2	30	0	0
			Pirellulales	Pirellulaceae		12	0	0	84	0	1
	Proteobacteria	Alpha-proteobacteria	Caulobacterales	Caulobacteraceae	*Phenylobacterium*	197	1	0	75	1	0
			Rhizobiales	Brucellaceae		106	1	0	11	0	0
				Hyphomicrobiaceae	*Pedomicrobium*	3	0	0	93	1	0
					Rhodomicrobium vannielii	79	0	0	303	0	1
					Rhodoplanes	65	1	0	250	1	1
				Phyllobacteriaceae	*Mesorhizobium*	8	0	0	164	1	0
				Xanthobacteraceae	*Labrys*	3	0	0	44	1	0
			Rhodobacterales	Hyphomonadaceae	*Woodsholea maritima*	0	0	0	71	1	0
			Rhodospirillales	Acetobacteraceae		30	0	0	553	4	0
				Rhodospirillaceae		452	3	0	1653	4	5
					Dongia mobilis	0	0	0	101	1	0
					Reyranella massiliensis	149	1	0	2	0	0
			Sphingomonadales	Sphingomonadaceae		2	0	0	161	1	0
		Beta-proteobacteria	Burkholderiales	Comamonadaceae		49	0	0	301	1	0
					Leptothrix	9	0	0	77	1	0
		Delta-proteobacteria	[Entotheonellales]	[Entotheonellaceae]		11	0	0	296	0	2
			Myxococcales	Myxococcaceae		10	0	0	142	0	1
			Syntropho-bacterales	Syntrophobacteraceae		2	0	0	304	0	2

						Landslide			*Forest*		
Kingdom	**Phylum**	**Class**	**Order**	**Family**	**Genus/Species**	**Ab**	**R**	**B**	**Ab**	**R**	**B**
		Gamma-proteobacteria	Alteromonadales	211ds20		1	0	0	44	1	0
				OM60		7	0	0	135	1	0
			HTCC2188	HTCC2089		15	0	0	208	1	0
			Thiotrichales	Piscirickettsiaceae		12	0	0	199	1	0
			Xanthomonadales	Sinobacteraceae		162	2	0	151	0	1
					Nevskia	92	1	0	4	0	0
					Steroidobacter	13	0	0	110	1	0
	Verrucomicrobia	[Pedosphaerae]	[Pedosphaerales]	auto67_4W		358	2	0	975	5	0
				Ellin515		2	0	0	71	0	1
		[Spartobacteria]	Chthoniobacterales	Chthoniobacteraceae	*Chthoniobacter*	92	1	0	18	0	0
					DA101	33	0	0	305	1	0
		Opitutae	Opitutales	Opitutaceae		63	0	0	455	2	0
					Opitutus	53	1	0	3	0	0
	WS3	PRR-12	Sediment-1	PRR-10		2	0	0	232	0	2
Fungi						*3519*	*1*	*3*	*1766*	*0*	*2*
	Ascomycota	Lecanoromycetes	Pertusariales	Megasporaceae	*Aspicilia*	403	0	1	0	0	0
		Leotiomycetes	Helotiales			2585	0	1	62	0	0
		Sordariomycetes				0	0	0	1258	0	1
			Hypocreales	Clavicipitaceae		0	0	0	440	0	1
			Xylariales	Xylariaceae	*Calceomyces lacunosus*	84	0	1	0	0	0
	Glomeromycota	Glomeromycetes	Diversisporales			447	1	0	6	0	0

Table S2.8. Differentially abundant ASVs per habitat in tiles and pellets. Selected differentially abundant ASVs had an effect value lower than -1.5 and higher than 1.5, and a Benjamini-Hochberg corrected *p*-value lower than 0.05. Each ASV was identified to the lowest taxonomical classification available.

	Habitat	Effect	Phylum	Class	Order	Family	Genus/Species
16S	Forest	-2.13	Actinobacteria	Actinobacteria	Actinomycetales	Micromonosporaceae	
16S	Forest	-2.05	Proteobacteria	Alpha-	Rhizobiales	Hyphomicrobiaceae	
16S	Forest	-1.98	Acidobacteria	Acidobacteriia	Acidobacteriales	Koribacteraceae	
16S	Forest	-1.94	Planctomycetes	Planctomycetia	Pirellulales	Pirellulaceae	*Pirellula*
16S	Forest	-1.88	Nitrospirae	Nitrospira	Nitrospirales	Leptospirillaceae	
16S	Forest	-1.80	Proteobacteria	Alpha-	Rhizobiales	Hyphomicrobiaceae	*Rhodoplanes*
16S	Forest	-1.74	Nitrospirae	Nitrospira	Nitrospirales	Nitrospiraceae	*Nitrospira*
16S	Forest	-1.67	Acidobacteria	Acidobacteriia	Acidobacteriales	Acidobacteriaceae	
16S	Forest	-1.67	Proteobacteria	Alpha-	Rhizobiales	Hyphomicrobiaceae	*Rhodoplanes*
16S	Forest	-1.64	Proteobacteria	Gamma-	Thiotrichales	Piscirickettsiaceae	
16S	Forest	-1.61	Proteobacteria	Gamma-	Xanthomonadales	Sinobacteraceae	
16S	Forest	-1.60	Proteobacteria	Gamma-	Xanthomonadales	Sinobacteraceae	
16S	Forest	-1.59	Proteobacteria	Alpha-	Rhizobiales	Hyphomicrobiaceae	*Rhodoplanes*
16S	Forest	-1.55	Proteobacteria	Alpha-	Rhizobiales	Hyphomicrobiaceae	*Rhodoplanes*
16S	Forest	-1.54	Acidobacteria	Chloracidobacteria	RB41	Ellin6075	
16S	Landslide	1.50	Verrucomicrobia	Spartobacteria	Chthoniobacterales	Chthoniobacteraceae	*DA101*
16S	Landslide	1.51	Actinobacteria	Thermoleophilia	Solirubrobacterales	Conexibacteraceae	
16S	Landslide	1.51	Planctomycetes	Planctomycetia	Pirellulales	Pirellulaceae	*Pirellula*

	Habitat	Effect	Phylum	Class	Order	Family	Genus/Species
16S	Landslide	1.52	Acidobacteria	Acidobacteriia	Acidobacteriales	Koribacteraceae	
16S	Landslide	1.52	Planctomycetes	Planctomycetia	Gemmatales	Gemmataceae	
16S	Landslide	1.53	Proteobacteria	Alpha-	Rhodospirillales	Rhodospirillaceae	
16S	Landslide	1.53	Acidobacteria	Solibacteres	Solibacterales	Solibacteraceae	
16S	Landslide	1.53	Planctomycetes	Planctomycetia	Gemmatales	Isosphaeraceae	
16S	Landslide	1.53	Actinobacteria	Actinobacteria	Actinomycetales	Mycobacteriaceae	*Mycobacterium*
16S	Landslide	1.54	Verrucomicrobia	Pedosphaerae	Pedosphaerales	auto67_4W	
16S	Landslide	1.54	Verrucomicrobia	Pedosphaerae	Pedosphaerales	auto67_4W	
16S	Landslide	1.55	Proteobacteria	Alpha-	Rhizobiales	Hyphomicrobiaceae	*Rhodoplanes*
16S	Landslide	1.55	Acidobacteria	Solibacteres	Solibacterales	Solibacteraceae	*Solibacter*
16S	Landslide	1.55	Proteobacteria	Gamma-	Xanthomonadales	Sinobacteraceae	
16S	Landslide	1.56	Chloroflexi	Ktedonobacteria	Thermogemmati-sporales	Thermogemmati-sporaceae	
16S	Landslide	1.56	Verrucomicrobia	Spartobacteria	Chthoniobacterales	Chthoniobacteraceae	*DA101*
16S	Landslide	1.58	Planctomycetes	Planctomycetia	Gemmatales	Isosphaeraceae	
16S	Landslide	1.58	Bacteroidetes	Saprospirae	Saprospirales	Chitinophagaceae	
16S	Landslide	1.59	Proteobacteria	Alpha-	Rhodospirillales	Acetobacteraceae	
16S	Landslide	1.59	Proteobacteria	Alpha-	Rhizobiales	Hyphomicrobiaceae	*Rhodoplanes*
16S	Landslide	1.61	Proteobacteria	Alpha-	Rhizobiales	Hyphomicrobiaceae	*Rhodoplanes*
16S	Landslide	1.62	Verrucomicrobia	Pedosphaerae	Pedosphaerales	auto67_4W	
16S	Landslide	1.62	Proteobacteria	Alpha-	Rhodospirillales	Rhodospirillaceae	
16S	Landslide	1.63	Acidobacteria	Acidobacteriia	Acidobacteriales	Acidobacteriaceae	
16S	Landslide	1.63	Proteobacteria	Alpha-	Rhodospirillales	Rhodospirillaceae	
16S	Landslide	1.64	Planctomycetes	Planctomycetia	Gemmatales	Gemmataceae	
16S	Landslide	1.65	Proteobacteria	Gamma-	Xanthomonadales	Xanthomonadaceae	
16S	Landslide	1.65	Verrucomicrobia	Spartobacteria	Chthoniobacterales	Chthoniobacteraceae	*DA101*
16S	Landslide	1.65	Acidobacteria	Acidobacteriia	Acidobacteriales	Koribacteraceae	
16S	Landslide	1.66	Proteobacteria	Beta-	A21b	EB1003	
16S	Landslide	1.68	Verrucomicrobia	Pedosphaerae	Pedosphaerales	auto67_4W	

	Habitat	Effect	Phylum	Class	Order	Family	Genus/Species
16S	Landslide	1.70	Verrucomicrobia	Pedosphaerae	Pedosphaerales	auto67_4W	
16S	Landslide	1.70	Bacteroidetes	Flavobacteriia	Flavobacteriales	Flavobacteriaceae	*Flavobacterium*
16S	Landslide	1.71	Bacteroidetes	Saprospirae	Saprospirales	Chitinophagaceae	
16S	Landslide	1.72	Planctomycetes	Planctomycetia	Gemmatales	Gemmataceae	
16S	Landslide	1.73	Verrucomicrobia	Spartobacteria	Chthoniobacterales	Chthoniobacteraceae	*Xiphinematobacter*
16S	Landslide	1.77	Proteobacteria	Alpha-	Rhodospirillales	Rhodospirillaceae	
16S	Landslide	1.77	Acidobacteria	Acidobacteriia	Acidobacteriales	Koribacteraceae	*Koribacter*
16S	Landslide	1.78	Proteobacteria	Alpha-	Rhodospirillales	Acetobacteraceae	
16S	Landslide	1.78	Proteobacteria	Gamma-	Xanthomonadales	Xanthomonadaceae	
16S	Landslide	1.79	Acidobacteria	Acidobacteriia	Acidobacteriales	Koribacteraceae	
16S	Landslide	1.83	Chloroflexi	Ktedonobacteria	Thermogemmati-sporales	Thermogemmati-sporaceae	
16S	Landslide	1.83	Proteobacteria	Beta-	Burkholderiales	Burkholderiaceae	*Burkholderia*
16S	Landslide	1.83	Planctomycetes	Planctomycetia	Gemmatales	Gemmataceae	
16S	Landslide	1.87	Acidobacteria	Acidobacteriia	Acidobacteriales	Koribacteraceae	*Koribacter*
16S	Landslide	1.88	Acidobacteria	Acidobacteriia	Acidobacteriales	Acidobacteriaceae	
16S	Landslide	1.90	Proteobacteria	Alpha-	Rhodospirillales	Acetobacteraceae	
16S	Landslide	1.90	Proteobacteria	Alpha-	Caulobacterales	Caulobacteraceae	*Phenylobacterium*
16S	Landslide	1.90	Planctomycetes	Planctomycetia	Gemmatales	Gemmataceae	
16S	Landslide	1.91	Proteobacteria	Alpha-	Rhodospirillales	Rhodospirillaceae	
16S	Landslide	1.91	Bacteroidetes	Saprospirae	Saprospirales	Chitinophagaceae	
16S	Landslide	1.91	Proteobacteria	Alpha-	Rhodospirillales	Rhodospirillaceae	
16S	Landslide	1.95	Proteobacteria	Alpha-	Rhodospirillales	Rhodospirillaceae	
16S	Landslide	1.95	Proteobacteria	Alpha-	Sphingomonadales	Sphingomonadaceae	*Kaistobacter*
16S	Landslide	1.96	Acidobacteria	Acidobacteriia	Acidobacteriales	Koribacteraceae	*Koribacter*
16S	Landslide	1.96	Bacteroidetes	Flavobacteriia	Flavobacteriales	Flavobacteriaceae	*Flavobacterium*
16S	Landslide	1.96	Acidobacteria	Acidobacteriia	Acidobacteriales	Acidobacteriaceae	
16S	Landslide	1.96	Acidobacteria	Acidobacteriia	Acidobacteriales	Acidobacteriaceae	
16S	Landslide	1.96	Proteobacteria	Alpha-	Rhodospirillales	Rhodospirillaceae	

	Habitat	Effect	Phylum	Class	Order	Family	Genus/Species
16S	Landslide	1.97	Acidobacteria	Acidobacteriia	Acidobacteriales	Acidobacteriaceae	*Edaphobacter*
16S	Landslide	2.05	Chloroflexi	Ktedonobacteria	Ktedonobacterales	Ktedonobacteraceae	*FFCH10602*
16S	Landslide	2.05	Proteobacteria	Beta-	Burkholderiales	Comamonadaceae	*Methylibium*
16S	Landslide	2.09	Proteobacteria	Alpha-	Rhodospirillales	Acetobacteraceae	
16S	Landslide	2.10	Verrucomicrobia	Pedosphaerae	Pedosphaerales	auto67_4W	
16S	Landslide	2.12	Planctomycetes	Planctomycetia	Gemmatales	Gemmataceae	*Gemmata*
16S	Landslide	2.15	Proteobacteria	Beta-	A21b	EB1003	
16S	Landslide	2.18	Proteobacteria	Alpha-	Rhodospirillales	Rhodospirillaceae	
16S	Landslide	2.34	Verrucomicrobia	Pedosphaerae	Pedosphaerales	auto67_4W	
16S	Landslide	2.38	Bacteroidetes	Saprospirae	Saprospirales	Chitinophagaceae	
16S	Landslide	2.47	Acidobacteria	Solibacteres	Solibacterales	Solibacteraceae	*Solibacter*
16S	Landslide	2.69	Acidobacteria	Acidobacteriia	Acidobacteriales	Koribacteraceae	*Koribacter versatilis*
ITS	Forest	-2.56	Ascomycota	Sordariomycetes	Hypocreales	Clavicipitaceae	
ITS	Forest	-1.92	Ascomycota	Sordariomycetes	Chaetosphaeriales	Chaetosphaeriaceae	*Chloridium*
ITS	Forest	-1.76	Basidiomycota	Agaricomycetes			
ITS	Landslide	1.76	Ascomycota	Leotiomycetes	Helotiales		
ITS	Landslide	1.92	Ascomycota				
ITS	Landslide	1.95	Ascomycota	Sordariomycetes	Sordariales	Sordariaceae	*Neurospora terricola*
ITS	Landslide	3.22	Ascomycota	Leotiomycetes	Helotiales	Helotiales_fam Incertae_sedis	*Leohumicola*

Table S2.9. GeoChip 5.0 functional genes array classifications of the differentially abundant KOs.

	Forest	Landslide
Carbon cycling	**1**	**1**
Carbon degradation	0	1
Carbon fixation	1	0
Metal Homeostasis	**2**	**0**
Mercury	1	0
Potassium	1	0
Microbial defense	**1**	**0**
Antibiotic resistance	1	0
Nitrogen Cycling	**1**	**0**
Nitrification	1	0
Plant Growth Promotion	**0**	**1**
Anti-pathogen	0	1
Stress	**2**	**0**
Osmotic stress	1	0
Oxygen limitation	1	**0**
Virulence	**0**	**1**
Secretion system	0	1
Not classified	**244**	**41**
Total	251	44

Table S2.10. CSR classification of differentially abundant KOs.

	Forest		Landslide	
	Count	**%**	**Count**	**%**
CSR	**123**	**0.49**	**8**	**0.18**
Competitive	8	0.03	3	0.07
Stress	17	0.07	2	0.05
Ruderal	95	0.38	2	0.05
Multiple	3	0.01	1	0.02
Other classifications	**14**	**0.06**	**11**	**0.25**
Foraging	6	0.02	0	0.00
Methylotrophs	1	0.00	0	0.00
Plant exudates metabolism	5	0.02	11	0.25
Multiple	2	0.01	0	0.00
Not classified	**114**	**0.45**	**25**	**0.57**
Total	251		44	

Figure S2.1. CoDa dendrogram (A) and PCA ordination (B) of orthonormal balances of soil nutrients. The V1-V12 variables are the orthonormal balances.

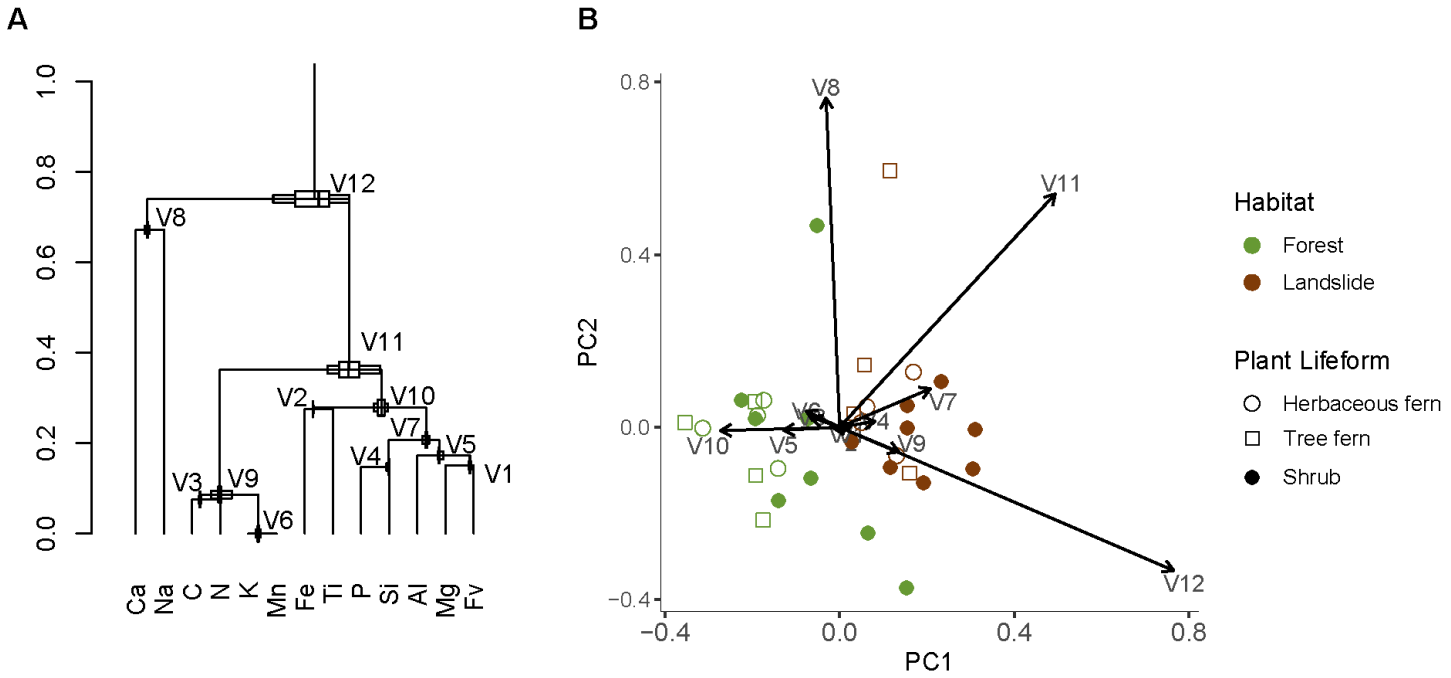

Figure S2.2. Pearson correlation matrix corresponding soil attributes in soils and their multicollinearity test results. Selected variables with its resulting Variance Inflation Factor (VIF) are shown the table.

Variables	VIF
$\delta^{13}C$	2.12
$\delta^{15}N$	1.86
Fe	4.72
K	4.26
Mn	3.07
V1	2.25
V2	1.38
V8	1.99
V11	1.47
CIW	3.56

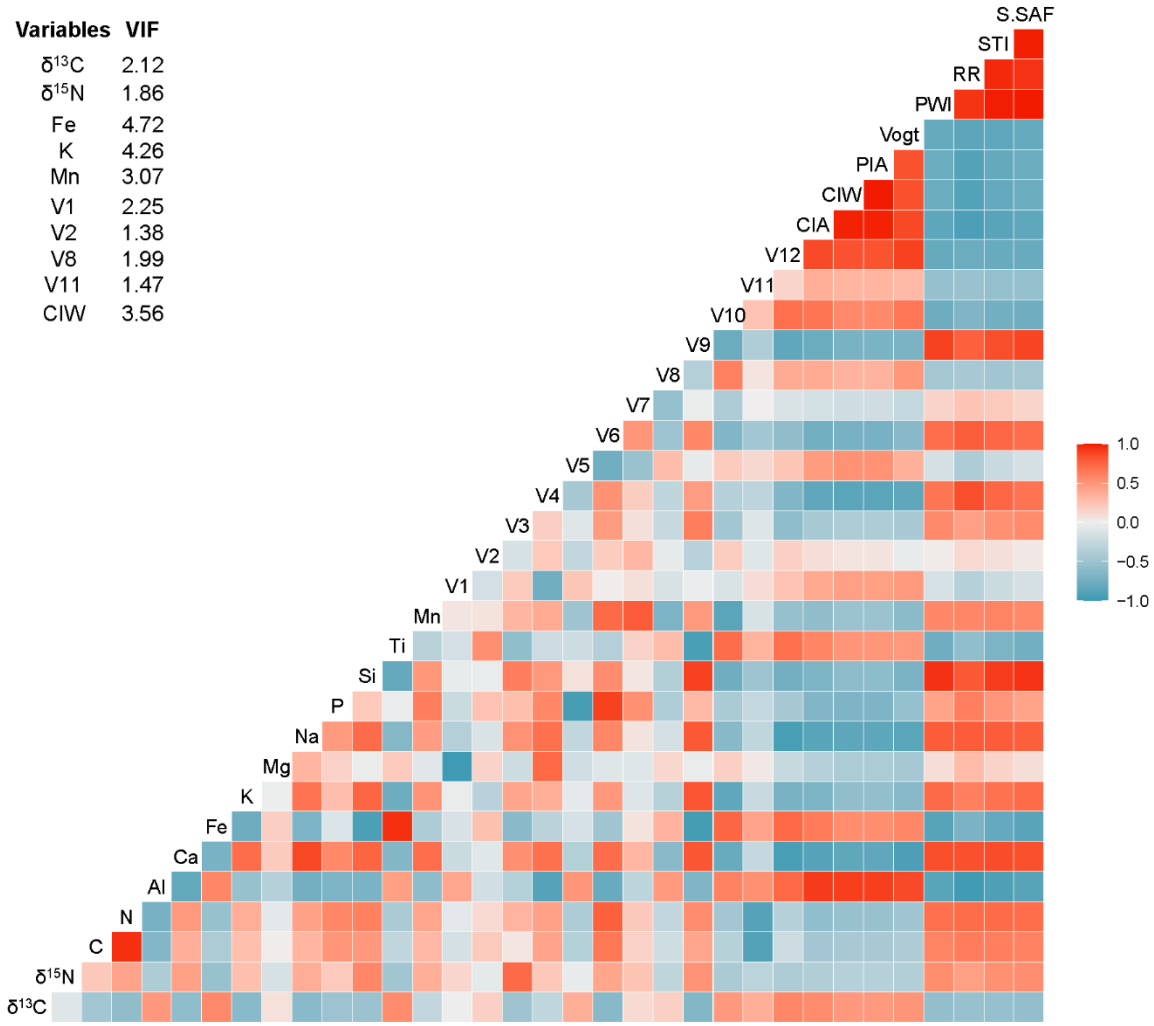

Figure S2.3. Species richness rarefaction curves for **A**) *16S* and **B**) *ITS* ASVs across habitats.

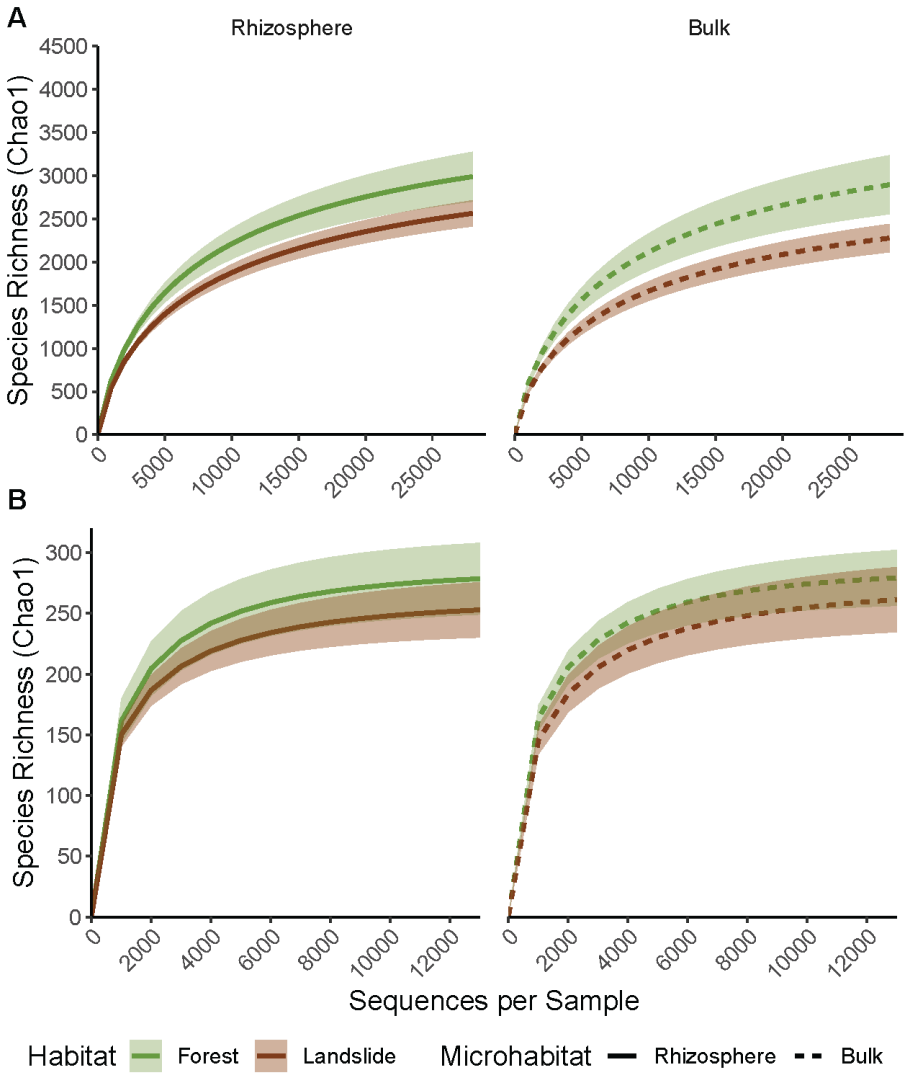

Figure S2.4. Taxonomic composition at phylum-level of low abundant bacteria, archaea and fungi across habitats, microhabitats, and plant species. Phyla with > 1% relative abundance were excluded.

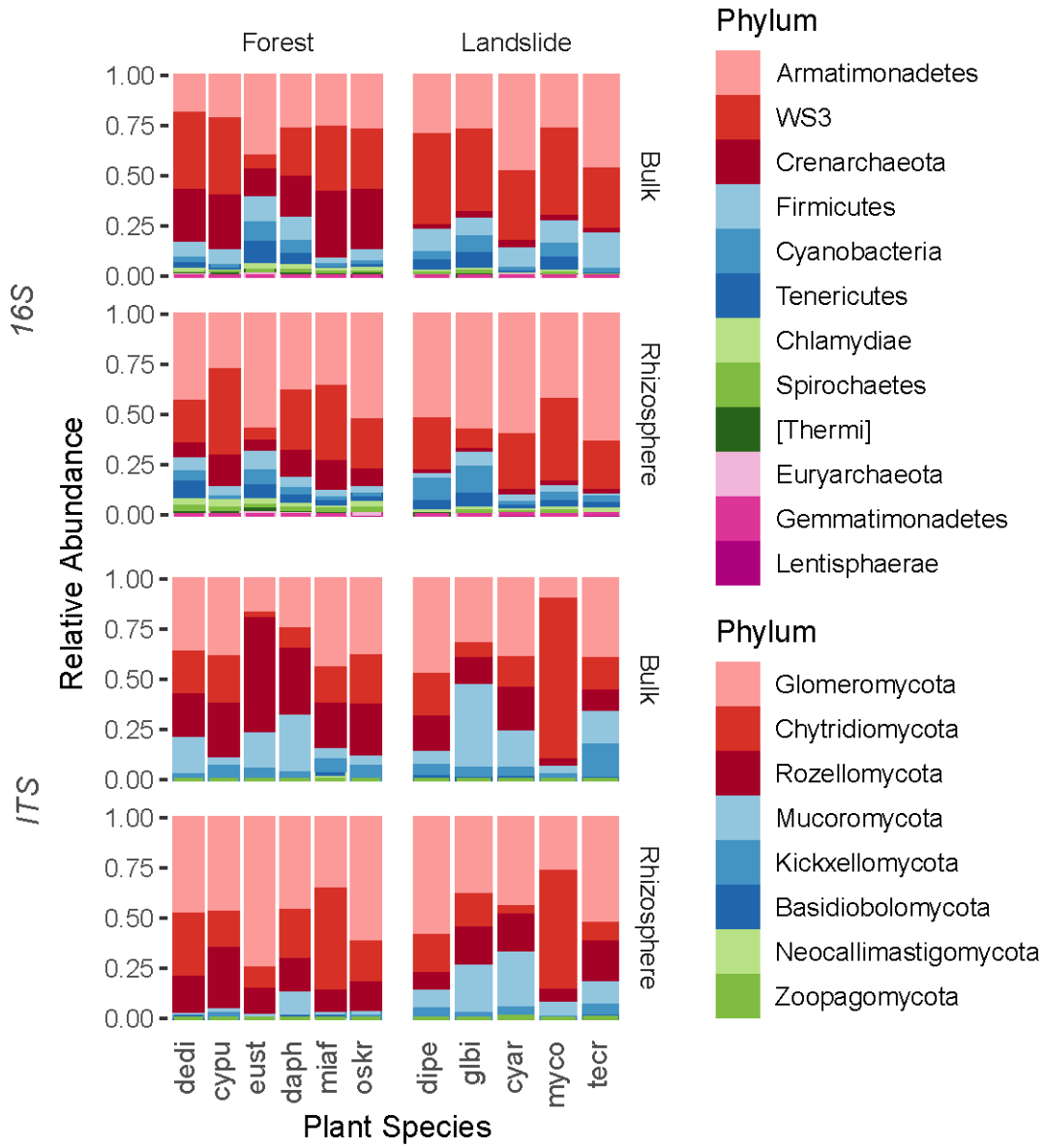

Figure S2.5. Principal Component Analysis (PCA) of *16S*, and *ITS* ASVs using Aitchison distances.

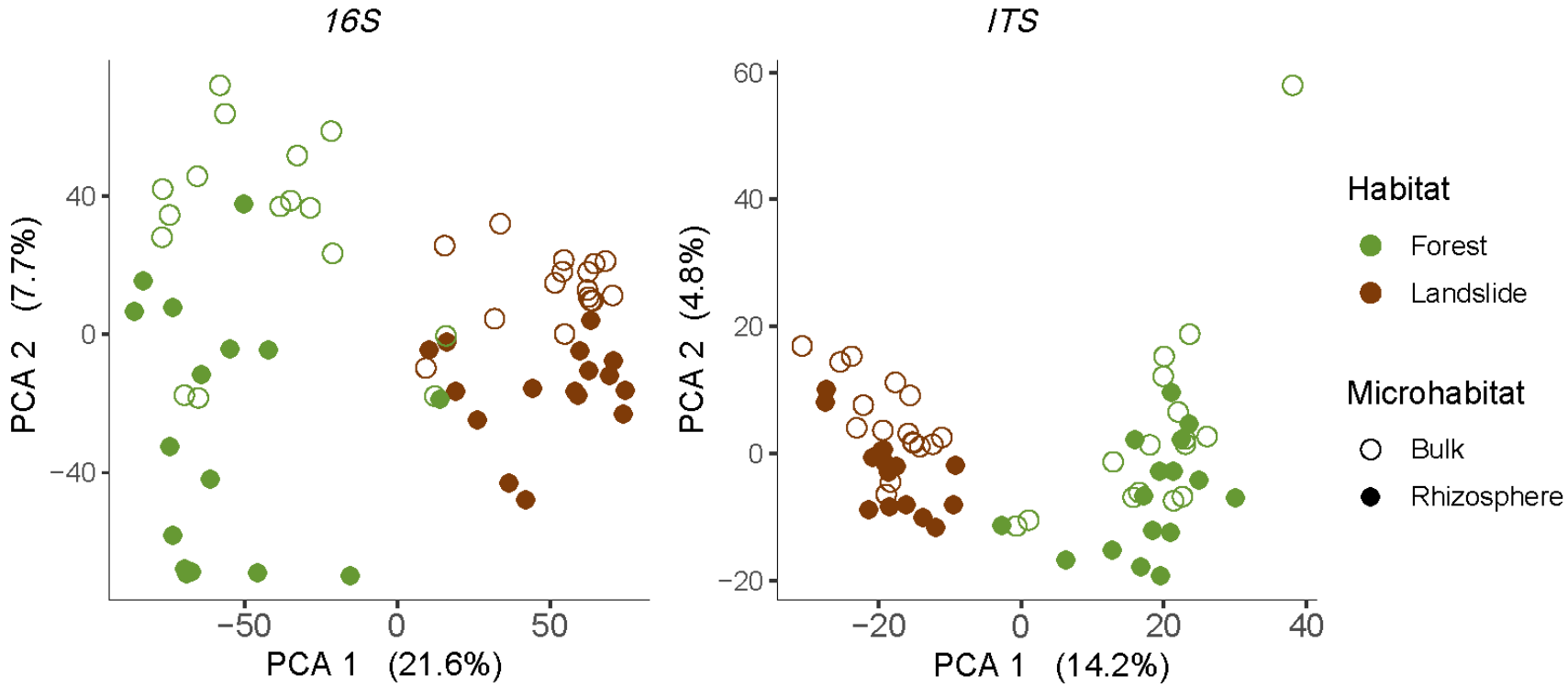

CHAPTER III: SILICATE ROCK WEATHERING IN AN IN-SITU EXPERIMENT DRIVES LANDSLIDE MICROBIAL DIVERSITY

INTRODUCTION

Rock weathering is a critical process central to most biogeochemical cycles. Of particular interest is the chemical weathering of calcium- and/or magnesium-bearing silicate rocks [(Ca|Mg)SiO_x] because their important role in the carbon cycle (Figure 1.1). In fact, a tight coupling between spatial and temporal scales contributes to distinct ecological processes. At small spatial and temporal scales, the chemical weathering of (Ca|Mg)SiO_x rocks contributes to the release of mineral nutrients essential for plant growth and the short-term sequestration of carbon dioxide (CO_2) by plants during photosynthesis (Beerling 2012, Uhlig et al. 2017). At large spatial and temporal scales, the weathering of these rocks contributes to uptake of mineral nutrients and CO_2 by marine algae leading to long-term sequestration of CO_2 in the ocean floor (Berner et al. 1983, Berner and Kothavala 2001, Beerling 2012, Uhlig et al. 2017). One open question is how tropical soils experiencing high physical denudation rates through landslides couple biotic processes at rhizobiomes with chemical weathering.

Work conducted mostly in temperate regions has shown that microorganisms associated with rocks and soils (Barker et al. 1998, Gleeson et al. 2006, Frey et al. 2010, Bernasconi et al. 2011, Brunner et al. 2011, Zumsteg et al. 2012), and rhizoplane of roots (Leyval and Berthelin 1991, Calvaruso et al. 2006, Calvaruso et al. 2007, Uroz et al. 2007, Uroz et al. 2009a, Uroz et al. 2009b, Calvaruso et al. 2010, Uroz et al. 2011) increase chemical weathering rates of (Ca|Mg)SiO_x minerals by up to 20 times compared to abiotic conditions (Kalinowski et al. 2000, Maurice et al. 2001, Calvaruso et al. 2006, Koele et al. 2009, Smits et al. 2012). In tropical regions, studies of deep regolith weathering in "stable" areas (Buss et al. 2005, Liermann et al. 2015) has shown that the abundance of

microorganisms is correlated with bioavailable nutrients throughout a vertical soil profile, and suggest that bacteria might play an important role in the weathering of bedrock.

The aforementioned studies use *ex situ* and *in situ* experiments to understanding of the role of microorganisms on chemical weathering of (Ca|Mg)SiO_x minerals. One set of *ex situ* experiments include batch reactors in which powdered rock or pure minerals (Vandevivere et al. 1994a, Kalinowski et al. 2000, Maurice et al. 2001, Balogh-Brunstad et al. 2008, Wu et al. 2008, Frey et al. 2010, Brunner et al. 2011) or solid pieces of silicate rocks (Vuorinen et al. 1981, Song et al. 2007, 2010) are inoculated with one or more microbial species at a time. Although these studies demonstrate quantitatively through nutrient release estimates, or qualitatively through pit formation, that mineral dissolution rates are significantly faster in the presence of certain bacterial species, it is difficult to infer what would happen in a natural setting under complex biogeochemical interactions such as plant-microbes-rocks systems.

A second group of *ex situ* experiments makes use of column weathering experiments, inoculating seedling roots with one or more microbial species and pure minerals (Leyval and Berthelin 1991, Calvaruso et al. 2006, Leake et al. 2008b, Koele et al. 2009, Smits et al. 2012). These studies have shown that inoculating roots with bacteria from the rhizosophere (e.g., *Burkholderia* spp.*)* or mycorrhizal fungi (e.g., *Scleroderma* and *Laccaria* spp.), significantly increases nutrient release from silicate minerals compared to roots that have not been inoculated. Although these studies offer a new level of biological understanding because they mimic natural conditions experienced by the plants and microorganisms compared to batch reactor experiments, they still miss the complex interactions observed under natural settings. The complex interactions include symbiotic

and competitive relationships between microorganisms, that could ultimately affect silicate weathering rates.

A few *in situ* studies have examined the contribution of microorganisms to weathering of (Ca|Mg)SiO_x rocks. Root exclusion experiments in temperate regions have shown that mycorrhizal fungi are capable of weathering crushed rocks and minerals through trenching (Quirk et al. 2012, Koele et al. 2014). Other studies have characterized microbial communities from mineral to landscape scales under field conditions. On the one hand, Gleeson et al. (2006) found that microbial communities composition was significantly different within the minerals of a (Ca|Mg)SiO_x rock, and found a strong correlation between microbial species and particular chemical elements within those minerals. On the other hand, Gleeson et al. (2016) found that microbial communities changed across soils with different weathering and disturbance degrees. Although the aforementioned work has been extremely valuable to understand the role of microorganisms on (Ca|Mg)SiO_x rocks, it may overlook the complexity in forest ecosystems that are subjected to high physical and chemical weathering. A point in case is provided by humid mountains in which landsliding and human-made disturbances contribute to physical weathering. Tiene que desarrollar esto un poco mas

Leveraging on a larger study aimed at characterizing taxonomic and functional diversity of microbiomes of "landslide-like" areas underlain by Ca,Mg-silicate rocks (Chapter 2), I focused on tree ferns of the genus *Cyathea* to design an *in situ* experiment aimed at evaluating the role of rhizobiomes on (Ca|Mg)SiO_x rock weathering in tropical mountains subjected to landsliding. The *in situ* experiment examined the role of four main drivers of chemical weathering, namely habitat, microhabitat, substrate, and presence of

roots on weathering of (Ca|Mg)SiO_x rocks. In this study I 1) quantify weathering rates of two experimental substrates, and 2) describe microbiomes in soil and those developing on experimental substrates. I hypothesized that a) weathering rate of (Ca|Mg)SiO_x substrates were going to be greater in landslides than forest habitats, b) soils and rocks microbiomes and their functions were mainly affected by habitats, and c) rock weathering will affect the microbial diversity. To my knowledge this is the first study that assess the role of rhizobiomes on (Ca|Mg)SiO_x rock weathering in landslides-like habitats in the tropics.

METHODS

STUDY AREA

This study took place in the vicinity of Cerro Punta, in the Central Mountain Range of Puerto Rico (centroid of sampling locations: 18° 9′ 55.44″ N, 66° 36′ 10.08″ W; mean elevation: 1060 m a.s.l.; Figure 2.1), a region classified as lower montane subtropical wet forest (Ewel and Whitmore 1973). Within this region, I chose two locations centered around Km 13 (“casa Gladys” or Site 2) and Km 14.5 (“casa Doris” or Site 1) of PR-143 to conduct the work that I describe below. The dominant land cover in the immediate surroundings of the study sites includes old growth forest interspersed with secondary forests of various ages, small-shaded coffee plantations, and pastures. Most of these high elevation sites are within or adjacent to the Toro Negro State Forest (Birdsey and Jimenez 1985).

This region is underlain by the Utuado pluton-UP, the second largest reservoir of intrusive igneous rocks in Puerto Rico emplaced 76 to 69 Mya (Chen 1967). The UP is an important source of sediments for the rivers that originate in the region, largely due to the

presence of granodiorite (65%) and diorite (~32%). The granodiorite of the UP has high concentrations of plagioclase minerals, that include an elevated concentrations of Ca and Mg (Table S2.1 and Table S3.0) (Chen 1967, Smith et al. 1998). A combination of elevated mean annual precipitation (2560 mm) and mean annual temperature (20.7 °C) (Weaver 1979, Birdsey and Jimenez 1985), creates ideal conditions for high chemical (Durgin 1977, Monroe 1979) and physical (Halsey et al. 1998) weathering activity, that together with historical forest clearing generates a high potential for landsliding.

EXPERIMENTAL DESIGN

At each of the two locations I selected an "old-growth" forest habitat site and paired it with a nearby road-cut that we used as a surrogate for landslides for a total of four sites. These road cuts were created during the construction of PR-143 in 1974 (Autoridad de Carreteras y Transportación). A combination of factors, including road maintenance and landslides, has kept the vegetation at these sites in early stages of succession, i.e., dominated by herbaceous plants, shrubs, and tree ferns. Many of these species are known to colonize landslides in the Caribbean, and more broadly speaking the Neotropics (Ewel and Whitmore 1973, Sugden et al. 1985, Guariguata 1990, Walker 1994, Keddy 2007, Judd and Ionta 2013). From now on, I refer to these road-cuts as landslide habitats.

At each site per habitat, I selected two tree ferns to characterize the microbial communities of rhizosphere and bulk soil and establish the *in-situ* experiment. The tree ferns are represented by two congeneric species: C*yathea arborea* and *C. pungens* found in landslides and forest, respectively. In January 2016, I collected root segments with attached soil and paired them with bulk soils collected one meter away from the base of

each plant. From now on I refer to these samples as *soil samples*. I removed the litter and used a 1.9 cm diameter soil corer to collect soil down to 10 cm. For each tree fern I collected three bundles of roots, from which rhizosphere soil was obtained, and three bulk soils samples to characterize their microbial communities; the three samples represent biological replicates". The bulk and rhizosphere soil were immediately stored in 25 Eppendorf tubes filled with 25 mL of phosphate buffered saline (PBS) solution with 10% glycerol and placed in dry ice for a period < 36 hours. Once in the laboratory I stored the samples at -80^{0}C until further processing.

In June of 2017, I located the tree ferns sampled in 2016 to establish the *in situ* experiment that included four variables of interest: habitat (landslide and forest), microhabitat or proximity to roots (close and far form roots), root accessibility (large and small mesh bags), and weathering substrate (tiles and pellets; see below) (Table 3.1). The two experimental rock weathering substrates were prepared from a fresh rock sample collected nearby Site 1 (18° 15′ 50.89″ N, 66° 36′ 0.23″ W) that was confirmed to be granodiorite by Dr. Stephen Hughes (UPR-Mayaguez). From now on I refer to the two experimental substrates as *rock samples*. The tiles exhibit the heterogenous characteristics of rocks found in nature, whereas the powder-pressed pellets the homogenous characteristics used in weathering experiments. The tiles and pellets were enclosed in mesh bags of two different sizes: large mesh bag (2-mm diameter opening; PELCO® Precision Woven Polyester Mesh from Ted Pella®) allowed the entrance of fine roots, whereas the small mesh bags (50-µm diameter opening) restricted the entrance of roots but allowed microorganisms, including mycorrhizal fungi hyphae (Wallander et al. 2001, Berner et al. 2012, Koele et al. 2014). The mesh bags were subsequently buried in the two

microhabitats. I periodically removed plants growing near bulk soil samples to prevent exogenous root contact. The first set of experimental units, i.e., one set of tiles and two sets of pellets, were collected in January 2018, after 7 months of incubation in the field. One of the set of pellets was used exclusively for microbial characterization, while the other for measuring element concentrations; the rock tiles were used for both. The rock samples used for microbial characterization were preserved following the same methodology used for soil samples. The incubation of the two substrates in landslides and forest represent a chronosequence, whereby the pellets and tiles represent fresh rock exposed by landslide disturbance and the landslides and forest first and second time points of succession, respectively.

GRANODIORITE TILE AND PELLET PREPARATION

The fresh sample of granodiorite was transported to the Department of Geology, University of Puerto Rico-Mayaguez campus. To prepare the granodiorite tiles, I cut the rock into 96-10 mm x 10 mm x 2 mm tiles (Thorn et al. 2002, Song et al. 2010) using a table-top wet tile saw (Figure 3.1A). On one side of each granodiorite tile, I bored a superficial mark using a Dremel® rotary tool (Figure 3.1B). This mark was used to quantify the elemental concentration in the same area before and after the field experiment using SEM-EDx spectroscopy (see below). Subsequently I sequentially abraded the granodiorite tiles with four silicon carbide sandpapers (average particle diameter: 58.5 µm, 25.8 µm, 21.8 µm and 15.3 µm) and ultrasonically cleaned the granodiorite tiles three times with distilled and deionized high purity water for 2 minutes each time (Song et al. 2007). Finally, I oven dried the tiles for 12 hrs at 80 ºC (Thorn et al. 2002) and weighed the tiles with an analytical

balance (± 0.001mg) prior to their analyses. To prepare the granodiorite pellets, I cut the rock it into small pieces (~5 cm) using a table-top wet tile saw (RIDGID®), then I crushed and grounded smaller pieces of rock in a shatterbox, and the resulting powder was sieved with a 270-mesh to obtain a 53 μm powder (Markowicz et al. 1997). Then, I weighed 0.9 (± 0.0001) g of powdered rock to which I added 0.1 (± 0.0001) g of SpectroBlend wax binder from Chemplex® (Markowicz et al. 1997, Mori et al. 1999). This mixture was placed in a stainless-steel sample holder (without the stainless-steel balls) in a Retsch® ball mill for 6 min at 17 rpm (Demir et al. 2006). Subsequently I transferred the rock-binder mixture to a 13 mm tungsten carbide pellet die set and applied 3.5 tons of hydraulic pressure for 3 min in a Carver® Bench Top Standard press.

The granodiorite tiles were analyzed twice, before and after retrieval, using a Scanning Electron Microscopy coupled with an Energy Dispersive X-Ray Spectroscopy (SEM-EDx) First, I acquired SEM images (JEOL – 20kV) at a 10X magnification for a complete view of the tiles. Then, I centered each tile with the aid of the bore-mark and analyzed them with EDx spectroscopy to obtain the quantitative elemental composition at a 30X magnification (Figure 3.1B). These analyzes were performed, at the Material Characterization Center of the University of Puerto Rico (MCC at UPR). The powdered-press pellets were analyzed through quantitative analyses using a RIGAKU ZSX Primus II WDXRF spectrometer coupled to the ZSX software (Version 7.07) following the methodology described in Chapter 2.

The soil and rock samples were allowed to slightly thaw within a week of retrieval, and to each 25 mL Eppendorf tube I added 12.5 μL of detergent polysorbate 20 (Tween 20) and subsequently placed them in a shaker (240 rpm) for 20 min (Ortiz et al. 2020). I removed the roots and tiles from the 25 mL tubes. Then, the samples were centrifuged at 4 ºC for 40 min at 4000 rpm. I discarded the supernatant and stored the remaining sediment at -80 ºC until further processing. To extract genomic DNA I used the PowerSoil™ DNA Isolation Kit (MO BIO Laboratories, Carlsbad, CA, United States) and followed their instructions.

I amplified and sequenced the *16S rRNA* V3-V4 region (*16S* primers: 515F, 805R) (Caporaso et al. 2011) and *Internal Transcribed Spacer-2* (*ITS-2* primers: 5.8-Fun; ITS4-Fun) (Taylor et al. 2016) region following Illumina's 16S Metagenomic Sequencing Library Preparation protocol with some modifications. Prior to amplification of each sample, I measured gDNA concentrations using QuantiFluor dsDNA system kit with the Promega platform.

I used slightly different parameters to amplify the *16S* and *ITS2* regions. For *16S*, I ran PCRs for each rhizosphere, bulk soil and rock replicates using 12.5 ng of genomic DNA, 0.5 μL of each primer (10 μM), 12.5 μL of 2x KAPA HiFi HotStart ReadyMix and subsequently filled with PCR water until reaching a 25-μL reaction mixture. For the *ITS*, I ran the PCRs for each rhizosphere, bulk soil and rock replicates using 10 ng of genomic DNA, 0.25 μL of each primer (25 μM), 0.25 μL of Phusion® High-Fidelity DNA Polymerase, 5 μL of Phusion HF Buffer (5X), 0.5 μL of dNTPs (10 mM), 0.75 μL of DMSO, and subsequently filled with PCR water until reaching a 21 μL reaction mixture. The thermocycling conditions for the *16S* were: initial denaturing at 95 °C for 3 min,

followed by 25 cycles of denaturation at 95 °C for 30 s, 55 °C for 30 s, 72 °C for 30 s, and a final extension at 72 °C for 5 min (Eppendorf Mastercycler Nexus). To verify the amplicon size, I ran 1 μL of the PCR product on an Agilent 2100 Bioanalyzer (Bioanalyzer DNA 1000 chip). The thermocycling conditions used for the *ITS2* samples were: initial denaturing at 96 °C for 2 min, followed by 27 cycles of denaturation at 94 °C for 30 s, 58 °C for 30 s, 72 °C for 2 min, and a final extension at 72 °C for 10 min. I added controls to the PCRs for the soil (*ITS*) and rock (*16S* and *ITS*) samples.

In contrast to the *16S*-PCR's, I merged the *ITS*-amplicons of the three biological replicates of rhizosphere and bulk soil, separately for each plant. I purified the merged-*ITS* amplicons using PureLink PCR Purification kit from Invitrogen®, and resuspended the samples in 40 μL. Finally, I measured the purified-amplicon DNA concentration using Invitrogen® Qubit 4 fluorometer and then normalized the DNA concentration to up to 5 ng/μL. I did not make any further modifications to Illumina's *16S* Metagenomic Sequencing Library Preparation protocol for any of the remaining steps. The sequencing was done using Illumina's MiSeq.

Preparation of the *16S* and *ITS* libraries was done at the University of Puerto Rico- Rio Piedras campus, whereas the sequencing of the *16S* soil samples and all *ITS* samples were done at UPR's Sequencing and Genomics Facility (SGF). A subset of soil samples representing technical replicates along with the *16S* rock samples and water samples related to other project were sequenced at the Louisiana State University Genomics Facility. Splitting the *16S* samples in two sequencing facilities created a slight batch effect (Figure S3.1) that was partially removed using filtering a custom filtering to remove ASVs overrepresented in control samples (see below).

The demultiplexed forward (fastq formatted) sequences from each MiSeq were downloaded from Illumina's BaseSpace® and imported into Quantitative Insights into Microbial Ecology 2 (QIIME2, v.2019.1) using the *demux emp-single* plugin (Boylen et al. 2018) and processed in three steps. First, I removed the primers using *Cutadapt* (Martin 2011), filtered using a max-ee of 1, denoised, and dereplicated the sequences, and removed chimeras using DADA2 *denoise-single* plugin (Callahan et al. 2016). I truncated all the *16S* sequences to 230 bp due to a drop in the nucleotide's quality whereas the *ITS* was truncated in variable sizes based on quality of the nucleotides (< Q7). The *ITS2* amplicon size is variable (267-511 bp) (Taylor et al. 2016) thus truncating all sequences to the same length can create a bias towards taxa with short amplicons (Ihrmark et al. 2012).

Second, following DADA2, I assigned taxonomy using Scikit-learn (Pedregosa et al. 2011) through the *classify-sklearn* plugin from QIIME 2. The classifier for *16S* was pre-trained using GreenGenes (99% similarity to V3-V4 region) (Pruesse et al. 2007, Quast et al. 2013, Yilmaz et al. 2014, Glockner et al. 2017) whereas for *ITS*, I used UNITE (dynamic similarity; version 8) (Nilsson et al. 2019) databases. ASVs that were overrepresented in control samples (samples abundance/negative control abundance > 0.75) were filtered out. I also removed the sequences belonging to chloroplast, mitochondria (*16S*), and unidentified taxa (*16S* and *ITS*) and ASV with less than 10 reads in > 3 samples. Lastly, I separately grouped the three biological replicates for *16S* rhizosphere and bulk soil per individual, that was previously done for the *ITS* at the PCR step.

The resulting *16S* and *ITS* ASVs were used to generate phylogenetic trees based on *de novo* construction. Towards this end, I aligned the representative sequences using Mafft (Katoh and Standley 2013), filtered the sequence gaps and highly un-conserved areas of

the sequences using Mask (Lane 1991), and subsequently built the phylogenetic trees with FastTree (Price et al. 2010) that I rooted with *phylogeny midpoint-root* plugin.

The third step involved partitioning the data in two subsets and rarefying each dataset to even depth. The first subset included the soil and rock samples, whereas the second subset included only the rock samples (Table 3.2). The rock samples subset was used to analyze the microbial diversity with the rock weathering indices.

Finally, I used Phylogenetic Investigation of Communities by Reconstruction of Unobserved States (PICRUSt2, v.2.3.0-b) to infer microbial gene content (Kegg Orthologs-KOs) from bacterial and archaeal taxa abundance (Douglas et al. 2020). I also used Funguild (Nguyena et al. 2016) to infer taxonomy-based ecological and fungal guild annotations.

DATA ANALYSES

Rock weathering - I used the elemental composition of the rock samples, i.e. tiles and pellets in two complimentary sets of analyses. The first set was aimed at quantifying nutrient mobilization in the rock samples using nutrient mobility indexes, whereas the second was aimed at characterizing their weathering status based on the ratio between immobile and mobile elements that are accumulated or depleted during weathering (Table S3.2). Both of these approaches were parent normalized indexes which allows to compare both types of experimental rock samples through incubation. Towards this end, I replaced all zeroes in the tile data set, but not in the pellets, with a small value using the *Bayesian-Multiplicative replacement of count zeros* function of *zCompositions* R package (Palarea-Albaladejo and Martín-Fernández 2015). The sum of oxides concentrations was closed to

100% using the *acomp* function in *compositions* R package (Egozcue et al. 2003, Egozcue and Pawlowsky-Glahn 2005, van den Boogaart 2008). Then, I calculated the nutrient mobility and rock weathering indexes. Finally, I replaced nutrient mobility outliers observed in tiles with NA values and then imputed these values using *imputePCA* (missMDA R package) (Josse and Husson 2016). These outliers were associated with zeroes that were replaced before.

To test for habitat, microhabitat, and root accessibility effects on rock samples, I used PERMANOVA test with *adonis2* in vegan R package (Anderson 2001, Oksanen et al. 2018) coupled with a PCA ordination with FactoMineR R package (Lê et al. 2008). In addition, I used ANOVAs to test the effect of the aforementioned variables on each index.

Microbiomes - I had to partially exclude variables to test for the effects of habitat, microhabitat, root accessibility, and weathering substrate on the microbiome analyses that follow. The reason for this was that insufficient gDNA, and low read counts after sequencing particularly among tiles incubated on small mesh-bag affected my original experimental design. I performed four sets of analyses on bacteria/archaea and fungi.

In a first set of analyses, I used species richness (Chao1), species diversity (Shannon), and rarefaction curves (Chao1) on both data subsets to characterize alpha diversity, coupled with ANOVAs to test for differences across habitats, microhabitats, and substrates. To test for the effect of root accessibility on alpha diversity, I used only the pellets. Alpha diversity metrics were calculated using Phyloseq R package (McMurdie and Holmes 2013b) and plotted using *ggplot2* (Wickham 2016). The rarefaction curves were generated with *ggrare* in Ranacapa R package (Kandlikar et al. 2018).

In the second set of analyses, I used barplots to examine the taxonomic structure of microbial communities. I identified indicator species (Dufrene and Legendre 1997) across habitats and habitat-substrate interactions using *labdsv* (Roberts 2016) and *Indicspecies* (De Cáceres and Legendre 2009, De Cáceres et al. 2011) R packages. Finally, I identified differentially abundant taxa using *ALDEx2* (v.1.16.0) (Fernandes et al. 2013, Fernandes et al. 2014, Gloor et al. 2015). Differentially abundant species were visualized using barplots with CLR-transformed abundances in *ggplot2*.

In a third set of was aimed at beta diversity analyses, I used a PERMANOVA to test for the effects of habitat, microhabitat, substrate and root accessibility on microbial community composition. I used Aitchison distances, which are Euclidean distances over the ASV abundances with prior zero-replacement and CLR transformation in a Principal Component Analysis (PCA) ordination to examine variation in the composition of microbial communities. I ran three sets of PCA ordinations, one per dataset, and a third set that of ordinations that were done per substrate for each amplicon. The last set of ordinations was used to test for microbiomes and rock weathering relationships.

Microbiome - rock weathering relationships – Prior to any analysis I used Variance Inflation Factor (vifcor function; *usdm* R package, v.1.1-18) to select nutrient mobility/weathering degree indices without collinearity using a VIF correlation threshold of 0.50. The variables were selected per weathering substrate for each amplicon (Figure S3.2). With this subset of variables, I examined relationships between microbiome alpha and beta diversity and nutrient mobility/weathering degree. Using Stepwise Regressions, I tested for the combined effect of nutrient mobility/weathering degree indices on species

diversity and the 1st and 2nd axis of the PCA ordinations per substrate for each amplicon (i.e. beta diversity).

Microbial functional characterization- I tested for genes (KOs) and fungal guilds differential abundances between habitats per weathering substrate using *ALDEx2* and the results were visualized using bar plots. A preliminary analysis of 7,111 KO's based on differential abundance revealed that 655 were differentially expressed as a function of habitat. These KO were annotated following three complimentary approaches: 1) based on KEGG Orthology (https://www.genome.jp/kegg/kegg2.html; accessed from July 2020 – April 2021) using Brite Hierarchy levels, 2) based on Geochip 5.0 functional gene array system (Shi et al. 2019), and 3) and on Grime's competitor/stress-tolerator/ruderal (CSR) traits (Wood et al. 2018). For the Brite Hierarchy levels, I searched the differentially abundant KOs in KEGG Orthology database and manually annotated each KO. For the GeoChip 5.0 genes, I searched the 1346 genes from Shi et al. (2019) in the KEGG database: a total of 918 genes matched 1 to 6 KO, 69 genes were associated to fungi and 359 genes were unclear or did not yield results. For the CSR traits, used the Brite Hierarchy levels and matched them to the CSR annotation based on Wood et al. (2018).

RESULTS

NUTRIENT MOBILITY AND ROCK WEATHERING

After 7 months of *in-situ* incubation, the relative mobility of the major oxides in tiles and pellets was small (Figure S3.3). Nonetheless, for half of nutrients in pellets I observed significant differences in mobility across habitats (Table 3.2). In pellets, I observed significant accumulation of one oxide (Al_2O_3) and significant depletion of CaO, MgO and

two other oxides (MnO, P_2O_5) in landslides compared to forests; while five oxides mobility (Fe_2O_3, TiO_2, SiO_2, K_2O, and Na_2O) did not differed with habitats. Similarly, I*mob* weathering index was significantly different across habitats in pellets, while CLI was significantly different between habitats in both pellets and tiles (Figure S3.2; Table 3.2). Finally, changes in analytical weight and bulk density were not significant across experimental treatments, pellets mean weight was significantly lower after the experiment (data not shown; T-test, $p < 0.05$).

A multivariate analysis of all nutrient mobility and weathering indices showed that the weathering patterns are differed between habitats, microhabitats and root accessibility (Table 3.3). Specifically, pellets in landslides were characterized by CaO and Na_2O mobilization as well as lower LF values (Figure 3.2).

MICROBIOMES

Species richness and diversity - After quality filtering, the analysis of 1,527,810 *16S* and 3,171,714 *ITS* reads yielded a total of 7,487 and 2,066 ASVs, respectively (Table S3.3). After rarefying to even depth (n = 1,363 seqs per sample), 2 *16S* samples were lost, yielding 81,780 reads and 5,404 ASVs, while *ITS* rarefaction (n = 11,194 seqs per sample) did not lead to any sample loss, yielding 727,610 reads and 2,065 ASVs. After sub-setting the rock samples subset (n=41), the total number of 16S reads was 231,611, yielding a total of 1,855 ASVs, while the 2,273,950 *ITS* reads yielded 1,367 ASVs (Table S3.3).

The species richness (Chao1) suggests that most of the bacterial and archaeal, and fungal species richness was captured with the sampling effort, although a slightly greater effort is needed to reach full-bacterial and archaeal species saturation (Figure S3.4). The

16S and *ITS* species diversity and richness did not differ with habitats nor microhabitats but did differ across substrates (Figure 3.3, Table 3.4), although when considering only rock samples, there were significant differences among microhabitats (Figure S3.5). Finally, restricting the analysis to only pellets samples, root restriction to substrates significantly reduced microbial species richness and diversity (Figure S3.5; Table 3.4).

Taxonomic structure of microbial communities - Overall, the *16S* microbial communities were represented by 15 bacterial and 2 archaeal phyla, and eight bacterial phyla had relative abundances > 2%: Proteobacteria (48%), Verrucomicrobia (12%), Acidobacteria (8%), Plactomycetes (8%), Actinobacteria (7%), Bacteroidetes (6%), Nitrospirae (3%) and Chloroflexi (3%) (Figure 3.4). The remaining 9 phyla represents 3.9% of the reads (Figure S3.6). Among Proteobacteria, the most abundant classes were the Alphaproteobacteria (54%), followed by the Betaproteobacteria (22%), Gammaproteobacteria (17%), and Deltaproteobacteria (7%). The fungal communities included 12 phyla, with Ascomycota (63%), Basidiomycota (21%), and Mortierellomycota (14%) comprising the 98% of the total fungal abundance (Figure 3.4). The remaining 9 phyla represents 2.6% of the reads (Figure S3.6). Among the Ascomycota, the most abundant fungal phylum, the most abundantclasses were Sordariomycetes (61%), Leotiomycetes (16%), Eurotiomycetes (12%), and Dothideomycetes (6%).

Indicator species and differentially abundant taxa – The Indicator Species Analysis identified a total of 99 indicator taxa: 37 in landslides and 62 in forests (Figure 3.5). In landslides, 7 ASVs were indicator only in tiles and 5 in pellets, whereas in forests, 32 were indicator only in tiles and 14 in pellets (Table S3.4). In pellets incubated at landslides, indicator species included *Variovorax* spp., and *Cupriavidus* spp. (Proteobacteria),

Anaerolineae (Cloroflexi), and *Staphylotrichum boninense* (Ascomycota), whereas at forests included *Reyranella massiliensis*, *Phenylobacterium* spp., *Rhodoplanes* spp., and *Steroidobacter* spp. (Proteobacteria), *Turneriella* spp. (Spirochaetes), and *Mortierella* spp. (Mortierellomycota). In tiles incubated at landslides, indicator species included Pedosphaerales (Verrucomicrobia), *Schizothecium dakotense* (Ascomycota), and *Apiotrichum scarabaeorum* and *A. sporotrichoides* (Basidiomycota), whereas at forests included SAGMA-X (Crenarchaeota), *Nitrospira* spp. (Nitrospirae), *Gemmata* spp., and *Pirellula* spp. (Planctomycetes), *Agrobacterium sullae*, *Pedomicrobium* spp. (Proteobacteria), and *Talaromyces palmae*, *Phialocephala humicola*, *Saccharomycopsis vini*, *Plectosphaerella cucumerina*, *Wallrothiella gmelinae*, *Acremonium stromaticum*, *Archaeorhizomyces* spp., *Volutella* spp. and *Pestalotiopsis* spp. (Ascomycota).

The differential abundance analysis with *ALDEx2* showed that 22 *16S* and 12 *ITS* ASVs were differentially abundant in the two habitats for each rock substrate (Table S3.5). In pellets, 1 archaeal, 8 bacterial and 5 fungal ASVs were differentially abundant between habitats (Figure 3.6A). Similarly, in tiles 13 bacterial and 7 fungal ASVs were differentially abundant between habitats (Table S3.5). In pellets incubated an landslides (Figure 3.6A), differentially abundant ASVs included *Koribacter versatilis* (Acidobacteria), and *Leohumicola* spp. and *Staphylotrichum* spp. (Ascomycota), whereas at forests differentially abundant ASVs included *Nitrosotalea devanaterra* (Crenarchaeota), *Rhodoplanes* spp. and *Steroidobacter* spp. (Proteobacteria), *Humicola* spp. (Ascomycota) and *Mortierella* spp. (Mortierellomycota). In tiles incubated an landslides (Figure 3.6B), differentially abundant ASVs included *Apiotrichum sporotrichoides* (Basidiomycota), *Mortierella beljakovae* (Mortierellomycota), *Koribacter* spp. (Acidobacteria) and

Xiphinematobacter spp. (Verrucomicrobia), while in forests differentially abundant ASVs included *Agrobacterium sullae* (Proteobacteria), *Nitrospira* spp. (Nitrospirae), and *Devosia*, spp. and *Rhodoplanes* spp. (Proteobacteria).

Beta diversity – A first set of analyses that included soils and rock samples, showed that microbial communities differed across habitat microhabitats and substrates (Table 3.5). In the *16S* Principal Component Analyses-PCA, soil, pellets and tiles were separated along the first axis and the landslides and forest were separated along the second axis (Figure S3.7). In contrast, for the *ITS* PCA, landslides and forest were separated along the first axis, whereas the substrates were distinguished along the second axis (Figure S3.7). Yet, there were other notable differences among the bacterial-archaeal and fungal communities. First, tiles' bacterial and archaeal community was more similar to that of pellets than soils. Second, tiles fungal community was more similar to soils than pellets.

In a second set of analysis, that only included the rock samples, habitat, substrate, and root accessibility explained the greatest variation in microbial community composition (Table 3.5). The PCA ordinations of both *16S* and *ITS* revealed that microbial communities were mainly differentiated by habitats throughout the first axis, and by weathering substrate on the second axis, particularly for the bacterial and archaeal community (Figure 3.7). For fungal communities, the separation of samples by weathering substrates was not evident in the first two axes of the ordination.

MICROBIOMES – ROCK WEATHERING RELATIONSHIP

Roughly 75% of the multiple linear regression models predicting *16S* and *ITS* alpha- and beta diversity were significant ($P < 0.10$; Table 3.6); among these all but one model (16S-Pellets) had $R^2 < 0.37$. Overall, the most important variables were Fe_2O_3 and CaO

mobilization as well as changes in bulk density. For alpha-diversity, regression models were better at explaining tiles' species diversity, while *16S* and *ITS* species diversity in pellets were poorly predicted by the models (R^2: 0.07-0.11). However, simple linear regressions showed that LF was had a fair power predicting *16S* species diversity, while no variable explained *ITS* species diversity on pellets (Table S3.7 – "Both"). For beta diversity, regression models were better at explaining *16S* and *ITS*-PCA first axis in pellets (R^2: 0.60-0.65), while they were better at explaining PCA second axis in tiles (R^2: 0.41-0.55). Among the simple linear regressions, only P_2O_5 had a good explanatory power in predicting ITS beta diversity in pellets ($R^2 = 0.30$).

MICROBIAL FUNCTIONAL CHARACTERIZATION

PICRUSt2 resulted in 7,111 KEGG functional Orthologs (KOs), where the overall 100 most abundant KOs were associated to Metabolism (Carbohydrate, Amino acids and Energy metabolism), Cellular Processes (Transporters and Cellular community), and Genetic Information Processing (Transcription and Translation). A total of 655 KOs were differentially abundant between habitats (Table S3.6): 229 were differentially abundant at landslides, and 426 in forests. I used three strategies to describe the function of these KOs: 1) KEGG Brite Hierarchy annotation, 2) GeoChip 5.0 functional array descriptions, and 3) Competitive-Stress-Ruderal strategies annotations.

Based on the Brite hierarchy (Table S3.7), I found that almost 50% of the differentially abundant genes of forests were related to genetic information processing (translation), and almost 35% were related to metabolism. At landslides, almost 60% of the differentially abundant genes belonged to metabolism, particularly carbohydrate metabolism and other unclassified metabolisms. Based on the Geochip 5.0 gene array, I found that landslides

differentially abundant genes related to carbon cycling (carbon degradation), plant growth promotion (anti-plant pathogens), stress (glucose limitation) and virulence (cellular function, immune evasion, soil-borne pathogen and toxins), whereas forests had genes related to carbon cycling (carbon fixation), metal transport (Ca, Fe, K, Hg, Na, Zn), nitrogen cycling (nitrification/denitrification) and stress (oxygen limitation and osmotic stress) (Table S3.8). Finally, based on the CSR classifications, differentially abundant genes at landslides were not related to a CSR strategy in particular, although a quarter of the genes were related to plant exudates metabolism (Table S3.9). In contrast, differentially abundant genes at forests were associated to a ruderal life-history strategy. Across all gene classifications, soil, pellets and tiles substrates followed a similar trend.

FUNguild analysis resulted in 69 highly probable, 685 probable, 129 possible and 1179 unassigned ASVs to fungal guilds. From the assigned guilds, 96 were pathotrophs, 319 were saprotrophs, 59 were symbiotrophs and 409 were assigned to multiple guilds. The fungal guilds with the most species were undefined saprotrophs, generalists (i.e., ASVs that matched with the three trophic modes: symbiotrophs, pathotrophs and saprotrophs), and plant pathogens. A total of 5 fungal guilds were differently abundant between habitats: 1 in soils, 1 in pellets and 3 in tiles. In soil and pellets, an undefined fungal saprotroph was more abundant in forest than landslides (Figure 3.8). In tiles, two differentially abundant guilds belonged to forests and 1 to landslides (Figure 3.8). All differentially abundant guilds in tiles had more than one classification.

DISCUSSION

The goal of this work was to closely examine the contribution of rhizobiomes to weathering of (Ca,Mg)-silicate rocks in the tropics. Three key findings may help elucidate the role of rhizobiomes in this pivotal mechanism that enables multiple biogeochemical cycles at local and large scales. First, nutrient mobility patterns and weathering rates differed between habitats in pellets but not tiles. Second, microbial diversity, composition , and their functional traits differed between habitat and substrate. Third, nutrient mobility and rocks weathering were associated to differences in microbial diversity and composition. Altogether, these results highlight the first time the biogeochemical interactions that leads to the weathering of Ca,Mg-silicate rocks through an *in-situ* experiment in the tropics.

Nutrient mobility and rock weathering - The weathering of (Ca|Mg)SiO_x rocks depended on substrate type. The weathering rate and nutrient mobility of pellets, but not tiles, differ across habitats. In pellets, CaO and MgO depletion, as well as an overall mobile nutrients depletion measured through CLI weathering index suggest that the weathering degree was higher in landslides (Ceryan 2008). Although I focused on Ca and Mg due to their role on the long-term carbon cycle, I discovered that other nutrients were also mobilized faster in landslides. Other nutrients were also mobilized or accumulated faster in landslides, such as MnO, P_2O_5 and Al_2O_3, which is partially consistent with weathering of granitic rocks in other studies (Middelburg et al. 1988). This is indirectly related to soil production functions, where the consensus states that at lower soil depths, rock weathering rates are higher (Cox 1980, Heimsath et al. 1997, Dixon and von Blanckenburg 2012, Dixon and Riebe 2014). Nonetheless, other factors other than soil depth affected rock weathering. Pellets proximity to plants (microhabitat) and root exclusion manipulations (mesh size),

which have not been quantitatively studied before (Quirk et al. 2012, Koele et al. 2014), affected the mobility of various oxides but did not altered the overall rock weathering rates in an experiment under natural settings. This is the first time that weathering indexes are measured taking in consideration these plant/microbes interactions combined, which helps construct the foundation to understand the bio-weathering signatures in a natural context. Although insignificant, the resulting weathering patterns are indicative of the complex microbial-geochemical interactions across the experimental variables in this work, and these could be best elucidated with a longer incubation time. Moreover, these results are surprising for an *in-situ* experiment after such as short time.

Microbiomes - Habitat and substrate had a strong effect on microbial species diversity, composition, and functional traits. Microbial diversity throughout habitats and substrates resembled that of a microbial succession in a chronosequence (Wojcik et al. 2020): it was lower in tiles and pellets at landslides, increased at landslide soils, and peaked at forest soils, which is consistent to what has been found in landslided areas (DeGrood et al. 2005). It is important to note that DeGrood et al. (2005) differed from this work in two ways: 1) they estimated diversity through phospholipid fatty acids measurements, and 2) their work was done in serpentine-derived soils. However, contrasting results have been found in other chronosequences, where species richness was higher in younger soils and lower older soils (Yeoh et al. 2017).

Between rock substrates, tiles had significantly higher species diversity than pellets. This result was partially unexpected, because the pellets have more readily available nutrients than tiles, as it was demonstrated by the differing weathering rates of tiles and pellets. Nonetheless, Gleeson et al. (2006) found that microbial colonization was mineral

specific within a whole rock. Thus, the heterogeneity of tile's surface, which is more similar to soils, might be the reason for tiles' microbial composition was closer to soils than to pellets. Other possibility is that the wax used for pelletizing interfered with the microbial colonization of the pellet's surface, creating a unique and distinctive niche to those naturally occurring in the study area.

Finally, habitats and substrates affected differentially abundant species and inferred functions. Landslides, which are considered highly disturbed habitats with low nutrient availability (Osksanen and Ranta 1992, Matthews 2014), included differentially abundant species from phyla associated to oligotrophic environments such as Acidobacteria, Verrucomicrobia and Basidiomycota (Fierer et al. 2007, Bergmann et al. 2011, Ho et al. 2017). The oligotrophic taxa are consistent with the differentially abundant functions found in landslides which were associated to carbon degradation, glucose limitation and virulence based on the Geochip 5.0 – functional microarray (Shi et al. 2019), and to the plant exudate metabolism genes based on (Wood et al. 2018). On the other hand, indicator species at forests included members of fungal copiotrophic genus *Acremonium* (Di Lionardo et al. 2013, Lunghini et al. 2013), which was coupled with genes related to carbon fixation and multiple metals homeostasis, (Shi et al. 2019) in addition to foraging and ruderal genes (Wood et al. 2018). The low number of copiotrophic taxa, and the genes related to foraging and ruderal strategies at forests suggest that this habitat is also the product of relatively recent disturbances.

Microbiomes-rock weathering relationships - The weathering of $(Ca|Mg)SiO_x$ rocks, measured through nutrient mobility and weathering indices, affected microbial diversity. I found that the variables that affected microbial diversity were different for alpha and beta

diversity, for *16S* and *ITS* and lastly for pellets and tiles. Overall, variables that more frequently affected microbial diversity were Fe_2O_3, CaO, MgO, P_2O_5 and K_2O, which are similar to those mobilized from the weathering of $(Ca|Mg)SiO_x$ rocks inoculated with one or two microbial species during *ex-situ* experiments (Vuorinen et al. 1981, Frey et al. 2010, Brunner et al. 2011). Various studies have focused only on iron mobilization during weathering (Barker et al. 1998, Kalinowski et al. 2000, Maurice et al. 2001), although CaO appeared to be the most important variable affecting alpha and beta diversity during this experiment. Calcium is an inorganic nutrient for plant nutrition, growth and health (Clarkson and Hanson 1980, Marschner 1995), which is a critical structural components of plant's cells. Thus, it is important for plants in landslide-ecosystems to mobilize such an essential nutrient. This is confirmed by the microbial functional trait inferences in landslides, where metabolism of plant exudates were differentially abundant. It is known that host plant exchanges carbon-rich exudates for mineral nutrients, driving microbial communities' dynamics (Bonfante and Genre 2010, Zhalnina et al. 2018).

With road constructions and other forest modifications, combined with climate extremes such as hurricanes, causing increases in landslide frequency (Larsen and Torres-Sánchez 1996, Hughes and Schulz 2020), it is important to understand the biogeochemical dynamics that control ecosystem succession. This *in-situ* experiment with granodiorite tiles and pellets, allowed to couple the microbial diversity, community composition and functional traits with the weathering of a $(Ca|Mg)SiO_x$ rock. I found that calcium is potentially driving the granodiorite weathering in the tropical mountains, as it is a highly depleted, yet essential nutrient for plant growth.

Amundson, R., D. D. Richter, G. S. Humphreys, E. G. Jobbágy, and J. Gaillardet. 2007. Coupling between biota and earth materials in the Critical Zone. Elements **3**:327-332.

Anderson, M. J. 2001. A new method for non-parametric multivariate analysis of variance. Austral Ecology **26**:32-46.

Anderson, S. P., W. E. Dietrich, and G. H. Brimhall. 2002. Weathering profiles, mass-balance analysis, and rates of solute loss: Linkages between weathering and erosion in a small, steep catchment. GSA Bulletin **114**:1143-1158.

Augusto, L., M. P. Turpault, and J. Ranger. 2000. Impact of forest tree species on feldspar weathering rates. Geoderma **96**:215-237.

Autoridad de Carreteras y Transportación, P. Plan de Manejo de la Ruta Panorámica. Departamento de Transportación y Obras Públicas de Puerto Rico.

Baldrian, P. 2006. Fungal laccases-occurrence and properties. FEMS Microbiol Rev **30**:215-242.

Balogh-Brunstad, Z., C. K. Keller, R. A. Gill, B. T. Bormann, and C. Y. Li. 2008. The effect of bacteria and fungi on chemical weathering and chemical denudation fluxes in pine growth experiments Biochemistry **88**:153-167.

Banfield, J. F., W. W. Barker, S. A. Welch, and A. Tauton. 1999. Biological impact on mineral dissolution: Application of the lichen model to understanding mineral weathering in the rhizosphere. Proc. Natl. Acad. Sci **96**:3404-3411.

Barker, W. W., S. A. Welch, S. Chu, and J. F. Banfield. 1998. Experimental observations of the effects of bacteria on aluminosilicate weathering. American Mineralogist **83**:1551-1563.

Beerling, D. J. 2012. Atmospheric carbon dioxide: a driver of photosynthetic eukaryote evolution for over a billion years? Phil. Trans. R. Soc. B:477-482.

Beerling, D. J., and R. A. Berner. 2005. Feedbacks and the coevolution of plants and atmospheric CO_2Feedbacks and the coevolution of plants and atmospheric CO2. Proc. Natl. Acad. Sci **102**:1302-1305.

Bennett, P. C., J. R. Rogers, W. J. Choi, and F. K. Hiebert. 2001. Silicates, silicate weathering, and microbial ecology. Geomicrobiology Journal **18**:3-19.

Berg, G., and K. Smalla. 2009. Plant species and soil type cooperatively shape the structure and function of microbial communities in the rhizosphere. Pages 1–13. FEMS Microbiol Ecol.

Bergmann, G. T., S. T. Bates, K. G. Eilers, C. Lauber, J. G. Caporaso, W. Walters, R. Knight, and N. Fierer. 2011. The under-recognized dominance of Verrucomicrobia in soil bacterial communities. Soil Biology & Biochemistry **43**:1450-1455.

Bernasconi, S. M., A. Bauder, B. Bourdon, I. Brunner, E. Bünemann, I. Christl, N. Derungs, P. Edwards, D. Farinotti, B. Frey, E. Frossard, G. Furrer, M. Gierga, H. Göransson, K. Gülland, F. Hagedorn, I. Hajdas, R. Hindshaw, S. Ivy-Ochs, J. Jansa, T. Jonas, M. Kiczka, R. Kretzschmar, E. Lemarchand, J. Luster, J. Magnusson, E. A. D. Mitchell, H. Olde-Venterink, M. Plötze, B. Reynolds, R. H. Smittenberg, M. Stähli, F. Tamburini, E. T. Tipper, L. Wacker, M. Welc, J. G. Wiederhold, J. Zeyer, S. Zimmermann, and A. Zumsteg. 2011. Chemical and Biological Gradients along the Damma Glacier Soil Chronosequence, Switzerland Vadose Zone Journal **10**:867 - 883.

Berner, C., T. Johansson, and H. Wallander. 2012. Long-term effect of apatite on ectomycorrhizal growth and community structure. Mycorrhiza **22**:615–621.

Berner, R. A. 1992. Weathering, plants, and the long-term carbon-cycle. Geochimica Et Cosmochimica Acta **56**:3225-3231.

Berner, R. A., and Z. Kothavala. 2001. GEOCARB III: A Revised model of atmospheric CO2. American Journal of Science **301**:182-204.

Berner, R. A., A. C. Lasaga, and R. M. Garrels. 1983. The carbonate-silicate geochemical cycle and its effect on atmospheric carbon dioxide over the past 100 million years. American Journal of Science **283**:641-685.

Bever, J. D., I. A. Dickie, J. M. Facelli, J. Klironomos, M. Moora, M. C. Rilling, W. D. Stock, M. Tibbett, and M. Zobel. 2010. Rooting theories of plant community ecology in microbial interactions. Trends in Ecology & Evolution **25**:468-478.

Birdsey, R. A., and D. Jimenez. 1985. The Forests of Toro Negro. Usda Forest Service Southern Forest Experiment Station Research Paper:1-&.

Birdsey, R. A., and D. Jiménez. 1985. The Forests of Toro Negro. Pages 1-29 *in* U. S. D. o. Agriculture, editor. Forest Service, New Orleans, Louisiana.

Bonfante, P., and A. Genre. 2010. Mechanisms underlying beneficial plant-fungus interactions in mycorrhizal symbiosis. Nature Communications **1**.

Bonneville, S., D. J. Morgana, A. Schmalenberger, A. Bray, A. Brown, S. A. Banwar, and L. G. Benning. 2011. Tree-mycorrhiza symbiosis accelerate mineral weathering: Evidences from nanometer-scale elemental fluxes at the hypha–mineral interface. Geochimica Et Cosmochimica Acta **75**:6988 – 7005.

Boylen, E., J. R. Rideout, M. Dillon, N. A. Bokulich, C. Abnet, G. A. Al-Ghalith, H. Alexander, E. J. Alm, M. Arumugam, F. Asnicar, Y. Bai, J. E. Bisanz, K.

Bittinger, A. Brejnrod, C. J. Brislawn, C. T. Brown, B. J. Callahan, A. M. Caraballo-Rodríguez, J. Chase, E. Cope, R. Da Silva, P. C. Dorrestein, G. M. Douglas, D. M. Durall, C. Duvallet, C. F. Edwardson, M. Ernst, M. Estaki, J. Fouquier, J. M. Gauglitz, D. L. Gibson, A. Gonzalez, K. Gorlick, J. Guo, B. Hillmann, S. Holmes, H. Holste, C. Huttenhower, G. Huttley, S. Janssen, A. K. Jarmusch, L. Jiang, B. Kaehler, K. B. Kang, C. R. Keefe, P. Keim, S. T. Kelley, D. Knights, I. Koester, T. Kosciolek, J. Kreps, M. G. Langille, J. Lee, R. Ley, Y. Liu, E. Loftfield, C. Lozupone, M. Maher, C. Marotz, B. D. Martin, D. McDonald, L. J. McIver, A. V. Melnik, J. L. Metcalf, S. C. Morgan, J. Morton, A. T. Naimey, J. A. Navas-Molina, L. F. Nothias, S. B. Orchanian, T. Pearson, S. L. Peoples, D. Petras, M. L. Preuss, Pruesse E, L. B. Rasmussen, A. Rivers, M. S. Robeson II, P. Rosenthal, N. Segata, M. Shaffer, A. Shiffer, R. Sinha, S. J. Song, J. R. Spear, A. D. Swafford, L. R. Thompson, P. J. Torres, P. Trinh, A. Tripathi, P. J. Turnbaugh, S. Ul-Hasan, J. J. van der Hooft, F. Vargas, Y. Vázquez-Baeza, E. Vogtmann, M. von Hippel, W. Walters, Y. Wan, M. Wang, J. Warren, K. C. Weber, C. H. Williamson, A. D. Willis, Z. Z. Xu, J. R. Zaneveld, Y. Zhang, Q. Zhu, R. Knight, and J. G. Caporaso. 2018. QIIME 2: Reproducible, interactive, scalable, and extensible microbiome data science. PeerJ Preprints **6**:e27295v27292.

Brantley, S. L., M. B. Goldhaber, and K. Vala Ragnarsdottlr. 2007. Crossing disciplines and scales to understand the Critical Zone. Elements **3**:307-314.

Brenning, A., M. Schwinn, A. P. Ruiz-Páez, and J. Muenchow. 2015. Landslide susceptibility near highways is increased by 1 order of magnitude in the Andes of southern Ecuador, Loja province. Nat. Hazards Earth Syst. Sci. **15**:45-57.

Brown, S. P., and A. Jumpponen. 2014. Contrasting primary successional trajectories of fungi and bacteria in retreating glacier soils. Molecular Ecology **23**:481-497.

Brunner, I., M. Plotze, S. Rieder, A. Zumsteg, G. Furrer, and B. Frey. 2011. Pioneering fungi fromthe Damma glacier forefield in the Swiss Alps can promote granite weathering. Geobiology **9**:266-279.

Burke, B. C., A. M. Heimsath, J. L. Dixon, J. Chappell, and K. Yoo. 2009. Weathering the escarpment: chemical and physical rates and processes, south-eastern Australia. Earth Surface Processes and Landforms **34**:768-785.

Buss, H. L., M. J. Schultz, C. F. Mathur, and S. L. Brantley. 2005. The coupling of biological iron cycling and mineral weathering during saprolite formation, Luquillo Mountains, Puerto Rico. Geobiology **3**:247-260.

Callahan, B. J., P. J. McMurdie, M. J. Rosen, A. W. Han, A. J. A. Johnson, and S. P. Holmes. 2016. DADA2: High-resolution sample inference from Illumina amplicon data. Nature Methods **13**:581-+.

Calvaruso, C., M.-P. Turpault, E. Leclerc, and P. Frey-Klett. 2007. Impact of ectomycorrhizosphere on the functional diversity of soil bacterial and fungal

communities from a forest stand in relation to nutrient mobilization processes. Pages 567-577. Microbial Ecology.

Calvaruso, C., M.-P. Turpault, E. Leclerc, J. Ranger, J. Garbaye, S. Uroz, and P. Frey-Klett. 2010. Influence of forest trees on the distribution of mineral weathering-associated bacterial communities of the Scleroderma citrinum mycorrhizosphere. Applied and Environmental Microbiology **76**:4780-4787.

Calvaruso, C., M. P. Turpault, and P. Frey-Klett. 2006. Root-associated bacteria contribute to mineral weathering and to mineral nutrition in trees: A budgeting analysis. Applied and Environmental Microbiology **72**:1258-1266.

Cammeraat, E., R. van Beek, and A. Kooijman. 2005. Vegetation succession and its consequences for slope stability in SE Spain. Plant and Soil **278**:135-147.

Campbell, B. 2014. The Family Acidobacteriaceae. Pages 405-415 *in* E. Rosenberg, editor. The Prokaryotes – Other Major Lineages of Bacteria and the Archaea. Springer-Verlag, Berlin.

Caporaso, J. G., C. Lauber, L. Walters, D. Berg-Lyons, C. Lozupone, P. J. Turnbaugh, N. Fierer, and R. Knight. 2011. Global patterns of 16S rRNA diversity at a depth of millions of sequences per sample. Proc Natl Acad Sci **108**:4416-4522.

Ceryan, S. 2008. New chemical weathering indices for estimating the mechanical properties of rocks: a case study from the Kürtün Granodiorite, NE Turkey. Turkish Journal of Earth Sciences **17**:187-207.

Che, V. B., K. Fontijn, G. G. J. Ernst, M. Kervyn, M. Elburg, E. Van Ranst, and C. E. Suh. 2012. Evaluating the degree of weathering in landslide-prone soils in the humid tropics: The case of Limbe, SW Cameroon. Geoderma **170**:378-389.

Chen, C., J. Zhang, M. Lu, C. Qin, Y. Chen, L. Yang, Q. Huang, J. Wang, Z. Shen, and Q. Shen. 2016. Microbial communities of an arable soil treated for 8 years with organic and inorganic fertilizers. Biology and Fertility of Soils **52**:455-467.

Chen, J. 1967. Petrological and chemical studies of Utuado Pluton, Puerto Rico. Rice University.

Chen, Y., X. Zhang, J. Ye, H. Han, and S. Wan. 2014. Six-year fertilization modifies the biodiversity of arbuscular mycorrhizal fungi in a temperate steppe in Inner Mongolia. Soil Biology & Biochemistry **69**.

Clarkson, D. T., and J. B. Hanson. 1980. The mineral nutrition of higher plants. Annual Review of Plant Physiology **31**:239-298.

Cox, N. J. 1980. On the relationship between bedrock lowering ans regolith thickness. Earth Surface Processes **5**:271-274.

De Cáceres, M., and P. Legendre. 2009. Associations between species and groups of sites: indices and statistical inference. Ecology **90**:3566-3574.

De Cáceres, M., D. Sol, O. Lapiedra, and P. Legendre. 2011. A framework for estimating niche metrics using the resemblance between qualitative resources. Synthesising Ecology **120**:1341-1350.

DeGrood, S. H., V. P. Claassen, and K. M. Scow. 2005. Microbial community composition on native and drastically disturbed serpentine soils. Soil Biology & Biochemistry **37**:1427–1435.

Demir, F., G. Budak, E. Bayas, and Y. Sahin. 2006. Standard deviations of the error effects in preparing pellet samples for WDXRF spectroscopy. Nuclear Instruments and Methods in Physics Research B **243**:423-428.

Di Lionardo, D. P., F. Pinzari, D. Lunghini, O. Maggi, V. M. Granito, and A. M. Persiani. 2013. Metabolic profiling reveals a functional succession of active fungi during the decay of Mediterranean plant litter. Soil Biology & Biochemistry **60**:210-219.

Dixon, J. L., and C. S. Riebe. 2014. Tracing and pacing soil across slopes. Elements **10**:363-368.

Dixon, J. L., and F. von Blanckenburg. 2012. Soils as pacemakers and limiters of global silicate weathering. Comptes Rendus Geoscience:597–609.

Douglas, G. M., V. J. Maffei, J. R. Zaneveld, S. N. Yurgel, B. J. R., C. M. Taylor, C. Huttenhower, and M. G. Langille. 2020. PICRUSt2 for prediction of metagenome functions. Nature Biotechnology **38**:685-688.

Drever, J. I. 1994a. The effect of land plants on weathering rates of silicate minerals. Geochimica Et Cosmochimica Acta **58**:2325-2332.

Drever, J. I. 1994b. The effect of land plants on weathering rates of silicate minerals. Geochimica et Cosmochimica Acta **58**:2325-2332.

Dufrene, M., and P. Legendre. 1997. Species assemblages and indicator species: the need for a flexible asymmetrical approach. Ecological Monographs **67**:345-366.

Durgin, P. B. 1977. Landslides and the weathering of granitic rocks. Reviews in Engineering Geology **3**:127-131.

Edwards, J., C. Johnson, C. Santos-Medellín, E. Lurie, N. Kumar Podishetty, S. Bhatnagar, J. A. Eisen, and V. Sundaresan. 2015. Structure, variation, and assembly of the root-associated microbiomes of rice. PNAS:E911-E920.

Egozcue, J. J., and V. Pawlowsky-Glahn. 2005. CoDa-Dendrogram: a new exploratory tool.*in* G. a. B.-V. In: Mateu-Figueras, C. (Eds.), editor. Proceedings of the 2nd International Workshop on Compositional Data Analysis. Universitat de Girona.

Egozcue, J. J., V. Pawlowsky-Glahn, G. Mateu-Figueras, and C. Barcelo-Vidal. 2003. Isometric logratio transformations for compositional data analysis. Mathematical Geology **35**:279-300.

Ehrenfeld, J. G., B. Ravit, and K. Elgersma. 2005. Feedback in the plant-soil system. Annu. Rev. Environ. Resour. **30**:75-115.

Eilers, K. G., C. L. Lauber, and N. Fierer. 2010. Shifts in bacterial community structure associated with inputs of low molecular weight carbon compounds to soil. Soil Biology & Biochemistry **42**:896-903.

Emberson, R., A. Galy, and N. Hovius. 2018. Weathering of reactive mineral phases in landslides acts as a source of carbon dioxide in mountain belts. JGR Earth Surface **123**:2695-2713.

Emmett, B. D., N. D. Youngblut, D. H. Buckley, and L. E. Drinkwater. 2017. Plant phylogeny and life history shape rhizosphere bacterial microbiome of summer annuals in an agricultural field. Frontiers in Microbiology **8**:1-16.

Ewel, J. J., and J. L. Whitmore. 1973. The ecological life zones of Puerto Rico and the U.S. Virgin Islands. Institute of Tropical Forestry, Rio Piedras, P.R.,.

Fedo, C. M., H. W. Nesbitt, and G. M. Young. 1995. Unraveling the effects of potassium metasomatism in sedimentary rocks and paleosols, with implications for paleoweathering conditions and provenance. Geology **23**:921-924.

Fernandes, A. D., J. M. Macklaim, T. G. Linn, G. Reid, and G. B. Gloor. 2013. ANOVA-Like Differential Expression (ALDEx) Analysis for Mixed Population RNA-Seq. Plos One **8**:e67019.

Fernandes, A. D., J. N. S. Reid, J. M. Macklaim, T. A. McMurrough, R. D. Edgell, and G. B. Gloor. 2014. Unifying the analysis of high-throughput sequencing datasets: characterizing RNA-seq, 16S rRNA gene sequencing and selective growth experiments by compositional data analysis. Microbiome **2**.

Fiantis, D., M. Nelson, J. Shamshuddin, T. B. Goh, and E. Van Ranst. 2010. Determination of the geochemical weathering indices and trace elements content of new volcanic ash deposits from Mt. Talang (West Sumatra) Indonesia. Eurasian Soil Science **43**:1477-1485.

Fierer, N., M. A. Bradford, and R. B. Jackson. 2007. Towards an ecological classification of soil bacteria. Ecology **88**:1354-1364.

Frey, B., S. R. Rieder, I. Brunner, M. Plotze, S. Koetzsch, A. Lapanje, H. Brandl, and G. Furrer. 2010. Weathering-associated bacteria from the Damma Glacier forefield: Physiological capabilities and impact on granite dissolution. Applied and Environmental Microbiology **76**:4788-4796.

Fu, D., X. Wu, C. Duan, L. Zhao, and B. Li. 2020. Different life-form plants exert different rhizosphere effects on phosphorus biogeochemistry in subtropical mountainous soils with low and high phosphorus content. Soil & Tillage Research **199**.

Fuerst, J. A. 2017. Planctomycetes—New models for microbial cells and activities. Pages 1-27 Microbial Resources: From Functional Existence in Nature to Applications. Academic Press.

Gadd, G. M. 2007. Geomycology: biogeochemical transformations of rocks, minerals, metals and radionuclides by fungi, bioweathering and bioremediation. Mycological Research **111**:3-49.

Gadd, G. M. 2013. Microbial roles in mineral transformations and metal cycling in the Earth's Critical Zone. Pages 115–165 *in* J. Xu and D. L. Sparks, editors. Molecular Environmental Soil Science. Springer Netherlands.

Gadd, G. M. 2017. Geomicrobiology of the built environment. Nature Microbiology **2**:1-9.

Geertsema, M., and J. J. Pojar. 2007. Influence of landslides on biophysical diversity — A perspective from British Columbia. Geomorphology **89**:55-69.

Gleeson, D., F. Mathes, M. Farrell, and M. Leopold. 2016. Environmental drivers of soil microbial community structure and function at the Avon River Critical Zone Observatory. Sci Total Environ **571**:1407-1418.

Gleeson, D. B., N. M. Kennedy, N. Clipson, K. Melville, G. M. Gadd, and F. P. McDermott. 2006. Characterization of bacterial community structure on a weathered pegmatitic granite. Microbial Ecology **51**:526-534.

Glockner, F. O., P. Yilmaz, C. Quast, J. Gerken, A. Beccati, A. Ciuprina, G. Bruns, P. Yarza, J. Peplies, R. Westram, and W. Ludwig. 2017. 25 years of serving the community with ribosomal RNA gene reference databases and tools. Journal of Biotechnology **261**:169-176.

Gloor, G. B., J. M. Macklaim, and A. D. Fernandes. 2015. Displaying Variation in Large Datasets: Plotting a Visual Summary of Effect Sizes. Journal of Computational and Graphical Statistics.

Gorbushina, A. A. 2007. Life on the rocks. Environmental Microbiology **9**:1613-1631.

Gorbushina, A. A., and W. J. Broughton. 2009. Microbiology of the atmosphere-rock interface: How biological interactions and physical stresses modulate a sophisticated microbial ecosystem.431-450.

Gorbushina, A. A., E. R. Kotlova, and O. A. Sherstneva. 2008. Cellular responses of microcolonial rock fungi to long-term desiccation and subsequent rehydration. Stud Mycol **61**:91-97.

Gorbushina, A. A., and W. E. Krumbein. 2005. Ch 3: Role of microorganisms in wear down of rocks and minerals. Pages 59-84 Soil Biology. Springer-Verlag Berlin Heidelberg.

Gorbushina, A. A., K. Whitehead, T. Dornieden, A. Niesse, A. Schulte, and J. I. Hedges. 2003. Black fungal colonies as units of survival: hyphal mycosporines synthesized by rock-dwelling microcolonial fungi. Canadian Journal of Botany **81**:131-138.

Grayston, S. J., D. Vaughan, and D. Jones. 1996. Rhizosphere carbon flow in trees, in comparison with annual plants: the importance of root exudation and its impact on microbial activity and nutrient availability. Applied Soil Ecology **5**:29-56.

Grime, J. P., and S. Pierce. 2012. The evolutionary strategies that shape ecosystems. John Wiley & Sons, Oxford.

Guariguata, M. R. 1990. Landslide disturbance and forest regeneration in the Upper Luquillo Mountains of Puerto Rico. Pages 814 - 832. Journal of Ecology.

Guida, M., P. Losanno Cannavacciuolo, M. Cesarano, M. Borra, E. Biffali, R. D'Alessandro, and B. De Felice. 2014. Microbial diversity of landslide soils assessed by RFLP and SSCP fingerprints. J Appl Genetics **55**:403–415.

Halsey, D. P., D. J. Mitchell, and S. J. Dews. 1998. Influence of climatically induced cycles in physical weathering. Quarterly Journal of Engineering Geology and Hydrogeology **31**:359-367.

Hambleton, S., N. L. Nickerson, and K. A. Seifert. 2005. Leohumicola, a new genus of heat-resistant hyphomycetes. Studies in Mycology **53**:29-52.

Harnois, L. 1988. The CIW Index: A new chemical index of weathering. Sedimentary Geology **55**:319-322.

Heimsath, A. M., W. E. Dietrich, K. Nishiizumi, and R. C. Finkel. 1997. The soil production function and landscape equilibrium. Nature **388**:358-361.

Hilley, G. E., and S. Porder. 2008. A framework for predicting global silicate weathering and CO2 drawdown rates over geologic time-scales. PNAS **105**:16855-16859.

Hiraishi, A., and Y. Ueda. 1994. Rhodoplanes gen. nov., a new genus of phototrophic bacteria including Rhodopseudomonas rosea as Rhodoplanes roseus comb. nov. and Rhodoplanes elegans sp. nov. International Journal of Systematic and Evolutionary Microbiology **44**:665-673.

Hirsch, P. 1992. The genus Nevskia. Pages 4089-4092 *in* B. e. al., editor. The Prokaryotes. Springer Science+Business Media, New York.

Ho, A., D. P. Di Lionardo, and P. L. E. Bodelier. 2017. Revisiting life strategy concepts in environmental microbial ecology. FEMS Microbiol Ecol **93**:1-14.

Hoppert, M., C. Flies, W. Pohl, B. Gunzl, and J. Schneider. 2004. Colonization strategies of lithobiontic microorganisms on carbonate rocks. Environmental Geology **46**:421-428.

Hughes, K. S., and W. H. Schulz. 2020. Map depicting susceptibility to landslides triggered by intense rainfall, Puerto Rico. U.S. Geological Survey.

Ihrmark, K., I. T. Bodeker, K. Cruz-Martinez, H. Friberg, A. Kubartova, J. Schenck, Y. Strid, J. Stenlid, M. Brandstrom-Durling, K. E. Clemmensen, and B. D. Lindahl. 2012. New primers to amplify the fungal ITS2 region--evaluation by 454-sequencing of artificial and natural communities. FEMS Microbiol Ecol **82**:666-677.

Imam, M. H., C. T. Ogushi, T. Wakatsuki, and M. Ueda. 2019. Assessment of climate-induced degree of chemical weathering in some granite and granodiorite slopes of Japan. Modeling Earth Systems and Environment **5**:1751–1767.

Irfan, T. Y. 1996. Mineralogy, fabric properties and classification of weathered granites in Hong Kong. Quarterly Journal of Engineering Geology **29**:5-35.

Jackson, C. R. 2003. Changes in community properties during microbial succession. Oikos **101**:444-448.

Jackson, O., R. S. Quilliam, A. Stott, H. Grant, and S. J. A. 2019. Rhizosphere carbon supply accelerates soil organic matter decomposition in the presence of fresh organic substrates. Plant and Soil **440**:473-490.

Jayawardena, U. S., and E. Izawa. 1994a. Application of present indices of chemical weathering for precambrian metamorphic rocks in Sri Lanka. Bulletin of the International Association of Engineering Geology **49**:55-61.

Jayawardena, U. S., and E. Izawa. 1994b. A new chemical index of weathering for metamorphic silicate rocks in tropical regions: A study from Sri Lanka. Engineering Geology **36**:303-310.

Jenny, H. 1941. Factors of Soil Formation: A System of Quantitative Pedology. McGraw-Hill, New York.

Josse, J., and F. Husson. 2016. missMDA: A Package for Handling Missing Values in Multivariate Data Analysis. Journal of Statistical Software **70**:1-31.

Judd, W. S., and G. M. Ionta. 2013. Taxonomic studies in the Miconieae (Melastomataceae). X. Revision of the species of the Miconia crotonifolia complex. Brittonia **65**:66-95.

Kalinowski, B. E., L. J. Liermann, S. Givens, and S. L. Brantley. 2000. Rates of bacteria-promoted solubilization of Fe from minerals: a review of problems and approaches Chemical Geology **169**:357-370.

Kandlikar, G. S., Z. J. Gold, M. C. Cowen, R. S. Meyer, A. C. Freise, N. J. B. Kraft, J. Moberg-Parker, J. Sprague, D. J. Kushner, and E. E. Curd. 2018. ranacapa: An R package and Shiny web app to explore environmental DNA data with exploratory statistics and interactive visualizations [version 1]. F1000Research **7**:1734-1751.

Katoh, K., and D. M. Standley. 2013. MAFFT multiple sequence alignment software version 7: Improvements in performance and usability. Molecular Biology and Evolution **30**:772-780.

Keddy, P. 2007. Plants and vegetation: Origins, processes, consequences. Cambridge University Press.

Kirtzel, J., N. Ueberschaar, T. Deckert-Gaudig, K. Krause, V. Deckert, G. M. Gadd, and E. Kothe. 2020. Organic acids, siderophores, enzymes and mechanical pressure for black slate bioweathering with the basidiomycete Schizophyllum commune. Environmental Microbiology **22**:1535-1546.

Knelman, J. E., T. M. Legg, S. P. O'neill, C. L. Washenberg, A. González, C. C. Cleveland, and D. R. Nemergut. 2012. Bacterial community structure and function change in association with colonizer plants during early primary succession in a glacier forefield. Soil Biology & Biochemistry **46**.

Koele, N., I. A. Dickie, J. D. Blum, J. D. Gleason, and L. de Graaf. 2014. Ecological significance of mineral weathering in ectomycorrhizal and arbuscular mycorrhizal ecosystems from a field-based comparison. Soil Biology & Biochemistry **69**:63-70.

Koele, N., M. P. Turpault, E. E. Hildebrand, S. Uroz, and P. Frey-Klett. 2009. Interactions between mycorrhizal fungi and mycorrhizosphere bacteria during mineral weathering: Budget analysis and bacterial quantification. Soil Biology & Biochemistry **41**:1935-1942.

Krause, S., X. Le Roux, P. A. Niklaus, P. M. Van Bodegom, J. T. Lennon, S. Bertilsson, H.-P. Grossart, L. Philippot, and P. L. E. Bodelier. 2014. Trait-based approaches for understanding microbial biodiversity and ecosystem functioning. Frontiers in Microbiology **5**:1-10.

Lambers, H., C. Mougel, B. Jaillard, and P. Hinsinger. 2009. Plant-microbe-soil interactions in the rhizosphere: an evolutionary perspective. Plant and Soil **321**:83-115.

Lane, D. J. 1991. 16s/23s rrna sequencing. John Wiley and Sons, New York.

Larsen, J., P. Jaramillo-López, M. Nájera-Rincón, and C. E. Gonzaléz-Esquivel. 2015. Biotic interactions in the rhizosphere in relation to plant and soil nutrient dynamics. Journal of Soil Science and Plant Nutrition **15**:449-463.

Larsen, M. C., and A. J. Torres-Sánchez. 1996. Geographic relations of landslide Distribution and assessment of landslide hazards in the Blanco, Cibuco, and Coamo basins, Puerto Rico. U.S. Geological Survey, San Juan, Puerto Rico.

Lê, S., J. Josse, and F. Husson. 2008. FactoMineR: A Package for Multivariate Analysis. Journal of Statistical Software **25**:1-18.

Leake, J. R., A. L. Duran, K. E. Hardy, I. Johnson, D. J. Beerling, S. A. Banwart, and M. M. Smits. 2008a. Biological weathering in soil: the role of symbiotic root-associated fungi biosensing minerals and directing photosynthate-energy into grain-scale mineral weathering. Mineralogical Magazine **72**:85-89.

Leake, J. R., A. L. Duran, K. E. Hardy, I. Johnson, D. J. Beerling, S. A. Banwart, and M. M. Smits. 2008b. Biological weathering in soil: the role of symbiotic root-associated fungi biosensing minerals and directing photosynthate-energy into grain-scale mineral weathering. Mineralogical Magazine **72**:85-89.

Leyval, C., and J. Berthelin. 1991. Weathering of a mica by roots and rhizospheric microorganisms of pine. Soil Sci. Soc. Am. J. **55**:1009-1016.

Li, Y., H. Ruan, X. Zou, and R. W. Myster. 2005. Response of major soil decomposers to landslide disturbance in a Puerto Rican rainforest. Soil Science **170**:202-211.

Liermann, L. J., I. Albert, H. L. Buss, M. Minyard, and S. L. Brantley. 2015. Relating microbial community structure and geochemistry in deep regolith developed on volcaniclastic rock in the Luquillo Mountains, Puerto Rico. Geomicrobiology Journal **32**:494-510.

Liu, Y., E. J. M. Carranza, K. Zhou, and Q. Xia. 2019. Compositional balance analysis: An elegant method of geochemical pattern recognition and anomaly mapping for mineral exploration Natural Resources Research **28**:1269-1283.

Lladó, S., R. López-Mondéjar, and P. Baldrian. 2018. Drivers of microbial community structure in forest soils. Appl Microbiol Biotechnol **102**:4331–4338.

Lopez, A. M., K. S. Hughes, and E. Vanacore. 2020. Puerto Rico's winter 2019–2020 seismic sequence leaves the island on edge: Temblor.

Lunghini, D., V. M. Granito, D. P. Di Lionardo, O. Maggi, and A. M. Persiani. 2013. Fungal diversity of saprotrophic litter fungi in a Mediterranean maquis environment. Mycologia **105**:1499-1515.

Mapelli, F., R. Marasco, M. Fusi, B. Scaglia, G. Tsiamis, E. Rolli, S. Fodelianakis, K. Bourtzis, S. Ventura, F. Tambone, F. Adani, S. Borin, and D. Daffonchio. 2018. The stage of soil development modulates rhizosphere effect along a High Arctic desert chronosequence. The ISME Journal **12**:1188-1198.

Marguí, E. V. G., R. 2013. Chapter 3: Qualitative and Quantitative X-Ray Fluorescence Analysis. Pages 33-59 *in* J. M. Chalmers, editor. X-Ray Fluorescence Spectrometry and Related Techniques: An Introduction. Momentum Press, New York.

Markowicz, A., M. Dargie, and R. L. Walsh. 1997. Analysis of geological materials. Pages 15-20 Sampling, storage and sample preparation procedures for X ray fluorescence analysis of environmental materials. International Atomic Energy Agency, Vienna, Austria.

Marschner, H. 1995. Mineral Nutrition of Higher Plants. Second Edition edition. Academic Press, ndon.

Martin, M. 2011. Cutadapt removes adapter sequences from high-throughput sequencing reads. EMBnet. journal **17**:10.

Matsukura, Y., T. Hattanji, C. T. Oguchi, and T. Hirose. 2007. Ten year measurements of weathering rates of rock tablets on a forested hillslope in a humid temperate region, Japan. Z. Geomorph. N. F. **51**:27-40.

Matsunami, H., K. Matsuda, S. Yamasaki, K. Kimura, Y. Ogawa, Y. Miura, I. Yamaji, and N. Tsuchiya. 2010. Rapid simultaneous multi-element determination of soils and environmental samples with polarizing energy dispersive X-ray fluorescence (EDXRF) spectrometry using pressed powder pellets. Soil Science & Plant Nutrition **56**:530-540.

Matthews, T. J. 2014. Integrating Geoconservation and Biodiversity Conservation: Theoretical Foundations and Conservation Recommendations in a European Union Context. Geoheritage **6**:57-70.

Maurice, P. A., M. A. Vierkorn, L. E. Hersman, and J. E. Fulghum. 2001. Dissolution of well and poorly ordered kaolinites by an aerobic bacterium. Chemical Geology **180**:81-97.

McAdams, B. C., A. M. Trierweiler, S. A. Welch, C. Restrepo, and A. E. Carey. 2015. Two sides to every range: Orographic influences on CO2 consumption by silicate weathering. Applied Geochemistry **63**:472-483.

McMurdie, and Holmes. 2013a. Phyloseq: An R Package for Reproducible Interactive Analysis and graphics of Microbiome Census Data. Plos One **8**:e61217.

McMurdie, P. J., and S. Holmes. 2013b. phyloseq: An R package for reproducible interactive analysis and graphics of microbiome census data. Plos One **8**.

McMurdie, P. J., and S. Holmes. 2014. Shiny-phyloseq: Web application for interactive microbiome analysis with provenance tracking. Bioinformatics **31**:282-283.

Mendes, L. W., E. E. Kuramae, A. A. Navarrete, J. A. van Veen, and S. M. Tsai. 2014. Taxonomical and functional microbial community selection in soybean rhizosphere. The ISME Journal **8**:1577-1587.

Middelburg, J. J., C. H. Van Der Weijden, and J. R. W. Woittiez. 1988. Chemical processes affecting the mobility of major, minor and trace elements during weathering of granitic rocks. Chemical Geology **68**:253-273.

Molinelli, J. A. 1984. Geomorphic processes along the Autopista Las Americas in north central Puerto Rico Implications for highway construction, design, and maintenance. Clark University, Ann Monroe, Michigan.

Monroe, W. H. 1979. Map showing landslides and areas of susceptibility to landsliding in Puerto Rico. Department of the Interior, U.S. Geological Survey:Map I-1148.

Mori, P. M., S. Reeves, C. Teixeira-Correia, and M. Haukka. 1999. Development of a fused glass disc XRF facility and comparison with the pressed powder pellet technique at Instituto de Geociencias, Sao Paulo University. Brazilian Journal of Geology **23**:441-446.

Muenchow, J., A. Brenning, and M. Richter. 2012. Geomorphic process rates of landslides along a humidity gradient in the tropical Andes. Geomorphology **139 - 140**:271-284.

Neaman, A., J. Chorover, and S. L. Brantley. 2006. Effects of organic ligands on granite dissolution in batch experiments at pH 6. American Journal of Science **306**:451-473.

Nemergut, D. R., S. P. Anderson, C. C. Cleveland, A. P. Martin, A. E. Miller, A. Seimon, and S. K. Schmidt. 2007. Microbial community succession in an unvegetated recently deglaciated soil. Microbial Ecology **53**:110-122.

Nesbitt, H. W., and G. M. Young. 1982. Early Proterozoic climates and plate motions inferred from major element chemistry or lutites. Nature **299**:715–717.

Nguyena, N. H., Z. Song, S. T. Bates, S. Branco, L. Tedersoo, J. Menk, J. S. Schilling, and P. G. Kennedy. 2016. FUNGuild: An open annotation tool for parsing fungal community datasets by ecological guild. Fungal Ecology **20**:241-248.

Nilsson, R. H., K. H. Larsson, A. F. S. Taylor, J. Bengtsson-Palme, T. S. Jeppesen, D. Schigel, P. Kennedy, K. Picard, F. O. Glockner, L. Tedersoo, I. Saar, U. Koljalg, and K. Abarenkov. 2019. The UNITE database for molecular identification of fungi: handling dark taxa and parallel taxonomic classifications. Nucleic Acids Research **47**:D259-D264.

Oksanen, J., F. G. Blanchet, M. Friendly, R. Kindt, P. Legendre, D. McGlinn, P. R. Minchin, R. B. O'Hara, G. L. Simpson, P. Solymos, M. H. H. Stevens, E. Szoecs, and H. Wagner. 2018. vegan: Community ecology package. R package version 2.5-3.

Olsson-Francis, K., A. E. Simpson, D. Wolff-Boenisch, and C. S. Cockell. 2012. The effect of rock composition on cyanobacterial weathering of crystalline basalt and rhyolite. Geobiology **10**:434-444.

Omelon, C. R. 2008. Endolithic microbial communities in Polar Desert habitats. Geomicrobiology Journal **25**:404-414.

Ortiz-Álvarez, R., N. Fierer, A. de los Ríos, E. O. Casamayor, and A. Barberán. 2018. Consistent changes in the taxonomic structure and functional attributes of bacterial communities during primary succession The ISME Journal **12**:1658-1667.

Ortiz, Y., C. Restrepo, B. Vilanova-Cuevas, E. Santiago-Valentin, S. G. Tringe, and F. Godoy-Vitorino. 2020. Geology and climate influence rhizobiome composition of the phenotypically diverse tropical tree Tabebuia heterophylla. Plos One **15**:e0231083.

Osksanen, L., and E. Ranta. 1992. Plant strategies along mountain vegetation gradients: a test of two theories. Journal of Vegetation Science **3**:175-186.

Palarea-Albaladejo, J., and J. A. Martín-Fernández. 2015. zCompositions — R package for multivariate imputation of left-censored data under a compositional approach. Chemometrics and Intelligent Laboratory Systems **143**:85-96.

Parent, S. E., L. E. Parent, J. J. Egozcue, D. E. Rozane, A. Hernandes, L. Lapointe, V. Hebert-Gentile, K. Naess, S. Marchand, J. Lafond, D. Mattos, Jr., P. Barlow, and W. Natale. 2013. The plant ionome revisited by the nutrient balance concept. Front Plant Sci **4**:39.

Parent, S. E., L. E. Parent, D. E. Rozanne, A. Hernandes, and W. Natale. 2012. Nutrient balance as paradigm of soil and plant chemometrics.*in* R. N. Issaka, editor. Soil Fertility. IntechOpen.

Parker, A. 1970. An index of weathering for silicate rocks. Geological Magazine **107**:501-504.

Pedregosa, F., G. Varoquaux, A. Gramfort, V. Michel, B. Thirion, O. Grisel, M. Blondel, P. Prettenhofer, R. Weiss, V. Dubourg, J. Vanderplas, A. Passos, D. Cournapeau, M. Brucher, M. Perrot, and E. Duchesnay. 2011. Scikit-learn: machine learning in Python. Journal of Machine Learning Research **12**:2825-2830.

Peiffer, J. A., A. Spor, O. Koren, Z. Jin, S. G. Tringe, J. L. Dangl, E. S. Buckler, and R. E. Ley. 2015. Diversity and heritability of the maize rhizosphere microbiome under field conditions. PNAS **110**:6548-6553.

Philippot, L., J. M. Raaijmakers, P. Lemanceau, and W. H. van der Putten. 2013. Going back to the roots: the microbial ecology of the rhizosphere Pages 789–799. Nature reviews Microbiology.

Price, M. N., P. S. Dehal, and A. P. Arkin. 2010. FastTree 2-approximately maximum-likelihood trees for large alignments. Plos One **5**.

Prince, J. R., and M. A. Velbel. 2003. Chemical weathering indices applied to weathering profiles developed on heterogeneous felsic metamorphic parent rocks. Chemical Geology **202**:397-416.

Pruesse, E., C. Quast, K. Knittel, B. M. Fuchs, W. G. Ludwig, J. Peplies, and F. O. Glockner. 2007. SILVA: a comprehensive online resource for quality checked and aligned ribosomal RNA sequence data compatible with ARB. Nucleic Acids Research **35**:7188-7196.

Quast, C., E. Pruesse, P. Yilmaz, J. Gerken, T. Schweer, P. Yarza, J. Peplies, and F. O. Glockner. 2013. The SILVA ribosomal RNA gene database project: improved data processing and web-based tools. Nucleic Acids Research **41**:D590-D596.

Quirk, J., D. J. Beerling, S. A. Banwart, G. Kakonyi, M. E. Romero-Gonzalez, and J. R. Leake. 2012. Evolution of trees and mycorrhizal fungi intensifies silicate mineral weathering. Biology Letters **8**:1006-1011.

R Core Team. 2013. R: A language and environment for statistical computing. R Foundation for Statistical Computing, Vienna, Austria.

Reiche, P. 1950. A survey of weathering processes and products. University of New Mexico Press, Albuquerque.

Restrepo, C., L. R. Walker, A. B. Shiels, R. Bussmann, L. Claessens, S. Fisch, P. Lozano, G. Negi, L. Paolini, G. Poveda, C. Ramos-Scharrón, M. Richter, and E. Velázquez. 2009. Landsliding and Its Multiscale Influence on Mountainscapes. BioScience **59**:685-698.

Riebe, C. S., J. W. Kirchner, and R. C. Finkel. 2003. Long-term rates of chemical weathering and physical erosion from cosmogenic nuclides and geochemical mass balance. Geochimica Et Cosmochimica Acta **67**:4411-4427.

Roberts, D. W. 2016. Labdsv: ordination and multivariate analysis for ecology.

Roberts, J. A. 2004. Inhibition and enhancement of microbial surface colonization: the role of silicate composition. Chemical Geology **212**:313-327.

Rocha Filho, P., F. S. Antuenes, and M. F. G. Falcao. 1985. Quantitative influence of the weathering upon the mechanical properties of a young gneiss residual soil. First Int. Conf. Geomech. Trop. Lateric Sprolitic Soils Brasilia **1**:281-294.

Roeselers, G., M. C. van Loosdrecht, and G. Muyzer. 2007. Heterotrophic pioneers facilitate phototrophic biofilm development. Microbial Ecology **54**:578-585.

Rogers, J. R., and P. C. Bennett. 2004. Mineral stimulation of subsurface microorganisms: release of limiting nutrients from silicates. Chemical Geology **203**:91-108.

Rogers, J. R., P. C. Bennett, and W. J. Choi. 1998. Feldspars as source of nutrients for microorganisms. American Mineralogist **83**:1532-1540.

Rollerson, T., D. Maynard, S. Higman, and E. Ortmayr. 2004. Klanawa landslide hazard mapping pilot project. Pages 1-24 oint Conference of IUFRO 3.06 Forest Operations under Mountainous Conditions and the 12th International Mountain Logging Conference, Vancouver B.C.

Rousseau, R. M. 2001. Detection limit and estimate of uncertainty of analytical XRF results. The Rigaku Journal **18**:33-47.

Ruxton, B. P. 1968. Measures of the degree of chemical weathering of rocks. Journal of Geology **76**:518-527.

Ruxton, B. P., and L. Berry. 1957. The weathering of granite and associated erosional features in Hong Kong. Bulletin of the Geological Society of America **68**:1263-1292.

Sajinkumar, K. S., S. Anbazhagan, A. P. Pradeepkumar, and V. R. Rani. 2011. Weathering and landslide occurrences in parts of Western Ghats, Kerala. geological Society of India **78**:249-257.

Schulz, S., R. Brankatschk, A. Dumig, I. Kogel-Knabner, M. Schloter, and J. Zeyer. 2013. The role of microorganisms at different stages of ecosystem development for soil formation. Biogeosciences **10**:3983-3996.

Schwartzman, D. W. 2017. Life's critical role in the long-term carbon cycle: the biotic enhancement of weathering. AIMS Geosciences **3**:216-238.

Shi, Z., H. Yin, J. D. Van Nostrand, J. W. Voordeckers, Q. Tu, Y. Deng, M. Yuan, A. Zhou, P. Zhang, N. Xiao, D. Ning, Z. He, L. Wu, and J. Zhou. 2019. Functional gene array-based ultrasensitive and quantitative detection of microbial populations in complex communities. Msystems **4**.

Singh, K. P., T. N. Mandal, and S. K. Tripathi. 2001. Patterns of restoration of soil physicochemical properties and microbial biomass in different landslide sites in the sal forest ecosystem of Nepal Himalaya. Ecological Engineering **17**:385-401.

Smith, A. L., J. H. Schellekens, and A. L. Muriel-Diaz. 1998. Batholiths as markers of tectonic change in the northeastern Caribbean. GSA Special Paper **322**:99-122.

Smits, M. M., S. Bonneville, L. G. Benning, S. A. Banwart, and J. R. Leake. 2012. Plant-driven weathering of apatite – the role of an ectomycorrhizal fungus Geobiology **10**:445–456.

Song, W., N. Ogawa, C. Takashima-Oguchi, T. Hatta, and Y. Matsukura. 2007. Effect of Bacillus subtilis on granite weathering: A laboratory experiment. Catena **70**:275-281.

Song, W., N. Ogawa, C. Takashima-Oguchi, T. Hatta, and Y. Matsukura. 2010. Laboratory experiments on bacterial weathering of granite and its constituent minerals. Géomorphologie: relief, processus, environnement **16**:327-336.

Sparling, G., G. Ross, N. Trustrum, G. Arnold, A. West, T. Speir, and L. Schipper. 2003. Recovery of topsoil characteristics after landslip erosion in dry hill country of New Zealand, and a test of the space-for-time hypothesis. Soil Biology and Biochemistry **35**:1575-1586.

Štyriaková, I., I. Štyriak, and H. Oberhänsli. 2012. Rock weathering by indigenous heterotrophic bacteria of Bacillus spp. at different temperature: a laboratory experiment. Mineral Petrology **105**:135-144.

Sugden, A. M., E. V. J. Tanner, and V. Kapos. 1985. Regeneration following clearing in a Jamaican montane forest: Results of a ten-year study. Journal of Tropical Ecology **1**:329-351.

Tang, J., Y. Mo, J. Zhang, and R. Zhang. 2011. Influence of biological aggregating agents associated with microbial population on soil aggregate stability. Applied Soil Ecology **47**:153-159.

Taylor, D. L., W. A. Walters, N. J. Lennon, J. Bochicchio, A. Krohn, J. G. Caporaso, and T. Pennanen. 2016. Accurate estimation of fungal diversity and abundance through improved lineage-specific primers optimized for Illumina amplicon sequencing. Applied and Environmental Microbiology **82**:7217-7226.

Taylor, L. L., J. R. Leake, J. Quirk, K. Hardy, S. A. Banwart, and D. J. Beerling. 2009. Biological weathering and the long-term carbon cycle: integrating mycorrhizal evolution and function into the current paradigm. Geobiology **7**:171-191.

Thorn, C. E., R. G. Darmody, J. C. Dixon, and P. Schlyter. 2002. Weathering rates of buried machine-polished rock disks, Karkevagge, Swedish Lapland. Earth Surf. Process. Landforms **27**:831-845.

Trustrum, N. A., and R. C. De Rose. 1988. Soil depth-age relationship of landslides on deforested hillslopes, Taranaki, New Zealand. Geomorphology **1**:143-160.

Turpault, M. P., C. Nys, and C. Calvaruso. 2009. Rhizosphere impact on the dissolution of test minerals in a forest ecosystem. Geoderma **153**:147-154.

Uhlig, D., J. A. Schuessler, J. Bouchez, J. L. Dixon, and F. Von Blanckenburg. 2017. Quantifying nutrient uptake as driver of rock weathering in forest ecosystems by magnesium stable isotopes. Biogeosciences **14**:3111-3128.

Ullman, W. J., D. L. Kirchman, S. A. Welch, and P. Vandevivere. 1996. Laboratory evidence for microbially mediated silicate mineral dissolution in nature. Chemical Geology **132**:11-17.

Uroz, S., C. Calvaruso, M.-P. Turpault, and P. Frey-Klett. 2009a. Mineral weathering by bacteria: ecology, actors and mechanisms. Trends in Microbiology **17**:378-387.

Uroz, S., C. Calvaruso, M. P. Turpault, J. C. Pierrat, C. Mustin, and P. Frey-Klett. 2007. Effect of the mycorrhizosphere on the genotypic and metabolic diversity of the bacterial communities involved in mineral weathering in a forest soil. Applied and Environmental Microbiology **73**:3019-3027.

Uroz, S., C. Calvaruso, M. P. Turpault, A. Sarniguet, W. de Boer, J. H. J. Leveau, and P. Frey-Klett. 2009b. Efficient mineral weathering is a distinctive functional trait of the bacterial genus Collimonas. Soil Biology and Biochemistry **41**:2178-2186.

Uroz, S., P. Oger, C. Lepleux, C. Collignon, P. Frey-Klett, and M.-P. Turpault. 2011. Bacterial weathering and its contribution to nutrient cycling in temperate forest ecosystems. Research in Microbiology **162**:820-831.

van den Boogaart, K. G. 2008. Using the R package "compositions".

van Scholl, L., T. W. Kuyper, M. M. Smits, R. Landeweert, E. Hoffland, and N. van Breemen. 2008. Rock-eating mycorrhizas: their role in plant nutrition and biogeochemical cycles. Plant and Soil **303**:35-47.

VanBuskirk, C. D., R. J. Neden, J. W. Schwab, and F. R. FSmith. 2005. Road and terrain attributes of road fill landslides in the Kalum Forest District. B.C. Ministry of Forests and Range, Province of British Columbia.

Vandevivere, P., S. A. Welch, W. J. Ullman, and D. L. Kirchman. 1994a. Enhanced dissolution of silicate minerals by bacteria at near-neutral pH. Microb Ecol **27**:241-251.

Vandevivere, P., S. A. Welch, W. J. Ullman, and D. L. Kirchman. 1994b. Enhanced dissolution of silicate minerals by bacteria at near-neutral pH. Microb Ecol **27**:241-251.

Visioli, G., S. D'Egidio, and A. M. Sanangelantoni. 2015. The bacterial rhizobiome of hyperaccumulators: future perspectives based on omics analysis and advanced microscopy. Frontiers in Plant Science **5**:1-12.

Vogt, T. 1927. Sulitjelmafeltets geologi og petrografi. Norges Geologiske Undersokelse **121**:1-560.

Volkmann, M., K. Whitehead, H. Rutters, J. Rullkotter, and A. A. Gorbushina. 2003. Mycosporine-glutamicol-glucoside: a natural UV-absorbing secondary metabolite of rock-inhabiting microcolonial fungi. Rapid Commun. Mass Spectrom. **17**:897-902.

Vuorinen, A., S. Mantere-Alhonen, R. Uusinoka, and P. Alhonen. 1981. Bacterial weathering of rapakivi granite. Geomicrobiology Journal **2**:317-325.

Wagner, M. R., D. S. Lundberg, T. G. del Rio, S. G. Tringe, J. L. Dangl, and T. Mitchell-Olds. 2016. Host genotype and age shape the leaf and root microbiomes of a wild perennial plant. Nature Communications **7**:1-15.

Walker, J. J., and N. R. Pace. 2007. Endolithic microbial ecosystems. Annu Rev Microbiol **61**:331-347.

Walker, L. R. 1994. Effects of fern thickets on woodland development on landslides in Puerto-Rico. Journal of Vegetation Science **5**:525-532.

Walker, L. R., and A. B. Shiels. 2008. Post-disturbance erosion impacts carbon fluxes and plant succession on recent tropical landslides Plant Soil **313**:205-216.

Wallander, H., L. O. Nilsson, D. Hagerberg, and E. Bååth. 2001. Estimation of the biomass and seasonal growth of external mycelium of ectomycorrhizal fungi in the field. New Phytol **151**:753–760.

Wang, G., J. Li, X. Liu, and L. X. 2013. Variations in carbon isotope ratios of plants across a temperature gradient along the 400 mm isoline of mean annual precipitation in north China and their relevance to paleovegetation reconstruction. Quaternary Science Reviews **63**:83-90.

Warscheid, T., and J. Braams. 2000. Biodeterioration of stone: a review. International Biodeterioration & Biodegradation **46**:343-368.

Weaver, P. L. 1979. Tree growth in several tropical forests of Puerto Rico. U.S. Dept. of Agriculture, Forest Service, Southern Forest Experiment Station, New Orleans, La.

Welch, S. A., W. W. Barker, and J. F. Banfield. 1999. Microbial extracellular polysaccharides and plagioclase dissolution. Geochimica Et Cosmochimica Acta **63**:1405-1419.

Welch, S. A., A. E. Taunton, and J. F. Banfield. 2002. Effect of microorganisms and microbial metabolites on apatite dissolution. Geomicrobiology Journal **19**:343-367.

Welch, S. A., and W. J. Ullman. 1993. The effect of organic acids on plagioclase dissolution rates and stoichiometry. Geochimica Et Cosmochimica Acta **57**:2725-2736.

Wickham, H. 2016. ggplot2: Elegant Graphics for Data Analysis. Springer-Verlag, New York.

Wickham, H., M. Averick, J. Bryan, W. Chang, L. D. McGowan, R. François, G. Grolemund, A. Hayes, L. Henry, J. Hester, M. Kuhn, T. L. Pedersen, E. Miller, S. M. Bache, K. Müller, J. Ooms, D. Robinson, D. P. Seidel, V. Spinu, K. Takahashi, D. Vaughan, C. Wilke, K. Woo, and H. Yutani. 2019. Welcome to the tidyverse. Journal of Open Source Software **4**:1686.

Wilford, J. 2012. A weathering intensity index for the Australian continent using airborne gamma-ray spectrometry and digital terrain analysis. Geoderma **183-184**:124-142.

Wills, C. J., M. W. Manson, K. D. Brown, C. W. Davenport, and C. J. Domrose. 2001. Landslides in the Highway 1 corridor: Geology and slope stability along the Big Sur coast between Point Lobos and San Carpoforo Creek, Monterey and San Luis Obispo counties, California. California Department of Transportation.

Wojcik, R., J. Donhauser, B. Frey, and L. G. Benning. 2020. Time since deglaciation and geomorphological disturbances determine the patterns of geochemical, mineralogical and microbial successions in an Icelandic foreland. Geoderma **379**:1-14.

Wood, J. L., and A. E. Franks. 2018. Understanding microbiomes through trait-based ecology. Microbiology Australia **39**:53-55.

Wood, J. L., C. Tang, and A. E. Franks. 2018. Competitive traits are more important than stress-tolerance traits in a cadmium-contaminated rhizosphere: a role for trait theory in microbial ecology. Frontiers in Microbiology **9**:1-12.

Wu, L., A. D. Jacobson, and M. Hausner. 2008. Characterization of elemental release during microbe–granite interactions at T=28°C. Geochimica Et Cosmochimica Acta **72**:1076-1095.

Yeoh, Y. K., P. G. Dennis, C. Paungfoo-Lonhienne, L. Weber, R. Brackin, M. A. Ragan, S. Schmidt, and P. Hugenholtz. 2017. Evolutionary conservation of a core root microbiome across plant phyla along a tropical soil chronosequence. Nature Communications **8**:1-9.

Yilmaz, P., L. W. Parfrey, P. Yarza, J. Gerken, E. Pruesse, C. Quast, T. Schweer, J. Peplies, W. Ludwig, and F. O. Glockner. 2014. The SILVA and "All-species Living Tree Project (LTP)" taxonomic frameworks. Nucleic Acids Research **42**:D643-D648.

Zhalnina, K., K. B. Louie, Z. Hao, N. Mansoori, U. Nunes da Rocha, S. Shi, H. Cho, U. Karaoz, D. Loqué, B. P. Bowen, M. K. Firestone, T. R. Northen, and E. L. Brodie. 2018. Dynamic root exudate chemistry and microbial substrate preferences drive patterns in rhizosphere microbial community assembly. Nature Microbiology **3**:470 - 480.

Zumsteg, A., J. Luster, H. Göransson, R. H. Smittenberg, I. Brunner, S. M. Bernasconi, J. Zeyer, and B. Frey. 2012. Bacterial, archaeal and fungal succession in the forefield of a receding glacier. Microbial Ecology **63**:552-564.

TABLES

`

Table 3.1. Experimental design of rock tiles and pellets buried close to roots and bulk soils surrounding *Cyathea arborea* (landslides) and *C. pungens* (forests) coupled with soil sampling.

		Soil	Tiles		Pellets	
Habitat	**Microhabitat**		**Small**	**Large**	**Small**	**Large**
Forest	Rhizosphere	4	4	4	4	4
	Bulk	4	4	4	4	4
Landslide	Rhizosphere	4	4	4	4	4
	Bulk	4	4	4	4	4

`

Table 3.2. Results of 3-way ANOVAs for mobility/weathering indices and physical variables of tiles and pellets across habitats (H), microhabitat (Mh), and mesh size (MS). Values are F values.

	Tiles				Pellets			
				H *x* Mh				H *x* Mh
	H	Mh	MS	*x* MS	H	Mh	MS	*x* MS
D*f*	**1**	**1**	**1**	**4**	**1**	**1**	**1**	**4**
Nutrient mobility								
Al_2O_3	0.5	0.2	1.3	0.2	6.5 *	3.7 *	0.8	6.3 **
Fe_2O_3	1.3	1.9	1.1	0.6	0.7	1.4	0.4	1.3
TiO_2	1.0	2.1	0.4	0.4	1.0	0.8	0.2	1.7
SiO_2	0.1	2.5	0.0	0.7	2.5	4.9 *	6.6 *	6.9 **
MnO	2.2	0.0	1.3	1.4	5.4 *	1.1	0.1	1.6
P_2O_5	0.7	1.5	1.2	0.9	23.6 **	1.1	0.7	0.3
CaO	3.9 .	0.2	0.1	0.4	5.2 *	5.8 *	0.4	2.5 .
K_2O	0.2	0.5	1.5	0.9	0.5	0.3	3.0 .	2.6 .
Na_2O	0.1	0.8	0.2	0.4	0.9	1.6	1.0	1.6
MgO	0.6	0.5	0.4	0.6	6.9 *	3.1 .	2.0	0.7
Weathering indices								
I*mob*	4.4 *	0.0	0.4	0.7	2.0	2.8	1.1	1.8
LF	0.5	0.1	0.6	0.9	0.6	0.8	2.5	0.8
CLI	4.9 *	0.4	0.2	2.0	5.3 *	1.2	2.4	1.3
Physical properties								
Δ Weight	0.6	2.8	0.6	0.3	1.0	0.2	0.0	1.4
Δ Bulk Density	0.8	0.8	0.2	0.6	0.9	0.4	0.1	1.4

** $p < 0.01$; * $p < 0.05$; . $p < 0.10$

`

Table 3.3. Results of a PERMANOVA testing for the effect of habitat, microhabitat, and mesh size on mobility/weathering indices.

	Tiles			Pellets		
	Df	**R^2**	**F-value**	**Df**	**R^2**	**F-value**
Habitat (H)	1	0.05	1.42	1	0.11	3.86 **
Microhabitat (Mh)	1	0.03	0.82	1	0.05	1.83 .
Mesh Size (MS)	1	0.02	0.64	1	0.04	1.29
H *x* Mh *x* MS	4	0.10	0.79	4	0.22	1.93 *

** $p < 0.01$; * $p < 0.05$; . $p < 0.10$

`

Table 3.4. Three-way ANOVAs for *16S* and *ITS* metric of species diversity across habitats, microhabitats, substrate and mesh size. Values are F values.

		16S				ITS			
	Df	**Shannon**		**Chao1**		**Shannon**		**Chao1**	
Soil and Rock substrates									
Habitat (H)	1	0.60		1.98		0.07		0.55	
Microhabitat (Mh)	1	2.83	.	0.69		0.29		0.63	
Substrate (S)	2	24.65	***	303.57	***	36.53	***	55.84	***
H x S	2	1.15		16.76	***	1.60		1.11	
H *x* MH *x* S	5	0.85		5.26	***	0.65		0.93	
Rock samples									
Habitat (H)	1	0.37		0.74		0.05		3.46	.
Microhabitat (Mh)	1	4.98	*	3.17	.	1.20		0.98	
Substrate (S)	1	12.13	**	3.54	.	28.05	***	46.98	***
H x S	1	0.34		0.35		0.74		0.19	
H x Mh x S	3	0.65		0.65		0.78		0.29	
Mesh size (Pellets)	1	28.86	***	30.76	***	7.28	*	17.80	***

*** $p < 0.001$; ** $p < 0.01$; * $p < 0.05$; . $p < 0.10$

`

Table 3.5. Results of a PERMANOVA testing for the effect of habitat, microhabitat, substrate, and mesh size on the microbial community composition.

		16S		*ITS*	
	D*f*	***F***	**R^2**	***F***	**R^2**
Soil and Rock samples					
Habitat (H)	1	3.56^{***}	0.05	7.23^{***}	0.09
Substrate (S)	2	3.29^{***}	0.10	2.77^{***}	0.07
Microhabitat (Mh)	1	1.29^{*}	0.02	1.42^{*}	0.02
H x S	2	1.88^{***}	0.05	1.85^{***}	0.05
H x S x Mh	5	1.18^{*}	0.09	1.17^{*}	0.08
Rock samples					
Habitat (H)	1	5.52^{***}	0.11	5.53^{***}	0.12
Substrate (S)	1	3.64^{***}	0.07	2.98^{***}	0.07
Microhabitat (Mh)	1	1.24	0.02	1.26	0.02
Mesh Size (MS)	1	2.19^{***}	0.04	1.90^{**}	0.02
H x S	1	1.54^{*}	0.03	1.61^{*}	0.04
H x S x Mh	3	1.01	0.06	1.09	0.01

*** $p < 0.001$; ** $p < 0.01$; * $p < 0.05$; **.** $p < 0.10$

`

Table 3.6. Stepwise regression coefficients for nutrient mobility and weathering indices as predictors of alpha and beta diversity metrics. Used alpha diversity metric was Shannon index (Sh) and beta diversity was PCA axes (PC1 and PC2 axes of Figure S3.8). In italics are the P and R^2 values of the linear models.

	16S						**ITS**					
	Tiles			**Pellets**			**Tiles**			**Pellets**		
Variable	**Sh.**	**PC1**	**PC2**	**Sh.**	**PC1**	**PC2**	**Sh.**	**PC1**	**PC2**	**Sh.**	**PC1**	**PC2**
Fe_2O_3	-0.4 *		-13.8 *		-151.0			-23.6 *			-125.2	
TiO_2								12.8				
SiO_2	-15.3 *						-11.6					
MnO			-4.8				-0.3					
P_2O_5					67.7 *						31.1	53.3 *
CaO				22.2	293.2 .			-172.8 *			478.3 *	
MgO											281.5	-195.0 *
Na_2O	1.8 *		-53.1									
K_2O	-2.0 *		-46.6				-4.0 *					
Δ BD	0.8 *		17.8.		162.7 *		1.4				119.3 .	153.5 *
P	*0.00*	*0.15*	*0.06*	*0.10*	*0.00*	*0.49*	*0.10*	*0.04*	*0.77*	*0.18*	*0.00*	*0.01*
R^2	*0.81*	*0.22*	*0.55*	*0.11*	*0.6*	*0.02*	*0.39*	*0.39*	*0.41*	*0.07*	*0.65*	*0.37*

* $p < 0.05$; . $p < 0.10$

`

FIGURES

`

Figure 3.1. Images of granodiorite tiles. (A) Seen under a dissection microscope. (B) Analyzed area in the EDX. The superficial mark is in the center of the tile.

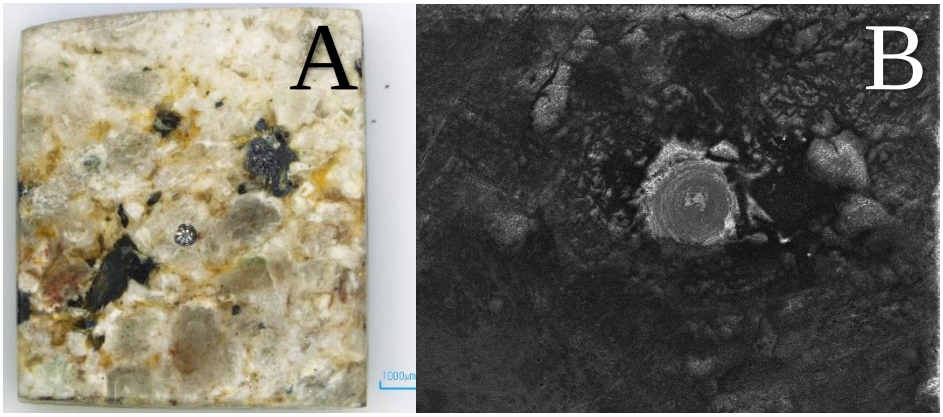

`

Figure 3.2. PCA biplots based on oxides mobility in tiles and pellets. The arrows direction indicates accumulation of the oxide after the experiment.

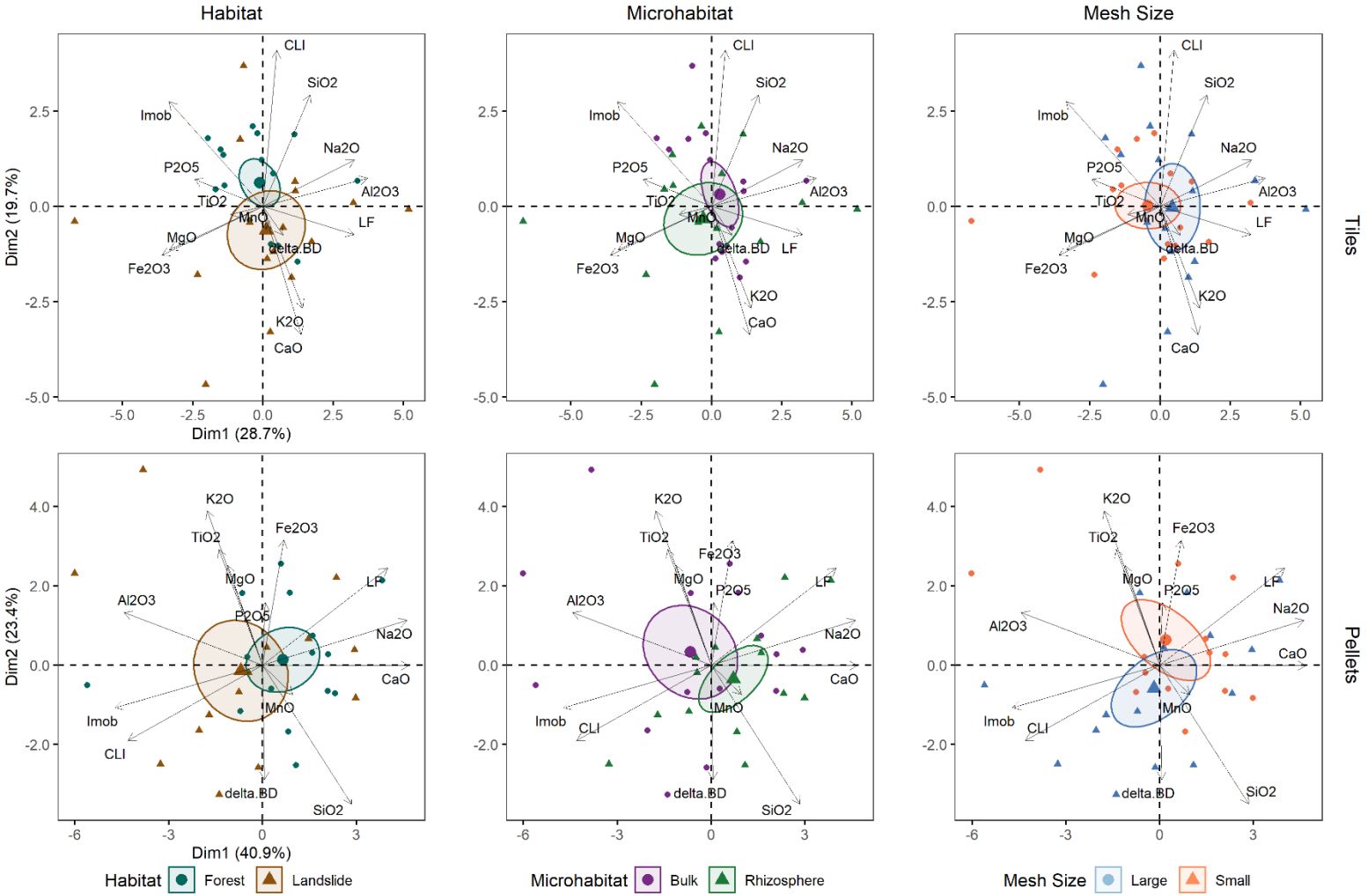

`

Figure 3.3. Mean species richness (Chao1) and diversity (Shannon) for *16S* and *ITS* ASVs across habitats, microhabitat, and substrates in the soil and rocks samples.

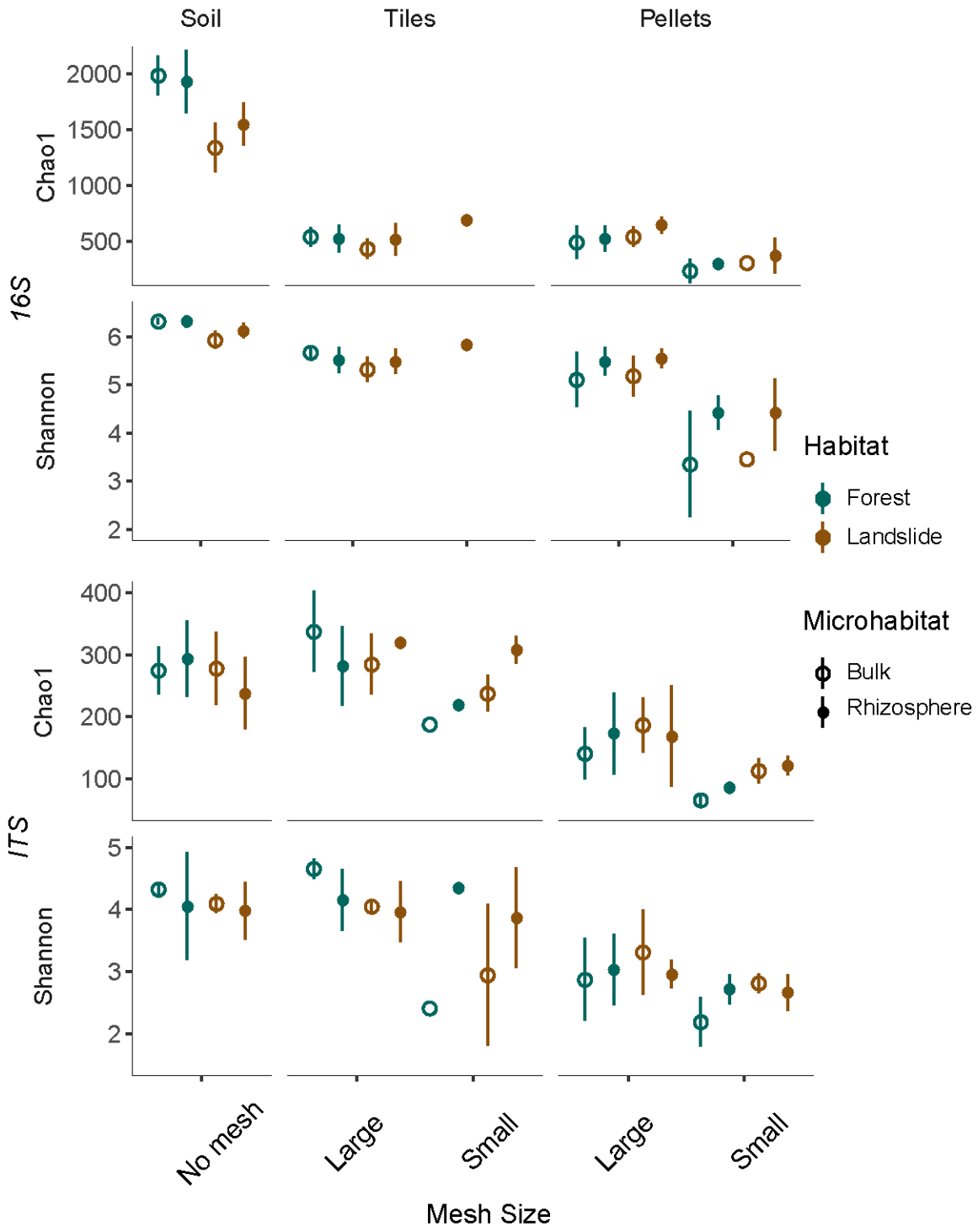

`

Figure 3.4. Taxonomic composition at phylum level of bacteria, archaea, and fungi at phylum level across habitat, microhabitat, substrate, and mesh size. Phyla with less than 1% total abundance were excluded.

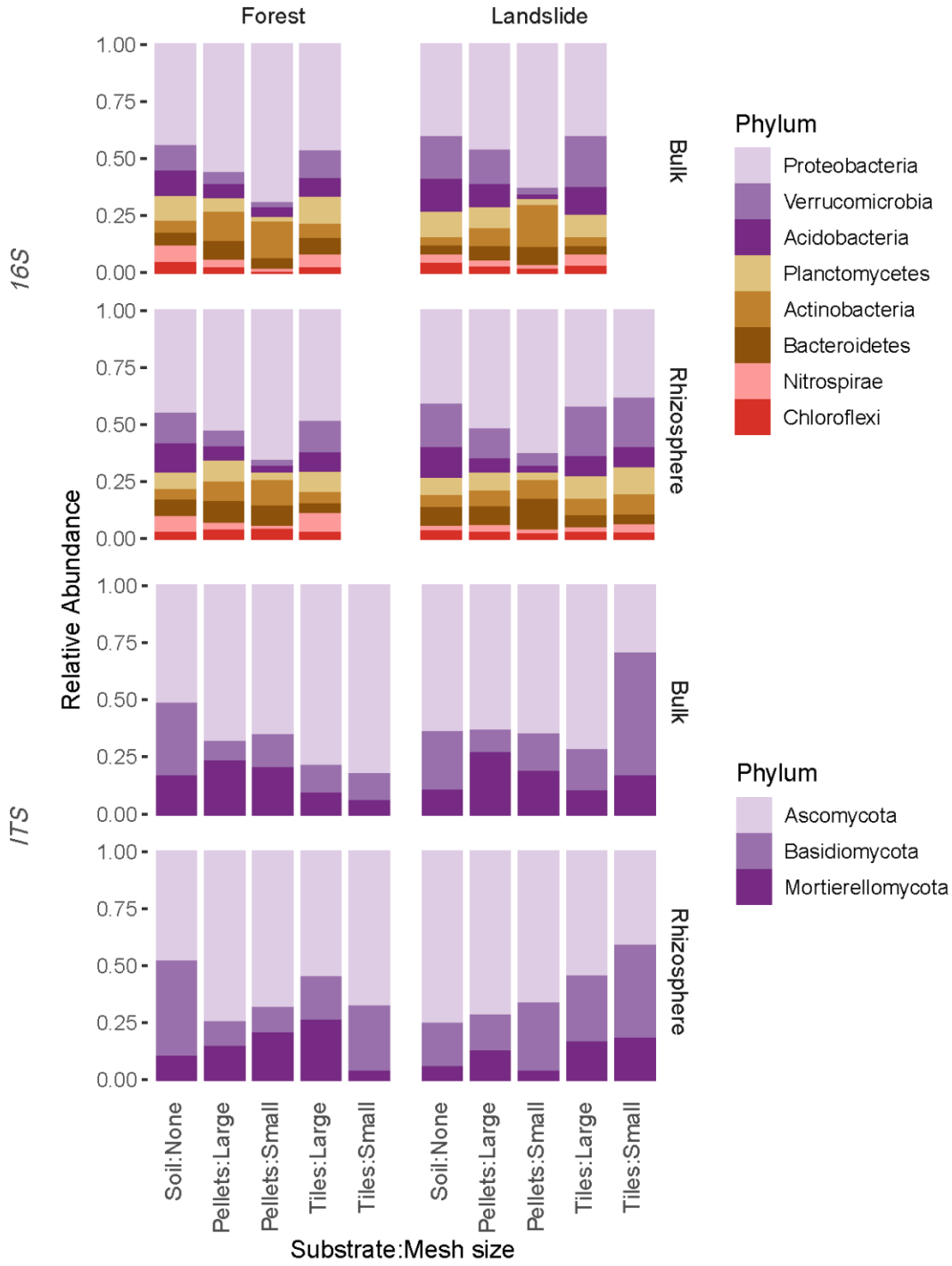

`

Figure 3.5. Extended Venn Diagram of Indicator Species.

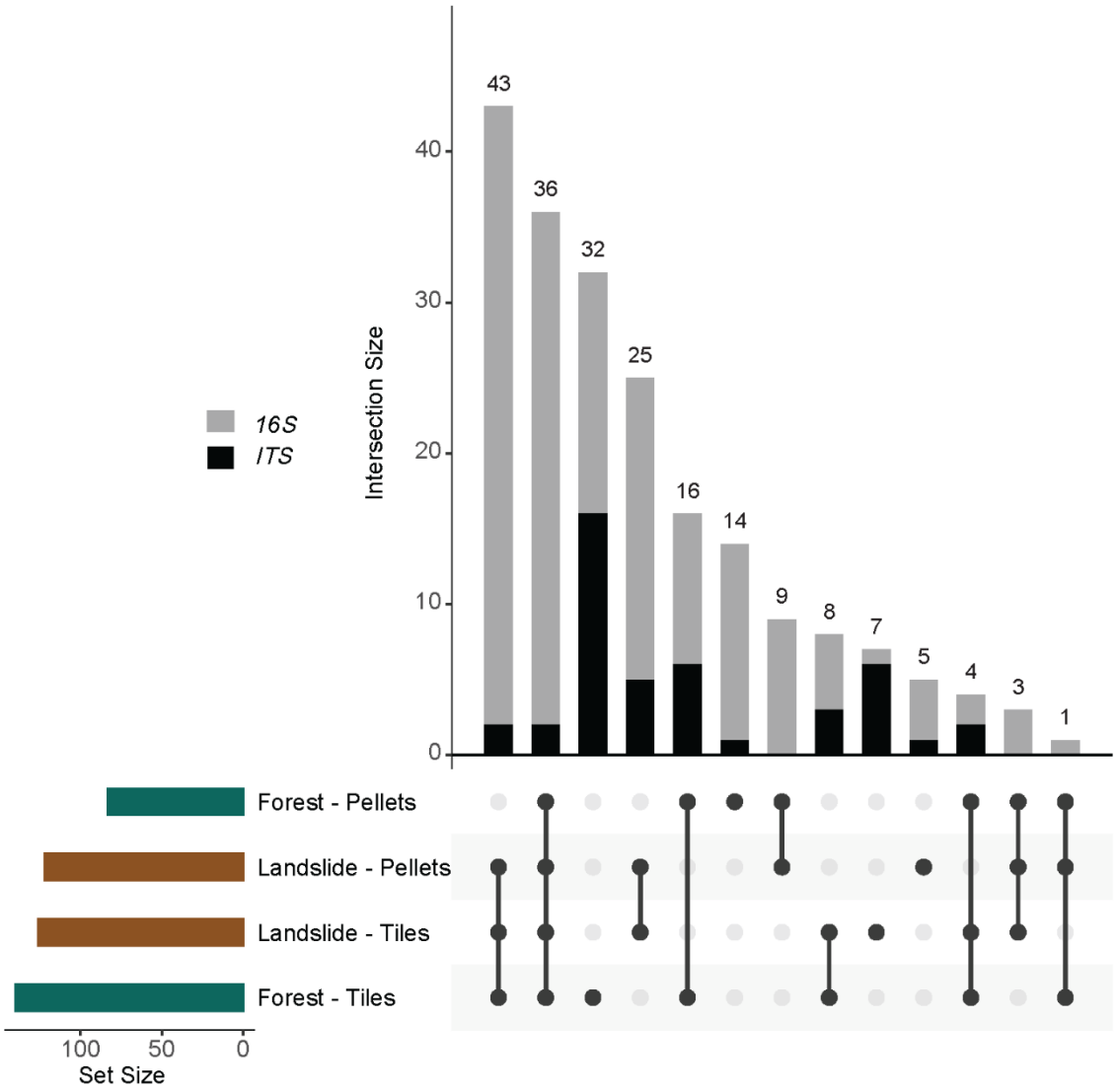

`

Figure 3.6. Mean CLR-transformed abundances of most differentially abundant ASVs between habitats in pellets and tiles. ASVs were identified by the phylum and lowest taxonomical classification available.

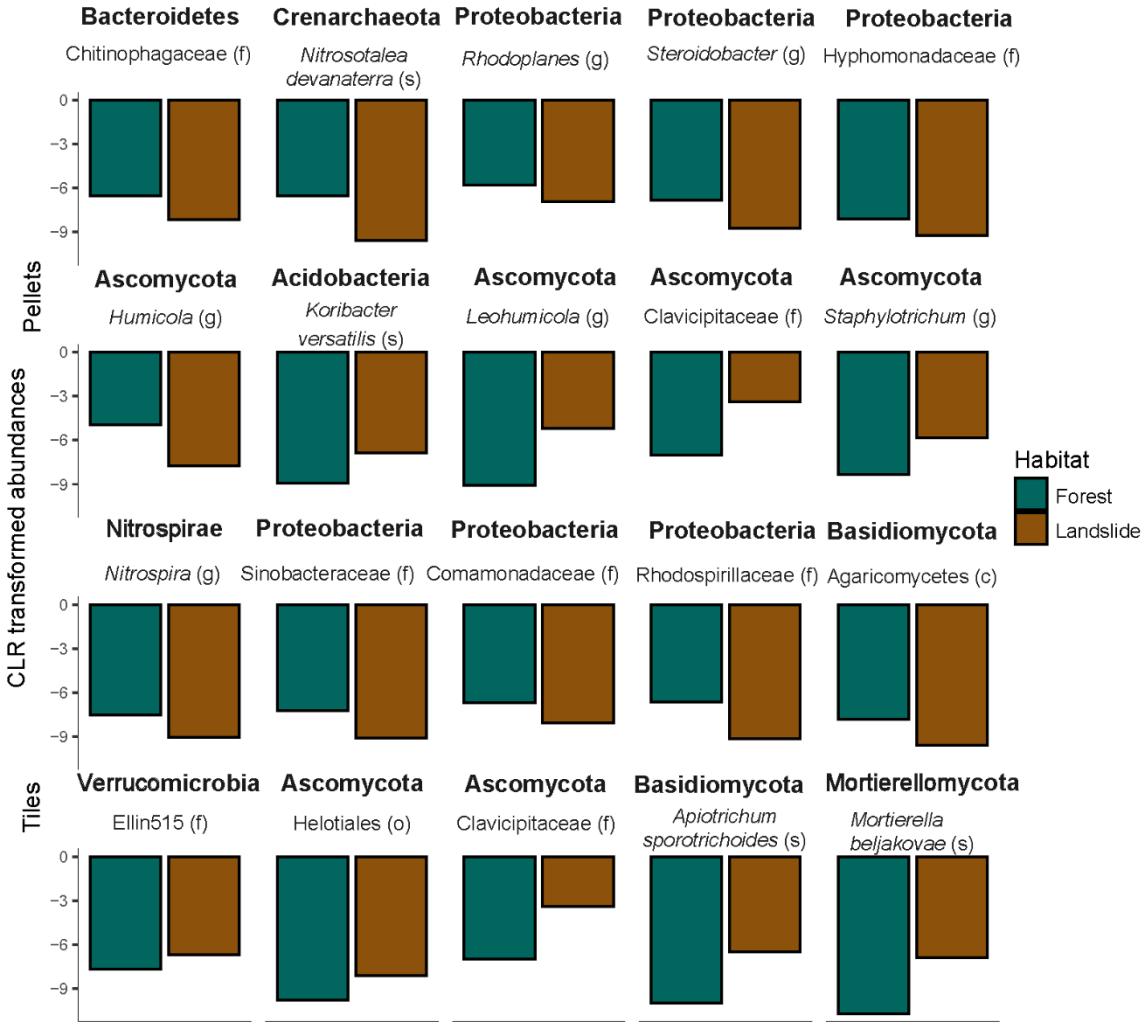

`

Figure 3.7. PCA ordination with Aitchison distances for bacterial, archaeal (*16S*) and fungal (*ITS*) ASVs in tiles and pellets across habitats.

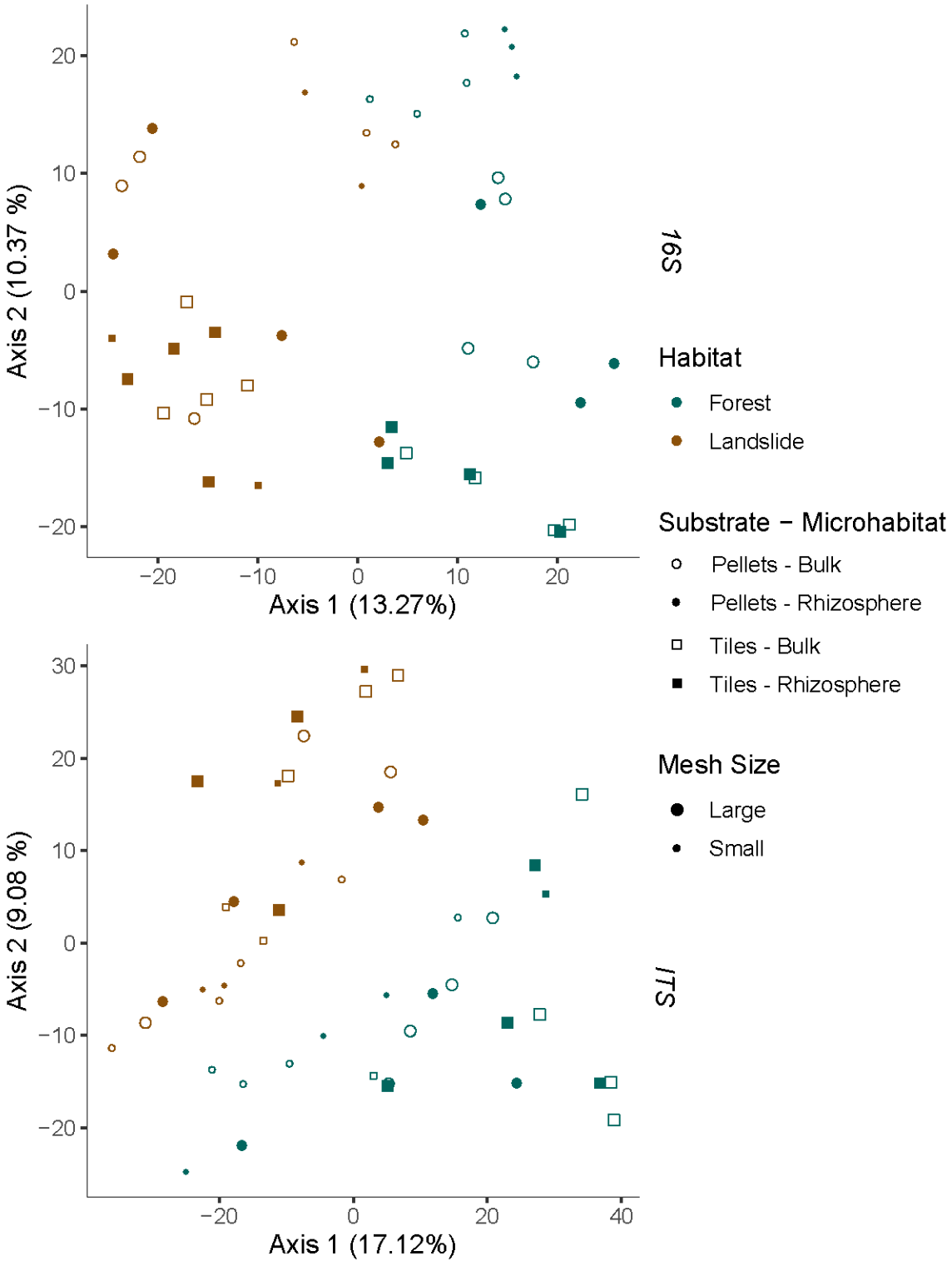

`

Figure 3.8. Mean CLR-transformed abundance of differentially abundant fungal guilds across habitats in soil, pellets, and tiles.

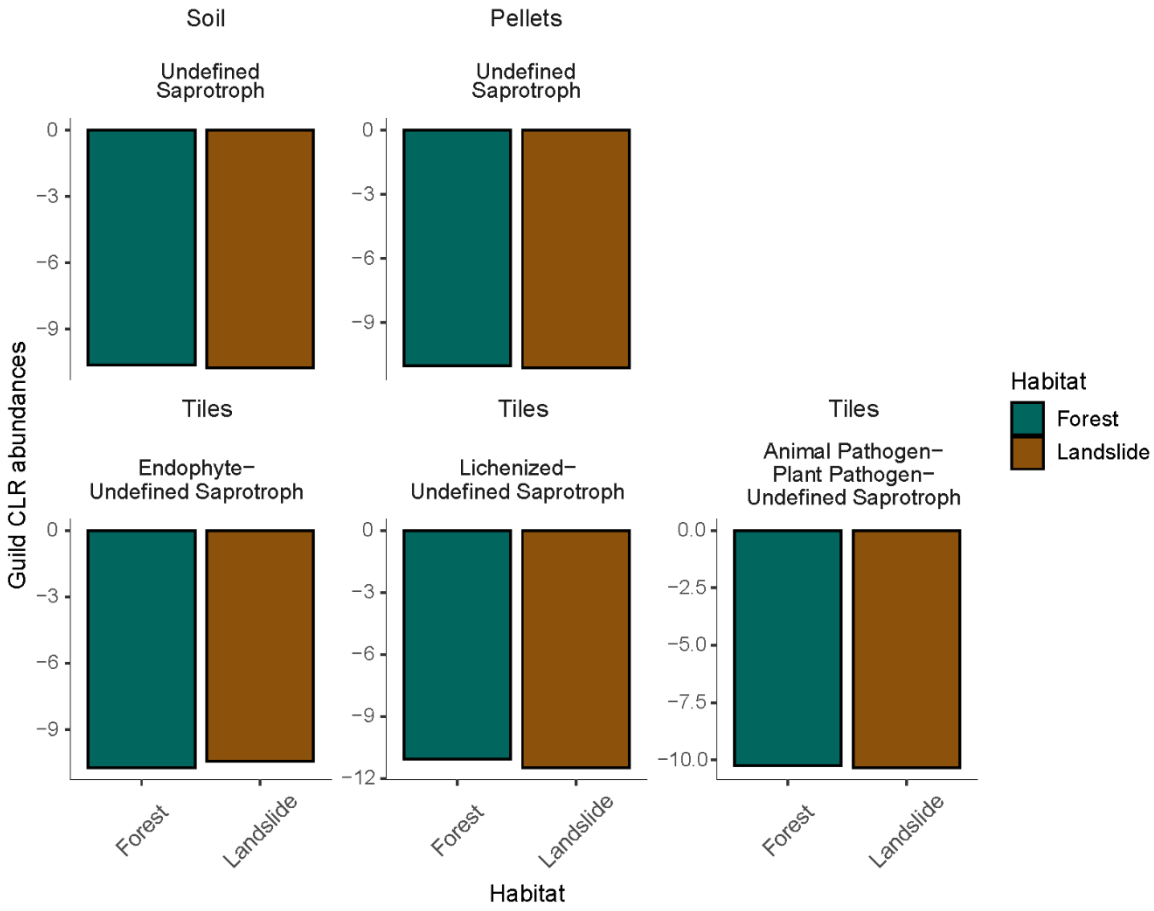

`

SUPPLEMENTAL TABLES AND FIGURES

`

Table S3.1. Average oxides concentration in granodiorite rocks (parental), and landslide-like and forest soils at the Utuado pluton. Parental, landslide and forest data was obtained following methodology at Chapter 2 of this work and were collected from the study area, whereas diorite and granodiorite data were obtained from (Chen 1967). Oxides are given in weight %.

	Diorite	**Granodiorite**	**Parental**	**Landslide**	**Forest**
TiO_2	0.62	0.64	0.43	1.24	0.84
Al_2O_3	17.95	15.30	17.93	29.94	24.20
Fe_2O_3	7.93	5.29	5.10	10.87	7.46
MnO	0.19	0.10	0.13	0.18	0.29
P_2O_5	-	-	0.16	0.18	0.25
K_2O	0.84	2.89	0.75	0.89	1.33
SiO_2	52.95	63.00	56.90	42.41	49.97
MgO	3.68	2.39	3.29	1.30	1.27
Na_2O	2.82	3.47	3.90	0.14	0.35
CaO	8.06	4.27	5.82	0.37	1.12

`

Table S3.2. Oxide mobility and weathering degree indexes used in this study.

Index	Formula	Reference
Relative Element Mobility	$\frac{X_{t1}}{X_{t0}}$	(Che et al. 2012)
Mobiles Index (Imob)	$\frac{C_{t0} - C_{t1}}{C_{t0}}; C = K_2O + Na_2O + CaO$	(Irfan 1996)
Chemical Leaching Index (CLI)	$100x\frac{C_{t0} - C_{t1}}{C_{t0}}; C = K_2O + Na_2O + CaO + MgO$	(Ceryan 2008)
K index (K)	$\frac{(SiO_2/Al_2O_3)_{t1}}{(K_2O + Na_2O + CaO/Al_2O_3)_{t0}}$	(Rocha Filho et al. 1985)
Leaching Factor (LF)	$\frac{C_{t1}}{C_{t0}}; C = \frac{K_2O + Na_2O}{SiO_2}$	(Jenny 1941)
Lixiviation Index (LI)	$\frac{C_{t1}}{C_{t0}}; C = \frac{K_2O + Na_2O}{Al_2O_3}$	(Rocha Filho et al. 1985)

[x] is the concentration of any element before (t0) and after (t1) the experiment. $[M]_x$ is the concentration of any mobile element, whereas $[I]_x$ is the concentration of any immobile element, although Al_2O_3 was selected as the immobile element in this work. $[C]_x$ is a given equation specified for specific indexes.

`

Table S3.3. Number of bacterial, archaeal, and fungal sequences and ASVs throughout the filtering and rarefaction steps for soil and rock, and rock data subsets.

		16S			ITS
		Bacteria	**Archaea**	**B+A**	**Fungi**
Soil and Rock samples					
Sequences	Raw	2,646,784	16,218	2,673,931	3,702,013
	Filt. Step 1	1,729,437	12,009	1,741,446	3,702,013
	Filt. Step 2	1,618,808	10,689	1,629,497	3,463,563
	Filt. Step 3	1,517,932	9,878	1,527,810	3,171,714
	Rarefied	80,831	949	81,780	727,610
ASVs	Raw	114,827	638	129,795	7,866
	Filt. Step 1	41,672	357	42,029	7,866
	Filt. Step 2	40,824	329	41,153	7,835
	Filt. Step 3	7,434	53	7,487	2,066
	Rarefied	5,361	43	5,404	2,065
Phyla	Raw	52	3	55	15
	Filt. Step 1	27	2	29	15
	Filt. Step 2	27	2	29	15
	Filt. Step 3	16	2	18	12
	Rarefied	15	2	17	12
Rock samples					
Sequences	Filt. Step 3	228,136	3,475	231,611	2,273,950
	Rarefied	55,775	799	56,574	522,922
ASVs	Filt. Step 3	1,843	24	1,867	1,367
	Rarefied	1,831	24	1,855	1,365
Phyla	Filt. Step 3	13	2	15	12
	Rarefied	13	2	15	12

Filtering step 1 consisted of removing unidentified, chloroplast and mitochondria associated sequences. Filtering step 2 consisted of filtering control predominant ASVs. Filtering step 3 consisted of filtering ASVs by abundance (minimum read 11) and occurrence (minimum samples 3).

`

Table S3.4. Indicator species per habitat and rock substrate. *Ab* is the taxon abundance, *P* and *T* refers to the number of ASVs associated to pellets and tiles within each habitat. Species included in this table had an indicator value higher than 0.8 and a p value <0.05. Indicator species in this table represent the individual dots at the bottom of the Extended Venn Diagram in Figure 3.6.

						Landslide			Forest		
Kingdom	**Phylum**	**Class**	**Order**	**Family**	**Genus/Species**	***Ab***	***T***	***P***	***Ab***	***T***	***P***
Archaea						***2***	***0***	***0***	***502***	***3***	***0***
	Crenarchaeota	Thaumarchaeota	Cenarchaeales	SAGMA-X		2	0	0	502	3	0
Bacteria						***2509***	***1***	***4***	***6089***	***13***	***13***
	Chloroflexi	Anaerolineae	SBR1031	oc28		428	0	1	31	0	0
	Nitrospirae	Nitrospira	Nitrospirales	Nitrospiraceae	*Nitrospira*	28	0	0	679	4	0
	Planctomycetes	Planctomycetia	Gemmatales	Gemmataceae	*Gemmata*	0	0	0	56	1	0
			Pirellulales	Pirellulaceae	*Pirellula*	9	0	0	36	1	0
	Proteobacteria	Alpha-	Caulobacterales	Caulobacteraceae	*Phenylobacterium*	33	0	0	732	0	2
			Rhizobiales	Hyphomicrobiaceae		1	0	0	153	1	0
					Pedomicrobium	22	0	0	115	1	0
					Rhodoplanes	116	0	0	1159	0	2
				Rhizobiaceae	*Agrobacterium sullae*	65	0	0	170	1	0
			Rhodobacterales	Hyphomonadaceae		44	0	0	399	0	2
			Rhodospirillales	Rhodospirillaceae		71	0	0	247	0	1
					Reyranella massiliensis	0	0	0	89	0	1
		Beta-	Burkholderiales	Alcaligenaceae		53	0	0	230	1	0
				Comamonadaceae		4	0	0	230	1	0
					Variovorax	524	0	1	69	0	0
				Oxalobacteraceae	*Cupriavidus*	892	0	2	96	0	0
		Delta-	Sva0853	JTB36		2	0	0	279	0	2
		Gamma-	Xanthomonadales	Sinobacteraceae		13	0	0	207	1	0
					Steroidobacter	4	0	0	399	0	2
	Spirochaetes	[Leptospirae]	[Leptospirales]	Leptospiraceae	*Turneriella*	8	0	0	673	0	1

`

						Landslide			Forest		
Kingdom	**Phylum**	**Class**	**Order**	**Family**	**Genus/Species**	***Ab***	***T***	***P***	***Ab***	***T***	***P***
Bacteria	Verruco-microbia	[Pedosphaerae]	[Pedosphaerales]	Ellin515		192	1	0	7	0	0
		Opitutae	Opitutales	Opitutaceae		0	0	0	33	1	0
Fungi						***14634***	***6***	***1***	***17585***	***16***	***1***
	Ascomycota					1483	2	0	111	1	0
		Archaeorhizo-mycetes	Archaeorhizo-mycetales	Archaeorhizo-mycetaceae	*Archaeorhizo-myces*	2	0	0	260	1	0
		Dothideomycetes	Pleosporales	Massarinaceae		7	0	0	113	1	0
				Melanommataceae		1	0	0	426	1	0
		Eurotiomycetes	Eurotiales	Trichocomaceae	*Talaromyces palmae*	21	0	0	1398	1	0
		Leotiomycetes	Helotiales			509	1	0	2	0	0
				Vibrisseaceae	*Phialocephala humicola*	5	0	0	328	1	0
		Saccharomycetes	Saccharomycetales	Saccharo-mycopsidaceae	*Saccharomycopsis vini*	0	0	0	499	1	0
		Sordariomycetes				2	0	0	128	1	0
			Glomerellales	Plectosphae-rellaceae	*Plectosphaerella cucumerina*	9	0	0	401	1	0
					Wallrothiella gmelinae	0	0	0	406	1	0
			Hypocreales	Hypocreales_fam Incertae_sedis		5	0	0	156	1	0
				Nectriaceae	*Volutella*	5	0	0	304	1	0
			Microascales	Ceratocystidaceae		1	0	0	121	1	0
			Sordariales	Lasiosphaeriaceae	*Schizothecium dakotense*	438	1	0	0	0	0
				Sordariales_fam Incertae_sedis	*Staphylotrichum boninense*	8543	0	1	2058	0	0
			Xylariales	Sporocadaceae	*Pestalotiopsis*	0	0	0	730	1	0

`

Kingdom	Phylum	Class	Order	Family	Genus/Species	Landslide			Forest		
						Ab	***T***	***P***	***Ab***	***T***	***P***
	Basidiomycota	Agaricomycetes				0	0	0	366	1	0
		Tremellomycetes	Trichosporonales	Trichosporonaceae	*Apiotrichum scarabaeorum*	2105	1	0	5	0	0
					Apiotrichum sporotrichoides	1489	1	0	73	0	0
	Mortierello-mycota	Mortierello-mycetes	Mortierellales	Mortierellaceae	*Mortierella*	9	0	0	9258	0	1
	Rozellomycota	Rozellomycotina	GS11			0	0	0	442	1	0

`

Table S3.5. Differentially abundant ASVs per habitat in tiles and pellets. Selected differentially abundant ASVs had an effect value lower than -1 and higher than 1, and a Benjamini-Hochberg corrected *p*-value lower than 0.05. Each ASV was identified to the lowest taxonomical classification available.

	Substrate	Habitat	Effect	Phylum	Class	Order	Family	Genus/Species
16S	Pellets	Forest	-1.87	Proteobacteria	Alpha-	Rhizobiales	Hyphomicrobiaceae	*Rhodoplanes*
16S	Pellets	Forest	-1.54	Proteobacteria	Gamma-	Xanthomonadales	Sinobacteraceae	*Steroidobacter*
16S	Pellets	Forest	-1.29	Crenarchaeota	Thaumarchaeota	Cenarchaeales	SAGMA-X	*Nitrosotalea devanaterra*
16S	Pellets	Forest	-1.25	Bacteroidetes	[Saprospirae]	[Saprospirales]	Chitinophagaceae	
16S	Pellets	Forest	-1.24	Proteobacteria	Alpha-	Rhodobacterales	Hyphomonadaceae	
16S	Pellets	Forest	-1.19	Proteobacteria	Gamma-	Xanthomonadales	Sinobacteraceae	*Steroidobacter*
16S	Pellets	Forest	-1.13	Proteobacteria	Alpha-	Rhizobiales	Hyphomicrobiaceae	*Rhodoplanes*
16S	Pellets	Forest	-1.00	Proteobacteria	Alpha-	Rhodobacterales	Hyphomonadaceae	
16S	Pellets	Landslide	1.05	Acidobacteria	Acidobacteriia	Acidobacteriales	Koribacteraceae	*Koribacter versatilis*
16S	Tiles	Forest	-2.14	Proteobacteria	Beta-	Burkholderiales	Comamonadaceae	
16S	Tiles	Forest	-1.74	Proteobacteria	Gamma-	Xanthomonadales	Sinobacteraceae	
16S	Tiles	Forest	-1.57	Proteobacteria	Alpha-	Rhodospirillales	Rhodospirillaceae	
16S	Tiles	Forest	-1.56	Nitrospirae	Nitrospira	Nitrospirales	Nitrospiraceae	*Nitrospira*
16S	Tiles	Forest	-1.45	Nitrospirae	Nitrospira	Nitrospirales	Nitrospiraceae	*Nitrospira*
16S	Tiles	Forest	-1.37	Proteobacteria	Alpha-	Rhizobiales	Hyphomicrobiaceae	*Devosia*
16S	Tiles	Forest	-1.31	Proteobacteria	Gamma-	Thiotrichales	Piscirickettsiaceae	
16S	Tiles	Forest	-1.27	Proteobacteria	Alpha-	Rhizobiales	Hyphomicrobiaceae	*Rhodoplanes*
16S	Tiles	Forest	-1.10	Proteobacteria	Alpha-	Rhizobiales	Rhizobiaceae	*Agrobacterium sullae*
16S	Tiles	Forest	-1.06	Proteobacteria	Alpha-	Rhizobiales	Hyphomicrobiaceae	*Rhodoplanes*
16S	Tiles	Landslide	1.26	Acidobacteria	Acidobacteriia	Acidobacteriales	Koribacteraceae	*Koribacter*
16S	Tiles	Landslide	1.34	Verrucomicrobia	[Spartobacteria]	[Chthoniobacterales]	[Chthonio-bacteraceae]	*Candidatus Xiphinematobacter*
16S	Tiles	Landslide	2.18	Verrucomicrobia	[Pedosphaerae]	[Pedosphaerales]	Ellin515	

`

	Substrate	Habitat	Effect	Phylum	Class	Order	Family	Genus/Species
ITS	Pellets	Forest	-1.51	Ascomycota	Sordariomycetes	Sordariales	Chaetomiaceae	*Humicola*
ITS	Pellets	Forest	-1.16	Mortierello-mycota	Mortierello-mycetes	Mortierellales	Mortierellaceae	*Mortierella*
ITS	Pellets	Landslide	1.47	Ascomycota	Sordariomycetes	Hypocreales	Clavicipitaceae	
ITS	Pellets	Landslide	1.49	Ascomycota	Sordariomycetes	Sordariales	Sordariales_fam Incertae_sedis	*Staphylotrichum*
ITS	Pellets	Landslide	1.71	Ascomycota	Leotiomycetes	Helotiales	Helotiales_fam Incertae_sedis	*Leohumicola*
ITS	Tiles	Forest	-2.17	Basidiomycota	Agaricomycetes			
ITS	Tiles	Landslide	1.61	Ascomycota				
ITS	Tiles	Landslide	1.80	Basidiomycota	Agaricomycetes			
ITS	Tiles	Landslide	1.86	Ascomycota	Sordariomycetes	Hypocreales	Clavicipitaceae	
ITS	Tiles	Landslide	1.91	Basidiomycota	Tremellomycetes	Trichosporonales	Trichosporonaceae	*Apiotrichum sporotrichoides*
ITS	Tiles	Landslide	2.12	Mortierello-mycota	Mortierello-mycetes	Mortierellales	Mortierellaceae	*Mortierella beljakovae*
ITS	Tiles	Landslide	2.51	Ascomycota	Leotiomycetes	Helotiales		

`

Table S3.6. Differentially abundant KOs per habitat in soil, tiles and pellets. Selected differentially abundant KOs had an effect value lower than -1.5 and higher than 1.5, and a Benjamini-Hochberg corrected *p*-value lower than 0.05. Each KO was identified using the KEGG Orthology classification (L1, L2, L3), CSR classification (Wood et al 2018) and Geochip Categories and Subcategories (Shi et al 2019). Substrates: S - Soil, T - Tile, P - Pellet; L1: CEP - Cellular Processes, EIP - Environmental Information Processing, GIP - Genetic Information Processing, MET - Metabolism, SCP - Signaling and Cellular Processes, PCP - Poorly characterized protein; CRS: C - Competitive, S - Stress, R - Ruderal, PE - Plant exudates metabolism, M - Mlotrophs, F - Foraging, nc - Not classified.

Substrate	Habitat	Effect	KO	L1	L2	L3	CSR	Category	Subcategory
S-T-P	Landslide	2.02	K01173	CEP	Cell growth and death	Apoptosis	nc	-	-
S-T-P	Landslide	4.23	K10557	CEP	Cellular community	Quorum sensing	C	-	-
S-T-P	Landslide	3.32	K03201	EIP	Membrane transport	Bacterial secretion system	nc	Virulence	Secretion system
S-T-P	Landslide	2.03	K11892	EIP	Membrane transport	Bacterial secretion system	nc	-	-
S-T-P	Landslide	2.45	K16299	EIP	Membrane transport	ABC transporters	nc	-	-
S-T-P	Landslide	2.79	K01147	GIP	Translation	Transfer RNA biogenesis	R	-	-
S-T-P	Landslide	2.79	K02443	GIP	Transcription	Transcription factors	nc	-	-
S-T-P	Landslide	2.42	K05799	GIP	Transcription	Transcription factors	nc	-	-
S-T-P	Landslide	2.27	K06970	GIP	Translation	Ribosome biosynthesis	R	-	-
S-T-P	Landslide	2.45	K07492	GIP	-	Replication and repair	S	-	-
S-T-P	Landslide	1.59	K07493	GIP	-	Replication and repair	S	-	-
S-T-P	Landslide	2.32	K07506	GIP	Transcription	Transcription factors	nc	-	-
S-T-P	Landslide	4.29	K15973	GIP	Transcription	Transcription factors	nc	-	-
S-T-P	Landslide	2.58	K17762	GIP	Transcription	Transcription machinery	nc	-	-
S-T-P	Landslide	2.01	K18828	GIP	Translation	Transfer RNA biogenesis	CR	-	-
S-T-P	Landslide	2.42	K00148	MET	Energy Metabolism	Methane metabolism	M	-	-
S-T-P	Landslide	3.17	K00661	MET	-	-	nc	-	-
S-T-P	Landslide	4.25	K01128	MET	-	-	nc	-	-
S-T-P	Landslide	2.29	K01176	MET	Carbohydrate metabolism	Starch and sucrose metabolism	PE	Carbon cycling	Carbon degradation
S-T-P	Landslide	4.03	K01193	MET	Carbohydrate metabolism	Starch and sucrose metabolism	PE	-	-
S-T-P	Landslide	2.31	K01194	MET	Carbohydrate metabolism	Starch and sucrose metabolism	PE	-	-

`

Substrate	Habitat	Effect	KO	L1	L2	L3	CSR	Category	Subcategory
S-T-P	Landslide	2.68	K01198	MET	Carbohydrate metabolism	Amino sugar and nucleotide sugar metabolism	nc	-	-
S-T-P	Landslide	2.23	K01432	MET	Carbohydrate metabolism	Glyoxylate and dicarboxylate metabolism	PE	-	-
S-T-P	Landslide	3.14	K01502	MET	Xenobiotics biodegradation and metabolism	Styrene degradation	nc	-	-
S-T-P	Landslide	4.78	K01575	MET	Carbohydrate metabolism	Butanoate metabolism	nc	-	-
S-T-P	Landslide	2.45	K01584	MET	Amino acid metabolism	Arginine and proline metabolism	PE	-	-
S-T-P	Landslide	4.23	K01596	MET	Carbohydrate metabolism	Citrate cycle	R	-	-
S-T-P	Landslide	1.67	K01598	MET	Metabolism of cofactors and vitamins	Pantothenate and CoA biosynthesis	nc	-	-
S-T-P	Landslide	2.97	K01729	MET	Carbohydrate metabolism	Fructose and mannose metabolism	PE	Carbon cycling	Carbon degradation
S-T-P	Landslide	2.26	K01730	MET	Carbohydrate metabolism	Pentose and glucuronate interconversions	nc	-	-
S-T-P	Landslide	2.28	K01753	MET	Amino acid metabolism	Glycine, serine and threonine metabolism	PE	-	-
S-T-P	Landslide	2.37	K01854	MET	Carbohydrate metabolism	Galactose metabolism	nc	-	-
S-T-P	Landslide	3.14	K03429	MET	Lipid metabolism	Glycerolipid metabolism	nc	-	-
S-T-P	Landslide	2.35	K03818	MET	-	-	nc	-	-
S-T-P	Landslide	2.41	K03889	MET	Energy Metabolism	Oxidative phosphorylation	R	-	-
S-T-P	Landslide	2.22	K03923	MET	-	-	nc	-	-
S-T-P	Landslide	2.44	K09844	MET	Metabolism of terpenoids and polyketids	Carotenoid biosynthesis	PE	Electron transport	Photosynthetic
S-T-P	Landslide	4.04	K10210	MET	Metabolism of terpenoids and polyketids	Carotenoid biosynthesis	PE	-	-
S-T-P	Landslide	4.26	K10211	MET	Metabolism of terpenoids and polyketids	Carotenoid biosynthesis	PE	-	-
S-T-P	Landslide	4.32	K10212	MET	Metabolism of terpenoids and polyketids	Carotenoid biosynthesis	PE	-	-
S-T-P	Landslide	1.98	K12308	MET	Carbohydrate metabolism	Galactose metabolism	nc	-	-
S-T-P	Landslide	2.00	K12349	MET	Lipid metabolism	Shingolipid metabolism	nc	-	-

`

Substrate	Habitat	Effect	KO	L1	L2	L3	CSR	Category	Subcategory
S-T-P	Landslide	1.59	K12957	MET	Carbohydrate metabolism	Glycolysis / Gluconeogenesis	PE	-	-
S-T-P	Landslide	3.11	K15372	MET	Metabolism of other amino acids	beta-Alanine metabolism	SR	-	-
S-T-P	Landslide	2.27	K15531	MET	-	-	nc	-	-
S-T-P	Landslide	1.66	K15894	MET	Carbohydrate metabolism	Amino sugar and nucleotide sugar metabolism	nc	Virulence	Immune evasion
S-T-P	Landslide	1.52	K16016	MET	Metabolism of terpenoids and polyketides	Biosynthesis of ansamycins	nc	-	-
S-T-P	Landslide	1.96	K16149	MET	Carbohydrate metabolism	Starch and sucrose metabolism	PE	-	-
S-T-P	Landslide	2.43	K16371	MET	Carbohydrate metabolism	Galactose metabolism	nc	-	-
S-T-P	Landslide	2.33	K17285	MET	Energy Metabolism	Sulfur metabolism	nc	-	-
S-T-P	Landslide	3.28	K17744	MET	Carbohydrate metabolism	Ascorbate and aldarate metabolism	S	-	-
S-T-P	Landslide	2.46	K17752	MET	-	Protein kinases	nc	-	-
S-T-P	Landslide	2.68	K18334	MET	Carbohydrate metabolism	Fructose and mannose metabolism	PE	-	-
S-T-P	Landslide	2.25	K03808	PCP	-	-	nc	-	-
S-T-P	Landslide	2.27	K06992	PCP	-	-	nc	-	-
S-T-P	Landslide	4.43	K08996	PCP	-	-	nc	-	-
S-T-P	Landslide	2.68	K09857	PCP	-	-	nc	-	-
S-T-P	Landslide	2.32	K09934	PCP	-	-	nc	-	-
S-T-P	Landslide	2.19	K09940	PCP	-	-	nc	-	-
S-T-P	Landslide	4.46	K02526	SCP	-	Transporters	nc	-	-
S-T-P	Landslide	3.43	K03303	SCP	-	Transporters	nc	-	-
S-T-P	Landslide	2.41	K05340	SCP	-	Transporters	nc	-	-
S-T-P	Landslide	3.16	K07175	SCP	-	Signaling proteins	nc	-	-
S-T-P	Landslide	2.41	K07290	SCP	-	Structural proteins	nc	-	-
S-T-P	Landslide	2.29	K08138	SCP	-	Transporters	nc	-	-
S-T-P	Landslide	2.02	K12542	SCP	-	Transporters	nc	-	-

`

Substrate	Habitat	Effect	KO	L1	L2	L3	CSR	Category	Subcategory
S-T-P	Landslide	3.12	K13021	SCP	-	Transporters (organic acid transporter)	nc	-	-
S-T-P	Landslide	4.92	K15549	SCP	-	Transporters	nc	-	-
S-T-P	Landslide	4.28	K18258	SCP	-	Exosome	nc	-	-
S-T-P	Landslide	2.79	K19585	SCP	-	Transporters	nc	-	-
S-T-P	Forest	-2.11	K02490	CEP	Cellular community	Quorum sensing	C	-	-
S-T-P	Forest	-4.54	K01539	EIP	Signal transduction	cAMP signaling pathway	F	-	-
S-T-P	Forest	-1.94	K11709	EIP	Membrane transport	ABC transporters	C	-	-
S-T-P	Forest	-5.24	K11710	EIP	Membrane transport	ABC transporters	C	-	-
S-T-P	Forest	-5.85	K15496	EIP	Membrane transport	ABC transporters	C	-	-
S-T-P	Forest	-6.50	K01170	GIP	Translation	Transfer RNA biogenesis	R	-	-
S-T-P	Forest	-6.44	K02877	GIP	Translation	Ribosome	R	-	-
S-T-P	Forest	-6.43	K02889	GIP	Translation	Ribosome	R	-	-
S-T-P	Forest	-6.65	K02908	GIP	Translation	Ribosome	R	-	-
S-T-P	Forest	-6.44	K02910	GIP	Translation	Ribosome	R	-	-
S-T-P	Forest	-6.30	K02912	GIP	Translation	Ribosome	R	-	-
S-T-P	Forest	-6.35	K02924	GIP	Translation	Ribosome	R	-	-
S-T-P	Forest	-6.50	K02977	GIP	Translation	Ribosome	R	-	-
S-T-P	Forest	-6.35	K02991	GIP	Translation	Ribosome	R	-	-
S-T-P	Forest	-6.47	K03047	GIP	Transcription	RNA polymerase	nc	-	-
S-T-P	Forest	-6.46	K03050	GIP	Transcription	RNA polymerase	nc	-	-
S-T-P	Forest	-6.32	K03051	GIP	Transcription	RNA polymerase	nc	-	-
S-T-P	Forest	-6.37	K03056	GIP	Transcription	RNA polymerase	nc	-	-
S-T-P	Forest	-4.83	K03124	GIP	Transcription	Basal transcription factors	nc	-	-
S-T-P	Forest	-6.40	K03237	GIP	Translation	RNA transport	nc	-	-
S-T-P	Forest	-6.44	K03238	GIP	Translation	RNA transport	nc	-	-
S-T-P	Forest	-3.85	K03552	GIP	Replication and repair	DNA repair and recombination proteins	S	-	-
S-T-P	Forest	-6.67	K03622	GIP	-	-	nc	-	-

`

Substrate	Habitat	Effect	KO	L1	L2	L3	CSR	Category	Subcategory
S-T-P	Forest	-6.37	K03627	GIP	-	-	nc	-	-
S-T-P	Forest	-6.57	K03679	GIP	Folding, sorting and degradation	RNA degradation	F	-	-
S-T-P	Forest	-2.31	K04074	GIP	-	Chromosome and associated proteins	nc	-	-
S-T-P	Forest	-1.54	K04794	GIP	Translation	Translation factors	nc	-	-
S-T-P	Forest	-6.50	K04802	GIP	Replication and repair	DNA replication	R	-	-
S-T-P	Forest	-6.69	K06174	GIP	Translation	Ribosome biogenesis	R	-	-
S-T-P	Forest	-6.46	K06932	GIP	Translation	Transfer RNA biogenesis	R	-	-
S-T-P	Forest	-6.43	K06947	GIP	Translation	Ribosome biogenesis	R	-	-
S-T-P	Forest	-6.47	K06963	GIP	Translation	Transfer RNA biogenesis	R	-	-
S-T-P	Forest	-6.40	K06965	GIP	Translation	mRNA surveillance pathway	nc	-	-
S-T-P	Forest	-6.37	K07398	GIP	-	-	nc	-	-
S-T-P	Forest	-3.65	K07446	GIP	-	Transfer RNA biogenesis	R	-	-
S-T-P	Forest	-4.55	K07463	GIP	Replication and repair	-	nc	-	-
S-T-P	Forest	-6.49	K07558	GIP	Translation	Transfer RNA biogenesis	R	-	-
S-T-P	Forest	-6.30	K07561	GIP	Translation	Translation factors	nc	-	-
S-T-P	Forest	-1.54	K07577	GIP	Translation	-	nc	-	-
S-T-P	Forest	-6.62	K10725	GIP	Replication and repair	DNA replication proteins	R	-	-
S-T-P	Forest	-6.30	K10726	GIP	Replication and repair	DNA replication	R	-	-
S-T-P	Forest	-1.91	K10839	GIP	Replication and repair	Nucleotide excision repair	S	-	-
S-T-P	Forest	-5.77	K10896	GIP	Replication and repair	-	nc	-	-
S-T-P	Forest	-6.49	K14568	GIP	Translation	Ribosome biogenesis	R	-	-
S-T-P	Forest	-6.35	K14574	GIP	Translation	Ribosome biogenesis	R	-	-
S-T-P	Forest	-6.26	K18532	GIP	Translation	Ribosome biogenesis	R	-	-
S-T-P	Forest	-3.64	K00169	MET	Carbohydrate metabolism	Citrate cycle	R	Carbon cycling	Carbon fixation
S-T-P	Forest	-1.92	K00245	MET	Carbohydrate metabolism	Citrate cycle	R	-	-
S-T-P	Forest	-1.96	K00246	MET	Carbohydrate metabolism	Citrate cycle	R	-	-

`

Substrate	Habitat	Effect	KO	L1	L2	L3	CSR	Category	Subcategory
S-T-P	Forest	-1.62	K00317	MET	Energy Metabolism	Methane metabolism	M	-	-
S-T-P	Forest	-1.80	K00346	MET	-	-	nc	-	-
S-T-P	Forest	-1.67	K00347	MET	-	-	nc	Metal Homeostasis	Sodium
S-T-P	Forest	-1.66	K00786	MET	-	Glycosyltransferases	nc	-	-
S-T-P	Forest	-1.51	K00813	MET	Amino acid metabolism	Alanine, aspartate and glutamate metabolism	S	-	-
S-T-P	Forest	-1.69	K01277	MET	-	Peptidases and inhibitors	C	-	-
S-T-P	Forest	-2.00	K01436	MET	-	Peptidases and inhibitors	C	-	-
S-T-P	Forest	-1.79	K01480	MET	Amino acid metabolism	Arginine and proline metabolism	PE	-	-
S-T-P	Forest	-1.55	K01486	MET	Nucleotide metabolism	Purine metabolism	nc	-	-
S-T-P	Forest	-4.79	K01537	MET	-	-	nc	-	-
S-T-P	Forest	-5.99	K02122	MET	Energy Metabolism	Oxidative phosphorylation	R	-	-
S-T-P	Forest	-5.50	K02191	MET	Metabolism of cofactors and vitamins	Porphyrin and chlorophyll metabolism	S	-	-
S-T-P	Forest	-1.59	K02486	MET	-	Protein kinases	nc	-	-
S-T-P	Forest	-5.51	K03399	MET	Metabolism of cofactors and vitamins	Porphyrin and chlorophyll metabolism	S	-	-
S-T-P	Forest	-6.52	K03726	MET	-	-	nc	-	-
S-T-P	Forest	-1.64	K03760	MET	Glycan biosynthesis and metabolism	Lipopolysaccharide biosynthesis	S	-	-
S-T-P	Forest	-1.83	K04068	MET	-	-	nc	-	-
S-T-P	Forest	-2.15	K04070	MET	-	-	nc	-	-
S-T-P	Forest	-2.12	K04748	MET	Energy Metabolism	-	nc	-	-
S-T-P	Forest	-3.81	K05830	MET	Amino acid metabolism	Lysine biosynthesis	R	-	-
S-T-P	Forest	-5.67	K06072	MET	-	-	nc	-	-
S-T-P	Forest	-2.25	K06897	MET	Metabolism of cofactors and vitamins	Folate biosynthesis	R	-	-
S-T-P	Forest	-6.40	K06982	MET	Metabolism of cofactors and vitamins	Pantothenate and CoA biosynthesis	nc	-	-

`

Substrate	Habitat	Effect	KO	L1	L2	L3	CSR	Category	Subcategory
S-T-P	Forest	-2.45	K07026	MET	Carbohydrate metabolism	Fructose and mannose metabolism	PE	-	-
S-T-P	Forest	-5.86	K08096	MET	Metabolism of cofactors and vitamins	Riboflavin metabolism	nc	-	-
S-T-P	Forest	-1.57	K11941	MET	-	-	nc	-	-
S-T-P	Forest	-1.62	K13039	MET	Energy Metabolism	Methane metabolism	M	-	-
S-T-P	Forest	-5.47	K13767	MET	Lipid metabolism	Fatty acid biosynthesis	S	-	-
S-T-P	Forest	-6.42	K17104	MET	Lipid metabolism	Glycerophospholipid metabolism	nc	-	-
S-T-P	Forest	-3.32	K17364	MET	Metabolism of cofactors and vitamins	Folate biosynthesis	R	-	-
S-T-P	Forest	-1.61	K17716	MET	Carbohydrate metabolism	Galactose metabolism	nc	Virulence	Adherence
S-T-P	Forest	-5.72	K17892	MET	-	-	nc	-	-
S-T-P	Forest	-1.62	K17989	MET	Amino acid metabolism	Glycine, serine and threonine metabolism	S	-	-
S-T-P	Forest	-5.81	K18594	MET	Energy Metabolism	Carbon fixation	R	Carbon cycling	Carbon fixation
S-T-P	Forest	-5.93	K18603	MET	Energy Metabolism	Carbon fixation	R	-	-
S-T-P	Forest	-5.79	K18604	MET	Energy Metabolism	Carbon fixation	R	-	-
S-T-P	Forest	-4.33	K19664	MET	Lipid metabolism	Glycerophospholipid metabolism	nc	-	-
S-T-P	Forest	-4.41	K01163	PCP	-	-	nc	-	-
S-T-P	Forest	-1.91	K06955	PCP	-	-	nc	-	-
S-T-P	Forest	-3.57	K07022	PCP	-	-	nc	-	-
S-T-P	Forest	-4.72	K07033	PCP	-	-	nc	-	-
S-T-P	Forest	-4.61	K07041	PCP	-	-	nc	-	-
S-T-P	Forest	-2.00	K07338	PCP	-	-	nc	-	-
S-T-P	Forest	-6.51	K09721	PCP	-	-	nc	-	-
S-T-P	Forest	-4.53	K02450	SCP	-	Secretion system	nc	-	-
S-T-P	Forest	-1.60	K02664	SCP	-	Bacterial motility proteins	F	-	-
S-T-P	Forest	-8.16	K06039	SCP	-	-	nc	-	-

`

Substrate	Habitat	Effect	KO	L1	L2	L3	CSR	Category	Subcategory
S-T-P	Forest	-3.89	K07330	SCP	-	Bacterial motility proteins	F	-	-
S-T-P	Forest	-3.87	K07331	SCP	-	Bacterial motility proteins	F	-	-
S-T-P	Forest	-2.60	K09820	SCP	-	Transporters	C	-	-
S-T-P	Forest	-3.62	K18235	SCP	-	Antimicrobial resistance	C	Microbial def.	Antibiotic resistance
T-P	Forest	-3.74	K07333	SCP	-	Bacterial motility proteins	F	-	-
S-P	Forest	-6.42	K09142	GIP	-	Chromosome and associated proteins	nc	-	-
S-T	Landslide	2.31	K04565	CEP	Transport and catabolism	Peroxisome	nc	Plant Growth Promotion	Anti-pathogen
S-T	Landslide	1.62	K11901	CEP	Cellular community	Biofilm formation	C	Virulence	Immune evasion
S-T	Landslide	1.57	K07484	GIP	-	Replication and repair	S	-	-
S-T	Landslide	3.61	K11921	GIP	Transcription	Transcription factors	nc	-	-
S-T	Landslide	1.66	K00117	MET	Carbohydrate metabolism	Pentose and phosphate pathway	nc	-	-
S-T	Landslide	1.52	K00364	MET	Nucleotide metabolism	Purine metabolism	nc	-	-
S-T	Landslide	3.45	K00469	MET	Carbohydrate metabolism	Ascorbate and aldarate metabolism	S	-	-
S-T	Landslide	3.19	K00594	MET	Carbohydrate metabolism	Fructose and mannose metabolism	PE	-	-
S-T	Landslide	5.29	K01392	MET	-	Peptidases and inhibitors	C	-	-
S-T	Landslide	1.78	K01654	MET	Carbohydrate metabolism	Amino sugar and nucleotide sugar metabolism	nc	Virulence	Immune evasion
S-T	Landslide	1.60	K01706	MET	Carbohydrate metabolism	Ascorbate and aldarate metabolism	S	-	-
S-T	Landslide	3.00	K01779	MET	Amino acid metabolism	Alanine, aspartate and glutamate metabolism	CS	-	-
S-T	Landslide	5.38	K01792	MET	Carbohydrate metabolism	Glycolysis / Gluconeogenesis	PE	-	-
S-T	Landslide	2.36	K03119	MET	Energy Metabolism	Sulfur metabolism	nc	Organic Contaminant Degradation	Others
S-T	Landslide	1.59	K03150	MET	Metabolism of cofactors and vitamins	Thiamine metabolism	S	-	-
S-T	Landslide	2.13	K03208	MET	-	Glycan metabolism	nc	-	-

`

Substrate	Habitat	Effect	KO	L1	L2	L3	CSR	Category	Subcategory
S-T	Landslide	1.58	K03418	MET	Carbohydrate metabolism	Glyoxylate and dicarboxylate metabolism	PE	-	-
S-T	Landslide	2.32	K03778	MET	Carbohydrate metabolism	Pyruvate metabolism	R	-	-
S-T	Landslide	1.65	K03831	MET	Metabolism of cofactors and vitamins	Folate biosynthesis	R	-	-
S-T	Landslide	3.48	K04486	MET	Amino acid metabolism	Histidine metabolism	PE	-	-
S-T	Landslide	1.77	K05337	MET	Energy Metabolism	-	nc	-	-
S-T	Landslide	1.57	K05826	MET	Amino acid metabolism	Lysine biosynthesis	R	-	-
S-T	Landslide	1.98	K05989	MET	-	-	nc	-	-
S-T	Landslide	1.68	K06113	MET	-	-	nc	-	-
S-T	Landslide	5.31	K06324	MET	-	-	nc	-	-
S-T	Landslide	1.96	K07404	MET	Carbohydrate metabolism	Pentose phosphate pathway	nc	-	-
S-T	Landslide	1.95	K08318	MET	Carbohydrate metabolism	Butanoate metabolism	nc	-	-
S-T	Landslide	1.59	K09788	MET	Carbohydrate metabolism	Propanoate metabolism	nc	-	-
S-T	Landslide	1.70	K13614	MET	-	Polyketide biosynthesis	CS	-	-
S-T	Landslide	2.68	K13935	MET	-	-	nc	-	-
S-T	Landslide	2.06	K14335	MET	Glycan biosynthesis and metabolism	Lipoarabinomannan (LAM) biosynthesis	nc	-	-
S-T	Landslide	1.52	K14682	MET	Amino acid metabolism	Arginine biosynthesis	nc	-	-
S-T	Landslide	1.58	K15329	MET	-	Polyketide biosynthesis	C	-	-
S-T	Landslide	1.62	K16044	MET	Carbohydrate metabolism	Inositol phosphate metabolism	PE	-	-
S-T	Landslide	2.12	K16147	MET	Carbohydrate metabolism	Starch and sucrose metabolism	PE	-	-
S-T	Landslide	1.76	K16148	MET	Carbohydrate metabolism	Starch and sucrose metabolism	PE	-	-
S-T	Landslide	1.66	K16164	MET	Amino acid metabolism	Tyrosine metabolism	PE	-	-
S-T	Landslide	2.24	K16840	MET	Nucleotide metabolism	Purine metabolism	nc	-	-
S-T	Landslide	1.75	K17228	MET	Energy Metabolism	Sulfur metabolism	nc	-	-
S-T	Landslide	1.69	K18115	MET	-	-	nc	-	-

`

Substrate	Habitat	Effect	KO	L1	L2	L3	CSR	Category	Subcategory
S-T	Landslide	1.92	K18981	MET	Carbohydrate metabolism	Ascorbate and aldarate metabolism	S	-	-
S-T	Landslide	1.86	K19746	MET	Metabolism of other amino acids	D-Arginine and D-ornithine metabolism	nc	-	-
S-T	Landslide	1.77	K06906	PCP	-	-	nc	-	-
S-T	Landslide	1.74	K09966	PCP	-	-	nc	-	-
S-T	Landslide	3.40	K11477	PCP	-	-	nc	-	-
S-T	Landslide	1.71	K02856	SCP	-	Transporters	S	-	-
S-T	Landslide	4.52	K07660	SCP	-	Antimicrobial resistance	C	Virulence	Cellular function
S-T	Landslide	1.77	K11897	SCP	-	Secretion system	nc	-	-
S-T	Landslide	1.95	K16300	SCP	-	Transporters	nc	-	-
S-T	Landslide	1.98	K18843	SCP	-	Prokaryotic defense system	C	-	-
S-T	Landslide	3.60	K19271	SCP	-	Antimicrobial resistance	C	-	-
S-T	Forest	-5.94	K08321	CEP	Cellular community	Quorum sensing	C	-	-
S-T	Forest	-1.58	K02000	EIP	Membrane transport	ABC transporters	S	Stress	Osmotic stress
S-T	Forest	-1.77	K02001	EIP	Membrane transport	ABC transporters	S	Stress	Osmotic stress
S-T	Forest	-6.53	K03234	EIP	Signal transduction	AMPK signaling pathway	nc	-	-
S-T	Forest	-1.79	K06857	EIP	Membrane transport	ABC transporters	C	-	-
S-T	Forest	-1.80	K10191	EIP	Membrane transport	ABC transporters	S	-	-
S-T	Forest	-2.59	K11705	EIP	Membrane transport	ABC transporters	C	-	-
S-T	Forest	-5.47	K14979	EIP	Signal transduction	Two-component system	nc	-	-
S-T	Forest	-2.18	K15497	EIP	Membrane transport	ABC transporters	C	-	-
S-T	Forest	-1.63	K19620	EIP	Signal transduction	Two-component system	nc	-	-
S-T	Forest	-6.39	K00586	GIP	Translation	Translation factors	nc	-	-
S-T	Forest	-1.53	K00974	GIP	Translation	RNA transport	nc	-	-
S-T	Forest	-6.41	K02319	GIP	Replication and repair	DNA replication	R	-	-
S-T	Forest	-3.84	K02875	GIP	Translation	Ribosome	R	-	-
S-T	Forest	-6.43	K02885	GIP	Translation	Ribosome	R	-	-
S-T	Forest	-3.71	K02922	GIP	Translation	Ribosome	R	-	-

`

Substrate	Habitat	Effect	KO	L1	L2	L3	CSR	Category	Subcategory
S-T	Forest	-3.62	K02927	GIP	Translation	Ribosome	R	-	-
S-T	Forest	-6.51	K02936	GIP	Translation	Ribosome	R	-	-
S-T	Forest	-3.67	K02944	GIP	Translation	Ribosome	R	-	-
S-T	Forest	-6.36	K02966	GIP	Translation	Ribosome	R	-	-
S-T	Forest	-6.62	K02975	GIP	Translation	Ribosome	R	-	-
S-T	Forest	-6.60	K02976	GIP	Translation	Ribosome	R	-	-
S-T	Forest	-6.34	K02979	GIP	Translation	Ribosome	R	-	-
S-T	Forest	-5.84	K03014	GIP	Transcription	RNA polymerase	nc	-	-
S-T	Forest	-6.34	K03049	GIP	Transcription	RNA polymerase	nc	-	-
S-T	Forest	-6.58	K03053	GIP	Transcription	RNA polymerase	nc	-	-
S-T	Forest	-3.65	K03055	GIP	Transcription	RNA polymerase	nc	-	-
S-T	Forest	-6.41	K03057	GIP	Transcription	RNA polymerase	nc	-	-
S-T	Forest	-6.32	K03120	GIP	Transcription	Basal transcription factors	nc	-	-
S-T	Forest	-5.64	K03167	GIP	Replication and repair	DNA replication proteins	R	-	-
S-T	Forest	-3.86	K03170	GIP	Replication and repair	DNA replication proteins	R	-	-
S-T	Forest	-6.17	K03231	GIP	Translation	RNA transport	nc	-	-
S-T	Forest	-6.41	K03232	GIP	Translation	Translation factors	nc	-	-
S-T	Forest	-6.40	K03264	GIP	Translation	Ribosome biogenesis	R	-	-
S-T	Forest	-6.47	K03330	GIP	Translation	Aminoacyl-tRNA biosynthesis	R	-	-
S-T	Forest	-7.41	K04479	GIP	Replication and repair	DNA repair and recombination proteins	S	-	-
S-T	Forest	-3.88	K04484	GIP	Replication and repair	DNA repair and recombination proteins	S	-	-
S-T	Forest	-6.54	K04796	GIP	-	-	nc	-	-
S-T	Forest	-6.43	K04797	GIP	-	Chaperones and folding catalysts	nc	-	-
S-T	Forest	-6.45	K04798	GIP	-	Chaperones and folding catalysts	nc	-	-
S-T	Forest	-6.58	K04801	GIP	Replication and repair	DNA replication	R	-	-
S-T	Forest	-1.80	K05499	GIP	Transcription	Transcription factors	nc	-	-

`

Substrate	Habitat	Effect	KO	L1	L2	L3	CSR	Category	Subcategory
S-T	Forest	-3.43	K06943	GIP	Translation	Ribosome biogenesis	R	-	-
S-T	Forest	-6.40	K07575	GIP	-	Messenger RNA biogenesis	nc	-	-
S-T	Forest	-3.58	K07728	GIP	Transcription	Transcription factors	nc	-	-
S-T	Forest	-6.34	K08851	GIP	Translation	Transfer RNA biogenesis	R	-	-
S-T	Forest	-6.33	K09716	GIP	Translation	Transfer RNA biogenesis	R	-	-
S-T	Forest	-3.91	K10848	GIP	Replication and repair	Nucleotide excision repair	SR	-	-
S-T	Forest	-6.53	K11600	GIP	Folding, sorting and degradation	RNA degradation	F	-	-
S-T	Forest	-4.13	K12600	GIP	Folding, sorting and degradation	RNA degradation	F	-	-
S-T	Forest	-1.58	K16138	GIP	Transcription	Transcription factors	nc	-	-
S-T	Forest	-5.28	K19592	GIP	Transcription	Transcription factors	nc	-	-
S-T	Forest	-2.05	K00158	MET	Carbohydrate metabolism	Pyruvate metabolism	R	-	-
S-T	Forest	-1.87	K00172	MET	Carbohydrate metabolism	Citrate cycle	R	Carbon cycling	Carbon fixation
S-T	Forest	-1.52	K00895	MET	Carbohydrate metabolism	Glycolysis / Gluconeogenesis	PE	-	-
S-T	Forest	-4.78	K00952	MET	Metabolism of cofactors and vitamins	Nicotinate and nicotinamide metabolism	nc	-	-
S-T	Forest	-1.62	K01565	MET	Glycan biosynthesis and metabolism	Glycosaminoglycan degradation	nc	-	-
S-T	Forest	-4.43	K01622	MET	Carbohydrate metabolism	Glycolysis / Gluconeogenesis	PE-M	-	-
S-T	Forest	-1.99	K02121	MET	Energy Metabolism	Oxidative phosphorylation	R	-	-
S-T	Forest	-6.52	K02201	MET	Metabolism of cofactors and vitamins	Pantothenate and CoA biosynthesis	nc	-	-
S-T	Forest	-5.14	K02573	MET	Energy Metabolism	-	nc	-	-
S-T	Forest	-8.22	K03146	MET	Metabolism of cofactors and vitamins	Thiamine metabolism	S	-	-
S-T	Forest	-6.59	K03943	MET	Energy Metabolism	Oxidative phosphorylation	R	-	-
S-T	Forest	-1.65	K04720	MET	Metabolism of cofactors and vitamins	Porphyrin and chlorophyll metabolism	S	-	-
S-T	Forest	-3.75	K05831	MET	Amino acid metabolism	Lysine biosynthesis	R	-	-
S-T	Forest	-1.50	K05919	MET	-	-	nc	-	-

`

Substrate	Habitat	Effect	KO	L1	L2	L3	CSR	Category	Subcategory
S-T	Forest	-6.72	K06863	MET	Nucleotide metabolism	Purine metabolism	nc	-	-
S-T	Forest	-3.68	K06928	MET	Nucleotide metabolism	Purine metabolism	nc	-	-
S-T	Forest	-2.14	K06937	MET	-	-	nc	-	-
S-T	Forest	-4.53	K06981	MET	Metabolism of terpenoids and polyketides	Terpenoid backbone biosynthesis	nc	-	-
S-T	Forest	-4.62	K06984	MET	Metabolism of cofactors and vitamins	Folate biosynthesis	R	-	-
S-T	Forest	-4.03	K08306	MET	-	Peptidoglycan biosynthesis and degradation proteins	S	-	-
S-T	Forest	-3.42	K11529	MET	Carbohydrate metabolism	Pentose phosphate pathway	nc	-	-
S-T	Forest	-5.98	K11646	MET	Amino acid metabolism	Phenylalanine, tyrosine and tryptophan biosynthesis	nc	-	-
S-T	Forest	-4.17	K12953	MET	-	-	nc	-	-
S-T	Forest	-1.67	K12978	MET	Glycan biosynthesis and metabolism	Lipopolysaccharide biosynthesis proteins	S	-	-
S-T	Forest	-1.53	K13086	MET	-	-	nc	-	-
S-T	Forest	-5.83	K16306	MET	Carbohydrate metabolism	Glycolysis / Gluconeogenesis	PE	-	-
S-T	Forest	-6.05	K18593	MET	Energy Metabolism	Carbon fixation	R	-	-
S-T	Forest	-5.78	K18605	MET	Energy Metabolism	Carbon fixation	R	-	-
S-T	Forest	-6.67	K18855	MET	-	-	nc	-	-
S-T	Forest	-4.50	K18978	MET	Carbohydrate metabolism	Glycolysis / Gluconeogenesis	PE	-	-
S-T	Forest	-1.57	K19295	MET	-	Glycan metabolism	nc	-	-
S-T	Forest	-6.46	K03626	PCP	-	-	nc	-	-
S-T	Forest	-1.68	K06885	PCP	-	-	nc	-	-
S-T	Forest	-4.49	K07023	PCP	-	-	nc	-	-
S-T	Forest	-1.87	K07096	PCP	-	-	nc	-	-
S-T	Forest	-1.55	K07502	PCP	-	-	nc	-	-
S-T	Forest	-3.41	K08984	PCP	-	-	nc	-	-
S-T	Forest	-1.74	K09120	PCP	-	-	nc	-	-
S-T	Forest	-3.49	K09717	PCP	-	-	nc	-	-

`

Substrate	Habitat	Effect	KO	L1	L2	L3	CSR	Category	Subcategory
S-T	Forest	-2.69	K02241	SCP	-	Secretion system	nc	-	-
S-T	Forest	-6.16	K06320	SCP	-	-	nc	-	-
Soil	Landslide	2.13	K00694	CEP	Cellular community	Biofilm formation	C	-	-
Soil	Landslide	1.70	K11907	CEP	Cellular community	Biofilm formation	C	-	-
Soil	Landslide	4.47	K12992	CEP	Cellular community	Biofilm formation	C	-	-
Soil	Landslide	1.67	K03194	EIP	Membrane transport	Bacterial secretion system	nc	-	-
Soil	Landslide	1.57	K03222	EIP	Membrane transport	Bacterial secretion system	nc	Virulence	Secretion system
Soil	Landslide	1.75	K10004	EIP	Membrane transport	ABC transporters	S	-	-
Soil	Landslide	1.51	K10019	EIP	Membrane transport	ABC transporters	nc	-	-
Soil	Landslide	1.58	K12541	EIP	Membrane transport	ABC transporters	nc	Virulence	Toxins
Soil	Landslide	1.74	K17326	EIP	Membrane transport	ABC transporters	nc	-	-
Soil	Landslide	1.55	K17327	EIP	Membrane transport	ABC transporters	nc	-	-
Soil	Landslide	3.79	K03169	GIP	Replication and repair	DNA repair and recombination proteins	SR	-	-
Soil	Landslide	1.55	K03577	GIP	Transcription	Transcription factors	nc	-	-
Soil	Landslide	1.79	K05817	GIP	Transcription	Transcription factors	nc	-	-
Soil	Landslide	1.52	K07237	GIP	Translation	Transfer RNA biogenesis	R	-	-
Soil	Landslide	2.05	K07494	GIP	-	Replication and repair	S	-	-
Soil	Landslide	1.72	K17763	GIP	Transcription	Transcription machinery	nc	-	-
Soil	Landslide	1.53	K00021	MET	Metabolism of terpenoids and polyketides	Terpenoid backbone biosynthesis	nc	-	-
Soil	Landslide	1.79	K00034	MET	Carbohydrate metabolism	Pentose phosphate pathway	nc	-	-
Soil	Landslide	1.62	K00146	MET	Amino acid metabolism	Phenylalanine metabolism	nc	-	-
Soil	Landslide	1.69	K00216	MET	Metabolism of terpenoids and polyketides	Biosynthesis of siderophore group nonribosomal peptides	C	-	-
Soil	Landslide	2.05	K00244	MET	Carbohydrate metabolism	Citrate cycle	R	-	-
Soil	Landslide	1.87	K00365	MET	Biosynthesis of other secondary metabolites	Caffeine metabolism	PE	-	-
Soil	Landslide	1.50	K00450	MET	Amino acid metabolism	Tyrosine metabolism	PE	-	-
Soil	Landslide	1.88	K00526	MET	Nucleotide metabolism	Purine metabolism	nc	-	-

`

Substrate	Habitat	Effect	KO	L1	L2	L3	CSR	Category	Subcategory
Soil	Landslide	2.01	K00675	MET	-	-	nc	-	-
Soil	Landslide	1.60	K00801	MET	Metabolism of terpenoids and polyketides	Sesquiterpenoid and triterpenoid biosynthesis	nc	-	-
Soil	Landslide	1.83	K00886	MET	Carbohydrate metabolism	Glycolysis / Gluconeogenesis	PE	-	-
Soil	Landslide	4.56	K01184	MET	Carbohydrate metabolism	Pentose and glucuronate interconversions	nc	Plant Growth Promotion	Anti-pathogen
Soil	Landslide	2.14	K01185	MET	-	-	nc	-	-
Soil	Landslide	1.79	K01195	MET	Carbohydrate metabolism	Ascorbate and aldarate metabolism	S	-	-
Soil	Landslide	1.51	K01212	MET	Carbohydrate metabolism	Starch and sucrose metabolism	PE	-	-
Soil	Landslide	1.72	K01569	MET	Carbohydrate metabolism	Glyoxylate and dicarboxylate metabolism	PE	-	-
Soil	Landslide	3.65	K01617	MET	Xenobiotics biodegradation and metabolism	Benzoate degradation	PE	-	-
Soil	Landslide	1.83	K01751	MET	-	-	nc	-	-
Soil	Landslide	1.66	K01800	MET	Amino acid metabolism	Tyrosine metabolism	PE	-	-
Soil	Landslide	1.80	K01820	MET	Carbohydrate metabolism	Fructose and mannose metabolism	PE	-	-
Soil	Landslide	1.85	K01829	MET	-	-	nc	-	-
Soil	Landslide	1.50	K01865	MET	Xenobiotics biodegradation and metabolism	Aminobenzoate degradation	nc	Organic Contaminant Degradation	Aromatics
Soil	Landslide	1.56	K02299	MET	Energy Metabolism	Oxidative phosphorylation	R	-	-
Soil	Landslide	1.53	K02362	MET	Metabolism of terpenoids and polyketides	Biosynthesis of siderophore group nonribosomal peptides	C	-	-
Soil	Landslide	1.64	K02564	MET	Carbohydrate metabolism	Amino sugar and nucleotide sugar metabolism	nc	-	-
Soil	Landslide	1.59	K03578	MET	-	-	nc	-	-
Soil	Landslide	3.16	K05350	MET	Carbohydrate metabolism	Starch and sucrose metabolism	PE	Stress	Glucose limitation
Soil	Landslide	1.77	K05995	MET	-	Peptidases and inhibitors	C	-	-

`

Substrate	Habitat	Effect	KO	L1	L2	L3	CSR	Category	Subcategory
Soil	Landslide	3.37	K07250	MET	Amino acid metabolism	Alanine, aspartate and glutamate	S	-	-
Soil	Landslide	1.70	K07407	MET	Glycan biosynthesis and metabolism	Glycosphingolipid biosynthesis	nc	-	-
Soil	Landslide	1.64	K08068	MET	Carbohydrate metabolism	Amino sugar and nucleotide sugar metabolism	nc	-	-
Soil	Landslide	1.89	K08092	MET	Carbohydrate metabolism	Ascorbate and aldarate metabolism	S	-	-
Soil	Landslide	1.66	K09011	MET	Amino acid metabolism	Valine, leucine and isoleucine biosynthesis	S	-	-
Soil	Landslide	2.21	K09836	MET	Metabolism of terpenoids and polyketids	Carotenoid biosynthesis	PE	-	-
Soil	Landslide	2.16	K09994	MET	Metabolism of other amino acids	Phosphonate and phosphinate metabolism	nc	-	-
Soil	Landslide	3.15	K12436	MET	-	Lipid biosynthesis	nc	-	-
Soil	Landslide	1.53	K12454	MET	Carbohydrate metabolism	Amino sugar and nucleotide sugar metabolism	nc	-	-
Soil	Landslide	2.01	K13541	MET	Metabolism of cofactors and vitamins	Porphyrin and chlorophyll metabolism	S	-	-
Soil	Landslide	1.70	K13930	MET	-	-	nc	-	-
Soil	Landslide	1.63	K13932	MET	-	-	nc	-	-
Soil	Landslide	1.67	K13933	MET	-	-	nc	-	-
Soil	Landslide	1.70	K13934	MET	-	-	nc	-	-
Soil	Landslide	1.81	K13992	MET	-	Photosynthesis	R	-	-
Soil	Landslide	1.71	K13995	MET	Metabolism of cofactors and vitamins	Nicotinate and nicotinamide metabolism	nc	-	-
Soil	Landslide	1.55	K15930	MET	Metabolism of terpenoids and polyketids	Biosynthesis of type II polyketide products	C	-	-
Soil	Landslide	1.51	K15986	MET	Energy Metabolism	Oxidative phosphorylation	R	-	-
Soil	Landslide	1.64	K16423	MET	Metabolism of terpenoids and polyketides	Biosynthesis of vancomycin group antibiotics	C	-	-
Soil	Landslide	2.05	K16856	MET	Nucleotide metabolism	Purine metabolism	nc	-	-

`

Substrate	Habitat	Effect	KO	L1	L2	L3	CSR	Category	Subcategory
Soil	Landslide	1.52	K17754	MET	Xenobiotics biodegradation and metabolism	Caprolactam degradation	nc	Organic Contaminant Degradation	Other hydrocarbons
Soil	Landslide	1.71	K18545	MET	-	Peptidases and inhibitors	C	-	-
Soil	Landslide	1.70	K18581	MET	-	-	nc	-	-
Soil	Landslide	1.88	K19689	MET	-	Peptidases and inhibitors	C	-	-
Soil	Landslide	1.83	K06908	PCP	-	-	nc	-	-
Soil	Landslide	1.91	K06986	PCP	-	-	nc	-	-
Soil	Landslide	1.55	K07034	PCP	-	-	nc	-	-
Soil	Landslide	1.57	K07065	PCP	-	-	nc	-	-
Soil	Landslide	1.53	K07099	PCP	-	-	nc	-	-
Soil	Landslide	1.78	K02505	SCP	-	Secretion system	nc	-	-
Soil	Landslide	2.08	K03098	SCP	-	Exosome	nc	-	-
Soil	Landslide	1.79	K03328	SCP	-	Transporters	nc	-	-
Soil	Landslide	1.75	K03453	SCP	-	Transporters	nc	-	-
Soil	Landslide	1.96	K03457	SCP	-	Transporters	nc	-	-
Soil	Landslide	2.12	K03535	SCP	-	Transporters	nc	-	-
Soil	Landslide	1.65	K03893	SCP	-	Transporters	nc	Metal Homeostasis	Arsenic
Soil	Landslide	1.50	K04338	SCP	-	Secretion system	nc	-	-
Soil	Landslide	1.62	K06077	SCP	-	Structural proteins	nc	-	-
Soil	Landslide	1.76	K06143	SCP	-	Structural proteins	nc	-	-
Soil	Landslide	1.52	K08191	SCP	-	Transporters	nc	-	-
Soil	Landslide	1.91	K10025	SCP	-	Transporters	C	-	-
Soil	Landslide	3.69	K10974	SCP	-	Transporters	nc	-	-
Soil	Landslide	1.59	K11896	SCP	-	Secretion system	nc	Virulence	Soil-borne pathogen
Soil	Landslide	5.93	K11928	SCP	-	Transporters	S	-	-
Soil	Landslide	1.71	K13929	SCP	-	Transporters	nc	-	-
Soil	Landslide	1.70	K13931	SCP	-	Transporters	nc	-	-
Soil	Landslide	5.20	K15547	SCP	-	Transporters	nc	-	-

`

Substrate	Habitat	Effect	KO	L1	L2	L3	CSR	Category	Subcategory
Soil	Landslide	1.54	K18303	SCP	-	Transporters	C	Microbial defense	Antibiotic resistance
Soil	Forest	-1.53	K07715	CEP	Cellular community	Quorum sensing	C	Virulence	Immune evasion
Soil	Forest	-1.75	K13585	CEP	Cell growth and death	Cell cycle	nc	-	-
Soil	Forest	-3.47	K13586	CEP	Cell growth and death	Cell cycle	nc	-	-
Soil	Forest	-5.47	K07777	EIP	Signal transduction	Two-component system	nc	Stress	Osmotic stress
Soil	Forest	-1.63	K09815	EIP	Membrane transport	ABC transporters	C	Metal Homeostasis	Zinc
Soil	Forest	-1.90	K11707	EIP	Membrane transport	ABC transporters	C	Metal Homeostasis	Zinc
Soil	Forest	-1.85	K11708	EIP	Membrane transport	ABC transporters	C	-	-
Soil	Forest	-2.00	K15495	EIP	Membrane transport	ABC transporters	C	-	-
Soil	Forest	-1.84	K16819	EIP	Signal transduction	Hippo signaling pathway	nc	-	-
Soil	Forest	-6.46	K00555	GIP	Translation	Transfer RNA biogenesis	R	-	-
Soil	Forest	-5.77	K02322	GIP	Replication and repair	DNA replication	R	-	-
Soil	Forest	-5.87	K02323	GIP	Replication and repair	DNA replication	R	-	-
Soil	Forest	-6.36	K02683	GIP	Replication and repair	DNA replication	R	-	-
Soil	Forest	-6.39	K02866	GIP	Translation	Ribosome	R	-	-
Soil	Forest	-6.56	K02869	GIP	Translation	Ribosome	R	-	-
Soil	Forest	-6.37	K02896	GIP	Translation	Ribosome	R	-	-
Soil	Forest	-6.41	K02921	GIP	Translation	Ribosome	R	-	-
Soil	Forest	-6.28	K02929	GIP	Translation	Ribosome	R	-	-
Soil	Forest	-6.55	K02930	GIP	Translation	Ribosome	R	-	-
Soil	Forest	-6.52	K02962	GIP	Translation	Ribosome	R	-	-
Soil	Forest	-6.44	K02974	GIP	Translation	Ribosome	R	-	-
Soil	Forest	-6.42	K02978	GIP	Translation	Ribosome	R	-	-
Soil	Forest	-6.38	K02983	GIP	Translation	Ribosome	R	-	-
Soil	Forest	-6.56	K02995	GIP	Translation	Ribosome	R	-	-
Soil	Forest	-6.32	K03041	GIP	Transcription	RNA polymerase	nc	-	-
Soil	Forest	-3.92	K03042	GIP	Transcription	RNA polymerase	nc	-	-

`

Substrate	Habitat	Effect	KO	L1	L2	L3	CSR	Category	Subcategory
Soil	Forest	-6.51	K03105	GIP	Folding, sorting and degradation	Protein export	nc	-	-
Soil	Forest	-5.90	K03163	GIP	Replication and repair	DNA replication proteins	R	-	-
Soil	Forest	-5.84	K03166	GIP	Replication and repair	DNA replication proteins	R	-	-
Soil	Forest	-6.48	K03242	GIP	Translation	RNA transport	nc	-	-
Soil	Forest	-6.41	K03243	GIP	Translation	RNA transport	nc	-	-
Soil	Forest	-6.65	K03263	GIP	Translation	Translation factors	nc	-	-
Soil	Forest	-6.19	K03265	GIP	Translation	mRNA surveillance pathway	nc	-	-
Soil	Forest	-4.46	K03432	GIP	Folding, sorting and degradation	Proteasome	S	-	-
Soil	Forest	-4.61	K03433	GIP	Folding, sorting and degradation	Proteasome	S	-	-
Soil	Forest	-3.73	K03537	GIP	Translation	Ribosome biogenesis	R	-	-
Soil	Forest	-6.52	K03538	GIP	Translation	Ribosome biogenesis	R	-	-
Soil	Forest	-1.55	K03540	GIP	Translation	RNA transport	R	-	-
Soil	Forest	-5.91	K04482	GIP	Replication and repair	Homologous recombination	F	-	-
Soil	Forest	-6.39	K04795	GIP	Translation	Ribosome biogenesis	R	-	-
Soil	Forest	-6.49	K04799	GIP	Replication and repair	DNA replication	SR	-	-
Soil	Forest	-6.36	K04800	GIP	Replication and repair	DNA replication	R	-	-
Soil	Forest	-6.56	K06961	GIP	Translation	Ribosome biogenesis	R	-	-
Soil	Forest	-3.90	K07179	GIP	Translation	Ribosome biogenesis	R	-	-
Soil	Forest	-6.46	K07254	GIP	Translation	Transfer RNA biogenesis	R	-	-
Soil	Forest	-1.87	K07442	GIP	Translation	Transfer RNA biogenesis	R	-	-
Soil	Forest	-6.55	K07466	GIP	Replication and repair	Nucleotide excision repair	SR	-	-
Soil	Forest	-3.99	K07562	GIP	Translation	Ribosome biogenesis	R	-	-
Soil	Forest	-6.49	K07569	GIP	Translation	Ribosome biogenesis	R	-	-
Soil	Forest	-6.40	K07572	GIP	Translation	-	nc	-	-
Soil	Forest	-6.50	K07573	GIP	Folding, sorting and degradation	RNA degradation	F	-	-
Soil	Forest	-3.54	K07579	GIP	Translation	-	nc	-	-

`

Substrate	Habitat	Effect	KO	L1	L2	L3	CSR	Category	Subcategory
Soil	Forest	-5.68	K07580	GIP	Translation	-	nc	-	-
Soil	Forest	-6.40	K07581	GIP	Translation	-	nc	-	-
Soil	Forest	-6.43	K07583	GIP	Translation	Transfer RNA biogenesis	R	-	-
Soil	Forest	-1.64	K07722	GIP	Transcription	Transcription factors	nc	-	-
Soil	Forest	-6.23	K07739	GIP	Translation	Transfer RNA biogenesis	R	-	-
Soil	Forest	-1.91	K07743	GIP	Transcription	-	nc	-	-
Soil	Forest	-4.60	K07744	GIP	Transcription	-	nc	-	-
Soil	Forest	-6.56	K09140	GIP	Translation	Ribosome biogenesis	R	-	-
Soil	Forest	-6.21	K09482	GIP	Translation	Aminoacyl-tRNA biosynthesis	R	-	-
Soil	Forest	-6.49	K09723	GIP	Replication and repair	DNA replication proteins	R	-	-
Soil	Forest	-1.80	K09765	GIP	-	Transfer RNA biogenesis	R	-	-
Soil	Forest	-6.36	K11130	GIP	Translation	Ribosome biogenesis	R	-	-
Soil	Forest	-6.36	K12589	GIP	Folding, sorting and degradation	RNA degradation	F	-	-
Soil	Forest	-1.60	K13525	GIP	-	Messenger RNA biogenesis	nc	-	-
Soil	Forest	-2.04	K13527	GIP	Folding, sorting and degradation	Proteasome	S	-	-
Soil	Forest	-1.58	K13652	GIP	Transcription	Transcription factors	nc	-	-
Soil	Forest	-3.94	K14561	GIP	Translation	Ribosome biogenesis	R	-	-
Soil	Forest	-6.47	K14564	GIP	Translation	Ribosome biogenesis	R	-	-
Soil	Forest	-6.55	K15429	GIP	Translation	Transfer RNA biogenesis	R	-	-
Soil	Forest	-6.46	K15449	GIP	Translation	Transfer RNA biogenesis	R	-	-
Soil	Forest	-6.35	K18779	GIP	Translation	Transfer RNA biogenesis	R	-	-
Soil	Forest	-6.63	K18882	GIP	Replication and repair	DNA replication	R	-	-
Soil	Forest	-1.66	K18992	GIP	Transcription	Transcription factors	nc	-	-
Soil	Forest	-1.52	K19736	GIP	Transcription	Transcription factors	nc	-	-
Soil	Forest	-1.56	K00043	MET	Carbohydrate metabolism	Butanoate metabolism	nc	-	-
Soil	Forest	-1.50	K00096	MET	Lipid metabolism	Glycerophospholipid metabolism	nc	-	-

`

Substrate	Habitat	Effect	KO	L1	L2	L3	CSR	Category	Subcategory
Soil	Forest	-1.87	K00122	MET	Carbohydrate metabolism	Glyoxylate and dicarboxylate metabolism	PE-M	-	-
Soil	Forest	-6.49	K00150	MET	Carbohydrate metabolism	Glycolysis / Gluconeogenesis	PE	-	-
Soil	Forest	-1.78	K00179	MET	-	-	nc	-	-
Soil	Forest	-1.88	K00180	MET	-	-	nc	-	-
Soil	Forest	-1.72	K00349	MET	-	-	nc	-	-
Soil	Forest	-1.71	K00350	MET	-	-	nc	-	-
Soil	Forest	-3.59	K00368	MET	Energy Metabolism	Nitrogen metabolism	nc	N Cycling	Denitrification
Soil	Forest	-5.82	K00371	MET	Energy Metabolism	Nitrogen metabolism	nc	Stress	Oxygen limitation
Soil	Forest	-4.96	K00463	MET	Amino acid metabolism	Tryptophan metabolism	PE	-	-
Soil	Forest	-4.55	K00569	MET	Xenobiotics biodegradation and metabolism	Drug metabolism - other enzymes	nc	-	-
Soil	Forest	-2.00	K00577	MET	Energy Metabolism	Methane metabolism	M	-	-
Soil	Forest	-3.42	K00588	MET	Biosynthesis of other secondary metabolites	Phenylpropanoid biosynthesis	nc	-	-
Soil	Forest	-3.17	K00621	MET	Carbohydrate metabolism	Amino sugar and nucleotide sugar metabolism	nc	-	-
Soil	Forest	-5.97	K00682	MET	Metabolism of other amino acids	Glutathione metabolism	S	-	-
Soil	Forest	-1.57	K00712	MET	-	Glycosyltransferases	nc	-	-
Soil	Forest	-6.55	K01001	MET	Glycan biosynthesis and metabolism	N-Glycan biosynthesis	nc	-	-
Soil	Forest	-3.44	K01611	MET	Amino acid metabolism	Cysteine and methionine metabolism	PE	-	-
Soil	Forest	-1.87	K01678	MET	Carbohydrate metabolism	Citrate cycle	R	-	-
Soil	Forest	-1.58	K01823	MET	Metabolism of terpenoids and polyketides	Terpenoid backbone biosynthesis	nc	-	-
Soil	Forest	-1.73	K01959	MET	Carbohydrate metabolism	Citrate cycle	R	-	-
Soil	Forest	-4.54	K02117	MET	Energy Metabolism	Oxidative phosphorylation	R	-	-

`

Substrate	Habitat	Effect	KO	L1	L2	L3	CSR	Category	Subcategory
Soil	Forest	-4.64	K02118	MET	Energy Metabolism	Oxidative phosphorylation	R	Metal Homeostasis	Potassium
Soil	Forest	-5.94	K02119	MET	Energy Metabolism	Oxidative phosphorylation	R	-	-
Soil	Forest	-4.61	K02120	MET	Energy Metabolism	Oxidative phosphorylation	R	-	-
Soil	Forest	-4.66	K02123	MET	Energy Metabolism	Oxidative phosphorylation	R	-	-
Soil	Forest	-4.57	K02124	MET	Energy Metabolism	Oxidative phosphorylation	R	-	-
Soil	Forest	-1.97	K02189	MET	Metabolism of cofactors and vitamins	Porphyrin and chlorophyll metabolism	S	-	-
Soil	Forest	-1.65	K02849	MET	Glycan biosynthesis and metabolism	Lipopolysaccharide biosynthesis	S	-	-
Soil	Forest	-4.67	K03151	MET	Metabolism of cofactors and vitamins	Thiamine metabolism	SR	-	-
Soil	Forest	-4.02	K05299	MET	Energy Metabolism	Carbon fixation	R	-	-
Soil	Forest	-1.52	K05360	MET	Metabolism of other amino acids	Glutathione metabolism	S	-	-
Soil	Forest	-1.71	K05827	MET	Amino acid metabolism	Lysine biosynthesis	R	-	-
Soil	Forest	-1.89	K05947	MET	Carbohydrate metabolism	Fructose and mannose metabolism	PE	-	-
Soil	Forest	-6.25	K07151	MET	Glycan biosynthesis and metabolism	N-Glycan biosynthesis	nc	-	-
Soil	Forest	-1.82	K07291	MET	Carbohydrate metabolism	Inositol phosphate metabolism	PE	-	-
Soil	Forest	-6.53	K07732	MET	Metabolism of cofactors and vitamins	Riboflavin metabolism	nc	-	-
Soil	Forest	-3.63	K07991	MET	-	Peptidases and inhibitors	C	-	-
Soil	Forest	-4.32	K08094	MET	Energy Metabolism	Methane metabolism	R	-	-
Soil	Forest	-3.89	K09722	MET	Metabolism of other amino acids	beta-Alanine metabolism	S	-	-
Soil	Forest	-6.53	K09735	MET	Metabolism of cofactors and vitamins	Pantothenate and CoA biosynthesis	nc	-	-
Soil	Forest	-1.63	K13058	MET	-	-	nc	-	-
Soil	Forest	-4.38	K13060	MET	Amino acid metabolism	Cysteine and methionine metabolism	C	-	-

`

Substrate	Habitat	Effect	KO	L1	L2	L3	CSR	Category	Subcategory
Soil	Forest	-1.83	K13659	MET	-	Glycosyltransferases	nc	-	-
Soil	Forest	-1.60	K13693	MET	-	Glycosyltransferases	nc	-	-
Soil	Forest	-3.12	K13747	MET	Amino acid metabolism	Arginine and proline metabolism	PE	-	-
Soil	Forest	-1.66	K13831	MET	Energy metabolism	Methane metabolism	M	-	-
Soil	Forest	-5.71	K14165	MET	-	Protein phosphatases	nc	-	-
Soil	Forest	-2.27	K14534	MET	Carbohydrate metabolism	Butanoate metabolism	R	Carbon cycling	Carbon fixation
Soil	Forest	-4.59	K14654	MET	Metabolism of cofactors and vitamins	Riboflavin metabolism	nc	-	-
Soil	Forest	-6.37	K14656	MET	Metabolism of cofactors and vitamins	Riboflavin metabolism	nc	-	-
Soil	Forest	-1.72	K14660	MET	-	-	nc	-	-
Soil	Forest	-1.69	K14661	MET	-	-	nc	-	-
Soil	Forest	-1.65	K14728	MET	-	-	nc	-	-
Soil	Forest	-6.02	K15230	MET	Carbohydrate metabolism	Citrate cycle	R	-	-
Soil	Forest	-6.00	K15231	MET	Carbohydrate metabolism	Citrate cycle	R	-	-
Soil	Forest	-6.45	K15888	MET	Carbohydrate metabolism	Fructose and mannose metabolism	PE-M	-	-
Soil	Forest	-6.19	K17105	MET	Lipid metabolism	Glycerophospholipid metabolism	nc	-	-
Soil	Forest	-1.62	K17230	MET	Energy Metabolism	Sulfur metabolism	nc	-	-
Soil	Forest	-6.34	K17884	MET	-	-	nc	-	-
Soil	Forest	-1.94	K18601	MET	-	-	nc	-	-
Soil	Forest	-5.83	K18602	MET	Energy Metabolism	Carbon fixation	R	-	-
Soil	Forest	-3.34	K18700	MET	-	-	nc	-	-
Soil	Forest	-1.58	K19189	MET	Metabolism of cofactors and vitamins	Nicotinate and nicotinamide metabolism	nc	-	-
Soil	Forest	-4.82	K19235	MET	-	Peptidoglycan biosynthesis and degradation proteins	CS	-	-
Soil	Forest	-6.30	K06865	PCP	-	-	nc	-	-
Soil	Forest	-3.73	K07049	PCP	-	-	nc	-	-

`

Substrate	Habitat	Effect	KO	L1	L2	L3	CSR	Category	Subcategory
Soil	Forest	-4.41	K07076	PCP	-	-	nc	-	-
Soil	Forest	-6.33	K07108	PCP	-	-	nc	-	-
Soil	Forest	-3.41	K07129	PCP	-	-	nc	-	-
Soil	Forest	-1.52	K07138	PCP	-	-	nc	-	-
Soil	Forest	-1.78	K07139	PCP	-	-	nc	-	-
Soil	Forest	-3.89	K07143	PCP	-	-	nc	-	-
Soil	Forest	-4.69	K07159	PCP	-	-	nc	-	-
Soil	Forest	-6.24	K08975	PCP	-	-	nc	-	-
Soil	Forest	-2.33	K09128	PCP	-	-	nc	-	-
Soil	Forest	-5.27	K09132	PCP	-	-	nc	-	-
Soil	Forest	-3.94	K09141	PCP	-	-	nc	-	-
Soil	Forest	-5.73	K09143	PCP	-	-	nc	-	-
Soil	Forest	-3.31	K09147	PCP	-	-	nc	-	-
Soil	Forest	-5.75	K09152	PCP	-	-	nc	-	-
Soil	Forest	-3.79	K09732	PCP	-	-	nc	-	-
Soil	Forest	-6.42	K09736	PCP	-	-	nc	-	-
Soil	Forest	-6.45	K09738	PCP	-	-	nc	-	-
Soil	Forest	-2.27	K09794	PCP	-	-	nc	-	-
Soil	Forest	-1.78	K09859	PCP	-	-	nc	-	-
Soil	Forest	-1.75	K03498	SCP	-	Transporters	nc	Metal Homeostasis	Potassium
Soil	Forest	-1.75	K03499	SCP	-	Transporters	nc	Metal Homeostasis	Potassium
Soil	Forest	-6.06	K06218	SCP	-	Prokaryotic defense system	C	-	-
Soil	Forest	-6.32	K07060	SCP	-	Prokaryotic defense system	C	-	-
Soil	Forest	-6.47	K07176	SCP	-	-	nc	-	-
Soil	Forest	-1.99	K07231	SCP	-	-	nc	-	-
Soil	Forest	-1.74	K07234	SCP	-	-	nc	-	-

`

Substrate	Habitat	Effect	KO	L1	L2	L3	CSR	Category	Subcategory
Soil	Forest	-5.89	K07285	SCP	-	Structural proteins	nc	-	-
Soil	Forest	-1.59	K07301	SCP	-	Transporters	nc	Metal Homeostasis	Calcium
Soil	Forest	-3.96	K07325	SCP	-	Secretion system	nc	-	-
Soil	Forest	-3.69	K07332	SCP	-	Bacterial motility proteins	F	-	-
Soil	Forest	-4.72	K08364	SCP	-	Transporters	nc	Metal Homeostasis	Mercury
Soil	Forest	-5.06	K09818	SCP	-	Transporters	C	-	-
Soil	Forest	-1.51	K12069	SCP	-	Secretion system	nc	-	-
Soil	Forest	-1.81	K13626	SCP	-	Bacterial motility proteins	F	-	-
Soil	Forest	-1.59	K16091	SCP	-	Transporters	C	Metal Homeostasis	Iron
Soil	Forest	-1.53	K16327	SCP	-	Transporters	nc	-	-
Soil	Forest	-1.57	K19591	SCP	-	Antimicrobial resistance	C	-	-
Tile	Landslide	1.92	K18148	-	Drug resistance: antimicrobial	beta-Lactam resistance	C	-	-
Tile	Landslide	1.50	K08604	CEP	Cellular community	Biofilm formation	C	-	-
Tile	Landslide	1.66	K06726	EIP	Membrane transport	ABC transporters	nc	-	-
Tile	Landslide	1.92	K04044	GIP	-	Chaperones and folding catalysts	nc	-	-
Tile	Landslide	1.73	K07486	GIP	-	Replication and repair	S	-	-
Tile	Landslide	3.85	K00865	MET	Carbohydrate metabolism	Glyoxylate and dicarboxylate metabolism	PE	-	-
Tile	Landslide	1.73	K01205	MET	Glycan biosynthesis and metabolism	Glycosaminoglycan degradation	nc	Carbon cycling	Carbon degradation
Tile	Landslide	1.61	K01707	MET	Carbohydrate metabolism	Ascorbate and aldarate metabolism	S	-	-
Tile	Landslide	1.75	K03274	MET	Glycan biosynthesis and metabolism	Lipopolysaccharide biosynthesis	S	-	-
Tile	Landslide	1.88	K03929	MET	-	-	nc	-	-
Tile	Landslide	1.99	K09252	MET	-	-	nc	-	-
Tile	Landslide	1.51	K06922	PCP	-	-	nc	-	-

`

Substrate	Habitat	Effect	KO	L1	L2	L3	CSR	Category	Subcategory
Tile	Landslide	2.20	K07118	PCP	-	-	nc	-	-
Tile	Landslide	2.10	K09990	PCP	-	-	nc	-	-
Tile	Landslide	1.54	K02445	SCP	-	Transporters	C	-	-
Tile	Landslide	1.63	K07448	SCP	-	Prokaryotic defense system	C	-	-
Tile	Forest	-1.59	K19733	CEP	Cellular community	Quorum sensing	C	-	-
Tile	Forest	-6.44	K01160	GIP	Replication and repair	DNA repair and recombination proteins	S	-	-
Tile	Forest	-6.46	K02883	GIP	Translation	Ribosome	R	-	-
Tile	Forest	-6.39	K02984	GIP	Translation	Ribosome	R	-	-
Tile	Forest	-6.54	K02987	GIP	Translation	Ribosome	R	-	-
Tile	Forest	-6.40	K03058	GIP	Transcription	RNA polymerase	nc	-	-
Tile	Forest	-6.26	K03059	GIP	Transcription	RNA polymerase	nc	-	-
Tile	Forest	-6.34	K03136	GIP	Transcription	Basal transcription factors	nc	-	-
Tile	Forest	-6.47	K03236	GIP	Translation	RNA transport	nc	-	-
Tile	Forest	-4.65	K04483	GIP	Replication and repair	DNA repair and recombination proteins	S	-	-
Tile	Forest	-6.41	K07342	GIP	Folding, sorting and degradation	Protein export	nc	-	-
Tile	Forest	-3.58	K07731	GIP	Transcription	Transcription factors	nc	-	-
Tile	Forest	-7.09	K08365	GIP	Transcription	Transcription factors	nc	-	-
Tile	Forest	-6.05	K10956	GIP	Folding, sorting and degradation	Protein export	nc	-	-
Tile	Forest	-6.51	K11131	GIP	Translation	Ribosome biogenesis	R	-	-
Tile	Forest	-2.14	K13571	GIP	Folding, sorting and degradation	Proteasome	S	-	-
Tile	Forest	-6.31	K13798	GIP	Transcription	RNA polymerase	nc	-	-
Tile	Forest	-3.59	K00170	MET	Carbohydrate metabolism	Citrate cycle	R	Carbon cycling	Carbon fixation
Tile	Forest	-1.75	K00348	MET	-	-	nc	-	-
Tile	Forest	-7.36	K00370	MET	Energy Metabolism	Nitrogen metabolism	nc	N Cycling	Nitrification
Tile	Forest	-1.86	K00610	MET	Nucleotide metabolism	Pyrimidine metabolism	SR	-	-

`

Substrate	Habitat	Effect	KO	L1	L2	L3	CSR	Category	Subcategory
Tile	Forest	-1.51	K01135	MET	Glycan biosynthesis and metabolism	Glycosaminoglycan degradation	nc	-	-
Tile	Forest	-1.69	K01136	MET	Glycan biosynthesis and metabolism	Glycosaminoglycan degradation	nc	-	-
Tile	Forest	-1.55	K01571	MET	Carbohydrate metabolism	Pyruvate metabolism	R	-	-
Tile	Forest	-1.74	K01663	MET	Amino acid metabolism	Histidine metabolism	PE	-	-
Tile	Forest	-1.81	K01677	MET	Carbohydrate metabolism	Citrate cycle	R	-	-
Tile	Forest	-3.63	K01960	MET	Carbohydrate metabolism	Citrate cycle	R	-	-
Tile	Forest	-1.51	K03824	MET	-	-	nc	-	-
Tile	Forest	-6.31	K07142	MET	Metabolism of cofactors and vitamins	Folate biosynthesis	R	-	-
Tile	Forest	-1.74	K07270	MET	-	Glycan metabolism	nc	-	-
Tile	Forest	-5.36	K08997	MET	-	-	nc	-	-
Tile	Forest	-2.20	K09123	MET	Amino acid metabolism	Arginine and proline metabolism	PE	-	-
Tile	Forest	-1.51	K10944	MET	Energy Metabolism	Methane metabolism	M	Carbon cycling	Methane Metabolism
Tile	Forest	-5.73	K11781	MET	Energy Metabolism	Methane metabolism	M	-	-
Tile	Forest	-3.71	K13378	MET	Energy Metabolism	Oxidative phosphorylation	R	-	-
Tile	Forest	-4.11	K15019	MET	Energy Metabolism	Carbon fixation	R	-	-
Tile	Forest	-3.59	K15778	MET	Biosynthesis of other secondary metabolites	Streptomycin biosynthesis	R	-	-
Tile	Forest	-3.49	K19068	MET	Glycan biosynthesis and metabolism	O-Antigen nucleotide and metabolism	nc	-	-
Tile	Forest	-5.86	K19712	MET	Metabolism of cofactors and vitamins	Porphyrin and chlorophyll metabolism	S	-	-
Tile	Forest	-6.37	K06869	PCP	-	-	nc	-	-
Tile	Forest	-4.10	K06874	PCP	-	-	nc	-	-
Tile	Forest	-2.34	K07086	PCP	-	-	nc	-	-
Tile	Forest	-6.40	K07158	PCP	-	-	nc	-	-
Tile	Forest	-6.19	K08979	PCP	-	-	nc	-	-
Tile	Forest	-1.65	K08982	PCP	-	-	nc	-	-

`

Substrate	Habitat	Effect	KO	L1	L2	L3	CSR	Category	Subcategory
Tile	Forest	-6.23	K09148	PCP	-	-	nc	-	-
Tile	Forest	-1.68	K09947	PCP	-	-	nc	-	-
Tile	Forest	-1.67	K02666	SCP	-	Bacterial motility proteins	F	-	-
Tile	Forest	-6.48	K06875	SCP	-	-	nc	-	-
Tile	Forest	-3.15	K19623	SCP	-	Two-component system	nc	-	-

`

Table S3.7. Brite hierarchy classification of differentially abundant KOs. Bold and plain text belong to the first and second level of the Brite classification, respectively.

	Forest								Landslide					
	Pellets		Soil		Tiles		Total		Soil		Tiles		Total	
	Count	%	Count	%	Count	%	Count	%	Count	%	Count	%	Count	%
Cellular Processes	**2**	**1.2**	**4**	**1.1**	**3**	**0.9**	**9**	**1.0**	**8**	**3.6**	**1**	**3.2**	**9**	**3.5**
Cell growth and death	1	0.6	2	0.5	0	0.0	3	0.3	1	0.4	0	0.0	1	0.4
Cellular community	1	0.6	2	0.5	3	0.9	6	0.7	6	2.7	1	3.2	7	2.7
Transport and catabolism	0	0.0	0	0.0	0	0.0	0	0.0	1	0.4	0	0.0	1	0.4
Environmental Information Processing	**2**	**1.2**	**14**	**3.8**	**11**	**3.1**	**27**	**3.0**	**10**	**4.5**	**1**	**3.2**	**11**	**4.3**
Membrane transport	1	0.6	8	2.2	7	2.0	16	1.8	10	4.5	1	3.2	11	4.3
Signal transduction	1	0.6	6	1.6	4	1.1	11	1.2	0	0.0	0	0.0	0	0.0
Genetic Information Processing	**119**	**69.2**	**158**	**43.4**	**157**	**44.9**	**434**	**49.0**	**20**	**8.9**	**2**	**6.5**	**22**	**8.6**
Folding, sorting and degradation	7	4.1	12	3.3	10	2.9	29	3.3	0	0.0	0	0.0	0	0.0
Replication and repair	18	10.5	26	7.1	26	7.4	70	7.9	1	0.4	1	3.2	2	0.8
Transcription	14	8.1	25	6.9	26	7.4	65	7.3	9	4.0	1	3.2	10	3.9
Translation	72	41.9	84	23.1	85	24.3	241	27.2	4	1.8	0	0.0	4	1.6
Others	8	4.7	11	3.0	10	2.9	29	3.3	6	2.7	0	0.0	6	2.4
Human Diseases	**0**	**0.0**	**0**	**0.0**	**0**	**0.0**	**0**	**0.0**	**1**	**0.4**	**0**	**0.0**	**1**	**0.4**
Drug resistance: antimicrobial	0	0.0	0	0.0	0	0.0	0	0.0	1	0.4	0	0.0	1	0.4
Metabolism	**34**	**19.8**	**124**	**34.1**	**121**	**34.6**	**279**	**31.5**	**131**	**58.5**	**17**	**54.8**	**148**	**58.0**
Amino acid metabolism	1	0.6	9	2.5	11	3.1	21	2.4	12	5.4	2	6.5	14	5.5
Biosynthesis of other secondary metabolites	**0**	0.0	2	0.5	2	0.6	4	0.5	1	0.4	0	0.0	1	0.4
Carbohydrate metabolism	3	1.7	24	6.6	17	4.9	44	5.0	47	21.0	7	22.6	54	21.2
Energy Metabolism	9	5.2	26	7.1	27	7.7	62	7.0	6	2.7	2	6.5	8	3.1
Glycan biosynthesis and metabolism	2	1.2	6	1.6	6	1.7	14	1.6	4	1.8	0	0.0	4	1.6
Lipid metabolism	2	1.2	4	1.1	5	1.4	11	1.2	2	0.9	1	3.2	3	1.2
Metabolism of cofactors and vitamins	11	6.4	18	4.9	18	5.1	47	5.3	5	2.2	0	0.0	5	2.0

`

	Forest								Landslide					
	Pellets		Soil		Tiles		Total		Soil		Tiles		Total	
	Count	%	Count	%	Count	%	Count	%	Count	%	Count	%	Count	%
Metabolism of other amino acids	0	0.0	2	0.5	3	0.9	5	0.6	3	1.3	0	0.0	3	1.2
Metabolism of terpenoids and polyketides	0	0.0	1	0.3	2	0.6	3	0.3	6	2.7	0	0.0	6	2.4
Metabolism of terpenoids and polyketids	0	0.0	0	0.0	0	0.0	0	0.0	6	2.7	0	0.0	6	2.4
Nucleotide metabolism	1	0.6	2	0.5	4	1.1	7	0.8	4	1.8	0	0.0	4	1.6
Xenobiotics biodegradation and metabolism	0	0.0	1	0.3	1	0.3	2	0.2	4	1.8	1	3.2	5	2.0
Others	5	2.9	29	8.0	25	7.1	59	6.7	31	13.8	4	12.9	35	13.7
Organismal systems	**1**	**0.6**	**1**	**0.3**	**1**	**0.3**	**3**	**0.3**	**0**	**0.0**	**0**	**0.0**	**0**	**0.0**
Signaling and Cellular Processes	**3**	**1.7**	**27**	**7.4**	**21**	**6.0**	**51**	**5.8**	**38**	**17.0**	**8**	**25.8**	**46**	**18.0**
Uncharacterized protein	**11**	**6.4**	**36**	**9.9**	**36**	**10.3**	**83**	**9.4**	**16**	**7.1**	**2**	**6.5**	**18**	**7.1**
Total	172		364		350		886		224		31		255	

`

Table S3.8. GeoChip 5.0 functional genes array classifications of the differentially abundant KOs.

	Forest				Landslide		
	Pellets	**Soil**	**Tiles**	**Total**	**Soil**	**Tiles**	**Total**
Carbon cycling	**1**	**4**	**5**	**10**	**3**	0	**3**
Carbon degradation	0	0	0	0	3	0	3
Carbon fixation	1	4	4	9	0	0	0
Methane Metabolism	0	0	1	1	0	0	0
Electron transport	0	0	0	0	1	0	1
Photosynthetic	0	0	0	0	1	0	1
Metal Homeostasis	**0**	**7**	**4**	**11**	**1**	0	**1**
Arsenic	0	0	0	0	1	0	1
Calcium	0	1	0	1	0	0	0
Iron	0	0	1	1	0	0	0
Mercury	0	1	1	2	0	0	0
Potassium	0	3	1	4	0	0	0
Sodium	0	1	0	1	0	0	0
Zinc	0	1	1	2	0	0	0
Microbial defense	0	**1**	**1**	**2**	**1**	0	**1**
Antibiotic resistance	0	1	1	2	1	0	1
Nitrogen Cycling	0	**2**	**2**	**4**	**0**	0	0
Denitrification	0	1	1	2	0	0	0
Nitrification	0	1	1	2	**0**	0	0
Organic Contaminant Degradation	0	0	0	0	**3**	0	**3**
Aromatics	0	0	0	0	1	0	1
Other hydrocarbons	0	0	0	0	1	0	1
Others	0	0	0	0	1	0	1
Plant Growth Promotion	0	0	0	0	**2**	**1**	**3**
Anti-pathogen	0	0	0	0	2	1	3
Stress	0	**2**	**4**	**6**	**1**	**1**	**2**
Glucose limitation	0	0	0	0	1	1	2
Osmotic stress	0	1	3	4	0	0	0
Oxygen limitation	0	1	1	2	0	0	0
Virulence	0	**1**	**1**	**2**	**7**	**2**	**9**
Adherence	0	0	1	1	0	0	0
Cellular function	0	0	0	0	1	1	2
Immune evasion	0	1	0	1	3	0	3
Secretion system	0	0	0	0	1	1	2
Soil-borne pathogen	0	0	0	0	1	0	1
Toxins	0	0	0	0	1	0	1
Not classified	**171**	**347**	**333**	**851**	**205**	**27**	**232**
Total	172	364	350	886	224	31	255

`

Table S3.9. CSR classification of differentially abundant KOs

	Forest								Landslide					
	Pellets		Soil		Tiles		Total		Soil		Tiles		Total	
	Count	%	Count	%	Count	%	Count	%	Count	%	Count	%	Count	%
CSR	**89**	**51.7**	**165**	**45.3**	**160**	**45.7**	**404**	**45.6**	**57**	**25.4**	**9**	**29.0**	**66**	**25.9**
Competitive	3	1.7	20	5.5	14	4.0	37	4.2	22	9.8	4	12.9	26	10.2
Stress	5	2.9	19	5.2	25	7.1	49	5.5	20	8.9	3	9.7	23	9.0
Rruderal	78	45.3	122	33.5	115	32.9	305	34.4	10	4.5	1	3.2	11	4.3
Multiple	3	1.7	4	1.1	6	1.7	13	1.5	5	2.2	1	3.2	6	2.4
Other classifications	**9**	**5.2**	**30**	**8.2**	**28**	**8.0**	**67**	**7.6**	**35**	**15.6**	**6**	**19.4**	**41**	**16.1**
Foraging	5	2.9	14	3.8	11	3.1	30	3.4	0	0.0	0	0.0	0	0.0
Methylotrophs	1	0.6	3	0.8	4	1.1	8	0.9	1	0.4	0	0.0	1	0.4
Plant exudates metabolism	2	1.2	10	2.7	9	2.6	21	2.4	34	15.2	6	19.4	40	15.7
Multiple	1	0.6	3	0.8	4	1.1	8	0.9	0	0.0	0	0.0	0	0.0
Not classified	**74**	**43.0**	**169**	**46.4**	**162**	**46.3**	**405**	**45.7**	**132**	**58.9**	**16**	**51.6**	**148**	**58.0**
Total	172	**100.0**	364	**100.0**	350	**100.0**	886	**100.0**	224	**100.0**	31	**100.0**	255	**100.0**

`

Figure S3.1. PCoA using two distance matrices (Hellinger and Jaccard) showing the batch effect from sequencing. Lines connect technical replicates sequenced on either the first or second sequencing run done in Puerto Rico and the third run done in Louisiana.

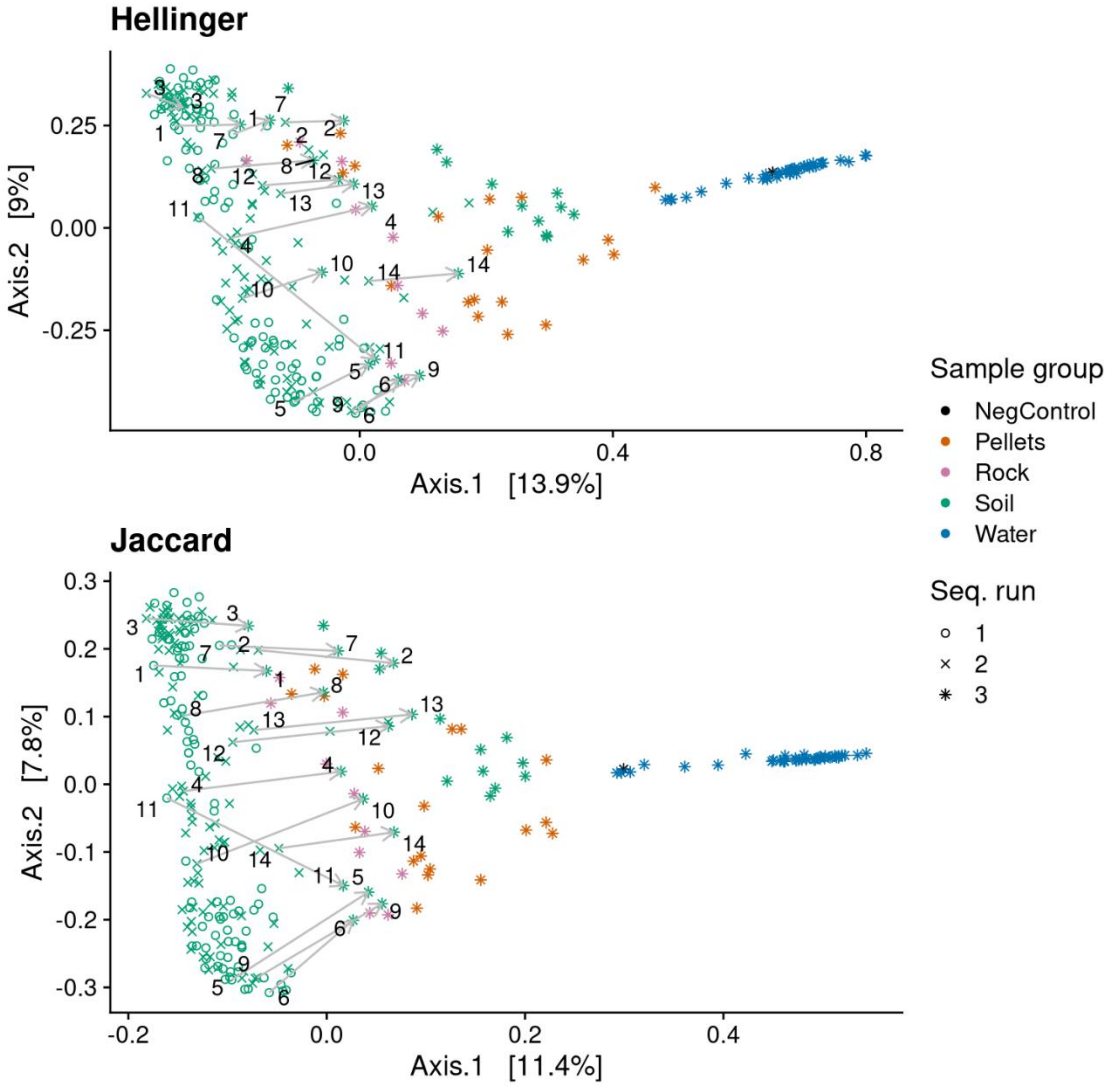

`

Figure S3.2. Pearson correlation matrix and multicollinearity test results corresponding to nutrient mobility/weathering indices calculated for pellets and tiles. Each table contains selected variables with its resulting Variance Inflation Factor (VIF).

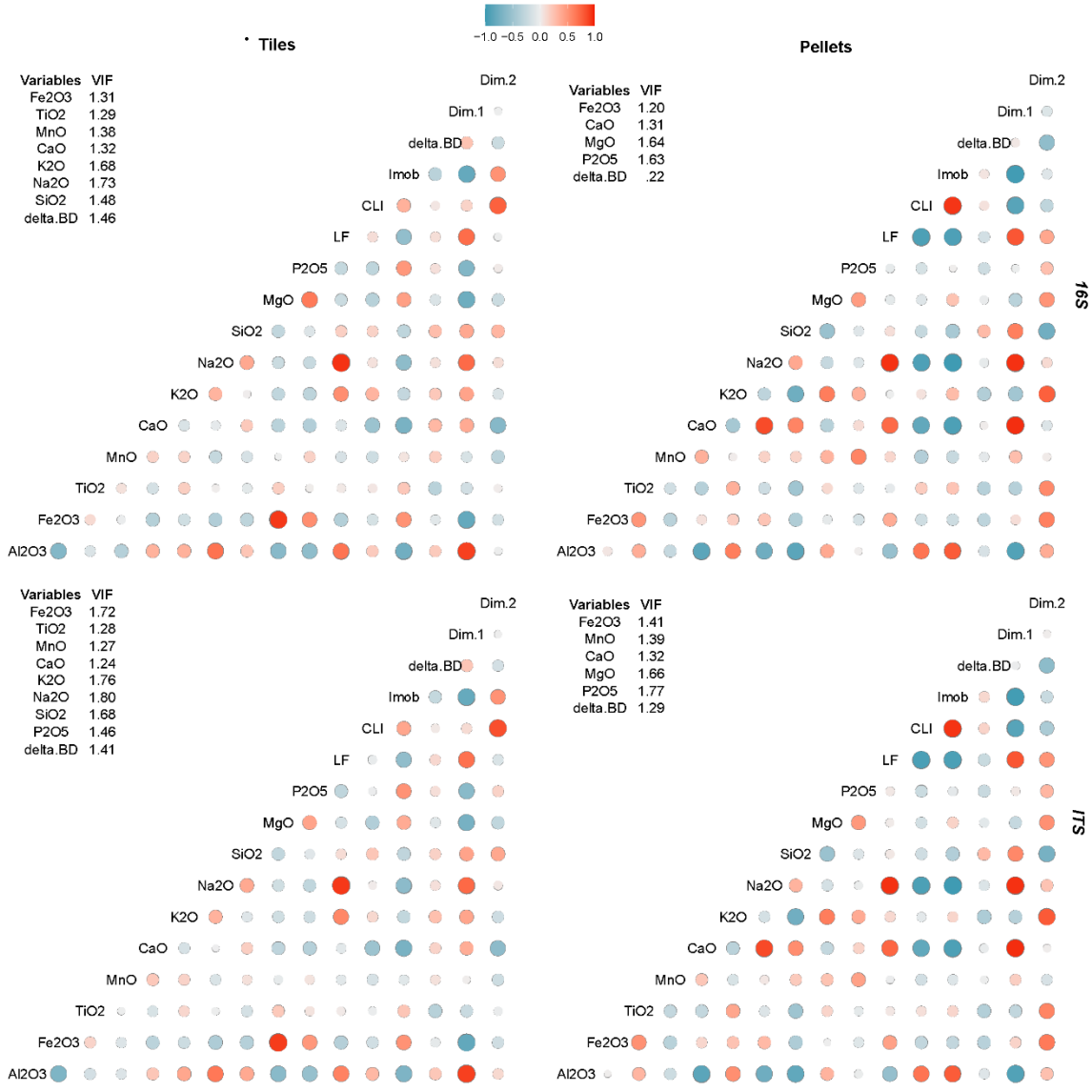

`

Figure S3.3. Mean nutrient mobility/weathering degree indices of A) tiles and B) pellets.

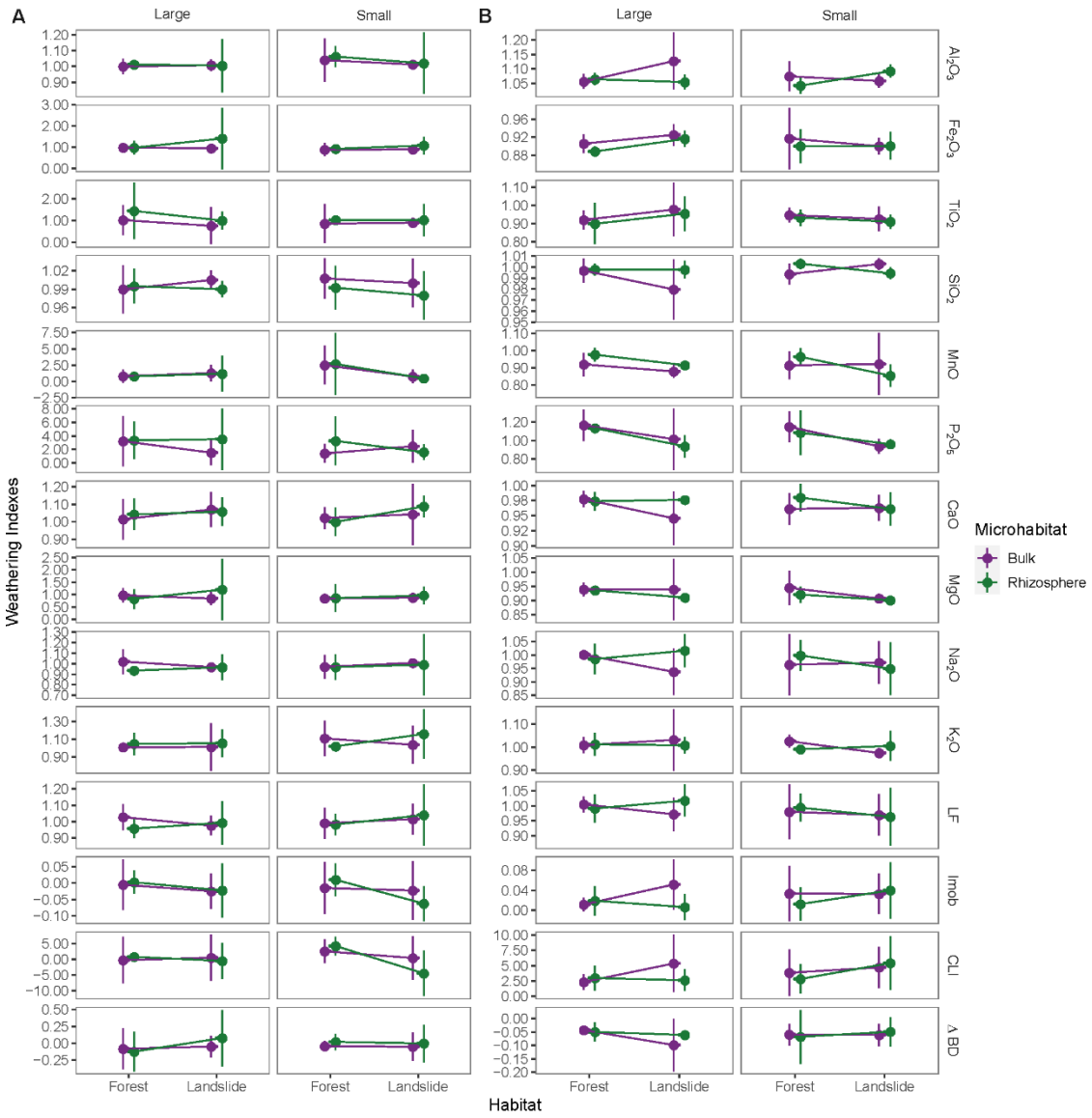

`

Figure S3.4. Rarefaction curves of species richness (Chao1) for *16S* and *ITS* ASVs at different habitats, microhabitat, substrates, and mesh size.

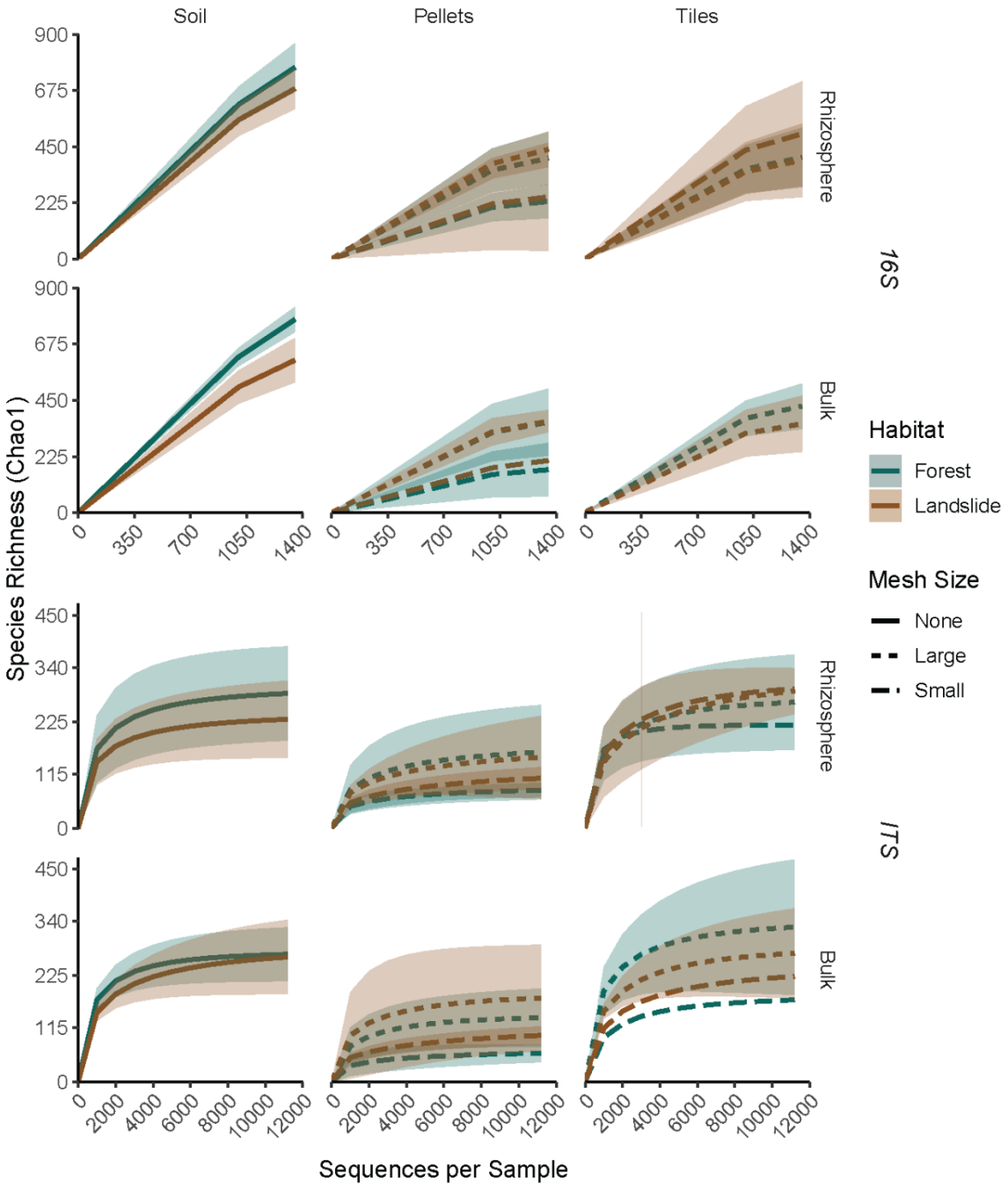

Figure S3.5. Average species richness (Chao1) and diversity (Shannon) for *16S* and *ITS* ASVs at different habitats, microhabitat, substrates, and mesh size in the rock samples.

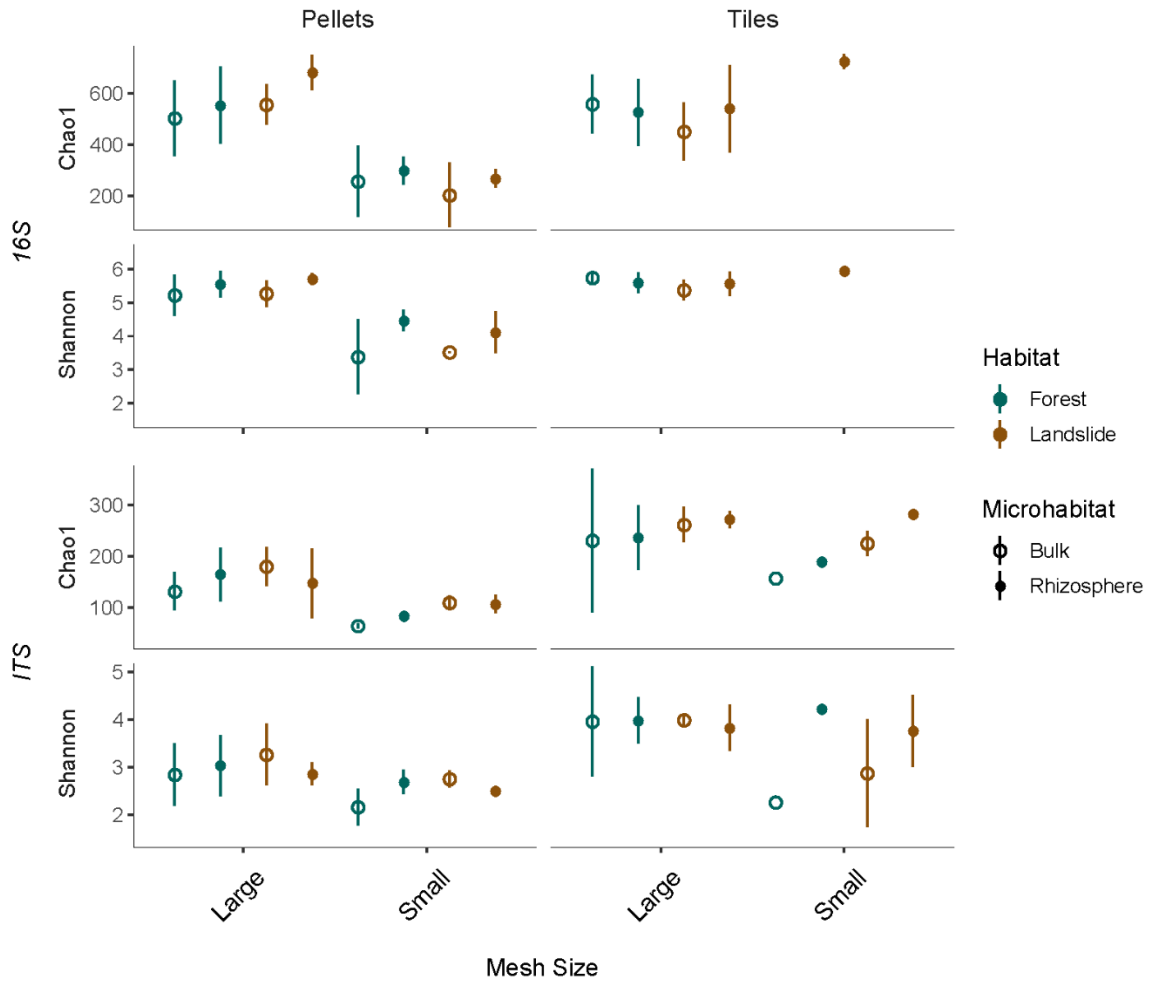

`

Figure S3.6. Taxonomic composition at phylum level of low abundant bacteria, archaea and fungi across habitat, microhabitat, substrate, and mesh size. Phyla with more than 1% total abundance were excluded.

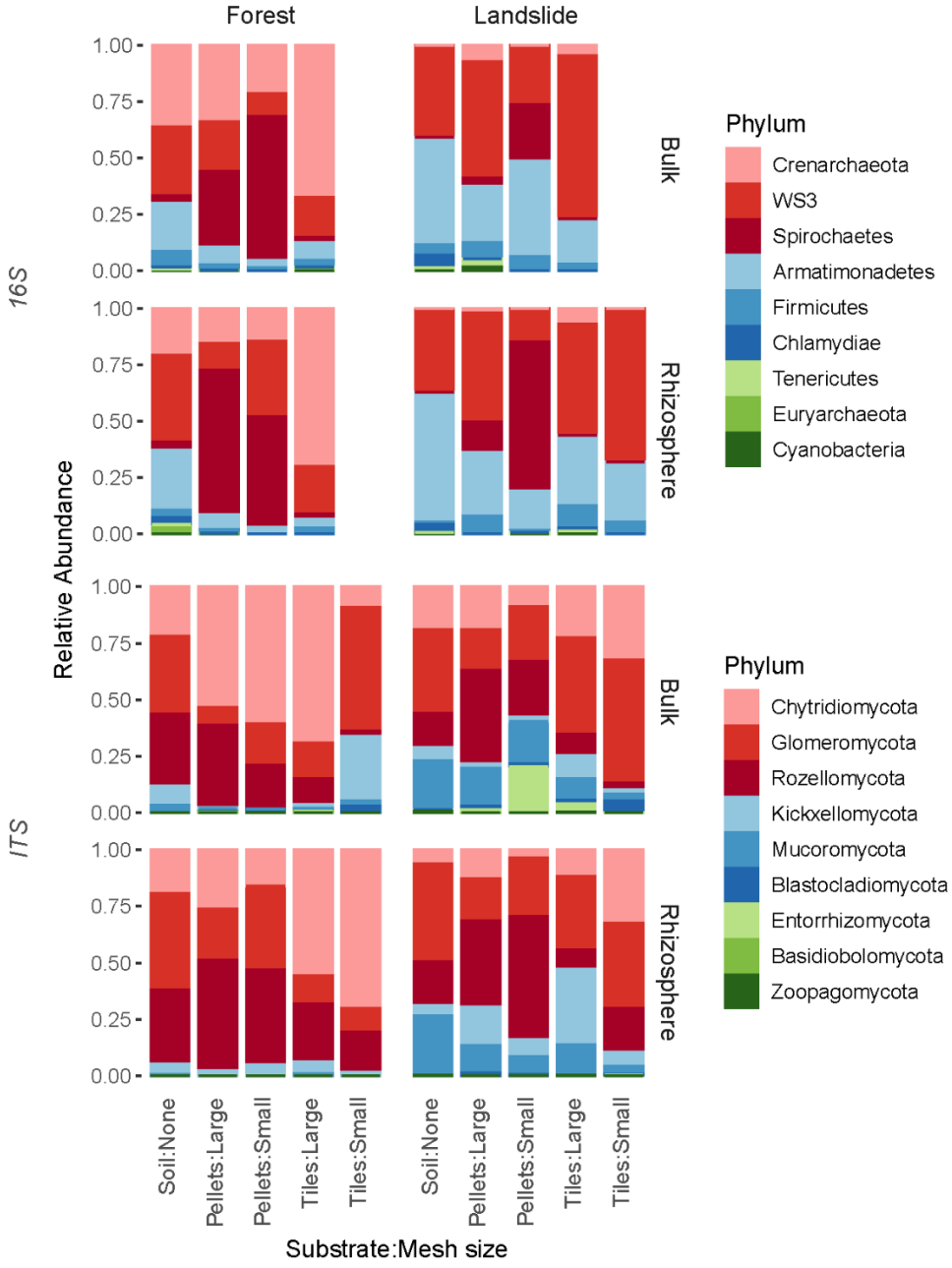

`

Figure S3.7. PCA ordination with Aitchison distances for bacterial and archaeal (*16S*) and fungal (*ITS*) ASVs found in soil, tiles and pellets at forests and landslides.

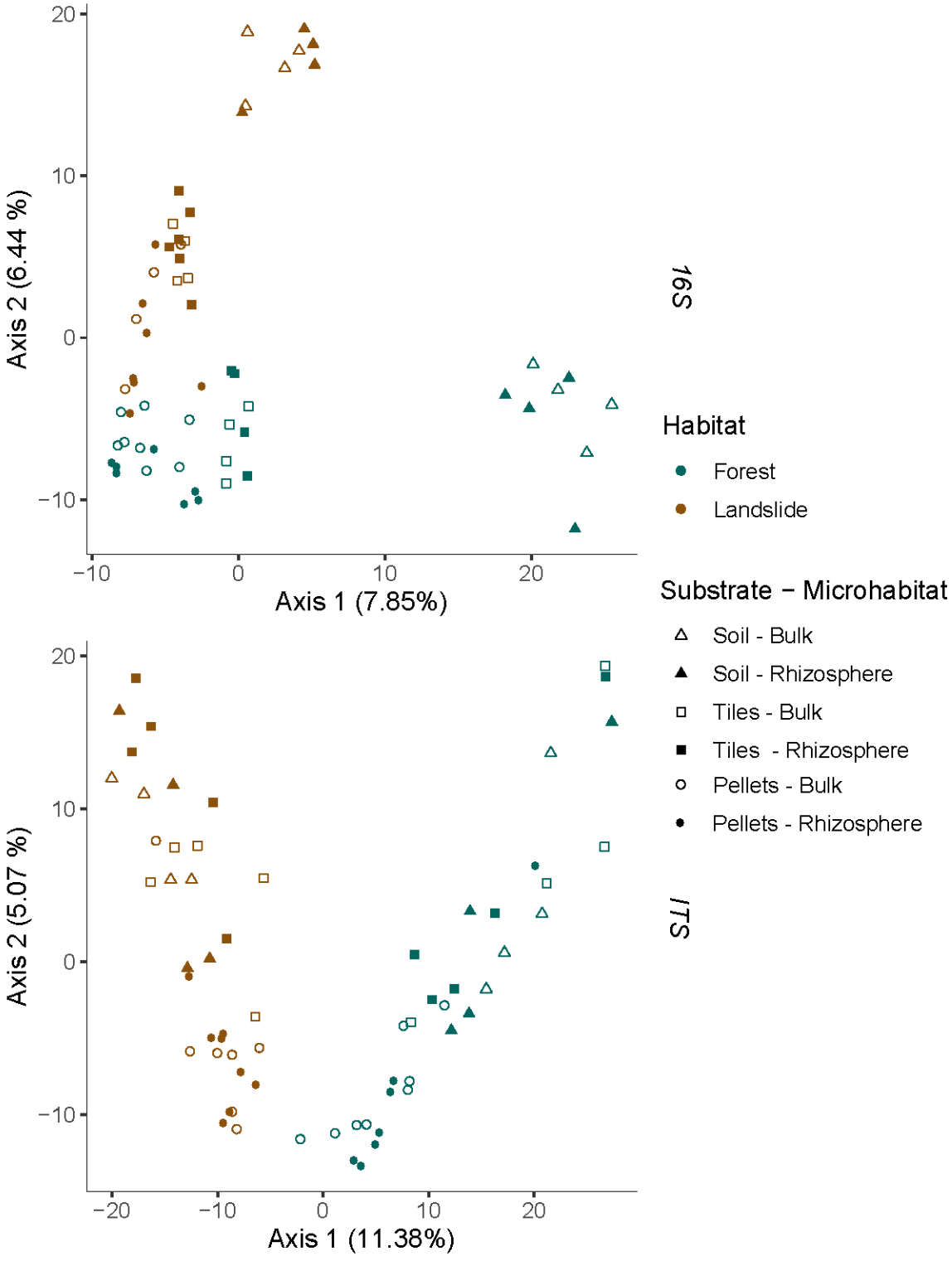

`

Figure S3.8. PCA ordinations with Aitchison distances for bacterial and archaeal (*16S*) and fungal (*ITS*) ASVs per rock weathering substrates.

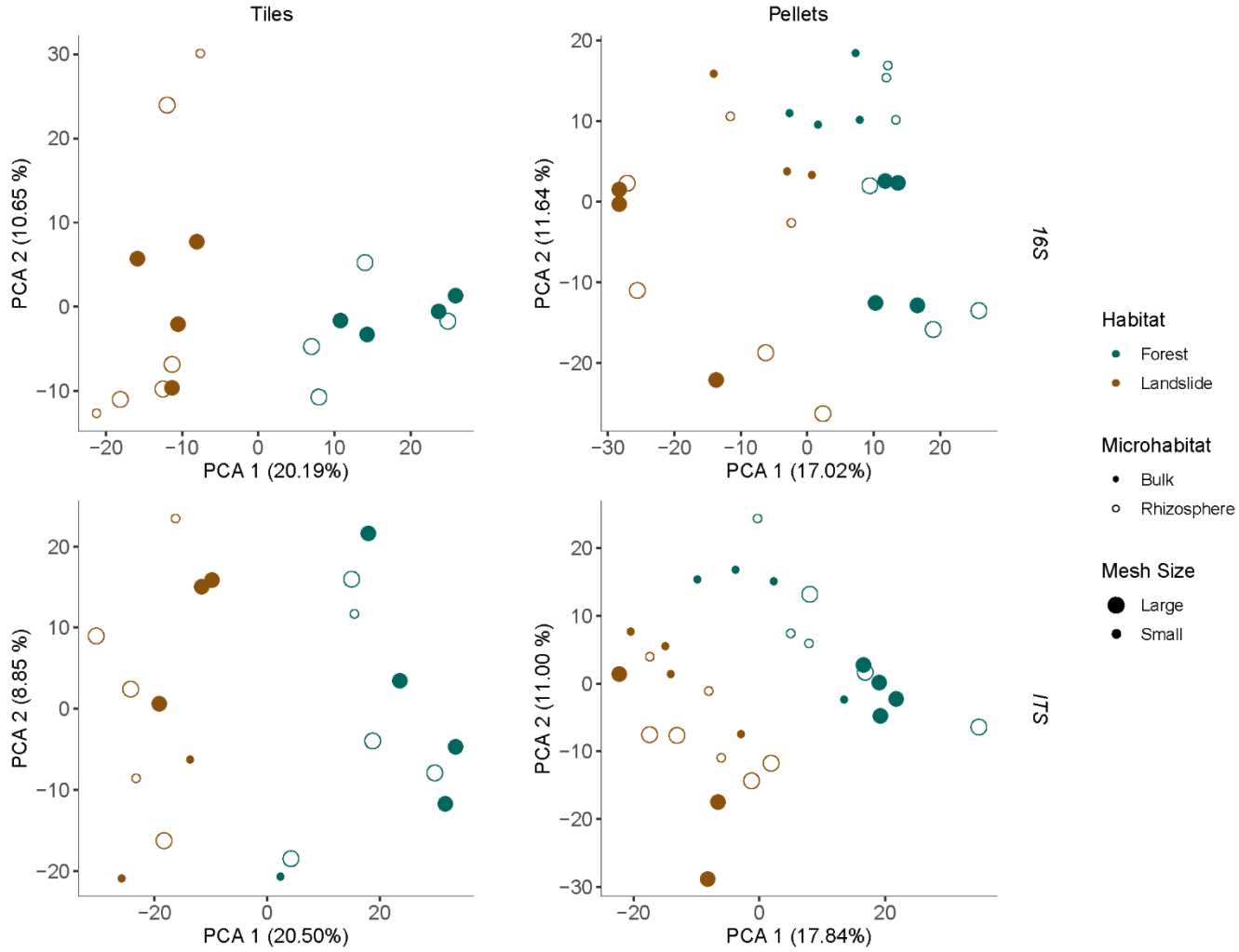

`

CHAPTER 4: CONCLUSIONS

In this final chapter, I summarize the main findings of my thesis which was aimed at characterizing the composition, structure, and function of plant rhizobiomes established in "landslide-like" areas, and evaluate the role of rhizobiomes in (Ca,Mg)-silicate rocks. This study represents a first effort to understand microbe-silicate rock interactions in landslides with a special emphasis on the tropics. Two general key findings are derived from this work: 1) landslide-like soils are highly weathered, and holds soil and root microbiomes with diversity, composition and functions disticnt to those at adjacent forest, and 2) rocks incubated at landslide-like soils and roots weathered faster than those at forest, and rocks incubated at each habitat inherited part of their respective root and soil microbiomes.

These results suggest that abiotic factors that diverge between the two habitats were more important than biotic ones in shaping microbial community composition and functioning. Indeed, landslides and similar disturbances causes modifications to ecosystems, such as changes in soil attributes measured in this study, in addition to other factors not measured here such as high UV radiation and extreme temperatures experienced in soils. Altogether, these factos ultimately affect soil microbial composition. Nonetheless, the losses in microbial inoculum and biomass caused by landslides (Singh et al. 2001, Li et al. 2005), might explain the huge microbial differences found across habitats. Other biotic factors were observed to affect microbial community diversity to a lesser extend, such as plant proximity (Mendes et al. 2014, Ortiz et al. 2020) and plant host identity and lifeform (Yeoh et al. 2017). Although separating the effect that biotic and abiotic factors exert in microbial community composition is a difficult task, it is clear that the interaction of these two sets of attributes controlled the microbial composition in landslides.

`

These results also suggest that rock weathering is occurring faster in landslides compared to forest, and that resulting nutrient mobilization drives microbial diversity and composition. This is the first time, to my knowledge, that a study uses NGS-technology coupled with an *in-situ* experiment to assess microbial silicate rock weathering. The study of landslides acquire greater relevance as their frequency is increased with road constructions, land use changes, and other forest modifications, combined with climate extremes such as hurricanes (Larsen and Torres-Sánchez 1996, Hughes and Schulz 2020). Thus, it is important to understand the biogeochemical dynamics triggered by landsliding and the factors controlling these ecosystems succession.